5 Anhang

I) Im Anhang befinden sich untenstehende Publikationen mit freundlicher Genehmigung der Bentham Science Publishers Ltd[4,7], Wiley-VCH Verlag GmbH & Co KGaA[8], S. Karger AG[6], Elsevier[1,3] und The American Society for Biochemistry and Molecular Biology[2] in der angegebenen Reihenfolge:

- B. Schmidt, D. K. Ehlert, H. A. Braun, *E*-1,2-Dichlorovinyl Ethers as Irreversible Protease Inhibitors, *Tetrahedron Lett.* **2004**, *45*, 1751.[1]

- H. A. Braun, S. Umbreen, M. Groll, U. Kuckelkorn, I. Mlynarczuk, M. E. Wigand, I. Drung, P.-M. Kloetzel, B. Schmidt, Tripeptide Mimetics Inhibit the 20 S Proteasome by Covalent Bonding to the Active Threonines, *J. Biol. Chem.* **2005**, *280*, 28394.[2]

- H. A. Braun, R. Meusinger, B. Schmidt, 2-Iodoethanols from Aldehydes, Diiodomethane and Isopropylmagnesium Chloride, *Tetrahedron Lett.* **2005**, *46*, 2551.[3]

- B. Schmidt, R. Narlawar, H. A. Braun, Drug Development and PET-Diagnostics for Alzheimer's Disease, *Curr. Med. Chem.* **2005**, *12*, 1677.[4]

- B. Schmidt, S. Baumann, R. Narlawar, H. A. Braun, G. Larbig, Modulators and Inhibitors of γ- and β-Secretases, *Neurodegenerative Diseases* **2006**, *3*, 290.[6]

- B. Schmidt, S. Baumann, H. A. Braun, G. Larbig, Inhibitors and Modulators of β- and γ-Secretase, *Curr. Top. Med. Chem.* **2006**, *6*, 377.[7]

- V. Limongelli, L. Marinelli, S. Cosconati, H. A. Braun, B. Schmidt, E. Novellino, Ensemble-Docking Approach on BACE-1: Pharmacophore Perception and Guidelines for Drug Design, *ChemMedChem* **2007**, DOI: 10.1002/cmdc.200600314, *in print.*[8] (Manuskript)

II) Daten der Kristallstrukturanalyse von Substanz (***S,S***)-**97** (Abb. 45).

Available online at www.sciencedirect.com
SCIENCE DIRECT®
Tetrahedron Letters 45 (2004) 1751–1753
Tetrahedron Letters

E-1,2-Dichlorovinyl ethers as irreversible protease inhibitors

Boris Schmidt,* Dennis K. Ehlert and Hannes A. Braun

Institute for Organic Chemistry and Biochemistry, Darmstadt Technical University, Petersenstr. 22, D-64287 Darmstadt, Germany

Received 4 November 2003; revised 9 December 2003; accepted 15 December 2003

Abstract—The synthesis of a novel motif for threonine protease inhibition is described. The desired *E*-1,2-dichlorovinyl ethers are obtained from alcohols and trichloroethylene as single diastereomers. Aqueous treatment at pH 11 unmasks the hidden α-chloroacetate, which is required for the reaction with the active site of the protease.

Cellular processes depend on the delicate balance of protein synthesis and degradation. Therefore cells feature two major pathways for protein degradation: proteolytic enzymes within the lysosome and the proteolytic core of the ubiquitin proteasome. The disregulation of protein half-life via disturbed destruction is common to many pathological processes. The selective inhibition of the multi-catalytic proteasome subunits is thus an attractive target for drug development in oncology and Alzheimer's disease.[1] For these therapeutic areas we investigate novel inhibitors of threonine proteases featuring reactive moieties, which bias their inhibition toward threonine over serine proteases. Several inhibitors of threonine proteases are known, both selective and unselective (Fig. 1).[2] Currently the most prominent threonine protease inhibitor: bortezomib **2**, is approved for the treatment of multiple myeloma by the FDA.[3]

We take the unspecific serine protease inhibitor **1** and its mode of action as our lead and intend to improve the selective inhibition of chymotrypsin-like activity of the 20S proteasome by reducing the inherent overkill. This over-activation derives from the dichlorovinyl ester, which reacts readily with all sorts of nucleophiles such as cysteine, serine and eventually threonine. The removal of the acyl function will significantly reduce the unspecific hydrolysis by ubiquitous nucleophiles and results in a reasonably stable dichlorovinyl ether. This ether tolerates acidic environment, but hydrolyses readily at pH 11 to be converted into an α-chloroacetate, which in turn reacts with nucleophiles. This dual reactivity, which is delivered in a cascade reaction, fulfils the specific requirements of an N-terminal threonine protease inhibitor. The general hydrolysis of an amide bond by a threonine protease is depicted in Scheme 1. Structural analysis of the proteasome β-subunits revealed that the 2°-hydroxyls of the N-terminal threonines serve as acyl

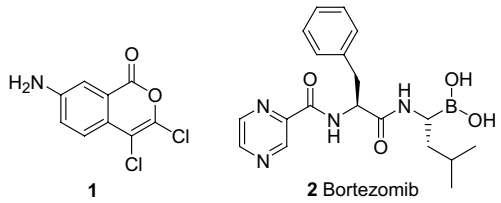

Figure. 1. Serine and threonine protease inhibitors.

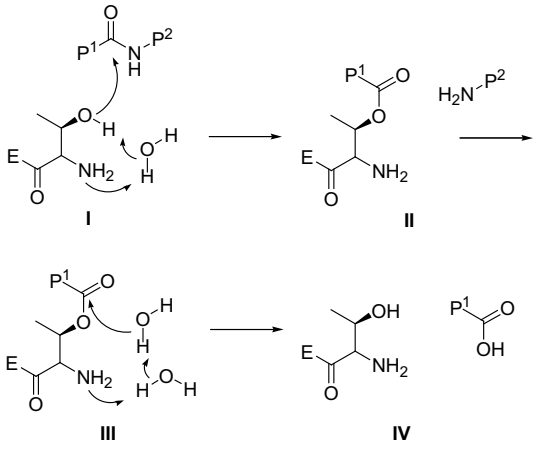

Scheme 1. Hydrolysis by threonine proteases.

Keywords: Enol ether; Protease.
* Corresponding author. Tel.: +49-6151-163075; fax: +49-6151-1632-78; e-mail: schmibo@oc.chemie.tu-darmstadt.de

0040-4039/$ - see front matter © 2003 Elsevier Ltd. All rights reserved.
doi:10.1016/j.tetlet.2003.12.088

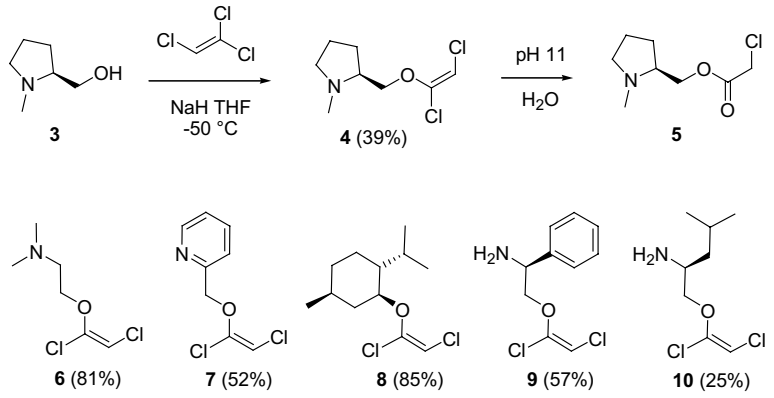

Scheme 2. Synthesis of dichlorovinyl ethers.

carriers. This difference from cysteine and serine proteases, which utilize less hindered 1° nucleophiles of an internal amino acid, holds potential for selective, mechanism-based inhibitors. The importance of the free amino terminus is apparent in the states **I** and **III**, where the amine directs a deprotonation cascade. These deprotonations result in hydrolysis of the amide and finally regenerate the catalytic site. Inhibitors addressing the active site may interact with the hydroxyl, the free amine or both. We have chosen compact, robust 2°-alcohols and aminoalcohols to explore the accessibility and stability of the required dichlorovinyl ethers. As it turned out, treatment of the alcohols with sodium hydride and trichloroethylene[4] in dry THF at −50 °C and slow warming to room temperature provided the desired ethers in moderate to excellent yields (Scheme 2).[5]

All compounds were obtained as single diastereomers, which were assigned the *E*-stereochemistry, based on the known menthyl ester **8**.[6] Further derivatization was accomplished by a palladium-mediated cross-coupling reaction, which resulted in the selective arylation of the 2-position (**11**, Scheme 3) by a magnesium acetylide species. All other methods and conditions for the cross-coupling (Stephens-Castro, Corey-House, Sonogashira) provided only trace amounts of the desired product. The initial work-up procedure involved extraction with sodium hydrogen carbonate solution and led to significant hydrolysis resulting in an α-chloroacyl ester. This reactivity suggests these derivatives as potential threonine protease inhibitors.

The introduction of amino acid sequences provides protease specificity and is accomplished by standard peptide synthesis in solution (Scheme 4). Condensation of the Z-protected Leucine–Leucine sequence is achieved using EDAC (1-ethyl-3-(3′-dimethylamino-

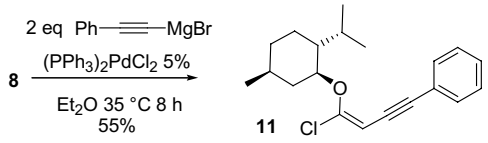

Scheme 3. Synthesis of an enyne chlorovinyl ether.

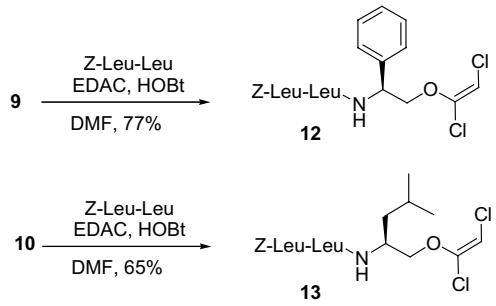

Scheme 4. Synthesis of tripeptide mimetics.

propyl)carbodiimide) and HOBt (*N*-hydroxybenzotriazole·H_2O) in DMF.

The resulting peptide mimetics are insensitive to air or moisture at neutral or slightly acid pH. However, exposure to strong nucleophiles or pH >11 leads to rapid hydrolysis. The inhibition of the β-subunits of the proteasome by the compounds **12**, **13** and close analogues thereof is subject to ongoing investigations.

Acknowledgements

We thank the Fonds der Chemischen Industrie, the DFG SPP1085 SCHM1012-3 and A. Hallberg, Uppsala Universitet for support of this work.

References and notes

1. Myung, J.; Kim, K. B.; Crews, C. M. *Med. Res. Rev.* **2001**, *21*, 245–273.
2. Hudig, D.; Allison, N. J.; Kam, C. M.; Powers, J. C. *Mol. Immun.* **1989**, *26*, 793–798.
3. Paramore, A.; Frantz, S. *Nat. Rev. Drug. Discov.* **2003**, *2*, 611–612.
4. Klementschitz, W. *Monatsh. Chemie* **1953**, *84*, 1201–1205.
5. A suspension of NaH (48 mg, 2.0 mmol) in dry THF (2 mL) was treated with (*S*)-(−)-1-methyl-2-pyrrolidinemethanol (115 mg, 1.0 mmol) and stirred at −15 °C for 30 min. The mixture was cooled to −50 °C prior to the addition of

trichloroethylene (1.23 mmol, 110 μL) in THF (2 mL). The mixture was warmed to +8 °C within 2 h and quenched with 2 mL sat. NH_4Cl solution and 6 mL Et_2O. The organic phase was washed with 2 mL H_2O, dried (Na_2SO_4) and concentrated. The crude oil was purified by filtration through Alox 90-II using $CHCl_3$/EtOH 100:1 R_f: 0.88 (Alox 60-N-E) to give the ether as a colorless oil (82.3 mg, 39%).

6. Moyano, A.; Charbonnier, F.; Greene, A. E. *J. Org. Chem.* **1987**, *52*, 2919–2922.

THE JOURNAL OF BIOLOGICAL CHEMISTRY
Vol. 280, No. 31, Issue of August 5, pp. 28394–28411, 2005
Printed in U.S.A.

Tripeptide Mimetics Inhibit the 20 S Proteasome by Covalent Bonding to the Active Threonines*

Received for publication, March 4, 2005, and in revised form, May 25, 2005
Published, JBC Papers in Press, May 26, 2005, DOI 10.1074/jbc.M502453200

Hannes A. Braun‡, Sumaira Umbreen‡, Michael Groll§, Ulrike Kuckelkorn¶, Izabela Mlynarczuk¶‖, Moritz E. Wigand¶, Ilse Drung¶, Peter-Michael Kloetzel¶, and Boris Schmidt‡

From the ‡Darmstadt University of Technology, Clemens Schöpf-Institute for Organic Chemistry and Biochemistry, D-64287 Darmstadt, Germany, §Institute for Physiological Chemistry, Ludwig Maximilian University München, D-81377 Munich, Germany, ¶Charité-Universitätsmedizin Berlin, Institute for Biochemistry, D-10117 Berlin, Germany, and ‖Department of Histology and Embryology, Center of Biostructure Research, The Medical University of Warsaw, 02-004 Warsaw, Poland

Proteasomes play an important role in protein turnover in living cells. The inhibition of proteasomes affects cell cycle processes and induces apoptosis. Thus, 20 S proteasomal inhibitors are potential tools for the modulation of neoplastic growth. Based on MG132, a potent but nonspecific 20 S proteasome inhibitor, we designed and synthesized 22 compounds and evaluated them for the inhibition of proteasomes. The majority of the synthesized compounds reduced the hydrolysis of LLVY-7-aminomethylcoumarin peptide substrate in cell lysates, some of them drastically. Several compounds displayed inhibitory effects when tested *in vitro* on isolated 20 S proteasomes, with lowest IC_{50} values of 58 nM (chymotrypsin-like activity), 53 nM (trypsin-like activity), and 100 nM (caspase-like activity). Compounds 16, 21, 22, and 28 affected the chymotrypsin-like activity of the β5 subunit exclusively, whereas compounds 7 and 8 inhibited the β2 trypsin-like active site selectively. Compounds 13 and 15 inhibited all three proteolytic activities. Compound 15 was shown to interact with the active site by x-ray crystallography. The potential of these novel inhibitors was assessed by cellular tolerance and biological response. HeLa cells tolerated up to 1 μM concentrations of all substances. Intracellular reduction of proteasomal activity and accumulation of polyubiquitinated proteins were observed for compounds 7, 13, 15, 22, 25, 26, 27, and 28 on HeLa cells. Four of these compounds (7, 15, 26, and 28) induced apoptosis in HeLa cells and thus are considered as promising leads for antitumor drug development.

The balance of protein synthesis and degradation processes is essential to maintain cellular homeostasis. Cells possess two major pathways to fulfill protein degradation: proteins are digested either by proteolytic enzymes within the lysosomes or via the ubiquitin-proteasome system. The imbalance of the protein synthesis and degradation processes causes many pathological processes (1).

* This work was supported by the Fonds der Chemischen Industrie, Deutsche Forschungsgemeinschaft Grants SPP1085 SCHM1012-3 and Ku1261, and EU Contract LSHM-CT-2003-503330 (APOPIS). The costs of publication of this article were defrayed in part by the payment of page charges. This article must therefore be hereby marked "*advertisement*" in accordance with 18 U.S.C. Section 1734 solely to indicate this fact.

** To whom correspondence should be addressed: Darmstadt University of Technology, Clemens Schöpf-Institute for Organic Chemistry and Biochemistry, Petersenstrasse 22, D-64287 Darmstadt, Germany. Tel.: 49-6151-16-3075; Fax: 49-6151-16-3278; E-mail: schmibo@oc.chemie.tu-darmstadt.de.

26 S proteasomes, multi-subunit protease complexes, perform ATP-dependent degradation of polyubiquitinated proteins and are responsible for most of the non-lysosomal proteolysis in eukaryotic cells. They consist of the proteolytic 20 S proteasome core particle and are capped at one or both ends by 19 S regulatory particles (2, 3). The 20 S core particle is a cylindrical assembly of 28 subunits arranged in four stacked heptameric rings; two rings are formed by 7 α-type subunits, and two rings are build of 7 β-type subunits (4, 5). The two inner β-rings form the central cavity of the cylinder and harbor the proteolytic sites. In contrast to prokaryotic 20 S proteasomes, which contain 14 identical proteolytically active β-type subunits, eukaryotic 20 S proteasomes belong to the family of N-terminal nucleophilic hydrolases (6, 7). They possess only three subunits with N-terminal active site threonines in the β-ring. In addition, the stimulation of mammalian cells by γ-interferon causes the replacement of the three active β-subunits β1, β2, and β5 by their immunohomologues β1i, β2i, and β5i, resulting in the formation of immunoproteasomes, which display modified cleavage patterns of substrate peptides. The functional integrity of proteasomes is indispensable for a variety of cellular functions, such as metabolic adaptation, cell differentiation, cell cycle control, stress response, degradation of abnormal proteins, and generation of epitopes presented by major histocompatibility complex class I receptors (for reviews, see Refs. 8 and 9). However, proteasomes are an important supplier (but not the exclusive supplier) of antigenic peptides (10, 11).

The deregulation of the ubiquitin-proteasome protein degradation pathway in humans causes several diseases, such as cancer and neurodegenerative, autoimmune, and metabolic disorders. Inhibition of proteasomes influences the stability of many proteins, especially those that are involved in the cell cycle regulation. In fact, most of the cells treated with proteasomal inhibitors become sensitive to apoptosis (12, 13). Thus, selective inhibitors of catalytic proteasome subunits are attractive targets for drug development (14). Interestingly, tumor cells are usually more sensitive to proteasomal inhibition than normal cells. Healthy cells display cell cycle arrest when treated with proteasomal inhibitors but, in contrast to tumor cells, are not as susceptible to apoptosis (15, 16). So far, several proteasomal inhibitors have been characterized, both selective (**4**, lactacystin; **5**, TMC-95A; and **6**, epoxomicin) and nonspecific (**1**, dichlorovinyl ester; **3**, MG132) (Fig. 1*A*) (17).

The most prominent proteasomal inhibitor **2** (Bortezomib®, VELCADE™) is approved by the United States Food and Drug Administration as a prescription drug for the treatment of multiple myeloma (18–20). Similar applications of proteasomal

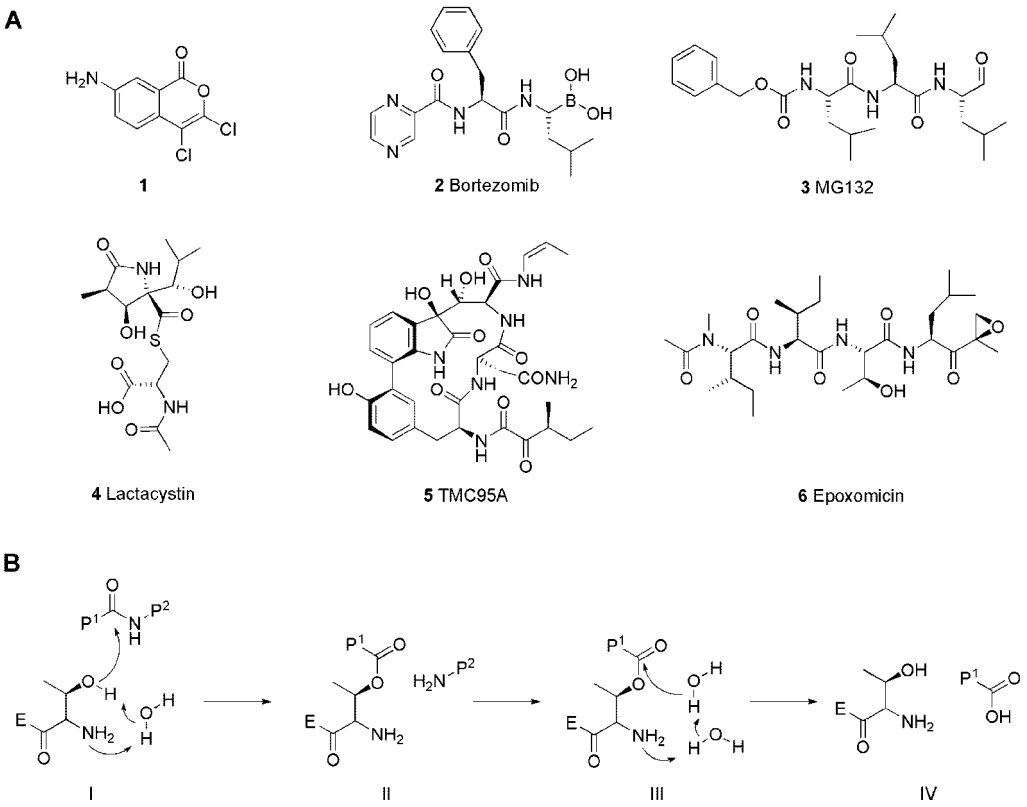

FIG. 1. *A*, serine and threonine protease inhibitors. *B*, hydrolysis by threonine proteases.

inhibitors in oncology and neurodegenerative diseases are at the focus of our interest (21). We intend to develop selective inhibitors for the three different proteolytic activities of the 20 S proteasome. Our goals may be achieved by creating compounds or reactive moieties, which bind covalently to the N-terminal threonine.

The proteasomal amide hydrolysis differs from all other classes of proteases and is performed by N-terminal threonines, as depicted in Fig. 1*B*. The crystal structure analysis of the 20 S proteasome revealed that the Thr-1Oγ functions as the nucleophile and that the N-terminal amino group serves as an acyl carrier (6). Covalent inhibitors can bind to the active site through the Thr-1Oγ hydroxyl group or both the free N terminus and Thr-1Oγ (for review, see Ref. 17).

Effective *in vivo* inhibitors of the 20 S proteasome require high selectivity and good penetration of the cellular membranes. We decided to address the selectivity problems of **3** (MG132) first. A focused set of peptide analogue aldehydes **13–18** aimed at the proteolytic activity of β5 subunit was synthesized and tested for inhibition of the 20 S proteasome and β-secretase (22, 23). These results encouraged us to address the design of irreversible and selective proteasome inhibitors. We concentrated on the nonspecific serine protease inhibitor **1** and introduced modifications to improve its selective inhibition of the chymotrypsin-like activity of the 20 S proteasome.

MATERIALS AND METHODS

Isolation of 20 S Proteasomes—20 S proteasomes were isolated from red blood cells. Cells were lysed with dithiothreitol (1 mM), and the stroma-free supernatant was applied to DEAE-Sepharose (Toyopearls). 20 S proteasome was eluted with a NaCl gradient in TEAD (20 mM Tris-HCl, pH 7.4, 1 mM EDTA, 1 mM azide, and 1 mM dithiothreitol) from 100 to 350 mM NaCl. 20 S proteasome was concentrated by ammonium sulfate precipitation (between 40 and 70% of saturation) and separated in a 10–40% sucrose gradient by centrifugation at 40,000 rpm for 16 h (SW40; L7; Beckman & Coulter). Finally, 20 S proteasome was purified on MonoQ column and eluted with a NaCl gradient at 280 mM NaCl. The fractions containing purified 20 S proteasome were dialyzed against 50 mM NaCl in TEAD and stored on ice. The purity was determined by SDS-PAGE.

Protease Assays—Suc-LLVY-AMC,[1] Z-VGR-AMC, and LLE-AMC (Bachem, Calbiochem) were used to estimate chymotrypsin-like, trypsin-like, and caspase-like (post-acidic) activities of the 20 S proteasome, respectively. Substrates were incubated with 20 S proteasome at 37 °C in assay buffer (20 mM Tris-HCl, pH 7.2, 1 mM EDTA, and 1 mM dithiothreitol) for 1 h. 100 ng of 20 S proteasome was preincubated with 0.01–10 μM of the inhibitors for 15 min. The reaction was started by addition of substrate (50 μM). The released AMC was detected by fluorescence emission at 460 nm (excitation at 390 nm) using a TECAN fluorometer. Activity was estimated in fluorescence units, and the inhibition is represented by IC_{50} values.

Cell Culture—HeLa cells and MeWo cells (human melanoma) were cultured in RPMI 1640 supplemented with 10% heat-inactivated fetal calf serum and penicillin/streptomycin at 5% CO_2. Inhibitors were applied from 100× stocks (in Me_2SO) at the indicated final concentrations and incubated for variable times.

Sensitivity of Cells against Added Compounds—The viability of HeLa cells was tested by crystal violet staining after incubation with inhibitors. The cells were washed once with PBS, fixed with 1% of glutardialdehyde for 30 min, and washed again. Finally, the fixed cells were stained with 0.1% crystal violet in PBS for 30 min and subsequently washed carefully with water to remove unbound dye. The remaining dye was eluted by 0.1% Triton X-100 in PBS and determined at 550 nm.

Inhibition of 20 S Proteasomes within Cells—Cells were harvested and lysed with 0.1% Nonidet P-40 in TEAD in the presence of the commercial protease inhibitor mixture Complete (Roche Applied Science). The proteasomal activity was measured in 10 μl of lysates by using Suc-LLVY-AMC as a substrate. The protein content was quantified by Bradford (Protein assay; Bio-Rad).

Detection of Accumulated Polyubiquitinated Proteins—50 μg of total cell lysate was separated by SDS-PAGE and blotted onto polyvinylidene difluoride membrane (Millipore). Blots were blocked by 5% of milk suspension. The polyubiquitinated proteins were detected by anti-ubiq-

[1] The abbreviations used are: AMC, 7-aminomethylcoumarin; Z, benzyloxycarbonyl; PBS, phosphate-buffered saline.

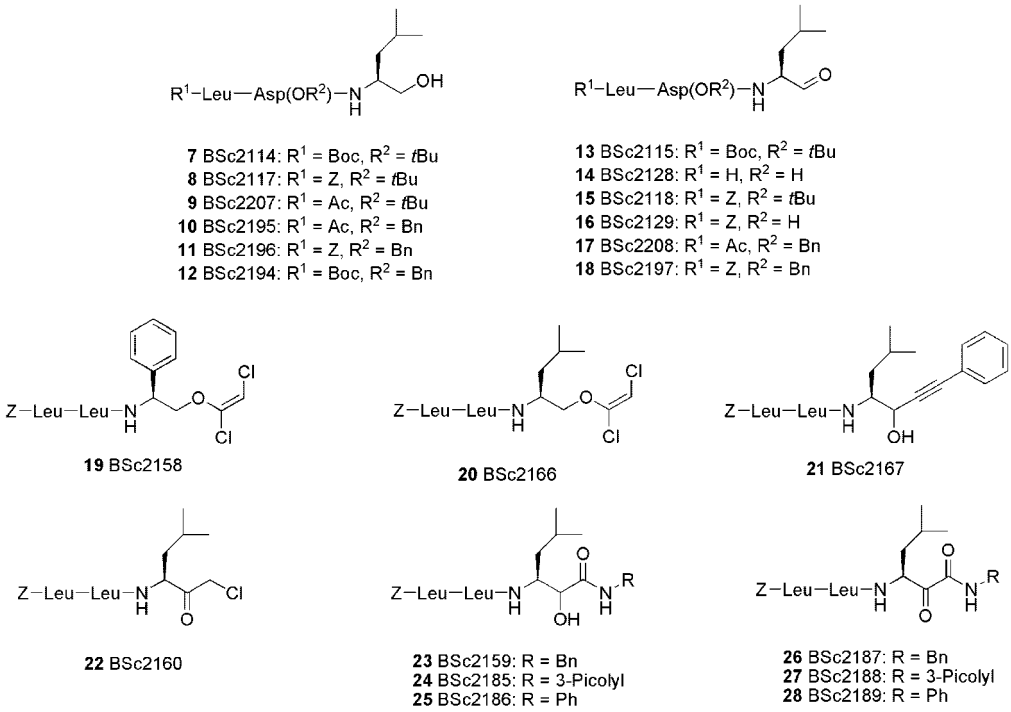

FIG. 2. **Peptidomimetics designed for 20 S proteasome inhibition.**

uitin antibody (DAKO) and anti-rabbit peroxidase-labeled as secondary antibody (DIANOVA) and then visualized by ECL.

Analysis of Cell Cycle—MeWo cells were treated with inhibitor **15** and MG132 for 24 h. Cells were trypsinized, washed with cold PBS, suspended in 70% ethanol, and fixed at −20 °C for 2 h. Fixed cells were washed twice with PBS, incubated with RNase A (Sigma) at room temperature for 20 min, and placed on ice. Propidium iodide was added to a final concentration of 5 μg/ml, and cells were stained at least for 2 h at 4 °C. The cells were analyzed after staining by flow cytometry (FACSCalibur flow cytometer; BD Biosciences) using CellQuest software. Statistical significance was determined by the χ^2 test.

Apoptosis Assay—HeLa cells (10,000 cells/well) were disseminated in a 96-well plate and treated with 1 μM of inhibitors for 20 h. The ongoing apoptosis was estimated by the Apo-One® assay (Promega).

Co-crystallization—Crystals of 20 S proteasome from *Saccharomyces cerevisiae* were grown in hanging drops at 24 °C as described previously (6) and incubated for 60 min with compound **15**. The protein concentration used for crystallization was 40 mg/ml in Tris-HCl (10 mM, pH 7.5) and EDTA (1 mM). The drops contained 3 μl of protein and 2 μl of the reservoir solution, which contained 30 mM magnesium acetate, 100 mM morpholinoethanesulfonic acid, pH 7.2, and 10% 2-methylpentane-2,4-diol.

The space group belongs to $P2_1$ with cell dimensions of a = 135.8 Å, b = 300.1 Å, c = 144.4 Å, and β = 113.1°. Data to 2.8 Å were collected using synchrotron radiation with λ = 1.05 Å on the BW6-beamline at DESY (Hamburg, Germany). Crystals were soaked in a cryoprotecting buffer (30% 2-methylpentane-2,4-diol, 20 mM magnesium acetate, 100 mM morpholinoethanesulfonic acid, pH 6.9) and frozen in a stream of liquid nitrogen gas at 90 K (Oxford Cryo Systems). X-ray intensities were evaluated by using the MOSFILM program package (version 6.1), and data reduction was performed with CCP4 (24). The anisotropy of diffraction was corrected by an overall anisotropic temperature factor by comparing observed and calculated structure amplitudes using the program X-PLOR (25). A total of 2,383,416 reflections yielding 248,616 unique reflections (96.9% completeness) was collected. The corresponding R_{merge} was 8.7% at 2.8 Å resolution (41.9% for the last resolution shell). Electron density was improved by averaging and back-transforming the reflections 10 times over the 2-fold noncrystallographic symmetry axis using the program package MAIN (26). Conventional crystallographic rigid body, positional, and temperature factor refinements were carried out with X-PLOR using the yeast 20 S proteasome structure as starting model (6). For model building, the program MAIN was used. The structure was refined to a R-factor of 21.7% (free R-factor, 24.9%) with root mean square deviations from target values of 0.007 Å for bonds and 1.30° for angles (27). Modeling experiments were performed using the coordinates of yeast 20 S proteasome with the program MAIN (26).

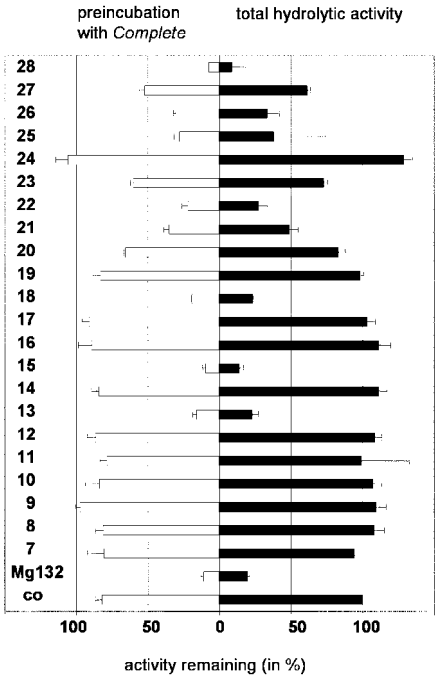

FIG. 3. **Estimation of proteolysis in cell lysates by addition of MG132 and 7–28.** Compounds (10 μM) were added to clarified lysates and preincubated for 30 min on ice prior to the proteolysis assay (*black bars*). In parallel, lysate was preincubated with the commercial protease inhibitor mixture Complete for 30 min, which inhibited most of the cytosolic serine/aspartate proteases, but not proteasomes (*white bars*). This partial inactivation was followed by incubation with the indicated compounds. The proteolytic activity was determined in 10 μl of the lysates by addition of LLVY-AMC (100 μl, 50 μM) in TEAD. The AMC released by non-inhibited lysate was set to 100%. MG132 was used as inhibition control.

Synthesis—Compounds **7–18** were synthesized as analogues of **3** (MG132) based on the established substrate preferences of β-secretase (23) by standard methodology or as published previously (28). The condensation of commercial protected dipeptides and amino acids with

TABLE I
Calculated IC_{50} values for compounds **7–28.**

IC_{50} values were calculated from inhibition of proteasomes at increasing amounts of inhibitors. Samples were preincubated for 15 min in ice. The assay was started by addition of 50 μM fluorogenic peptide substrate. LLVY-AMC and GLL-AMC for chymotryptic-like, VGR-AMC for tryptic-like, and LLE-AMC for caspase-like activity. The release of AMC was determined at 460 nm emission (excitation, 390 nm). Calculated IC_{50} values for MG132 served as controls.

Inhibitor	Access no.	IC_{50}			
		β5 Chymotrypsin-like (Y)	β5 Ch-I (L)	β2 Trypsin-like (R)	β1 Caspase-like (E)
		μM	μM	μM	μM
7	BSc2114	>10	–[a]	0.053	>10
8	BSc2117	>10	–	5.481	>10
9	BSc2207	>10	–	–	–
10	BSc2195	>10	–	–	–
11	BSc2196	>10	–	–	–
12	BSc2194	>10	–	–	–
13	BSc2115	0.382	0.102	0.495	0.098
14	BSc2128	>10	>10	>10	>10
15	BSc2118	0.058	0.031	0.155	1.791
16	BSc2129	7.26	–	>10	>10
17	BSc2208	–	–	–	–
18	BSc2197	1.731	–	–	3.122
19	BSc2158	–	–	–	–
20	BSc2166	>10		>10	>10
21	BSc2167	1.303	>10	–	–
22	BSc2160	2.196	–	–	–
23	BSc2159	–	–	–	–
24	BSc2185	–	–	–	–
25	BSc2186	0.981		–	4.04
26	BSc2187	0.441		–	1.72
27	BSc2188	0.350		–	7.966
28	BSc2189	0.072		–	>10
3	MG132	0.0242	2.240	9.215	2.288

[a] –, no inhibition.

commercial amino alcohols was followed by oxidation to the aldehydes by 2-iodooxybenzoic acid in Me_2SO.

RESULTS

The intermediate alcohol derivatives **7–12** and the tripeptidic aldehydes **13–18** were investigated for enzyme inhibition. Inhibition of β-secretase was rather poor ($IC_{50} \gg 200$ μM),[2] but several compounds turned out to be potent inhibitors of the 20 S proteasome. Peptide aldehydes generally lack selectivity in enzyme inhibition. Therefore, other moieties were tested for their ability to inhibit threonine proteases. The nonselective dichlorovinyl ester **1,** which reacts readily with all sorts of nucleophiles such as cysteine, serine, and, eventually, threonine, served as our lead, but we intended to reduce the inherent overactivation. The removal of the acyl group may reduce the nonspecific hydrolysis by ubiquitous nucleophiles and results in reasonably stable dichlorovinyl ethers (28). Such ethers (**19** and **20**) tolerate acidic environment but hydrolyze readily at pH 11 to be converted into α-chloroacetates, which in turn may react with nucleophiles. This dual reactivity, which is delivered in a cascade reaction, meets the specific requirements of an N-terminal threonine protease inhibitor. An analogue dual reactivity may be observed for propargylic ketones. A similar compound was synthesized, but unfortunately, the alcohol **21** resisted oxidation to the desired ketone. Therefore, we focused on transition state mimetics as inhibitors. Lead structures, such as statines (34), α-ketoamides, and chloromethyl ketones, are well established in protease inhibition. Combination of these structures with a β5 selective tripeptide furnished the compounds **22–28** (Fig. 2). Compound **22** was prepared from commercial Z-LL and chloromethyl leucine. Compounds **23–25** were obtained by a Passerini reaction of MG132 with three isonitriles. The subsequent oxidation by 2-iodooxybenzoic acid in Me_2SO furnished the α-ketoamides **26–28**.

All peptide mimetics (**7–28**) were tested for their ability to inhibit the 20 S proteasome. Initially, we investigated the inhibition of cellular soluble proteases. 10 μM solutions of compounds **7–28** were added to the cytosolic fraction of HeLa cells and incubated for 30 min on ice. Subsequently, the proteolytic process was monitored by addition of the peptidic substrate Suc-LLVY-AMC. In parallel, the cytosolic fraction was treated with the broad specific protease inhibitor mixture Complete (Roche Applied Science) prior to the addition of substrate. This inhibitor mixture did not affect 20 S proteasomes. 11 of 22 investigated compounds diminished proteolysis in the cytosolic fraction as well as in the Complete-pretreated lysate (Fig. 3). The inhibition rates differed drastically. Some of the compounds displayed no inhibition, whereas five of the analyzed compounds decreased the hydrolysis of Suc-LLVY-AMC by >75%.

To ensure that the inhibitory effect observed in the cytosolic fraction was indeed caused by inhibition of 20 S proteasomes, the inhibitors were added at different concentrations to isolated 20 S proteasomes. The effect of the inhibitors was compared with that of the frequently employed 20 S proteasome inhibitor **3** (MG132). The chymotryptic-like (Suc-LLVY-AMC), tryptic-like (Bz-VGR-AMC), and caspase-like (Z-LLE-AMC) activities of 20 S proteasomes were determined after incubation at 37 °C for 1 h. The strongest inhibitory effects were observed for chymotryptic-like activity. Six of the tested inhibitors (**13**, **15**, **25**, **26**, **27**, and **28**) displayed IC_{50} values of <1 μM. The inhibition of tryptic-like activity was <1 μM for the inhibitors **7**, **13**, and **15**. Only compounds **7** and **8** showed exclusive inhibition of tryptic-like activity. The inhibition of caspase-like activity was even weaker (Table I). 20 S proteasomes isolated from HeLa cells contain more constitutive proteasomes than immunoproteasomes. Therefore, we repeated the inhibition experiments with immunoproteasomes isolated from stably transfected T2.27 cells. These experiments revealed that immunoproteasomes and constitutive proteasomes display similar sensitivities to the inhibitors (data not shown). 26 S proteasomes are responsible for ATP-dependent degradation of

[2] M. Willem, S. Umbreen, and B. Schmidt, unpublished results.

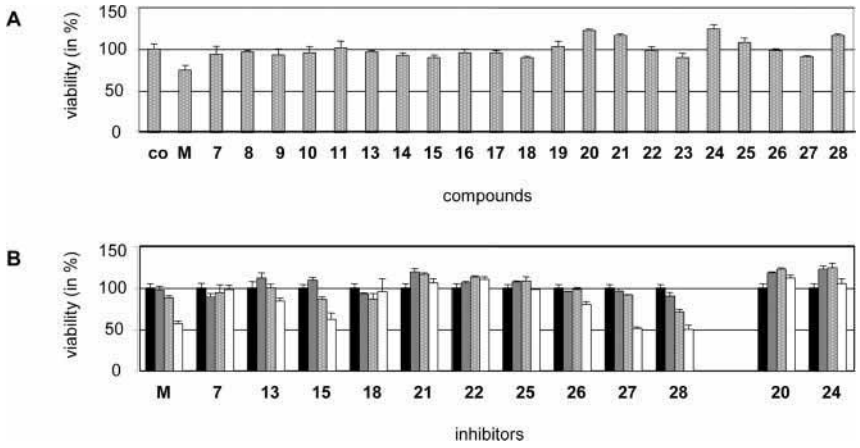

FIG. 4. *A*, viability of HeLa cells after incubation with MG132 and **7–28**. The viability of HeLa cells incubated with inhibitors (1 μM) was determined by crystal violet staining after 20 h. *B*, the viability of HeLa cells is dependent on inhibitor concentrations. HeLa cells were cultured in the presence of increasing concentrations (100 nM, *gray bars*; 1 μM, *white dotted bars*; 10 μM, *white bars*) of inhibitors for 20 h. Control cells are indicated by *black bars*. Cell survival was determined by crystal violet staining.

polyubiquitin-tagged proteins within living cells. They exhibited a similar susceptibility to the most potent inhibitor (**15**) *in vitro* (data not shown).

Protease inhibitors are often very toxic for organisms or single cells (1). Therefore, selected inhibitors were tested on cell cultures for cell lysis or cell death. The viability of HeLa cells in the presence of different compounds was tested in 24-h cultures. HeLa cells tolerated 1 μM concentrations of inhibitory and non-inhibitory substances (Fig. 4*A*). The relative survival rate of the cells was clearly diminished at concentrations of 10 μM. This effect was pronounced for the most potent inhibitors from the *in vitro* experiments (**15**, **28**, and **27**) (Fig. 4*B*).

The impact of inhibitors on living cells and organisms crucially depends on adequate cell permeability. Therefore, we analyzed the proteasome function within cells at different inhibitor concentrations. The application to cell cultures or animals required the concentrations of the inhibitors to be as low as possible. The specific proteasome activity was reduced below 50% (Fig. 5*A*) in cells treated with 1 μM solutions of **15**, **22**, **25**, **26**, and **28**. Compounds **7**, **13**, and **27** exhibited weaker effects on the specific activity, whereas compounds **18** and **21** hardly inhibited the cellular proteasome at all. Remarkably, inhibitors **15**, **22**, and **28** reduced the proteolytic activity already at a concentration of 100 nM (Fig. 5*A*). Specific inhibition of proteasomes results in the accumulation of polyubiquitinated proteins. Indeed, the amounts of polyubiquitinated proteins increased during incubation with the inhibitors. First effects were observed after 2 h for the potent compound **15** (Fig. 5*B*) and for compounds **20**, **22**, **25**, and **28** (data not shown). The accumulation of polyubiquitinated proteins via proteasome inhibition depended strongly on the applied concentrations (Fig. 5*C*). Thus, several of these new inhibitors are able to permeate cells and affect the activity of proteasomes. The consequences of proteasome inhibition for distinct cellular functions are subject to ongoing investigations.

The particular sensitivity of tumor cells to proteasome inhibitors (1) was evaluated in the melanoma cell line MeWo at different concentrations of compound **15** for 72 h. The viability was compared with MeWo cells treated with MG132 under the same conditions (Fig. 6*A*). 50% of the MeWo cells treated with 35 nM MG132 were still alive after 72 h. Very few cells survived the treatment with inhibitor **15**, which demonstrated its potency. Proteasome inhibitors can induce a cell cycle arrest in the G_1/S or G_2 phase, therefore the cell cycle progress was analyzed after 24-h inhibitor treatment of MeWo cells (Fig. 6, *B* and *C*). Compound **15** led to a cell cycle arrest in the G_2 phase, like MG132, albeit at considerably lower concentrations.

Proteasomes determine the delicate balance of life and death of the cells by controlling transcription factors and proteins involved in apoptosis. The reduction of proteasomal capacity

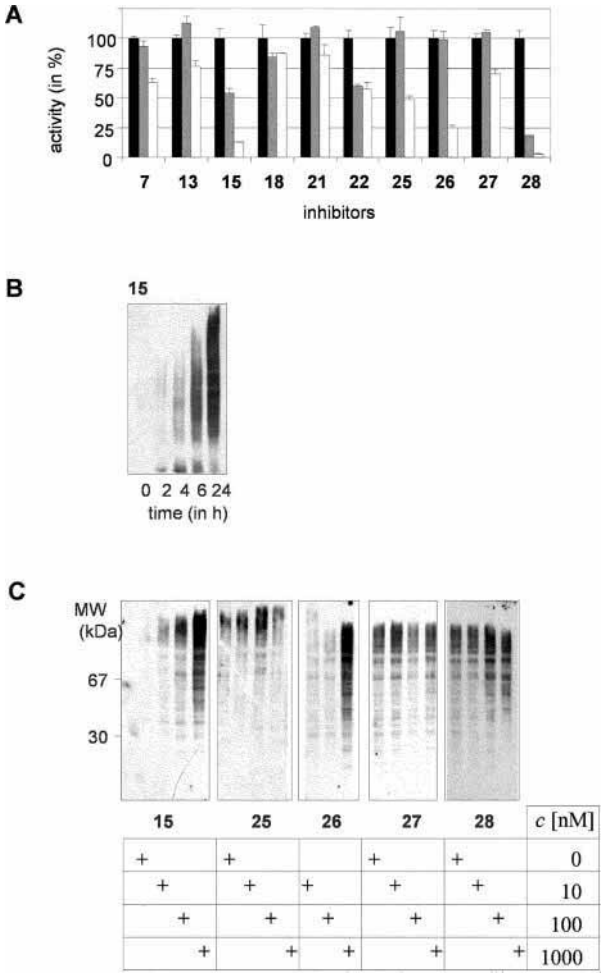

FIG. 5. **Inhibition of proteasomes within cells.** The proteasome activity and intracellular accumulation of polyubiquitinated proteins in cells co-cultured with inhibitors were tested in lysed cells. *A*, HeLa cells were cultured in the presence of inhibitors for 24 h. After lysis of cells, the protein concentration was measured according to Bradford to normalize the different cell amounts. Thereafter, Complete (Roche Applied Science) was added to all lysates, and the proteasomal activity was determined by hydrolysis of Suc-LLVY-AMC. Lysates of HeLa cells cultured without inhibitors served as control (*black bars*) and were compared with cell lysates cultivated at 100 nM (*gray bars*) and 1 μM (*white bars*). *B*, HeLa cells were cultured with 1 μM compound **15** for 2, 4, 6, and 24 h. Cells were lysed, and proteins were separated by SDS-PAGE in a 10% gel, blotted onto a polyvinylidene difluoride membrane, and detected in Western blot by an anti-ubiquitin antibody (DAKO). *C*, HeLa cells were treated with increasing concentrations of the inhibitors **15**, **25**, **26**, **27**, and **28** for 24 h (*c*, inhibitor concentration). Cells were lysed, proteins were separated in 15% gels, and the accumulation of polyubiquitinated proteins was controlled by Western blots.

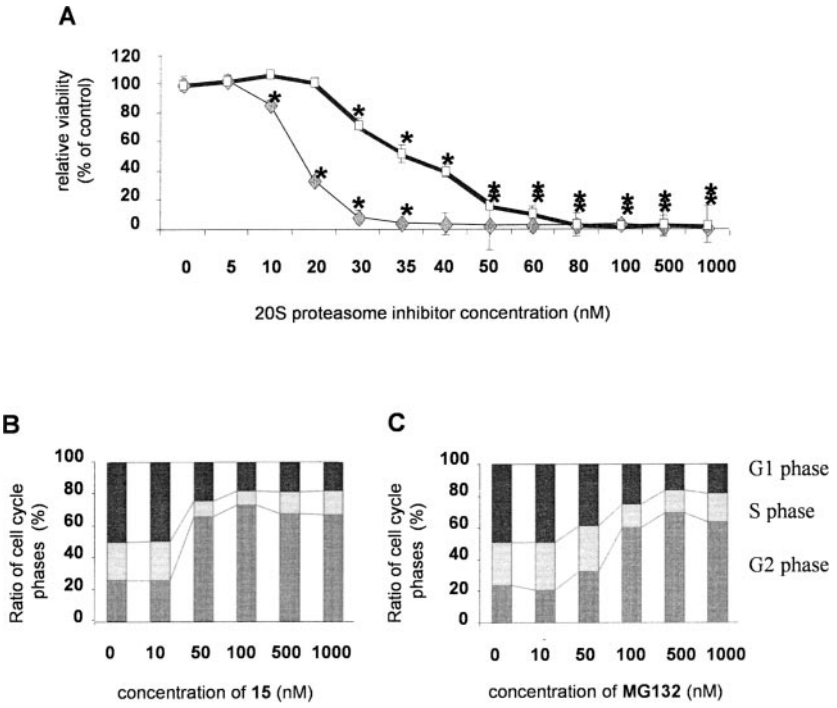

FIG. 6. **Higher susceptibility of human melanoma cells to inhibitor 15.** *A*, human melanoma cells (MeWo) were treated with increasing concentrations of inhibitor **15** or **3** (MG132) for 72 h. The viability of the cells after treatment with **15** (*gray diamonds*) or MG132 (*white squares*) was estimated by crystal violet staining. Statistical significance (*asterisks*) was calculated by Student's *t* test. *B* and *C*, investigation of cell cycle arrest. MeWo Cells were cultured with inhibitors **15** and **3** (MG132) for 24 h. The harvested cells were washed and fixed in 70% ethanol. Subsequently, the cells were incubated with RNase A. DNA was stained by addition of propidium iodide to a final concentration of 5 μg/ml. DNA was analyzed by fluorescence-activated cell sorting (FACSCalibur flow cytometer; BD Biosciences). Statistical significance was calculated by the χ^2 test. The relative distribution of cells that resided in G_1 (*black bar*), S (*white bar*), or G_2 phase (*checkered bar*) is shown for inhibitor **15** in *B* and for MG132 in *C*.

may result in the initiation of apoptosis, as reported for the proteasome inhibitor MG132 (29). Therefore, HeLa cells cocultured with 1 μM solutions of the inhibitors **7**, **8**, **11**, **13–16**, **18**, **20–23**, and **25–28** for 24 h were monitored for the induction of apoptosis by measuring caspase 3/7 activity. Most of the tested inhibitors did not affect cell viability. In contrast, application of the inhibitors **7**, **15**, **26**, and **28** caused an activation of caspase 3/7, signaling apoptotic events (Fig. 7).

We determined the crystal structure of the yeast 20 S proteasome in complex with inhibitor **15** to reveal the inhibition mechanism of the most potent inhibitor, **15**. This compound binds in a similar orientation to the active site threonine as observed for calpain inhibitor I (6). Defined electron density was found in all active sites, indicating that compound **15** lacks subunit specificity at the high concentrations employed (10 mM). The functional aldehyde of the inhibitor forms a covalent hemiacetal bond to the Thr-1Oγ. The peptide backbone of **15** adopts a β-conformation and fills the gap between β-strands and generates an anti-parallel β-sheet structure (Fig. 8). The leucine side chain projects into the S1 pocket, whereas the P2 side chain at P2 is not in contact with the protein. The leucine side chain at P3 closely interacts with the amino acids of the adjacent β-subunit. In general, both S1 and S3 specificity pockets play a prominent role in inhibitor binding as observed in the crystal structures of the 20 S proteasome in complex with lactacystin (6) and vinylsulfone (30). The neutral character of Met-45 in subunit β5 has a dominant role for the specificity of this subunit. The crystallographic data (Fig. 8) reveal that the P1-Leu side chain of **15** causes a structural rearrangement of Met-45. In contrast to the crystal structure of the 20 S proteasome in complex with lactacystin, Met-45 is rearranged by 3 Å, avoiding a clash with the leucine side chain in P1 of **15,** thereby making the S1 pocket more spacious. Remarkably, the hydrophobic interactions between the Leu residue of the inhibitor and Met-45 are only weak, thus reducing the mean residence time of the compound at the active center. The specificity defining pockets of subunits β1 and β2 have positive and negative charges, respectively, which destabilize the protein-ligand interactions. However, the inherent reactivity of the aldehyde in compound **15** causes binding to all proteolytically active sites. These observations indicate that the functional group of this inhibitor plays the dominant role in binding.

DISCUSSION

Proteasomes are involved in a number of different cellular processes. They are important for control of the cell cycle and protect cells from apoptosis by maintaining the balance of anti-apoptotic and pro-apoptotic proteins (9, 31, 32). The interest in potent and specific inhibitors that may be used as potential drugs against cancer or neoplastic growth is very high. Here we report the synthesis of inhibitors based on the proteasomal peptide inhibitor MG132, which is a potent yet nonspecific inhibitor. We assumed that side chain modifications of the tripeptide might offer higher potency, selectivity, and site-specific inhibition of the 20 S proteasome. This assumption is based on a couple of known and potent peptidic inhibitors (16, 17, 33, 35).

All novel compounds were tested for their inhibitory capacity in cell lysates. Therefore, serine proteases, cysteine proteases, and metalloproteases were blocked by the protease inhibitor mixture Complete (Roche Applied Science) during the assay with the synthesized mimetics. The proteolysis of the hydrophobic Suc-LLVY-AMC substrate was diminished by 11 of the investigated compounds in two assays. The specific inhibition of a single catalytic site is of special interest for drug development; therefore, we analyzed the inhibition of the different proteasomal activities. The different cleavage preferences of proteasomes were determined by specific substrates for the hydrophobic (chymotrypsin-like), trypsin-like, and post-acidic (caspase-like) activities on isolated proteasomes. 12 of 22 derivatives inhibited proteasomal activities with IC_{50} values below 10 μM. The peptidic aldehydes **13** and **15** inhibited all proteasomal hydrolytic activities, whereas four compounds (**18**, **24**, **25**, and **26**) inhibited the chymotryptic and caspase-like sites. However, the purpose of this investigation was the identification of fully selective inhibitors of proteasomal activity. The tripeptidic alcohol **7** (and with lower potency, **8**) specifically reduced the trypsin-like activity, and compounds **16**, **21**, **22**, and **28** resulted in an exclusive reduction of chymotryptic

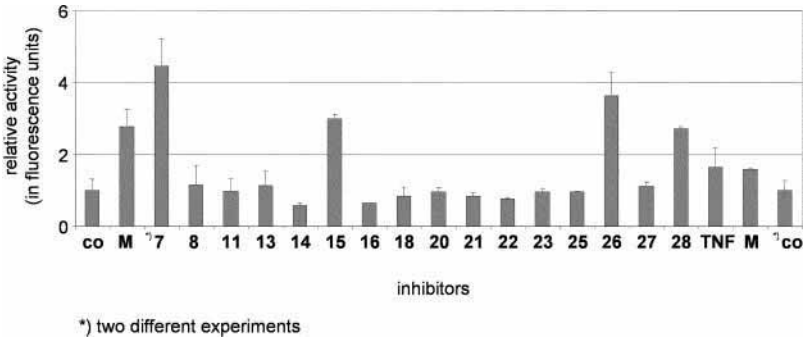

FIG. 7. **Proteasomal inhibition by 7, 15, 26, and 28 resulted in induction of apoptosis.** HeLa cells treated with 1 μM of the indicated inhibitors for 20 h were incubated with caspase substrates (Apo-One®; Promega) for 2 h. The activation of caspase 3/7 was measured at 538 nm (excitation, 485 nm). Treatment of cells with tumor necrosis factor α (*TNF*) or MG132 (*M*) served as positive controls; controls without treatment are indicated as *co*.

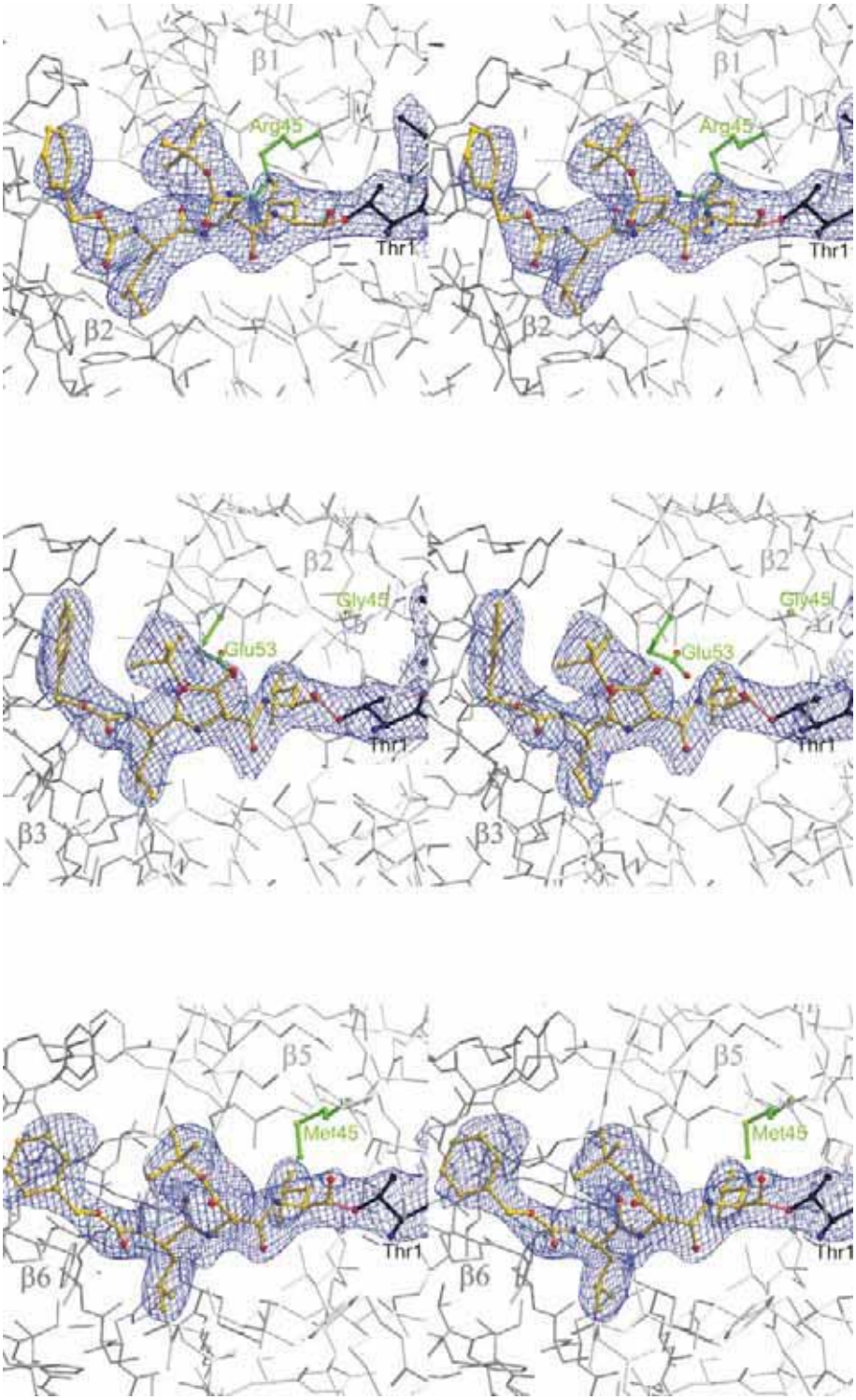

FIG. 8. **Stereoview of a 30 Å sector of the crystal structures of the (*top panel*) β1, (*middle panel*) β2, and (*bottom panel*) β5 active sites of the yeast 20 S proteasome in complex with the aldehyde 15. 15** is depicted in *yellow* and shown for each subunit with its unbiased electron density. The active site Thr-1 is highlighted in *black*, and the covalent bond between **15** and Thr-1Oγ is highlighted in *pink*. Residues that are particularly responsible for the character of the S1 subsite are drawn in *green*.

activity. Notably, the most potent of the new inhibitors feature IC_{50} values below 100 nM (**7**, **15**, and **28**). This is in the range of novel proteasomal inhibitors, which are in clinical trials (33).

Remarkably, the tetrapeptide inhibitor PSI (Z-IE(O^tBu)AL-CHO) is structurally related to our component **15** (Z-LD(O^t-Bu)L-CHO) (36), which is among the strongest inhibitors (IC_{50}, <60 nM). Moreover, it exhibited low toxicity and was able to permeate cellular membranes. The comparison of our inhibitors indicates the major contributions of the ligand side chains to the specific tight interactions with the various proteolytically active sites (Fig. 8). Similar observations were made for the alcohol derivates, with compound **7** being more effective than the other six compounds. Furthermore, very potent inhibitors were identified in the chloromethyl ketone (**22**) and in compounds **25–28**.

Tumor cells with their accelerated and neoplastic growth are often more sensitive to proteasomal inhibitors than normal cells. The clinically approved proteasomal inhibitor Bortezomib® causes growth arrest and apoptosis in the sensitive tumor cells, whereas "normal" cells tolerate higher inhibitor concentrations (37). The restriction to myeloma tumors may be overcome by more specific inhibitors, such as PSI, which blocks angiogenesis and modulates the growth of solid tumors (36). The differences in cellular features and the predictable resistance mechanisms require continuous development of new proteasomal inhibitors. Efficient cell permeation, stability in aquatic systems, and potent induction of cellular events are all mandatory for clinical applications. Therefore, we tested the permeation ability of our compounds and their *in vivo* impact on proteasomes, and we monitored the accumulation of polyubiquitinated proteins in cultured cells. A >50% reduction of cellular proteasome activity was observed for five of the new inhibitors (**15**, **22**, **25**, **26**, and **28**). The most potent inhibitions were achieved by compounds **15**, **26**, and **28**, which reduced the proteasome activity to 10% at a concentration of 1 μM. Even 50 nM solutions of compound **15** arrested 70% of the melanoma cells. Our results indicate potency, membrane permeation, and sufficient stability throughout the incubation period for the inhibitors **15**, **22**, **25**, **26**, and **28**. The cellular proteasomal activity was clearly reduced and accompanied by strong induction of apoptosis after 20 h treatment with 1 μM of inhibitors (**15**, **26**, and **28**). The prevalent enhanced sensitivity of tumor cells toward proteasomal inhibition was confirmed for inhibitor **15**. Compound **15** exerts its effects at considerably lower concentrations than MG132 and exhibits an almost identical inhibitory profile as Bortezomib®, which is characterized by a lower K_i value. The low toxicity of our new compounds and the effective proteasome inhibition encourage us to continue our evaluation of the lead compounds, **15**, **26**, and **28**.

Acknowledgment—We thank Dr. B. Dahlmann (Charité) for the gift of 26 S proteasome.

REFERENCES

1. Adams, J. (2004) *Proteasome Inhibitors in Cancer Therapy*, pp. 77–84, Humana Press Inc., Totowa, NJ
2. Glickman, M. H., and Ciechanover, A. (2002) *Physiol. Rev.* **82,** 373–428
3. Voges, D., Zwickl, P., and Baumeister, W. (1999) *Ann. Rev. Biochem.* **68,** 1015–1068
4. Peters, J. M., Cejka, Z., Harris, J. R., Kleinschmidt, J. A., and Baumeister, W. (1993) *J. Mol. Biol.* **234,** 932–937
5. Coux, O., Tanaka, K., and Goldberg, A. L. (1996) *Annu. Rev. Biochem.* **65,** 801–847
6. Groll, M., Ditzel, L., Loewe, J., Stock, D., Bochtler, M., Bartunik, H. D., and Huber, R. (1997) *Nature* **386,** 463–471
7. Baumeister, W., Walz, J., Zuhl, F., and Seemuller, E. (1998) *Cell* **92,** 367–380
8. Kloetzel, P.-M., and Ossendorp, F. (2004) *Curr. Opin. Immunol.* **16,** 76–81
9. Kloetzel, P. M. (2001) *Nat. Rev. Mol. Cell. Biol.* **2,** 179–187
10. Serwold, T., Gonzalez, F., Kim, J., Jacob, R., and Shastri, N. (2002) *Nature* **419,** 480–483
11. Seifert, U., Maranon, C., Shmueli, A., Desoutter, J.-F., Wesoloski, L., Janek, K., Henklein, P., Diescher, S., Andrieu, M., de la Salle, H., Weinschenk, T., Schild, H., Laderach, D., Galy, A., Haas, G., Kloetzel, P.-M., Reiss, Y., and Hosmalin, A. (2003) *Nat. Immunol.* **4,** 375–379
12. Golab, J., Bauer Thomas, M., Daniel, V., and Naujokat, C. (2004) *Clin. Chim. Acta* **340,** 27–40
13. An, B., Goldfarb, R. H., Siman, R., and Dou, Q. P. (1998) *Cell Death Differ.* **5,** 1062–1075
14. Orlowski, R. Z., Small, G. W., and Shi, Y. Y. (2002) *J. Biol. Chem.* **277,** 27864–27871
15. Orlowski, R. Z., Eswara, J. R., Lafond-Walker, A., Grever, M. R., Orlowski, M., and Dang, C. V. (1998) *Cancer Res.* **58,** 4342–4348
16. Kisselev, A. F., and Goldberg, A. L. (2001) *Chem. Biol.* **8,** 739–758
17. Groll, M., and Huber, R. (2004) *Biochim. Biophys. Acta* **1695,** 33–44
18. Cusack, J. C., Jr., Liu, R., Houston, M., Abendroth, K., Elliott, P. J., Adams, J., and Baldwin, A. S., Jr. (2001) *Cancer Res.* **61,** 3535–3540
19. Orlowski, R. Z., Stinchcombe, T. E., Mitchell, B. S., Shea, T. C., Baldwin, A. S., Stahl, S., Adams, J., Esseltine, D.-L., Elliott, P. J., Pien, C. S., Guerciolini, R., Anderson, J. K., Depcik-Smith, N. D., Bhagat, R., Lehman, M. J., Novick, S. C., O'Connor, O. A., and Soignet, S. L. (2002) *J. Clin. Oncol.* **20,** 4420–4427
20. Paramore, A., and Frantz, S. (2003) *Nat. Rev. Drug Discov.* **2,** 611–612
21. Myung, J., Kim, K. B., and Crews, C. M. (2001) *Med. Res. Rev.* **21,** 245–273
22. Schmidt, B. (2003) *Chembiochem.* **4,** 366–378
23. John, V., Beck, J. P., Bienkowski, M. J., Sinha, S., and Heinrikson, R. L. (2003) *J. Med. Chem.* **46,** 4625–4630
24. Leslie, A. G. W. (1994) *Mosflm User Guide, Mosflm Version 5.20*, MRC Laboratory of Molecular Biology, Cambrige, UK
25. Brünger, A. T. (1992) *X-PLOR, Version 3.1. A System for X-ray Crystallography and NMR*, Yale University Press, New Haven, CT
26. Turk, D. (1992) *Weiterentwicklung eines Programms für Molekülgraphik und Electronendichte-Manipulation und seine Anwendung auf verschiedene Protein-Strukturaufklärungen.* Ph.D. thesis, Technische Universität München, Munich
27. Engh, R., and Huber, R. (1991) *Acta Crystallogr.* **A47,** 392–400
28. Schmidt, B., Ehlert, D. K., and Braun, H. A. (2004) *Tetrahedron Lett.* **45,** 1751–1753
29. Guzmen, M. L., Swiderski, C. F., Howard, D. S., Grimes, B. A., Rossi, R. M., Szilvassy, S. J., and Jordan, C. T. (2002) *Proc. Natl. Acad. Sci. U. S. A.* **99,** 16220–16225
30. Groll, M., Nazif, T., Huber, R., and Bogyo, M. (2002) *Chem. Biol.* **9,** 655–662
31. Ling, Y. H., Liebes, L., Ng, B., Buckley, M., Elliott, P. J., Adams, J., Jiang, J. D., Muggia, F. M., and Perez-Soler, R. (2002) *Mol. Cancer Ther.* **1,** 841–849
32. Meiners, S., Heyken, D., Wellej, A., Ludwig, A., Stangl, K., Kloetzel, P.-M., and Krüger, E. (2003) *J. Biol. Chem.* **278,** 21517–21525
33. Adams, J. (2004) *Nat. Rev. Cancer* **4,** 349–360
34. Garcia-Echeverria, C., Imbach, P., France, D., Fürst, P., Lang, M., Noorani, A. M., Scholz, D., Zimmermann, J., and Furet, P. (2001) *Bioorg. Med. Chem. Lett.* **11,** 1317–1319
35. Traenker, E. B., Wilk, S., and Baeuerle, P. A. (1994) *EMBO J.* **13,** 5433–5441
36. Stoklosa, T., Golab, J., Wojcik, C., Wlodarski, P., Jalili, A., Januszko, P., Giermasz, A., Wilczynski, G. M., Pleban, E., Marczak, M., Wilk, S., and Jakobisiak, M. (2004) *Apoptosis* **9,** 193–204
37. Hideshima, T., Richardson, P., Chauhan, D., Palombella, V. J., Elliott, P. J., Adams, J., and Anderson, K. C. (2001) *Cancer Res.* **61,** 3071–3076

Syntheses of Peptidomimetics

Chemistry. General Comments. The 1H- and 13CNMR spectra were recorded on a Bruker AC 300 spectrometer at 300 (75). Chemical shifts are reported as ‰ values (ppm) downfield from Me_4Si. Mass spectrometry was performed on a Bruker-Franzen Esquire LC mass spectrometer. Flash column chromatography was carried out using Merck silica gel 60 (40-63 and 15-40 μm) and 60G (5-40 μm). Thin-layer chromatography (TLC) was carried out using aluminum sheets precoated with silica gel 60 F254 (0.2 mm; E. Merck). Chromatographic spots were visualized by UV and/or spraying with an acidic, ethanolic solution of p-anisaldehyde or an ethanolic solution of ninhydrin followed by heating. For preparative TLC, plates precoated with silica gel 60 F254 (2.0 mm; E. Merck) were used. Amino acid derivatives were bought from Fluka Chemie (Switzerland), NovaBiochem (Switzerland), or Bachem (Switzerland). THF was dried and distilled from sodium and benzophenone. DMF was stored over 3 Å molecular sieves. All other commercial chemicals were used without further purification.

7 (BSc 2114). Ethyl-3-(3′-dimethylaminopropyl)carbodiimide hydrochloride (EDAC, 191 mg, 1.0 mmol) and *N*-hydroxybenzotriazole hydrate (HOBt, 183 mg, 1.2 mmol) were added to a solution of Z-Asp(O*t*Bu)-OH (**29,** 323 mg, 1.0 mmol) dissolved in CH_2Cl_2 (10 mL). The resulting mixture was stirred at ambient temperature for 5 min, then treated with *L*-leucinol (117 mg, 1.0 mmol) and triethylamine (151 mg, 1.5 mmol) for 24 h. CH_2Cl_2 (20 mL) was added and the solution was washed with HCl (0.1 N, 5 x 30 mL), NaOH (0.1 N, 3 x 30 mL), brine (1 x 30 mL), dried over Na_2SO_4, and concentrated to obtain the product **31** (350 mg, 83%). A solution of **31** (422 mg, 0.8 mmol) in ethanol (10 mL, abs.) was treated with palladium on activated carbon (100 mg) under hydrogen atmosphere at room temperature. The suspension was filtered after 3 h and the solvent was removed *in vacuo* to yield **33** (228 mg, 100%). EDAC (157 mg, 0.82 mmol) and HOBt (132 mg, 0.98 mmol) were added to the solution of Boc-Leu-OH (189 mg, 0.82 mmol) in CH_2Cl_2 (10 mL). The resulting mixture was stirred at ambient temperature for 5 min, then treated with **33** (228 mg, 0.82 mmol) and

triethylamine (124 mg, 1.23 mmol) for 24 h. DCM (20 mL) was added and the solution was washed with HCl (0.1 N, 5 x 30 mL), NaOH (0.1 N, 3 x 30 mL), and brine (1 x 30 mL). The solvent was removed after drying (Na_2SO_4) *in vacuo* to yield (400 mg, 97%) **7** (BSc2114). **^{1}H-NMR** ($CDCl_3$, 300 MHz): δ = 7.65 (d, 1H, ^3J = 8.3 Hz), 6.8 (d, 1H, ^3J = 8.3 Hz), 5.03 (d, 1H, ^3J = 8.3 Hz), 4.55-4.45 (m, 1H), 3.99-3.89 (m, 2H), 3.57 (dd, 1H, ^3J = 3.3 Hz, ^2J = 11.0 Hz), 3.47 (dd, 1H, ^3J = 3.3 Hz, ^2J = 11.0 Hz), 2.99 (d, 1H, ^3J = 4.3 Hz), 2.58 (d, 1H, ^3J = 4.3 Hz), 2.48 (d, 1H, ^3J = 4.3 Hz), 2.15-2.14 (m, 2H), 1.44 (s, 9H), 1.34 (s, 9H), 0.90-0.87 (m, 6H), 0.80-0.75 (m, 6H) ppm. **^{13}C-NMR** ($CDCl_3$, 75 MHz): δ = 173.0, 171.5, 170.5, 156.3, 81.9, 81.0, 65.6, 54.3, 50.6, 50.5, 40.8, 39.7, 35.9, 28.4, 28.0, 24.9, 23.2, 22.2, 21.6, 21.1 ppm. **MS** (EI): *m/z* = 501 (M^+).

13 (BSc2115). Compound **7** (BSc2114) (400mg, 0.8 mmol) was oxidized with IBX (2-oodoxybenzoic acid, 268 mg, 0.95 mmol) in DMSO (5 mL) at room temperature for 6 h. CH_2Cl_2 (30 mL) was added and the solution was washed with water (3 x 30mL), $NaHCO_3$ solution (3 x 30 mL, sat.), and brine (1 x 30 mL). The solvent was removed after drying (Na_2SO_4) under vacuum to yield **13 (**BSc2115) (390 mg, 98%). **^{1}H-NMR** ($CDCl_3$, 300 MHz): δ = 9.4 (s, 1H), 7.54 (d, 1H, ^3J = 8.3 Hz), 7.27 (d, 1H, ^3J = 8.3 Hz), 4.89 (d, 1H, ^3J = 8.3 Hz), 4.66-4.56 (m, 2H), 4.22-4.15 (m, 2H), 3.99 (dd, 1H, ^3J = 3.3 Hz, ^2J = 11.0 Hz), 2.99 (dd, 1H, ^3J = 3.3 Hz, ^2J = 11.0 Hz), 2.90 (d, 1H, ^3J = 4.3 Hz), 2.58 (d, 1H, ^3J = 4.3 Hz), 2.48 (d, 1H, ^3J = 4.3 Hz), 1.66-1.55 (m, 1H),1.47-1.45 (m, 1H), 1.44 (s, 9H), 1.34 (s, 9H), 0.9-0.86 (m, 6H,), 0.80-0.76 (m, 6H) ppm. **^{13}C-NMR** ($CDCl_3$, 75 MHz): δ = 200.1, 172.6, 171.6, 170.9, 156.2, 82.0, 80.8, 54.3, 50.6, 50.5, 40.8, 39.7, 35.9, 28.4, 28.0, 24.9, 23.2, 22.2, 21.6, 21.1 ppm. **MS** (EI): *m/z* = 499 (M^+).

14 (BSc2128). TFA (1 mL) was added to the stirred solution of **7** (BSc2114. 390 mg, 0.78 mmol) in CH_2Cl_2 (4 mL). The solvent was evaporated after 3h (260 mg, 97%) to obtain **14** (BSc2128). **^{1}H-NMR** (DMSO-d_6, 300 MHz): δ = 9.37 (s, 1H), 8.85 (d, 1H, ^3J = 8.3 Hz), 8.19 (d, 1H, ^3J = 8.3 Hz), 4.67-4.56 (m, 1H), 4.05-3.89 (m, 2H), 3.77-3.65 (m, 2H), 3.70-3.67 (m, 1H), 2.89 (dd, 1H, ^3J = 4.1 Hz, ^2J = 16.0 Hz), 2.78 (d, 1H, ^3J = 4.1 Hz, ^2J = 16.0 Hz), 2.58 (d, 1H, ^3J = 4.1 Hz), 2.48 (d, 1H, , ^3J = 4.1 Hz), 1.60-1.58 (m, 1H), 1.46-1.44 (m, 1H), 0.80-0.76 (m, 6H), 0.70-0.66 (m, 6H) ppm. **^{13}C-NMR** (DMSO-d_6, 75 MHz): δ = 200.1, 171.1, 171.0,

169.9, 55.2, 53.8, 50.4, 40.8, 39.7, 35.9, 23.2, 22.2, 21.6, 21.1 ppm . **MS** (ESI): *m/z* = 343.4 (M^+).

Compounds **16** BSc2129, **9** BSc2207, **17** BSc2208, **18** BSc2197, and **12** BSc2194 were generated by analogue procedures.

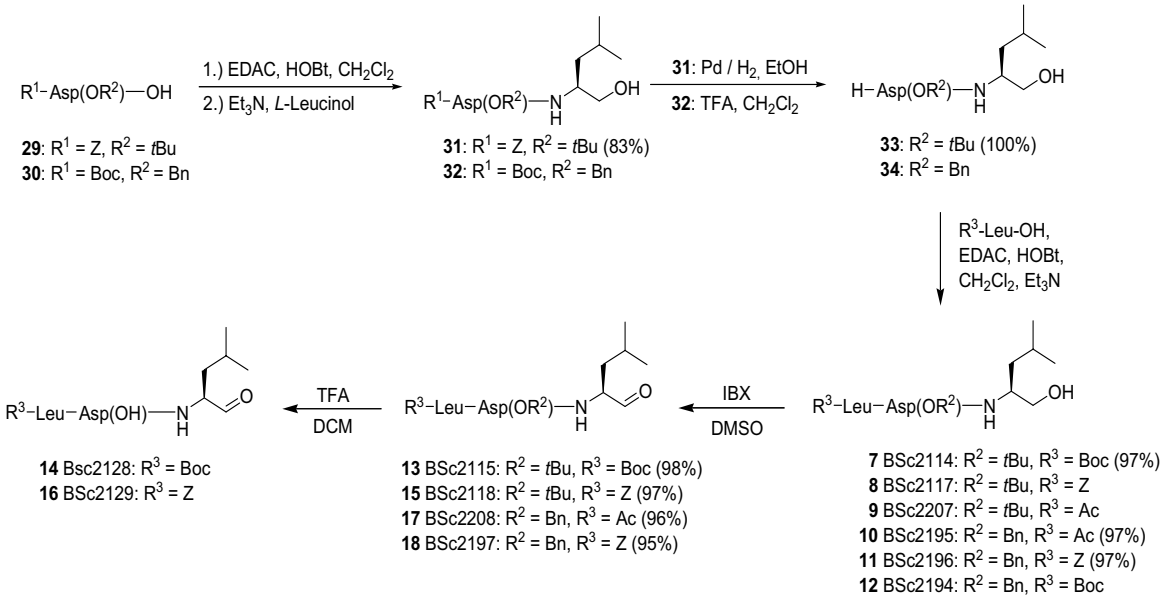

Scheme 1 Synthesis of tripeptide mimetics

8 (BSc2117). The title compound was prepared from **33** according to the same procedure in 80% yield. **^{1}H-NMR** ($CDCl_3$, 300 MHz): δ=7.51 (d, 1H, ^3J = 8.3 Hz),7.29-7.19 (m, 5H), 6.70 (d, 1H, ^3J = 8.3 Hz), 5.35 (d, 1H, ^3J = 8.3 Hz), 5.50 (s, 2H), 4.60-4.58 (m, 1H), 4.10-4.75 (m, 1H), 3.95-3.87 (m, 1H), 3.58 (dd, 1H, ^3J = 3.3 Hz, ^2J = 11.0 Hz), 3.45 (dd, 1H, ^3J = 3.3 Hz, ^2J = 11.0 Hz), 2.89 (dd, 1H, ^3J = 4.1 Hz, ^2J = 16.0 Hz), 2.80 (d, 1H, ^3J = 4.1 Hz, ^2J = 16.0 Hz), 2.59 (d, 1H, ^3J = 4.3 Hz,), 2.50 (d, 1H, ^3J = 4.3 Hz,), 2.0-1.96 (m, 2H), 1.55-1.53 (m, 1H), 1.34 (s, 9H), 1.25-1.23 (m, 1H), 0.89 (dd, 6H, ^3J = 4.3 Hz, ^3J = 7.0 Hz), 0.80 (dd, 6H, ^3J = 4.3 Hz, ^3J = 7.0 Hz) ppm. **^{13}C-NMR** ($CDCl_3$, 75 MHz): δ =167.0, 166.2, 165.1, 151.4, 130.4, 123.3, 123.1, 123.1, 122.8, 77.1, 62.2, 60.2, 49.0, 45.8, 45.2, 35.6, 34.4, 31.1, 22.7, 22.7, 22.7, 21.6, 21.1, 19.5, 17.8 ppm. **MS** (EI): *m/z* = 535(M^+).

15 (BSc2118). The title compound was prepared from **8** (BSc2117) according to the same procedure in 94% yield. **^{1}H-NMR** ($CDCl_3$, 300 MHz): δ = 9.49 (s, 1H), 7.48 (d, 1H, ^3J = 8.3 Hz), 7.35-7.33 (m, 5H), 7.25 (d, 1H, ^3J = 7.3 Hz), 5.23-5.22 (m, 1H), 5.12 (s, 2H), 4.80-4.79 (m, 1H), 4.38-4.37 (m, 1H), 4.15-4.14 (m, 1H), 3.00 (d, 1H, ^3J = 3.3 Hz), 2.98 (d, 1H, ^3J = 3.3

Hz), 2.60 (d, 1H, ^{3}J = 6.3 Hz), 2.55 (d, 1H, ^{3}J = 6.3 Hz), 2.30-2.28 (m, 1H), 2.23-2.22 (m, 1H), 2.05-1.99 (m, 2H), 1.77-1.76 (m, 1H), 1.44 (s, 9H), 1.35-1.34 (m, 1H), 0.89-0.86 (m, 6H), 0.80-0.78 (m, 6H) ppm. **^{13}C-NMR** ($CDCl_3$, 75 MHz): δ=200, 172.1, 171.6, 170.8, 67.4, 156.6 , 135.9, 128.7, 128.4, 128.1, 122.8, 82.1, 57.5, 54.5, 49.8, 45.8, 45.2, 41.1, 37.4, 36.5, 28.0, 28.0, 28.0, 24.5, 23.3, 23.0, 21.7 ppm. **MS** (ESI): *m/z* = 533 (M^+).

16 (BSc2129). The title compound was prepared from **15** (BSc2118) according to the same procedure in 84% yield. **^{1}H-NMR** (DMSO-d_6, 300 MHz): δ = 9.8 (s, 1H), 9.37 (s, 1H), 8.30 (d, 1H, ^{3}J = 8.3 Hz), 8.24 (d, 1H, ^{3}J = 7.3 Hz), 7.36-7.34 (m, 5H), 5.22-5.21 (m, 1H), 5.12 (s, 2H), 4.80-4.79 (m, 1H), 4.5-4.45 (m, 1H), 4.15-4.10 (m, 1H), 3.30-3.29 (m, 1H), 2.98-2.97 (m, 1H), 2.60-2.59 (m, 1H), 2.55-2.54 (m, 1H), 2.30-2.29 (m, 1H), 2.23-2.22 (m, 1H), 2.05-1.99 (m, 2H), 1.77-1.76 (m, 1H), 1.35-1.34 (m, 1H), 0.89-0.88 (m, 6H), 0.80-0.79 (m, 6H) ppm. **^{13}C-NMR** (DMSO-d_6, 75 MHz): δ=200, 172.1, 171.6, 170.8, 67.4, 156.6, 135.9, 128.7, 128.4, 128.1, 122.8, 82.1, 57.5, 54.5, 49.8, 45.8, 45.2, 41.1, 37.4, 36.5, 24.5, 23.3, 23.0 , 21.7 ppm. **MS** (ESI): *m/z* = 476 (M^+).

9 (BSc2207). The title compound was prepared from **33** according to the same procedure in 93% yield. **^{1}H-NMR** ($CDCl_3$, 300 MHz): δ=7.67 (d, 1H, ^{3}J = 8.3 Hz), 7.4 (d, 1H, ^{3}J = 9.2 Hz), 7.26 (d, 1H, ^{3}J = 8.4 Hz), 4.7-4.63 (m, 2H), 4.43-4.33 (m, 2H), 4.04-3.94 (m, 2H), 3.59-3.54 (m, 1H), 3.53-3.43 (m, 1H), 3.30 (dd, 1H, ^{3}J = 4.8 Hz, ^{2}J = 17.0 Hz), 2.8 (dd, 1H, ^{3}J = 4.8 Hz, ^{2}J = 17.0 Hz), 2.65-2.55 (m, 1H), 2.54-2.45 (m, 1H), 2.15-2.05 (m, 2H), 2.0 (d, 3H, ^{3}J = 15.0 Hz), 1.44 (s, 9H), 0.9-0.87 (m, 6H), 0.80-0.78 (m, 6H) ppm. **^{13}C-NMR** ($CDCl_3$, 75 MHz): δ = 172.5, 172.3, 171.6, 169.9, 82.0, 66.6, 53.4, 50.4, 49.5, 40.8, 39.7, 35.9, 28.4, 25.0, 24.7, 22.9, 23.2, 22.1 ppm. **MS** (EI): *m/z* = 443 (M^+).

10 (BSc2195). The title compound was prepared from **34** according to the same procedure in 88 % yield. **^{1}H-NMR** ($CDCl_3$, 300 MHz): δ = 8.26 (d, 1H, ^{3}J = 7.2 Hz), 7.59 (m, 5H, ArH), 6.70 (d, 1H, ^{3}J = 7.3 Hz), 6.35 (d, 1H, ^{3}J = 7.0 Hz), 5.20 (s, 2H), 4.62-4.48 (m, 1H), 4.44-4.42 (m, 1H), 4.01-4.00 (m, 1H), 3.98-3.97 (m, 1H), 3.91-3.90 (m, 1H), 2.89-2.88 (dm, 1H), 2.80-2.78 (m, 1H), 2.59-2.58 (m, 1H), 2.50-2.49 (m, 1H), 2.0-1.99 (m, 2H), 1.55-1.54 (m, 1H), 1.34 (s, 3H), 1.25-1.24 (m, 1H), 0.89 (dd, 6H, ^{3}J = 3.8 Hz, 6.7 Hz), 0.80 (dd, 6H, ^{3}J = 3.8 Hz, 6.7 Hz) ppm. **^{13}C-NMR** ($CDCl_3$, 75 MHz): δ = 175.5, 173.7, 173.0, 169.7, 128.8, 128.3, 68.5,

66.5, 41.4, 40.8, 40.2, 35.6, 34.4, 31.1, 23.5, 22.1, 23.9, 23.6, 22.9 ppm. **MS** (EI): *m/z* = 477 (M^+).

17 (BSc2208). The title compound was prepared from **10** (BSc2195) according to the same procedure in 74% yield. **^{1}H-NMR** ($CDCl_3$, 300 MHz): δ = 9.40 (s, 1H), 8.26 (d, 1H, ^3J = 7.0 Hz), 7.28-7.19 (m, 5H), 6.70 (d, 1H, ^3J = 7.0 Hz), 5.65 (d, 1H, ^3J = 7.0 Hz), 5.30 (s, 2H), 4.82-4.81 (m, 1H), 4.35-4.33 (m, 1H), 3.96-3.95 (m, 1H), 2.80-2.79 (m, 1H), 2.75-2.74 (m, 1H), 2.49-2.48 (m, 1H), 2.45-2.44 (m, 1H), 2.0-1.98 (m, 2H), 1.51-1.50 (m, 1H), 1.30 (s, 3H), 1.25-1.24 (m, 1H), 0.89 (dd, 6H, ^3J = 3.8 Hz, 6.4 Hz), 0.80 (dd, 6H, ^3J = 3.8 Hz, 6.4 Hz) ppm. **^{13}C-NMR** ($CDCl_3$, 75 MHz): δ = 200, 174.5, 173.5, 173.0, 166.7, 128.6, 128.3, 68.5, 41.4, 40.8, 40.2, 35.6, 34.4, 31.1, 23.5, 22.1, 23.9, 23.6, 22.9. **MS** (EI): *m/z* = 475 (M^+).

11 (BSc2196). The title compound was prepared from **34** according to the same procedure in 77 % yield. **^{1}H-NMR** ($CDCl_3$, 300 MHz): δ = 7.29-7.19 (m, 10H), 6.65 (d, 1H, ^3J = 7.0 Hz), 6.33 (d, 1H, ^3J = 7.0 Hz), 5.35 (d, 1H, ^3J = 7.0 Hz), 5.28-5.17 (m, 4H), 4.22-4.21 (m, 1H), 4.0-3.99 (m, 1H), 3.74-3.73 (m, 1H), 3.66-3.65 (m, 1H), 3.22-3.21 (m, 1H), 2.99-2.98 (m, 1H), 2.92-2.91 (m, 1H), 2.62-2.60 (d, 1H), 2.50-2.51 (d, 1H,), 2.4-2.3 (m, 2H), 1.57-1.56 (m, 1H), 1.24-1.23 (m, 1H), 0.87 (dd, 6H, ^3J = 3.8 Hz, 6.4 Hz), 0.80 (dd, 6H, ^3J = 3.8 Hz, 6.4 Hz) ppm. **^{13}C-NMR** ($CDCl_3$, 75 MHz): δ = 172.4, 172.0, 170.2, 156.8, 142.8, 135.8, 128.7, 68.5, 67.2, 62.2, 52.0, 49.8, 49.2, 41.6, 40.4, 33.1, 22.4, 22.1, 21.6, 21.1, 19.5, 18.3 ppm. **MS** (EI): *m/z* = 569 (M^+).

18 (BSc2197). The title compound was prepared from **11** (BSc2196) according to the same procedure in 74% yield. **^{1}H-NMR** ($CDCl_3$, 300 MHz): δ = 9.33 (s, 1H), 7.26-7.19 (m, 10H), 7.03 (d, 1H, ^3J = 7.0 Hz), 6.41 (d, 1H, ^3J = 7.0 Hz), 5.66 (d, 1H, ^3J = 7.0 Hz), 5.23-4.95 (m, 4H), 4.26-4.13 (m, 1H), 4.12-4.03 (m, 1H), 3.57-3.54 (m, 1H), 2.94 (d, 1H, ^3J = 7.3 Hz), 2.72 (d, 1H, ^3J = 7.3 Hz), 2.02 (d, 1H, ^3J = 10.0 Hz), 1.99 (d, 1H, ^3J = 10.0 Hz), 1.57-1.44 (m, 2H), 1.45-1.42 (m, 1H), 1.24-1.99 (m, 1H), 0.87 (dd, 6H, ^3J = 3.8 Hz, 6.4 Hz), 0.80 (dd, 6H, ^3J = 3.8 Hz, 6.4 Hz) ppm. **^{13}C-NMR** ($CDCl_3$, 75 MHz): δ = 200, 173.4, 172.6, 171.2, 156.8, 142.8, 138.8, 128.7, 128.7, 66.5, 65.2, 52.0, 49.7, 48.2, 41.7, 40.6, 33.5, 22.6, 22.3, 21.9, 21.5, 19.4, 18.0 ppm. **MS** (ESI): *m/z* = 567 (M^+).

12 (BSc2194). The title compound was prepared from **34** according to the same procedure in 90 % yield. **^{1}H-NMR** ($CDCl_3$, 300 MHz): δ = 7.32-7.28 (m, 5H), 7.01 (d, 1H, ^3J = 7.0 Hz),

6.33 (d, 1H, ^3J = 7.0 Hz), 5.32 (s, 2H), 4.91 (d, 1H, ^3J = 7.0 Hz), 4.25-4.22 (m, 1H), 4.08-4.06 (m, 1H), 3.98-3.97 (m, 1H), 3.68-3.65 (dd, 2H), 2.99-2.97 (m, 1H), 2.92 (d, 1H, ^3J = 7.3 Hz), 2.59 (d, 1H, ^3J = 7.3 Hz), 2.50 (d, 1H, ^3J = 7.3 Hz), 1.97-1.87 (m, 2H), 1.55-1.54 (m, 1H), 1.34 (s, 9H), 1.24.1.23 (m, 1H), 0.89 (dd, 6H, ^3J = 3.8 Hz, 6.4 Hz), 0.80 (dd, 6H, ^3J = 3.8 Hz, 6.4 Hz) ppm. **^{13}C-NMR** ($CDCl_3$, 75 MHz): δ = 172.8, 172.4, 170.1, 155.8, 135.4, 128.6, 77.1 , 76.6, 67.2, 62.2, 49.0, 45.8, 45.2, 35.6, 34.4, 33.1, 23.7, 22.4, 22.1, 21.6, 21.1, 19.5, 18.3 ppm. **MS** (EI): *m/z* = 535 (M^+).

19 (BSc2158). A suspension of NaH in mineral oil (60%, 291 mg, 7.3 mmol) in THF (2 mL, abs.) was treated with (*S*)-(-)-phenylglycinol (500 mg, 3.6 mmol) at -15°C under argon atmosphere and stirred for 20 min. The mixture was cooled to -55°C prior to the addition of trichloroethylene (400 µl, 4.5 mmol) in THF (2 mL). The mixture was warmed to ambient temperature within 5 h, quenched with water (40 mL) and extracted with Et_2O (60 mL). The organic layer was separated, washed with brine (40 mL), dried (Na_2SO_4), and concentrated. The crude oil was purified by LC to give dichlorovinyl ether **35** (347 mg, 56%).
To a mixture of Z-Leu-Leu-OH (378 mg, 1.0 mmol), EDAC (192 mg, 1.0 mmol) and HOBt (170 mg, 1.1 mmol) DMF (2 mL) was added. The resulting solution was stirred vigorously for 10 min, then dichlorovinyl ether **35** (200 mg, 1.2 mmol) and Et_3N (0.28 mL, 2.0 mmol) were added. The solution was stirred for 2 h. DCM (40 mL) was added and washed with hydrochloric acid (0.1 N, 3 x 30 mL), aqueous $NaHCO_3$ (sat., 3 x 30 mL), and water (3 x 30 mL). The organic layer was dried (Na_2SO_4) and the solvent removed under vacuum to yield **19** (BSc2158) (403 mg, 77%). **^{1}H-NMR** (DMSO-d_6, 300 MHz): δ = 8.52 (d, 1H, ^3J = 8.3 Hz), 8.33 (d, 1H, ^3J = 8.3 Hz), 7.44 (d, 1H, ^3J = 8.2 Hz, NH-Leu1), 7.40-7.28 (m, 10H), 6.07 (s, 1H), 5.19-5.12 (m, 1H), 5.00 (s, 2H), 4.45-4.40 (m, 1H), 4.22-4.11 (m, 2H), 4.08-4.01 (m, 1H), 1.65-1.35 (m, 6H), 0.90-0.78 (m, 12H) ppm. **^{13}C-NMR** (DMSO-d_6, 75 MHz): δ = 172.0, 171.5, 155.8, 142.2, 138.4, 136.9, 128.2, 127.7, 127.6, 127.4, 127.5, 126.9, 97.7, 73.0, 65.2, 53.0, 51.4, 50.8, 40.8, 40.6, 24.1, 24.0, 22.6, 21.9, 21.6, 21.3 ppm. **MS** (EI): *m/z* = 480 (Z-Leu-Leu-$C_8H_9^+$), 371 (CO-Leu-$C_{10}H_{10}Cl_2NO^+$).

20 (BSc2166). Dichlorovinyl ether **36** (178 mg, 25%) was synthesized from (*S*)-(-)-leucinol (400 mg, 3.4 mmol) according to the synthesis of dichlorovinyl ether **35**. The reaction was started at -70°C, warmed to ambient temperature over night, then stirred for another 60 h.

Coupling of **36** (100 mg, 0.47 mmol) with Z-Leu-Leu-OH (100 mg, 0.47 mmol) afforded product **20** (BSc2166) (143 mg, 63%). **^{1}H-NMR** (DMSO-d_6, 300 MHz): δ = 7.92 (d, 1H, ^3J = 5.1 Hz), 7.70 (d, 1H, ^3J = 5.1 Hz), 7.48 (d, 1H, ^3J = 4.2 Hz), 7.40-7.31 (m, 5H), 6.05 (s, 1H), 5.05 (s, 2H), 4.33-4.29 (m, 1H), 4.08-4.03 (m, 2H), 3.87-3.85 (m, 2H), 1.60-1.41 (m, 9H,) 0.90-0.88 (m, 18H) ppm. **^{13}C-NMR** (DMSO-d_6, 75 MHz): δ = 171.9, 171.5, 155.8, 142.9, 137.0 128.2, 127.7, 127.5, 97.9, 73.3, 65.3, 53.1, 50.9, 45.7, 40.9, 40.0, 39.8, 24.11, 24.08, 23.85, 23.16, 22.92, 22.87, 21.80, 21.50, 21.5 ppm. **MS** (EI): *m/z* = 460 (Z-Leu-Leu-$C_6H_{14}N^+$), 295 (CO-Leu-$C_4H_6Cl_2NO^+$).

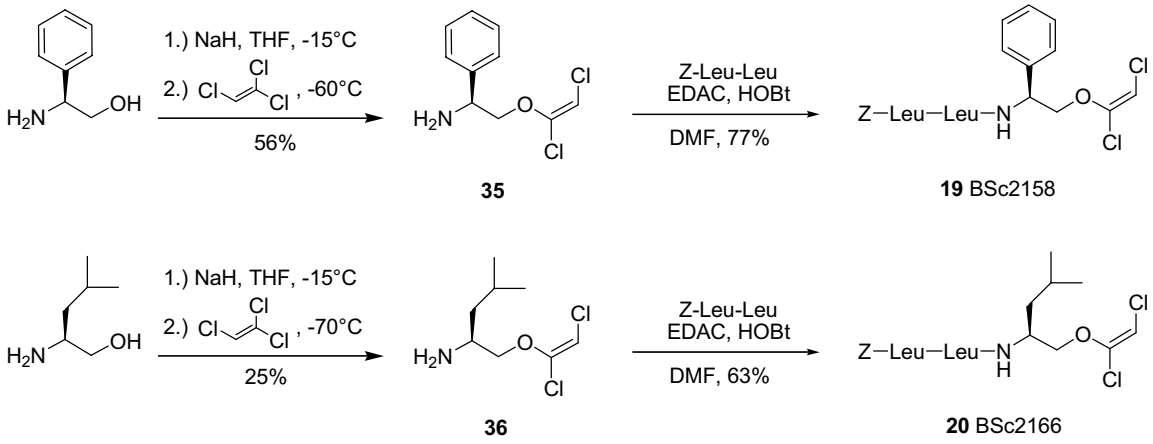

Scheme 2 Synthesis of dichlorovinyl ethers 19 (BSc2158) and 20 (BSc2166)

21 (BSc2167). An oven dried round bottom flask was charged with $Zn(OTf)_2$ (168 mg, 0.45 mmol) and (-)-ephedrine (84 mg, 0.50 mmol) under argon atmosphere. Et_3N (51 mg, 70 µL, 0.50 mmol) was added in dry toluene (2 mL) and stirred at room temperature for 2 h. **3** (MG132) (200 mg, 0.42 mmol) and phenylacetylene (52 mg, 56 µL, 0.50 mmol) were added after further 15 min and stirred at 60°C for 20 h. CH_2Cl_2 (40 mL) and an aqueous KH_2PO_4/Na_2HPO_4-buffer (30 mL, pH = 5.5) were added, the organic layer was separated and the aqueous phase extracted with CH_2Cl_2 (2 x 30 mL). The combined organic layers were dried (Na_2SO_4) and the solvent removed *in vacuo*. The crude product was purified by LC to yield **21** (BSc2167) (260 mg, 54%). **^{1}H-NMR** (DMSO-d_6, 300 MHz): δ = 8.46-8.37 (m, 1H), 7.50-7.47 (m, 1H), 7.43-7.19 (m, 10H), 5.20-5.11 (m, 1H), 5.00-4.95 (m, 2H), 4.57-4.49 (m,

2H), 4.13-4.03 (m, 2H), 1.80-1.24 (m, 9H), 0.90-0.53 (m, 18H) ppm. **^{13}C-NMR** (DMSO-d_6, 75 MHz): δ = 174.2, 174.7, 156.9, 139.5, 131.2, 127.9, 127.8, 127.6, 127.3, 126.5, 126.3, 98.1, 80.0, 63.1, 62.8, 54.5, 52.9, 46.8, 40.9, 40.3, 36.9, 24.7, 24.2, 24.0, 23.2, 23.1, 22.9, 21.4, 21.2, 20.7 ppm. **MS** (EI) *m/z* = 446 (Z-Leu-Leu-$C_5H_{11}^+$), 257 (CO-Leu-$C_6H_{13}O^+$).

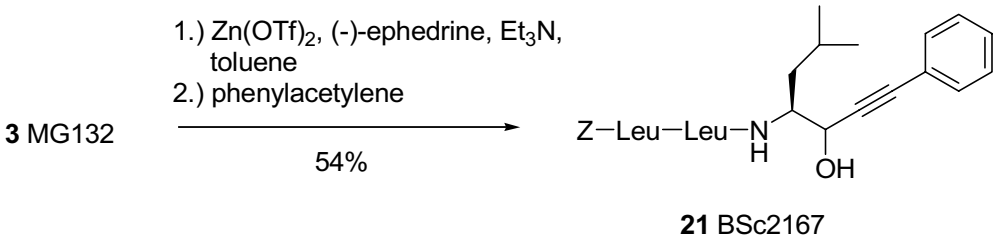

21 BSc2167

Scheme 3 Addition of phenylacetylene to aldehyde 3 (MG132)

22 (BSc2160). Z-Leu-Leu-OH (151 mg, 0.4 mmol) and (*S*)-3-amino-1-chloro-5-methylhexan-2-one (80 mg, 0.4 mmol) were coupled as described for **19** (BSc2158). The crude product was purified by LC to give **22** (BSc2160) (32 mg, 16%). **^{1}H-NMR** ($CDCl_3$, 300 MHz): δ = 7.35-7.19 (m, 5H), 6.81-6.73 (m, 1H), 6.41-6.32 (m, 1H), 5.16 (d, 1H, ^3J = 5.1 Hz), 5.03 (s, 2H), 4.64-4.61 (m, 1H), 4.35-4.06 (m, 3H), 1.87-1.40 (m, 9H), 0.92-0.73 (m, 18H) ppm. **^{13}C-NMR** ($CDCl_3$, 75 MHz): δ = 201.4, 172.7, 172.3, 156.6, 136.2, 128.6, 128.3, 128.0, 67.2, 55.0, 53.8, 51.8, 47.1, 41.4, 40.6, 39.6, 24.9, 24.8, 23.3, 22.9, 22.7, 22.6, 22.3, 22.2, 21.5 ppm. **MS** (EI): *m/z* = 488 (Z-Leu-Leu-Leu-CH_2^+), 432 (OCO-Leu-Leu-Leu-CH_2Cl^+).

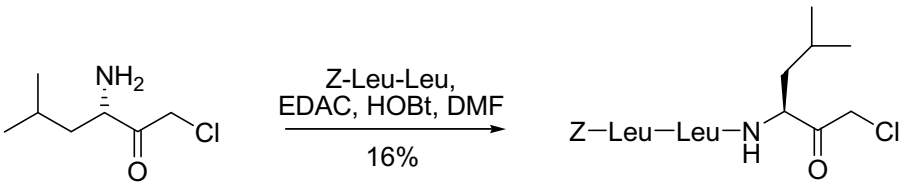

22 BSc2160

Scheme 4 Synthesis of α-chloromethyl ketone 22 (BSc2160)

23 (BSc2159). 3 (MG132) (300 mg, 0.63 mmol), benzyl isonitrile (116 µl, 0.95 mmol), and pyridine (204 µl, 2.53 mmol) were dissolved in CH_2Cl_2 (2.0 mL) and cooled to -10°C. Trifluoroacetic acid (97 µL, 1.26 mmol) was added dropwise (T < 0°C) under argon

atmosphere over 15 min. Cooling was maintained for 2 h, followed by additional 72 h at room temperature. CH_2Cl_2 (50 mL) was added and washed with hydrochloric acid (0.1 N, 3 x 30 ml), aqueous $NaHCO_3$ (sat., 3 x 30 mL) and brine (3 x 40 ml). The organic phase was dried (Na_2SO_4) and purified by LC to give **23** (BSc2159) (191 mg, 50%). **^{1}H-NMR** ($CDCl_3$, 300 MHz): δ = 7.51-7.27 (s, 1H), 7.26-7.14 (m, 10H), 6.91-6.80 (m, 1H) 5.82-5.63 (m, 2H), 5.02-4.90 (m, 2H), 4.35 (d, 1H, ^3J = 10.7 Hz), 4.30-4.01 (m, 5H), 1.55-1.31 (m, 9H), 0.81-0.73 (m, 18H) ppm. **^{13}C-NMR** ($CDCl_3$, 75 MHz): δ = 173.3, 172.7, 172.6, 157.5, 138.0, 136.2, 128.9, 128.8, 128.6, 128.1, 127.9, 127.8, 73.5, 67.3, 53.9, 52.0, 51.7, 43.2, 42.4, 41.6, 25.0, 24.8, 23.3, 23.0, 22.1, 22.0, 21.6 ppm. **MS** (EI): m/z = 610 (M^+).

24 (BSc2185). **3** MG132 (145 mg, 0.3 mmol) and 3-picolyl isonitrile (52 mg, 0.45 mmol) were converted into α-hydroxyl amide **24** (BSc2185) according to the preparation of **23** (BSc2159). Purification by LC resulted **24** (BSc2185) (103 mg, 56%). **^{1}H-NMR** ($CDCl_3$, 300 MHz): δ = 8.62-8.36 (m, 2H), 7.71-7.50 (m, 2H), 7.28-7.20 (m, 6H), 7.05-6.96 (m, 1H) 5.92-5.57 (m, 2H), 5.00 (s, 2H), 4.72-4.56 (m, 1H), 4.46-4.10 (m, 5H), 1.79 (s, 1H), 1.62-1.18 (m, 9H), 0.92-0.73 (m, 18H) ppm. **^{13}C-NMR** (DMSO-d_6, 75 MHz): δ = 172.4, 171.9, 171.2, 155.8, 148.9, 147.9, 137.0, 135.2, 135.0, 128.2, 127.7, 127.6, 123.2, 73.8, 65.2, 53.0, 51.0, 49.2, 42.8, 40.6, 37.1, 24.1, 23.7, 22.2, 23.0, 21.8, 21.7, 21.6, 21.1 ppm. **MS** (EI) m/z = 611 (M^+).

25 (BSc2186). **3** MG132 (200 mg, 0.42 mmol) and phenyl isonitrile (65 mg, 0.63 mmol) were converted into α-hydroxyl amide **25** (BSc2186) according to the preparation of **23** (BSc2159). The crude product was purified by LC to give **25** (BSc2186) (70 mg, 28%). **^{1}H-NMR** (DMSO-d_6, 300 MHz): δ = 8.27 (s, 1H), 7.72-7.57 (m, 2H), 7.37-7.20 (m, 7H), 7.11-7.01 (m, 2H), 6.11-6.08 (m, 1H), 5.95-5.92 (m, 1H), 5.07 (s, 2H), 4.30-4.24 (m, 2H), 4.07-3.99 (m, 2H), 1.57-1.32 (m, 9H), 0.88-0.61 (m, 18H) ppm. **^{13}C-NMR** (DMSO-d_6, 75 MHz): δ = 172.0, 171.1, 171.0, 155.7, 138.3, 137.0, 128.4, 128.2, 127.6, 127.5, 123.5, 119.5, 65.2, 52.7, 52.9,

49.2, 40.5, 40.3, 40.0, 24.1, 23.9, 23.8, 23.1, 23.0, 22.6, 22.0, 21.3, 21.2 ppm. **MS** (EI) *m*/*z* = 596 (M^+).

26 (BSc2187). α-Hydroxyl amide **23** (BSc2159) (40 mg, 0.065 mmol) and IBX (36 mg, 0.13 mmol) were dissolved in DMSO and stirred at room temperature for 12 h. DCM (40 mL) and water (30 mL) were added prior to filtration The organic layer was separated and washed with water (2 x 40 mL), aqueous $NaHCO_3$ (1 x 40 mL, 0.05 N) and water (1 x 30 mL). The organic layer was dried (Na_2SO_4) and the solvent removed *in vacuo* to give **26** (BSc 2187) (22 mg, 56%). **^{1}H-NMR** ($CDCl_3$, 300 MHz): δ = 7.50-7.41 (m, 1H), 7.41-7.14 (m, 10H), 6.91-6.80 (m, 1H) 5.58-5.54 (m, 1H), 5.27-5.21 (m, 1H), 5.03-4.94 (m, 2H), 4.43-4.31 (m, 3H), 4.19-4.03 (m, 2H), 1.64-1.12 (m, 9H), 0.92-0.74 (m, 18H) ppm. **^{13}C-NMR** ($CDCl_3$, 75 MHz): δ = 191.8, 172.6, 171.8, 161.4, 156.4, 136.9, 136.3, 128.9, 128.9, 128.6, 128.3, 128.1, 128.0, 67.2, 53.6, 53.3, 51.6, 43.4, 41.5, 40.86, 40.0, 25.3, 24.8, 23.8, 23.7, 23.3, 23.0, 22.8, 22.4, 22.1, 21.5 ppm. MS (EI) *m*/*z* = 474 (Z-Leu-Leu-$C_6H_{12}NO^+$).

27 (BSc2188). 24 (BSc2185) was oxidized according to the synthesis of **26** (BSc2187). Purification by LC afforded **27** (BSc2188) (60 mg, 49%). **^{1}H-NMR** ($CDCl_3$, 300 MHz): δ = 8.46-8.44 (m, 2H), 7.64-7.47 (m, 2H), 7.24-7.12 (m, 6H), 6.85-6.82 (m, 1H), 5.54-5.47 (m, 1H), 5.22-5.15 (m, 1H), 5.04-4.93 (m, 2H), 4.46-3.99 (m, 4H), 1.62-1.16 (m, 9H), 0.92-0.76 (m, 18H) ppm. **^{13}C-NMR** ($CDCl_3$, 75 MHz): δ = 196.4, 172.6, 171.9, 159.8, 156.4, 149.3, 149.2, 136.2, 135.9, 133.0, 128.7, 128.3, 128.0, 123.8, 67.2, 53.7, 53.3, 51.5, 41.4, 40.8, 40.6, 39.9, 25.0, 24.8, 23.3, 23.0, 22.1, 22.0 ppm. **MS** (EI): *m*/*z* = 609 (M^+), 474 (Z-Leu-Leu-$C_6H_{12}NO^+$).

28 (BSc2189). 25 (BSc2185) (200 mg, 0.35 mmol) was oxidized according to the synthesis of **26** (BSc2187). Purification by LC afforded **28** (BSc2189) (30 mg, 50%). **^{1}H-NMR** ($CDCl_3$, 300 MHz): δ = 8.58 (s, 1H), 7.56-7.54 (m, 2H), 7.29-7.19 (m, 7H), 7.11-7.00 (m, 1H), 6.75 (d, 1H, ^3J = 9.0 Hz), 6.63 (d, 1H, ^3J = 9.1 Hz), 5.36-5.28 (m, 2H), 5.07 (s, 2H), 4.51-4.41 (m, 1H), 4.19-4.11 (m, 1H), 1.97-1.41 (m, 9H), 0.93-0.77 (m, 18H) ppm. **^{13}C-NMR** ($CDCl_3$, 75

MHz): δ = 196.8, 172.5, 171.8, 157.2, 156.4, 136.3, 136.2, 129.3, 129.2, 128.7, 125.5, 120.0, 67.3, 53.7, 53.0, 51.6, 41.3, 40.6, 40.9, 25.4, 25.4, 24.8, 23.3, 23.0, 22.8, 22.2, 22.1, 21.5 ppm. MS (EI): *m*/*z* = 474 (Z-Leu-Leu-$C_6H_{12}NO^+$).

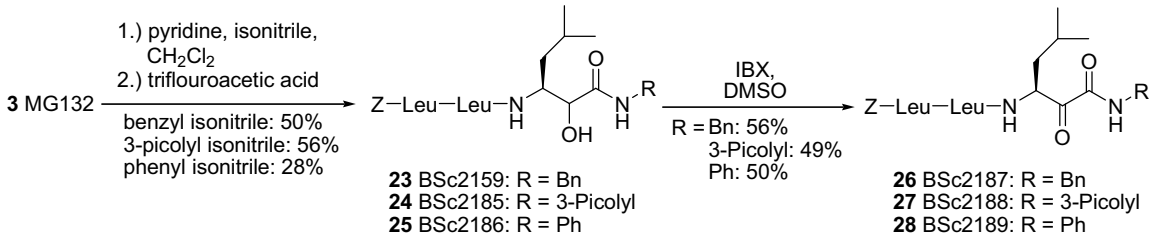

Scheme 5 Passerini reaction and following oxidation to α-keto amides.

Available online at www.sciencedirect.com
SCIENCE DIRECT®
Tetrahedron Letters
Tetrahedron Letters 46 (2005) 2551–2554

2-Iodoethanols from aldehydes, diiodomethane and isopropylmagnesium chloride

Hannes A. Braun, Reinhard Meusinger and Boris Schmidt*

Darmstadt Technical University, Clemens Schöpf-Institute for Organic Chemistry and Biochemistry, Petersenstr. 22, D-64287 Darmstadt, Germany

Received 18 January 2005; revised 15 February 2005; accepted 16 February 2005

Abstract—Diiodomethane and iodoform react with *i*-PrMgCl by halogen–metal exchange. The resulting magnesium reagents tolerate several functional groups, but aldehydes are converted selectively into iodoethanols in good to high yields. These mild reagents preserve racemization prone centres. The substrate controlled diastereoselectivity provides straightforward access to important intermediates of peptidomimetics.

Amino acid derived epoxides and 2-haloethanols are extremely versatile intermediates for the synthesis of protease inhibitors.[1–3] Several synthetic strategies are known, but they are either lengthy, require diazomethane or harsh conditions. Most organic chemists have rather mixed feelings using diazomethane for the synthesis of the intermediate α-chloroketones. The less hazardous siladiazomethane is significantly more expensive and therefore limited to small scale reactions. However, it can be replaced by dimethylsulfoxonium methylide.[4] Nevertheless, a reliable, straightforward and inexpensive approach is still very desirable. Some of these requirements are fulfilled by lithium organyls,[5] their strong basicity impedes the conversion of di- and oligopeptides, yet they provide access to α-chloroketones from *N*,*N*-dibenzylated amino acid esters.[15] The umpolung of $ClCH_2I$ or CH_2I_2 and subsequent addition to aldehydes provides access to epoxides,[6] but requires methyllithium at −78 °C. The deprotonation of CH_2Cl_2 by *n*-BuLi and addition to ketones furnished tertiary β-dichloroalcohols.[7] A more recent approach to the respective iodo species utilized diiodomethane or iodoform and air-sensitive and expensive SmI_2, which can be replaced by metallic samarium and iodoform.[8,9]

Here we report the efficient synthesis of 2-iodoethanols and 2,2-diiodoethanols from safe and convenient precursors. Seeking a safer replacement of methyllithium, we decided to investigate *i*-PrMgCl, which has a remarkable potential for iodine–magnesium exchanges. The late G. Köbrich already reported the halogen–metal exchange of bromoform and dibromomethane with *n*-BuLi. On the contrary, the analogous chloro compounds react by deprotonation.[10] The former reactivity continues in diiodomethane and iodoform, and may be improved by magnesium alkyls. We expected these magnesium reagents to favour late transition states, to tolerate a wide range of functional groups, to display reduced basicity, and thus allow stereoselective conversion of polyfunctional peptides.[11] The rate of the halogen–metal exchange depends on the electron density to a great extent that the stepwise activation of geminal diiodides is feasible. The detailed kinetics and energetics were reported by Hoffmann and the potential of this reaction was revealed in a number of publications already.[12–14] The activation of iodoform or diiodomethane by *i*-PrMgCl proceeded rapidly in tetrahydrofuran at −78 °C (Scheme 1).

The addition of *i*-PrMgCl to aldehydes was considerably slower at this temperature. Addition of an aldehyde after complete iodo-magnesium exchange (15 min) resulted in similar yields and selectivities as obtained for the simultaneous addition (Table 1). Both C1 nucleophiles, which are derived from long-lived ate complexes,[12] reacted with aldehydes (**1a**–**d**) at −78 °C

Keywords: Halogen–metal exchange; Iodomethane; Protease inhibitors.
* Corresponding author. Tel.: +49 6151 163075; fax: +49 6151 163278; e-mail addresses: boris.schmidt@imail.de; schmibo@oc.chemie.tu-darmstadt.de

0040-4039/$ - see front matter © 2005 Elsevier Ltd. All rights reserved.
doi:10.1016/j.tetlet.2005.02.093

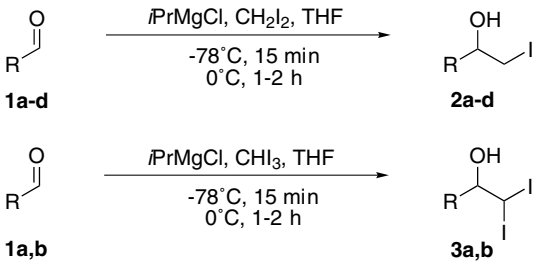

Scheme 1.

Table 1. Reactions of aldehydes, ketones and carboxylic acid derivatives according to Scheme 1 with 2.0 equiv of CH_2I_2 or CHI_3 and *i*-PrMgCl

Reagent	Aldehyde	Product	Yield[a] [%]
CH_2I_2/*i*-PrMgCl	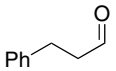 **1a**	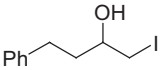 **2a**	96
CH_2I_2/*i*-PrMgCl	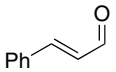 **1b**	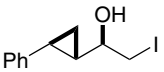 **2b**	91[b]
CH_2I_2/*i*-PrMgCl	 **1c**	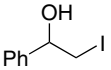 **2c**	73
CH_2I_2/*i*-PrMgCl	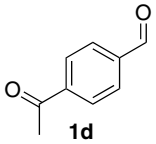 **1d**	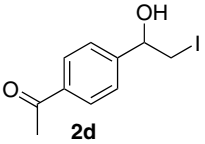 **2d**	69
CH_2I_2/*i*-PrMgCl	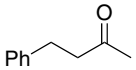 **1e**	Conversion < 10[c]	
CHI_3/*i*-PrMgCl	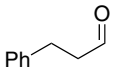 **1a**	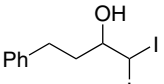 **3a**	91
CHI_3/*i*-PrMgCl	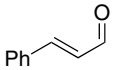 **1b**	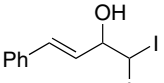 **3b**	82[d]
CH_2I_2/*i*-PrMgCl	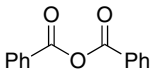 **1f**	Sluggish reaction	
CH_2I_2/*i*PrMgCl	 **1g**	No reaction	

[a] Isolated yields.
[b] Diastereomeric mixture: *syn*/*anti* 96:4, assigned by NMR.[17]
[c] Determined by HPLC.
[d] Contains 4% of 2,2-diiodo-1-(2-iodo-3-phenylcyclopropyl)ethanol (mixture of diastereomers, d.r. > 3:1) and 3% of 2,2-diiodo-1-(2-phenylcyclopropyl)ethanol.

to the β-iodo-(**2a**–**d**) and β-diiodo compounds (**3a** and **b**). The formation of epoxides was not observed even at 0 °C for 2 h. These results are similar to the samarium methodology,[8] but complement the diiodomethane derived lithium reagents, which provide epoxides.[6]

The turnover of **1e** was remarkably slow, it reacted just marginally under these conditions. Consequently, the formylacetophenone **1d** underwent iodomethylation at the aldehyde only. The benzoic anhydride **1f** underwent rapid conversion into a multitude of unidentified products. The conversion of the acid chloride **1g** did not take place, but reactivity could have been enhanced by either chelation assistance or the reported *trans*-metallation into a copper reagent.[15] The differences between the two nucleophilic reagents (Scheme 1) became apparent in the reaction with cinnamic aldehyde, which was converted into the cyclopropyl-methanol **2b** by diiodomethane and into the anticipated diiodinated allyl alcohol **3b** by CHI_3. Two pathways lead to the cyclopropane **2b**: (a) an initial Michael addition is followed by cyclization and iodomethylation,[16] or (b) an iodomethylation of the aldehyde is followed by a Simmons–Smith-like cyclopropanation, which is reported to occur with high *syn*-stereoselectivity, but modest yields for CH_2I_2/*i*-PrMgCl and allyl alcohols.[17] Therefore, we have monitored the reaction at different ratios of aldehyde and CH_2I_2/*i*-PrMgCl to establish the mode of action. The allyl alcohol **4** (Scheme 2) was identified as the dominant intermediate, which was converted into **2b** by a second equivalent of CH_2I_2/*i*-PrMgCl. The exclusive *anti* configuration of the cyclopropane was determined by NMR spectroscopy and revealed the dormant carbenoid reactivity. The relative configuration of the alcohol was tentatively assigned in analogy to the results of Bolm and Pupowicz.[17]

The reaction of the Evans imide **5** with CH_2I_2/*i*-PrMgCl (Scheme 3) resulted in the unexpected, selective iodomethylation of the urethane to furnish the iodoacetate **6**, initially in low yield. However, when the reaction mixture was kept at −25 °C for three days we obtained **6** as a single product. There is precedence for this reactivity of Evans imides.[18] Vinylmagnesium chloride reacted in a similar fashion to result in vinylation of the urethane. A tetrahedral intermediate, similar to Weinreb-amides, was suggested for this monoalkylation.

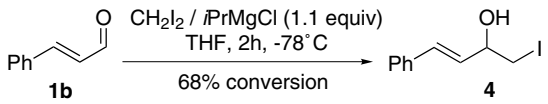

Scheme 2.

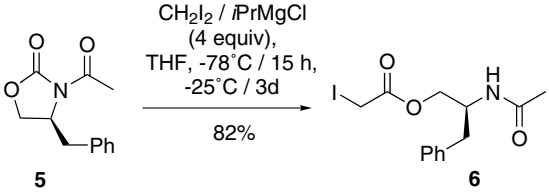

Scheme 3.

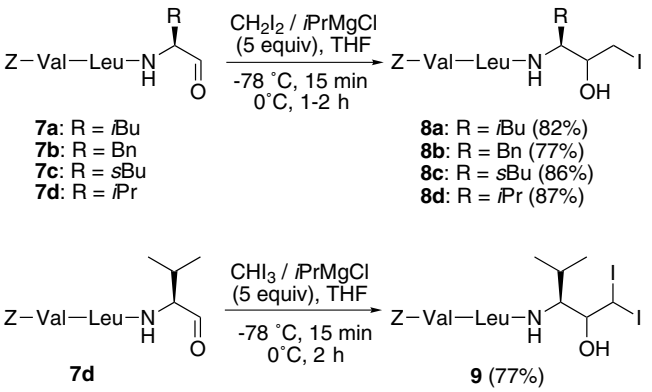

Scheme 4.

After these initial experiments we addressed the iodomethylation of peptide aldehydes, which are important intermediates for the synthesis of protease inhibitors. The deprotonation of the acidic amides required 5-fold excess of the reagent. This was not a nuisance, because the deprotonation froze the configuration of the P1–P3 positions of the tripeptide mimetics **7a**–**d**. The aldehydes were used as 3:1 mixtures of diastereomers, as obtained from the oxidation of alcohols by IBX in DMSO, followed by aqueous work up. The iodomethylation and diiodomethylation provided the compounds **8a**–**d** and **9** (Scheme 4), apparently without epimerization of the P1 position as judged by HPLC. The diastereoselectivity of the reaction was always better than 2:1 as judged by HPLC.

The diastereoselectivity of the iodomethylation was investigated for the phenylalanine derived aldehyde **10** (Scheme 5). The conversion into β-iodoalcohol **11** was followed by substitution of the iodide with diethylamine. The product **12** was deprotected and the resulting amino alcohol was treated with triphosgene to give oxazolidinone **13** and care was taken not to separate the diastereomers.

NMR spectroscopy (^{13}C NMR: γ-effect,[19] NOE) confirmed the relative configuration (*anti*/*syn* d.r. = 86:14). This is in accordance with a chelation controlled Cram transition state and complements the samarium methodology[20] which provides access to the diastereomer when the nitrogen is dibenzylated. The substrate controlled diastereoselectivity provides straightforward access to important intermediates of peptidomimetics. The chiral induction by additional ligands is subject to ongoing investigations.

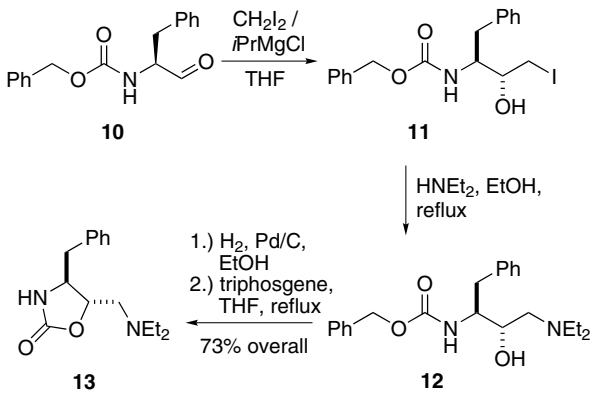

Scheme 5.

Acknowledgements

This work was supported by the Deutsche Forschungsgemeinschaft (SPP1085 SCHM1012-3) and the EU contract LSHM-CT-2003-503330 (APOPIS).

Supplementary data

Supplementary data associated with this article can be found, in the online version, at doi:10.1016/j.tetlet.2005.02.093.

References and notes

1. Fairlie, D. P.; Tyndall, J. D. A.; Reid, R. C.; Wong, A. K.; Abbenante, G.; Scanlon, M. J.; March, D. R.; Bergman, D. A.; Chai, C. L. L.; Burkett, B. A. *J. Med. Chem.* **2000**, *43*, 1271.
2. Powers, J. C.; Asgian, J. L.; Ekici, O. D.; James, K. E. *Chem. Rev.* **2002**, *102*, 4639.
3. Schmidt, B. *ChemBioChem* **2003**, *4*, 366.
4. Wang, D.; Schwinden, M. D.; Radesca, L.; Patel, B.; Kronenthal, D.; Huang, M.-H.; Nugent, W. A. *J. Org. Chem.* **2004**, *69*, 1629.
5. Fernández-Megía, E.; Iglesias-Pintos, J. M.; Sardina, F. J. *J. Org. Chem.* **1997**, *62*, 4770.
6. Concellón, J. M.; Llavona, L.; Bernad, P. L., Jr. *Tetrahedron* **1995**, *51*, 5573.
7. (a) Entmayr, P.; Köbrich, G. *Chem. Ber.* **1976**, *109*, 2175; (b) Taguchi, H.; Yamamoto, H.; Nozaki, H. *J. Org. Chem.* **1974**, *96*, 3010.
8. (a) Concellón, J. M.; Rodriguez-Solla, H.; Bardales, E.; Huerta, M. *Eur. J. Org. Chem.* **2003**, 1775; (b) Concellón, J. M.; Bernad, P. L.; Pérez-Andrés, J. A. *Tetrahedron Lett.* **1998**, *39*, 1409.
9. (a) Imamoto, T.; Hatajima, T.; Takiyama, N.; Takeyama, T.; Kamiya, Y.; Yoshizawa, T. *J. Chem. Soc., Perkin Trans. 1* **1991**, 3127; (b) Imamoto, T.; Takeyama, T.; Koto, H. *Tetrahedron Lett.* **1986**, *27*, 3243; (c) Tabuchi, T.; Inanaga, J.; Yamaguchi, M. *Tetrahedron Lett.* **1986**, *27*, 3891.
10. (a) Köbrich, G.; Fischer, R. H. *Chem. Ber.* **1968**, *101*, 3208; (b) Köbrich, G. *Angew. Chem.* **1967**, *79*, 15; *Angew. Chem., Int. Ed. Engl.* **1967**, *6*, 41; (c) Köbrich, G.; Büttner, H.; Wagner, E. *Angew. Chem.* **1970**, *82*, 177; *Angew. Chem., Int. Ed. Engl.* **1970**, *9*, 169.
11. Schulze, V.; Nell, P. G.; Burton, A.; Hoffmann, R. W. *J. Org. Chem.* **2003**, *68*, 4546.
12. Müller, M.; Brönstrup, M.; Knopff, O.; Schulze, V.; Hoffmann, R. W. *Organometallics* **2003**, *22*, 2931.
13. (a) Knochel, P.; Dohle, W.; Gommermann, N.; Kneisel, F. F.; Kopp, F.; Korn, T.; Sapountzis, I.; Vu, V. A. *Angew. Chem., Int. Ed.* **2003**, *42*, 4302; (b) Vu, V. A.; Marek, I.; Polborn, K.; Knochel, P. *Angew. Chem., Int. Ed.* **2002**, *41*, 351; (c) Rottlander, M.; Boymond, L.; Bérillon, L.; Leprêtre, A.; Varchi, G.; Avolio, S.; Laaziri, H.;

Quéguiner, G.; Ricci, A.; Cahiez, G.; Knochel, P. *Chem. Eur. J.* **2000**, *6*, 767.
14. (a) Villieras, J. *Bull. Soc. Chim. Fr.* **1967**, 1520; (b) Villieras, J.; Kirschleger, B.; Tarhouni, R.; Rambaud, M. *Bull. Soc. Chim. Fr.* **1986**, 470.
15. Barluenga, J.; Baragaña, B.; Concellón, J. M. *J. Org. Chem.* **1995**, *60*, 6696.
16. Oudeyer, S.; Aaziz, A.; Léonel, E.; Paugam, J. P.; Nédélec, J.-Y. *Synlett* **2003**, 485.
17. Bolm, C.; Pupowicz, D. *Tetrahedron Lett.* **1997**, *38*, 7349.
18. Schmidt, B.; Wildemann, H. *J. Chem. Soc., Perkin Trans. 1* **2002**, *8*, 1050.
19. Pihlaja, K.; Kleinpeter, E. *Carbon-13 NMR Chemical Shifts in Structural and Stereochemical Analysis*; VCH: Weinheim, 1994.
20. Concellón, J. M.; Cuervo, H.; Fernández-Fano, R. *Tetrahedron* **2001**, *57*, 8983.

Supplementary data

2-Iodoethanols from aldehydes, diiodomethane and *iso*-propylmagnesium chloride

Hannes A. Braun, Reinhard Meusinger, Boris Schmidt*

Darmstadt Technical University, Clemens Schöpf-Institute for Organic Chemistry and Biochemistry, Petersenstr. 22, D-64287 Darmstadt, Germany

1-Iodo-4-phenylbutan-2-ol (2a). *i*PrMgCl (4.0 mmol, 2.0 mL of a 2.0 M solution in Et_2O) was added dropwise to a solution of diiodomethane (1.07 g, 4.0 mmol) in THF (8 mL, abs.) at -78°C under argon atmosphere. A solution of 3-phenylpropanal (274 mg, 2.04 mmol) in THF (1 mL, abs.) was added and the resulting mixture was stirred at the same temperature for 15 min and at 0°C for 1 h. The mixture was quenched with aqueous NH_4Cl (5 mL, sat.) and extracted with CH_2Cl_2 (3x 20 mL). The combined organic layers were dried (Na_2SO_4) and concentrated under vacuum. The crude product was purified by LC ($CHCl_3$) to give alcohol **2a** (541 mg, 96%). ^{1}H-NMR ($CDCl_3$, 300 MHz): δ = 7.37-7.01 (m, 5H), 3.46-3.41 (m, 1H), 3.31-3.26 (m, 1H), 3.19-3.13 (m, 1H), 2.75-2.59 (m, 2H), 1.99 (s, 1H), 1.82-1.75 (m, 2H) ppm. ^{13}C-NMR ($CDCl_3$, 75 MHz): δ = 141.4, 128.7, 128.6, 126.2, 70.3, 38.3, 32.1, 16.7 ppm. MS (EI): *m/z* = 276 (M^+).

(*S*)-2-Acetamido-3-phenylpropyl 2-iodoacetate (6). *i*PrMgCl (2.3 mmol, 1.15 mL of a 2.0 M solution in THF) was added dropwise to a solution of diiodomethane (616 mg, 2.3 mmol) in THF (4 mL, abs.) at -78°C under argon atmosphere. A solution of (*S*)-3-acetyl-4-benzyloxazolidin-2-one (100 mg, 0.46 mmol) in THF (1 mL, abs.) was added and the resulting mixture was stirred at the same temperature for 15 h and at -25°C for 3 d. The mixture was quenched with aqueous NH_4Cl (5 mL, sat.) and extracted with CH_2Cl_2 (3x 20 mL). The combined organic layers were dried (Na_2SO_4) and concentrated under vacuum. The crude product was purified by LC ($CHCl_3$) to give acetate **6** (138 mg, 82%). ^{1}H-NMR ($CDCl_3$, 300 MHz): δ = 7.27-7.12 (m, 5H), 5.70 (d, *J* = 6.0 Hz, 1H), 4.44-4.34 (m, 1H), 4.11-4.00 (m, 2H), 3.65 (s, 2H), 2.89-2.74 (m, 2H), 1.89 (s, 3H) ppm. ^{13}C-NMR ($CDCl_3$, 75 MHz): δ = 169.9, 168.9, 136.9, 129.3, 128.8, 127.0, 66.0, 49.6, 37.4, 23.5, -5.7 ppm. MS (EI): *m/z* = 361.2 (M^+).

(*4S*,*5S*)-5-((Diethylamino)methyl)-4-benzyloxazolidin-2-one (13). *i*PrMgCl (3.08 mmol, 1.54 mL of a 2.0 M solution in THF) was added dropwise to a solution of diiodomethane (825 mg, 3.08 mmol) in THF (8 mL, abs.) at -78°C under argon atmosphere. A solution of benzyl (*S*)-1-formyl-2-phenylethylcarbamate **10** (248 mg, 0.88 mmol) was added and the resulting mixture was stirred at the same temperature for 15 min and at 0°C for 90 min. The mixture was quenched with aqueous NH_4Cl (5 mL, sat.) and extracted with CH_2Cl_2 (3x 20 mL). The combined organic layers were dried (Na_2SO_4) and concentrated under vacuum. The crude product was purified by LC ($CHCl_3$) to give alcohol **11** (292 mg, 78%). Alcohol **11** (244 mg, 0.57 mmol) was dissolved in EtOH (5 mL, abs.) and $HNEt_2$ (419 mg, 5.7 mmol). The mixture was heated under argon atmosphere to 60°C for 2 h and under reflux for 2 h. The crude product was purified by LC (system $CHCl_3$ to $CHCl_3$/MeOH 10:1) to afford amine **12** (201 mg, 95%). Amine **12** (201 mg, 0.54 mmol) was stirred with Pd/C catalyst (200 mg, 10wt%) in EtOH (4 mL, abs.) under H_2 atmosphere for 3 d to yield the deprotected compound (128 mg, quant.). The product (52 mg, 0.22 mmol) was dissolved in THF (8 mL, abs.). Triphosgene (130 mg, 0.44 mmol) was added and the reaction mixture was heated under reflux (argon

atmosphere) for 15 h. After 4 h and 8 h further triphosgene (2x 130 mg, 0.44 mmol) was added. Ethyl acetate (50 ml) was added and washed with aqueous K_2CO_3 (3x 30 mL, conc.). The organic layer was dried (Na_2SO_4) and concentrated under vacuum. The crude product was purified by LC ($CHCl_3$) to give oxazolidinone **13** (57 mg, 98%). ^{1}H-NMR ($CDCl_3$, 300 MHz): δ = 7.29-7.10 (m, 5H), 5.51 (s, 1H), 4.28 (q, *J* = 5.8 Hz, 1H), 3.76 (q, *J* = 6.0 Hz 1H), 2.87-2.72 (m, 2H), 2.62-2.37 (m, 6H), 0.88 (t, 6H) ppm. ^{13}C-NMR ($CDCl_3$, 75 MHz): δ = 158.7, 136.4, 129.2, 129.0, 127.2, 80.5, 57.6, 55.9, 47.9, 41.8, 12.0 ppm. MS (EI): *m/z* = 262.2 (M^+).

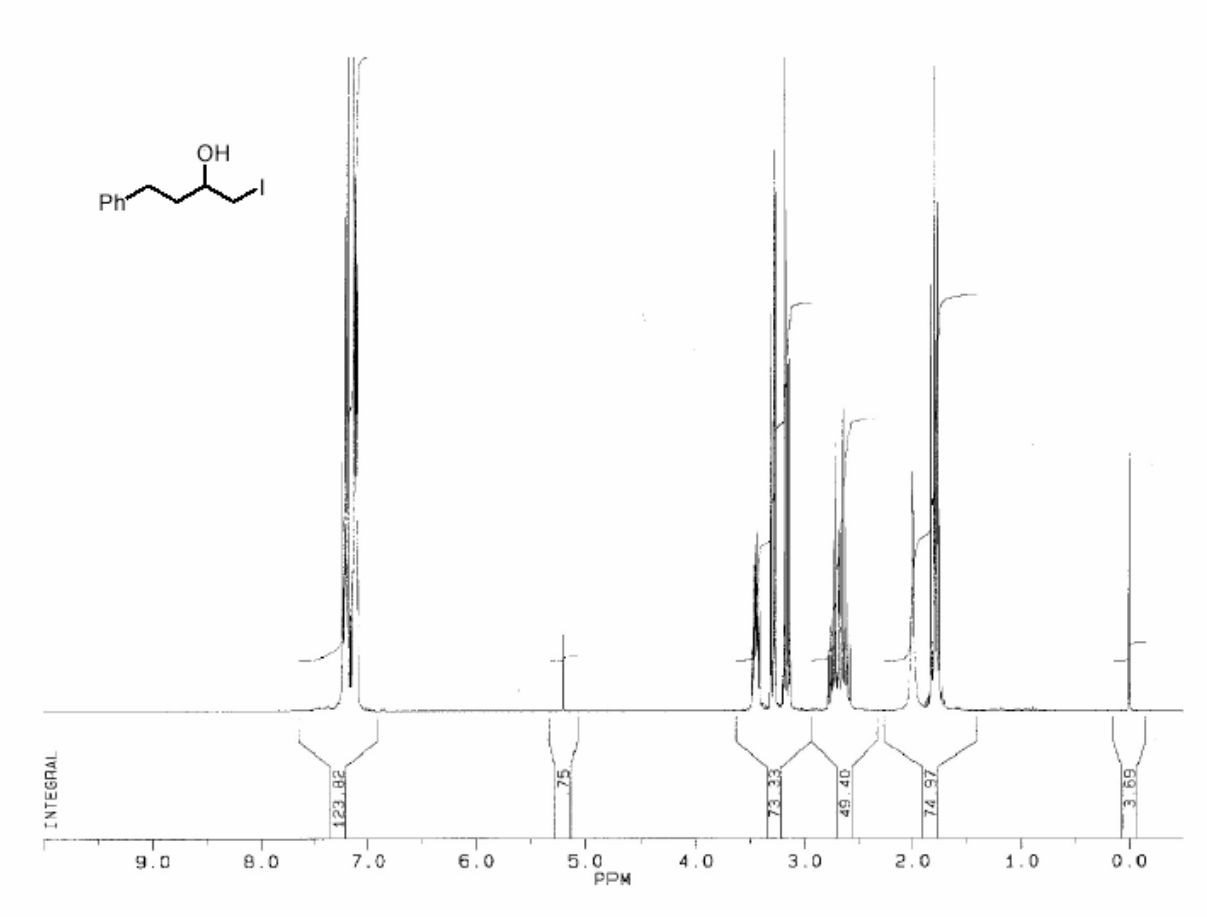
OH
Ph
I
INTEGRAL
123.82
7.5
73.33
49.40
74.97
3.69
9.0
8.0
7.0
6.0
5.0
4.0
3.0
2.0
1.0
0.0
PPM

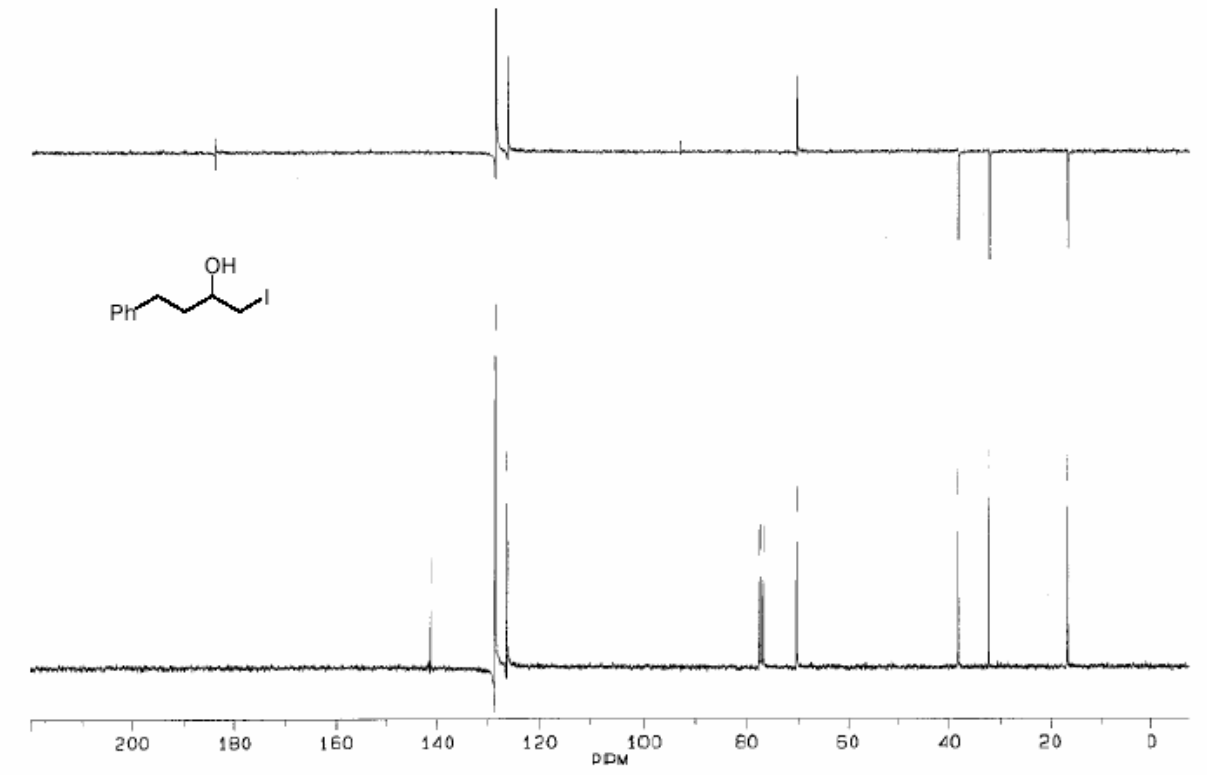
OH
Ph
I
200
180
160
140
120
100
80
60
40
20
0
PPM

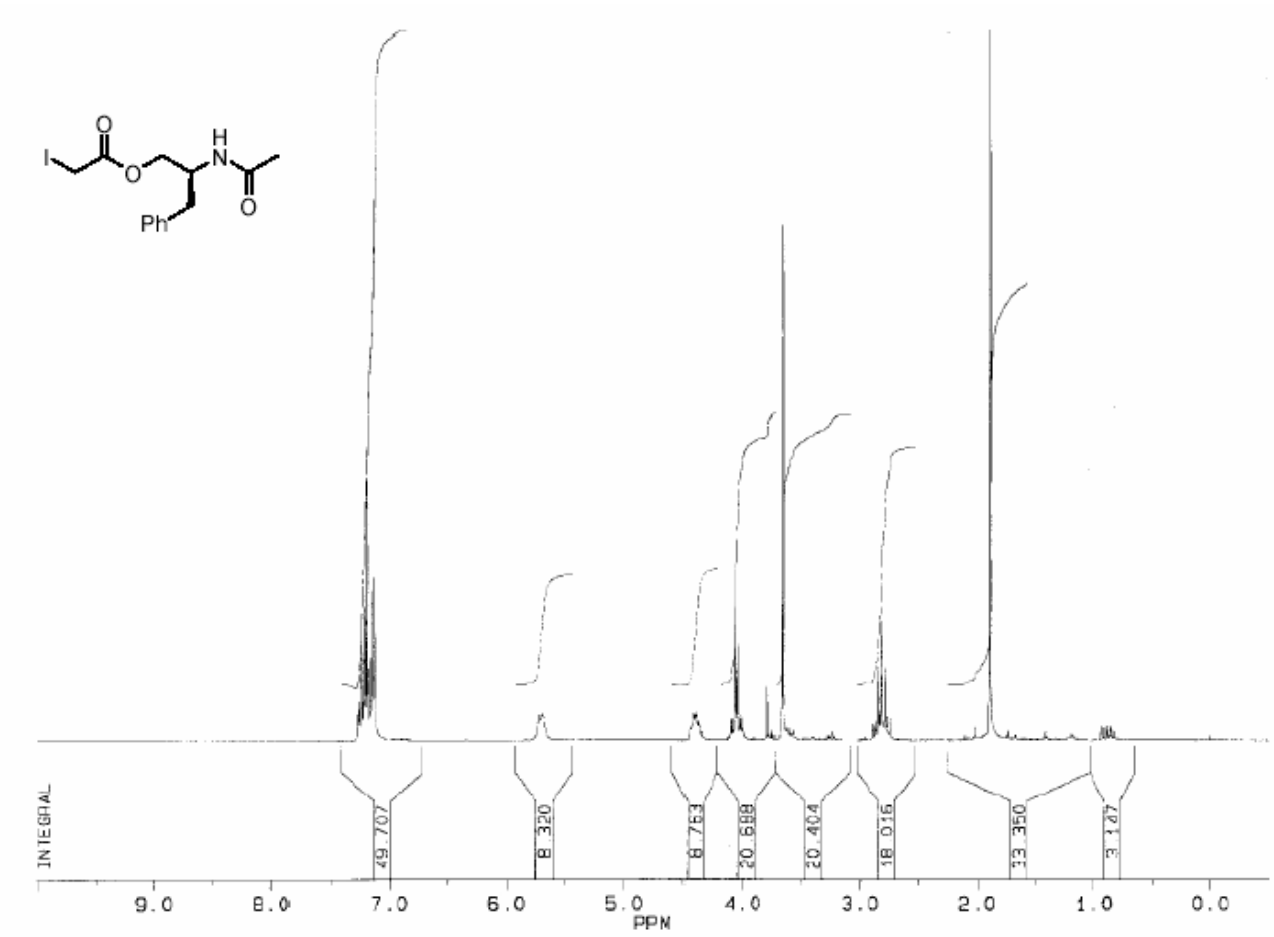
INTEGRAL
49.707
8.320
8.763
20.688
20.404
18.016
13.350
3.187
9.0
8.0
7.0
6.0
5.0
4.0
3.0
2.0
1.0
0.0
PPM

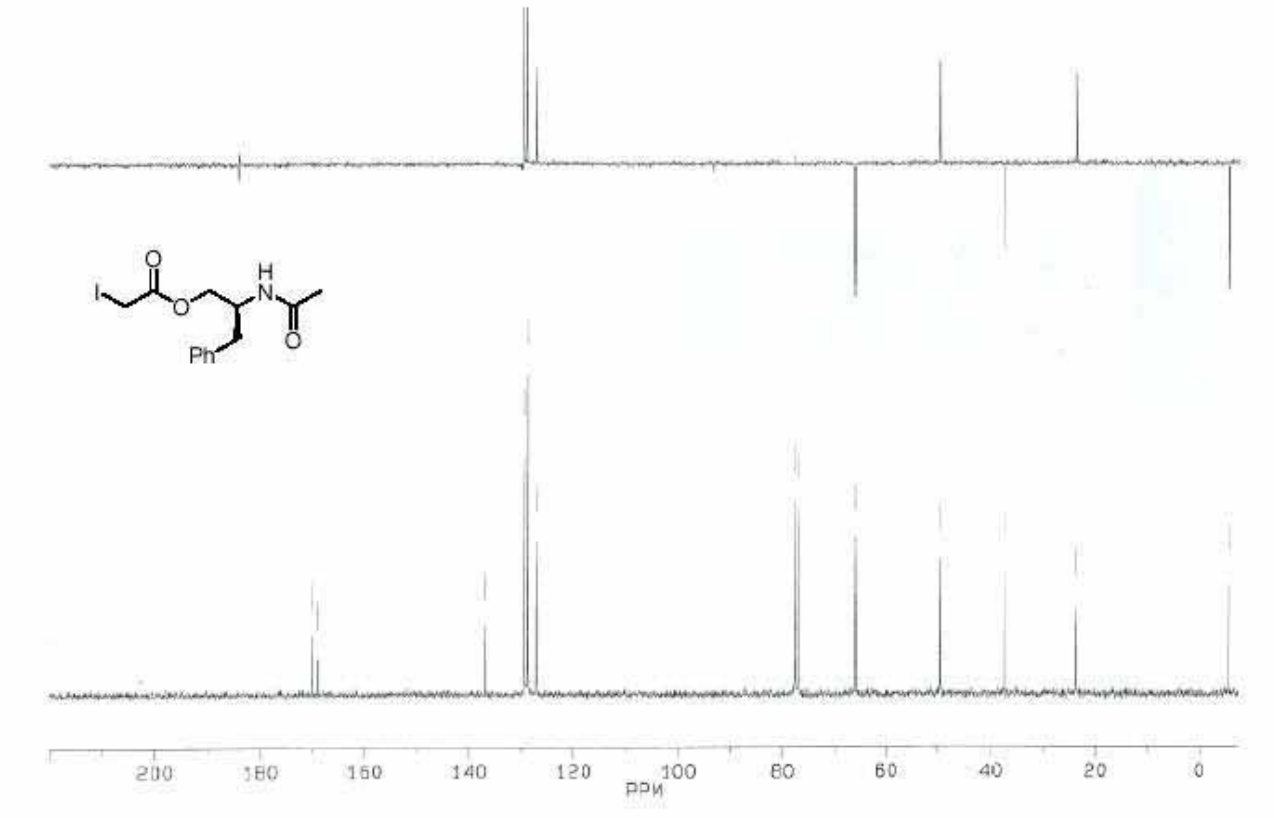
200
180
160
140
120
100
80
60
40
20
0
PPM

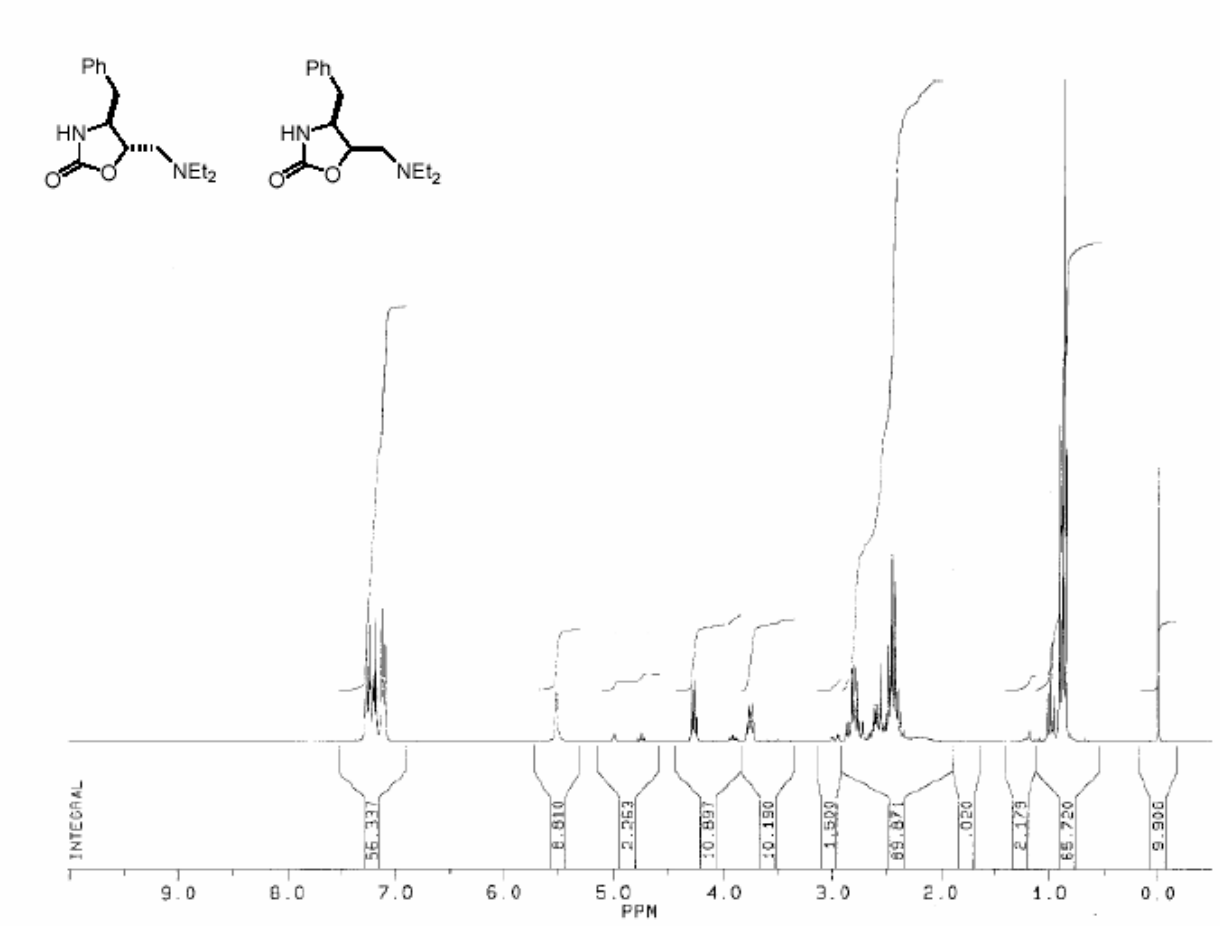
Ph
HN
O
O
NEt2
INTEGRAL
56.337
8.810
2.263
10.897
10.190
1.500
89.871
.020
2.179
65.720
9.900
9.0
8.0
7.0
6.0
5.0
4.0
3.0
2.0
1.0
0.0
PPM

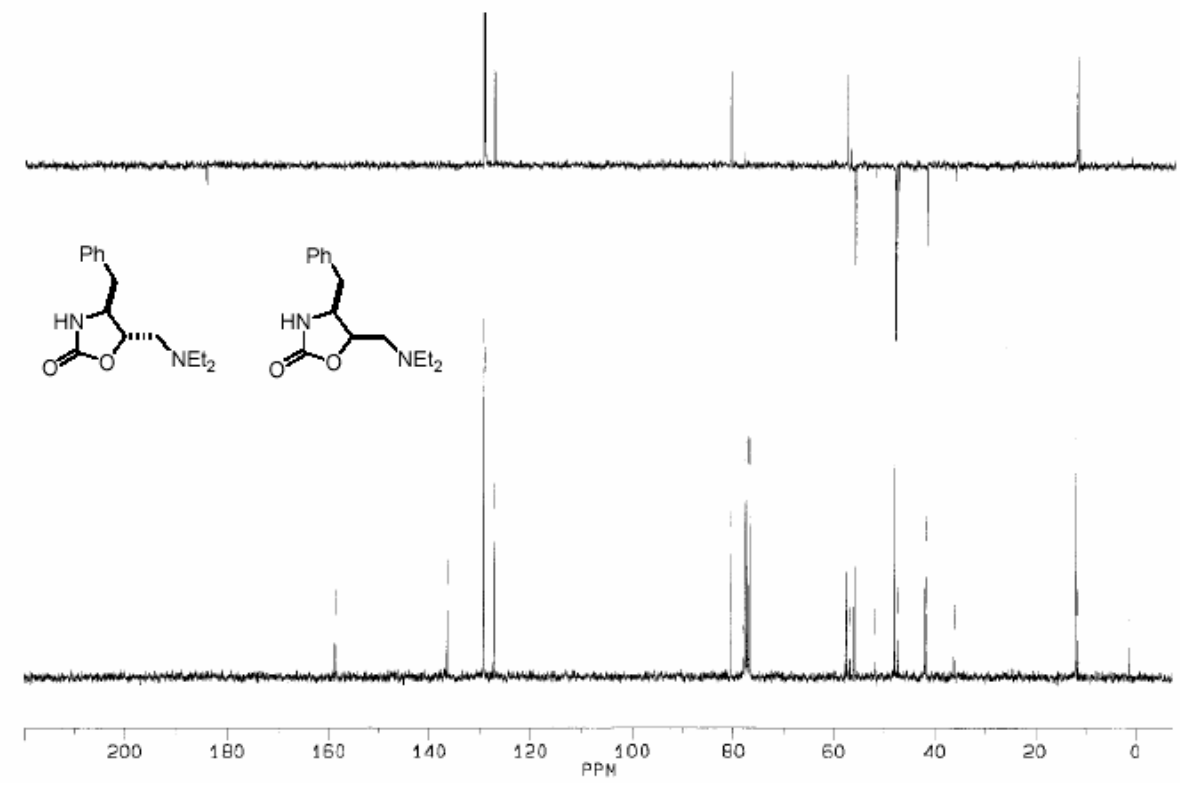
Ph
HN
O
O
NEt2
200
180
160
140
120
100
80
60
40
20
0
PPM

Drug Development and PET-Diagnostics for Alzheimer's Disease

Boris Schmidt*, Hannes A. Braun and Rajeshwar Narlawar

Clemens Schöpf-Institute for Organic Chemistry and Biochemistry, TU Darmstadt, Petersenstr. 22, D-64287 Darmstadt, Germany

Abstract: The exact cause of Alzheimer's disease is still unknown; despite the dramatic progress in understanding. Most gene mutations associated with Alzheimer's disease point to the amyloid precursor protein and amyloid β. The α-, β- and γ-secretases are the three executioners of amyloid precursor protein processing. Significant progress has been made in the selective inhibition of these proteases, regardless of the availability of structural information. Several peptidic and non-peptidic leads were identified and first drug candidates are in clinical trials. Cholesterol lowering drugs and metal chelators are also in advanced clinical stages as disease modifiers. Successful trials demand either large cohorts or reliable markers for Alzheimer's disease. Therefore, several radiomarkers are under investigation to support such clinical trials.

Keywords: Alzheimer's disease, secretase, copper, statine, aspartic protease, cholesterol, imaging.

INTRODUCTION

Alzheimer's disease (AD), the most common dementia in elderly people, affects nearly 2% of the population in industrialised countries (http://www.alz.org). This epidemic neurodegenerative disorder claims millions of victims per year, not just erasing the memory of the patient, buteffecting severe implications on the social environment. The AD prevalence equals 5.5 % above 60 years of age and increases for elderly people (clinical AD: 16% 85y, 22% 90y) [1, 2]. The onset of Alzheimer's disease is usually after 65 years of age, though earlier onset is not uncommon. As age advances, the incidence increases rapidly and roughly doubles every 5 years [1]. Age is the dominant risk factor overruling even the positive impacts of nutrition (low-fat diets), nutritional supplements after onset or education [3-5]. The socio-economic impact of AD, the care needed for disabled and chronically wasting patients, the consequences for patients, relatives and caretakers alike is a major social and financial issue for the coming decades. Current annual AD related expenditures total $83.9 billion in the US [6]. 14 million Americans are likely to be stricken by 2050 [7]. Despite all efforts, the exact cause of Alzheimer's disease is still unknown, but the pathways towards and away from Alzheimer's disease become better understood [8]. The process results in neuron and synapse degeneration, reduction of brain regions, memory loss and ultimately in death. There is progress in the definite diagnosis of AD prior to a post-mortem diagnosis. Problems arise from other causes of memory loss (e.g. vascular dementia). Several steps in the process offer potential for intervention, these include the amyloid cascade and plaque-related proteins [9], hyperphosphorylated tau protein [10, 11], zinc, copper and aluminium cations [12-14].

*Address correspondence to this author at the Clemens Schöpf-Institute for Organic Chemistry and Biochemistry, TU Darmstadt, Petersenstr. 22, D-64287 Darmstadt, Germany E-mails: schmibo@oc.chemie.tu-darmstadt.de or BSC2@gmx.net or boris.schmidt@imail.de

Established Therapies and Novel Approaches

Some 500 compounds are in development to treat neurodegenerative diseases. At least 10% of these are related to AD [15, 16]. The targets derive from a whole range of sometimes well-known receptors and enzymes: GSK-3, PDE 4 and muscarinic M1. nACh modulators, AChE inhibitors, NMDA modulators, 5-HT agonists and several vaccination projects (e.g. Elan, Cytos Biotechnology) are in advanced stages of research or development. The early rush on fibril formation inhibition resulted in a number of potent inhibitors thereof. However, the activities were confined to *in vitro* experiments or limited by poor DMPK properties, which excluded further development [17, 18]. Few drug candidates (e.g. SKF-74652, **1** [19], Scheme **1**) went beyond animal testing and convincing clinical data are still wanted. Furthermore, the view on Aβ toxicity has changed dramatically. Plaques were seen as the true culprit and their removal was one of the therapy goals until 2001. Now, soluble Aβ and early oligomers have to take the blame for the Aβ associated effects. Thus, mature Aβ plaques may rather rest in peace.

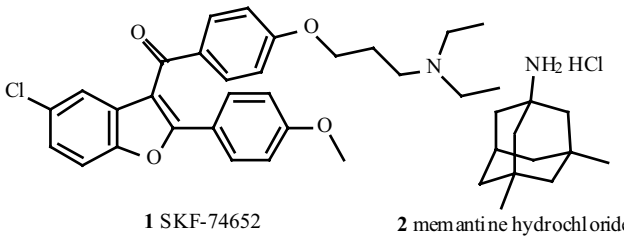

1 SKF-74652 **2** memantine hydrochloride

Scheme 1. Aβ fibril formation inhibitor and memantine hydrochloride: NMDA receptor antagonist.

Cholinesterase inhibitors (AChEI) produce small improvements in cognitive and global assessments [20-23], but galanthamine, tacrine, donepezil and rivastigmine do not address the severe mortality in the final stages of AD. 565 patients with mild to moderate Alzheimer's disease entered a 12-week run-in period, in which they were randomly allocated to donepezil or placebo. There were no significant benefits for the 486 patients who completed the 2nd period until the primary endpoints: entry to institutional care and

0929-8673/05 $50.00+.00

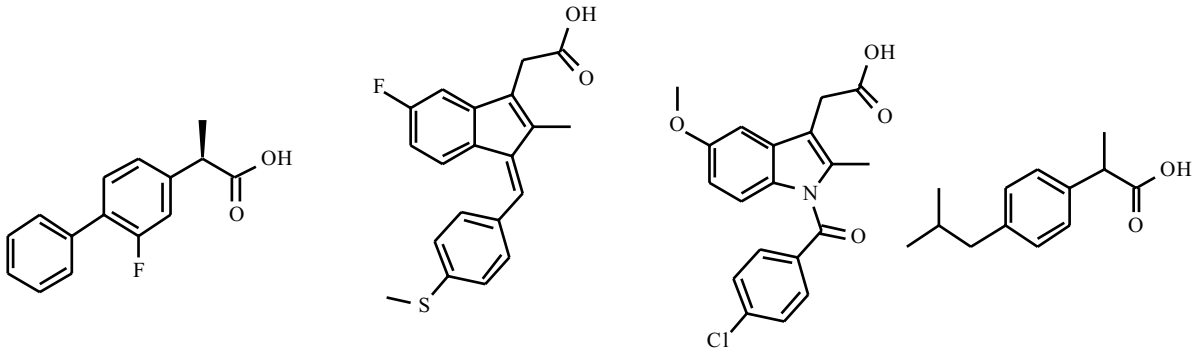

Scheme 2. NSAIDs effect Aβ levels [28, 29].

progression of disability [24, 25]. This outcome contradicts a previous report: the chosen AChEI was not cost effective, with benefits below minimally relevant thresholds [22]. Tacrine is losing ground to the other 3 AChE inhibitors because of hepatotoxic effects [6]. The message of these studies is obvious: better drugs are needed to target the cause of Alzheimer's disease.

Memantine hydrochloride (**2**), first made in 1960 by Ely Lilly as an anti-diabetic agent, protects neurons against overactivation of *N*-methyl-*D*-aspartate receptors and was approved for the treatment of moderate to severe Alzheimer's disease in 2002 as first of its class [26]. Previous attempts utilising this non-competitive antagonism failed. This was due to CNS side effects such as hallucinations. Memantine hydrochloride was tested in a 28 weeks trial at 20 mg/day against placebo, indicating a significant cognitive improvement. The current strategy to use memantine hydrochloride in combination therapy with the AChEI donezepil was concluded from the outcome of a 24 week trial against placebo. The combinations halted or showed further decline, but the magnitude of these effects was modest [6]. Furthermore, these results have become questionable in the light of the recent extended donezepil trials.

Thus, a causal therapy is still in utter demand, as no existing therapy effectively stops or even cures the disease. The incidence of early-onset of Alzheimer's disease in Down's syndrome patients indicated chromosome 21 as a likely hotspot for gene location. Mutations linked to early-onset Alzheimer's disease afflicted families in London and Sweden, and additional polymorphisms, that either cause or further AD, provided some insight into the biological pathways and the involvement of the amyloid precursor protein (APP) [41-44]. The genetic background of AD is quite heterogeneous; a large number of gene associations has been made with localisations on almost every chromosome [45]. Replicated or confirmed associations are few: the late-onset AD is linked to the ε4-allele of APOE, but its presence is neither necessary nor sufficient to cause the disease, but there is a dose-dependent relation to the age of onset [46]. Another cluster of mutations is located on chromosome 14, on the gene encoding for presenilin 1 [47]. Mouse models expressing mutated human APP and presenilin 1 display many symptoms of AD, although no model represents the full range of pathologies of the human disease. Particularly, the inflammation processes in humans and mice do not adequately relate to each other [48]. The observed loss of neurons (mice [49]) is accompanied by

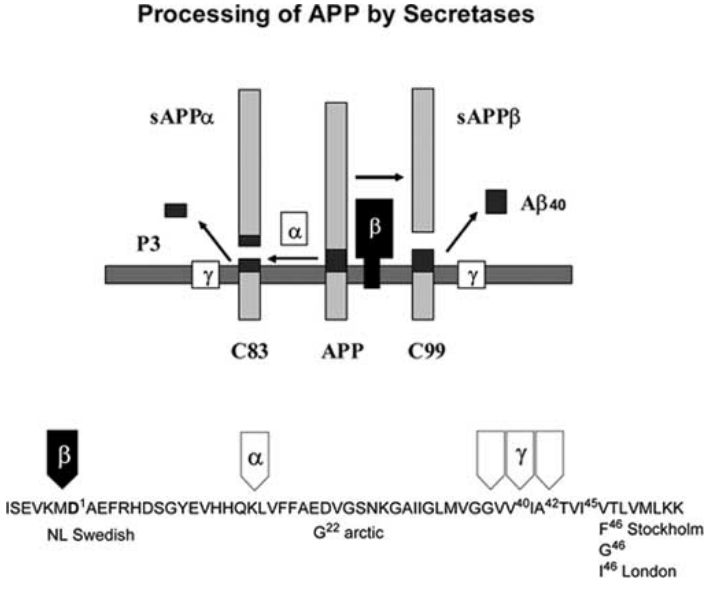

Scheme 3. APP amino acid sequence close to the cleavage sites and point mutations in Aβ numbering.

plaque formation consisting of amyloid β-peptide in the human perfrontal cortices. But there is mounting evidence for a second pool of insoluble Aβ in cholesterol enriched low-density membranes, where it moderates membrane fluidity [50].

A rational approach to a successful, causal therapy is based on the detailed understanding of Aβ formation, deposition and the inflammatory consequences. Decisive functions were assigned to the amyloid precursor protein (APP) and its degrading aspartic proteases β-secretase and the presenilins. A simplified APP processing is depicted in (Scheme **3**). APP occurs in 3 isoforms: APP695, APP751 and APP771, this includes a large extramembranous sequence and the crucial membrane spanning domain, followed by a short cytoplasmic tail. The non-pathological cleavage occurs between Lys687-Leu688 (resp. K16L17 in Scheme **3**) by the α-secretase, which belongs to the ADAM family and is suspected to be TACE or ADAM10.

This dominating event leaves just 10% of the APP behind for the β-secretase, produces α-APP and ultimately leads to the fragments p3 and C83. The α-secretase is sensitive to membrane cholesterol levels and can thus be modulated [51]. The most relevant point mutations for Aβ formation are K670-M671->NL and V717->Phe (Stockholm or Indiana), which cause familial Alzheimer's dementia (FAD). The molecular basis of these point mutations is explained by their modulation of the secretases. The rate limiting β-secretase usually cleaves between the Met671-Asp672 residues, but prefers the preceding amino acids Asn670-Leu671 of the Swedish mutation over Lys670-Met671. The V717->Phe mutation accelerates cleavage after Ala714, which leads to the notorious $A\beta_{42}$, the decisive factor in plaque formation. The released *C*-terminal fragment interacts in the cytoplasm with an adapter protein, Fe65, and finally induces apoptosis in H4 cells [52, 53]. It seemed too obvious to address Aβ deposits directly, either by inhibition of plaque formation or by enhanced plaque degradation. Several companies pursued strategies related to "plaque busters" [54], but clinical data for this mode of action are still lacking, and there is mounting evidence that plaques are not the real culprit, e.g. AD does not correlate well with total plaque load [247]. Both soluble Aβ and *early oligomers* are now commonly blamed to be toxic, particularly in the presence of copper cations (see copper section below). This hypothesis has its merits and is hard to falsify *in vivo,* as neither copper nor *early fibrils* are detectable at the necessary sub-cellular resolution by antibodies or atomic absorption spectroscopy (AAS) of brain slices. Fortunately, there is evidence for a common mechanism in amyloidogenic diseases. The identification of minimal amyloidic sequences and the detailed understanding of protein misfolding may hold the key to treat Aβ, tau and PrP^{Sc} associated pathologies [55, 56].

β-Secretase

β-Secretase was identified as an aspartic protease, despite the initial lack of selective inhibitors [57]. The key features of an aspartic protease were confirmed: the flexible flap region, which is crucial for substrate docking. The kinetics of statine-based inhibitors revealed a two state mechanism with structural reorganisation and activity modulation [58]. The two states: open and closed, contribute to selectivity and activity of the enzyme [59]. Two β-secretases are known BACE1 (ASP2 or memapsin2) and BACE2 (ASP1 or memapsin1), with high homology, but subtle differences in the active site and an additional disulfide bridge for BACE1 [7]. BACE2 causes additional cleavages close to Phe20, which are reminiscent of α-secretase activity [60, 61]. BACE1 is anchored to the membrane via its transmembrane domain (455-480) and may be active as a dimer [62]. BACE1 has a pro-peptide domain, which is cleaved by furin-like proteases to form mature enzyme. The *C*-terminal transmembrane domain of BACE1 is not strictly required for activity, but the localisation of both enzyme and substrate in the same membrane enhances kinetics and specificity. The *C*-terminal truncation seems to influence enzyme kinetics even in the absence of membranes. BACE1 maturation requires cysteine formation (Cys216/Cys420, Cys278/Cys443, Cys330/Cys380), *N*-glycosylation and pro-peptide removal. Cysteine mutants undergo impaired maturation, but obtain catalytic activity. The Cys330/Cys380 bridge was found to be the most important [63]. Crucial for assay development and animal models: BACE1 -/- knockout mice are fertile and healthy, and display reduced Aβ levels [64]. Selectivity issues arise not only by other aspartic proteases, but by the homologous BACE2, which displays a less pathogenic APP cleavage pattern and a distinctly different localisation [60, 65, 66]. The Aβ peptide is released by a subsequent proteolysis at Val711-Ile712 or Ala713-Thr714 by the intramembrane protease: γ-secretase, resulting in $A\beta_{40}$ and $A\beta_{42}$. A detailed analysis of BACE distribution, structure, species variation, degradation and properties was published recently [67]. BACE inhibition is not the only way to modulate the BACE dependent APP cleavage. High levels of ceramide or improved raft association can extend the half life of BACE1 (16 h) [68].

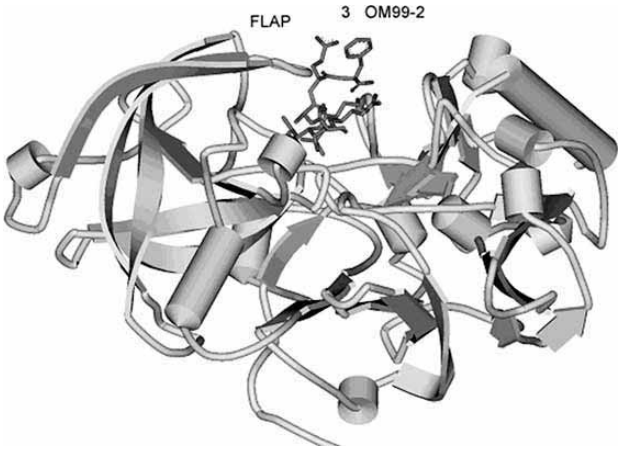

Fig. (1). BACE complexed to OM99-2 (8).

β-Secretase Inhibitors

Several inhibitors for β-secretase were identified in cellular assays, but more often than not, the true nature of the inhibition mechanism was not reported. Broad spectrum protease inhibitors such as pepstatin **7**, known aspartic

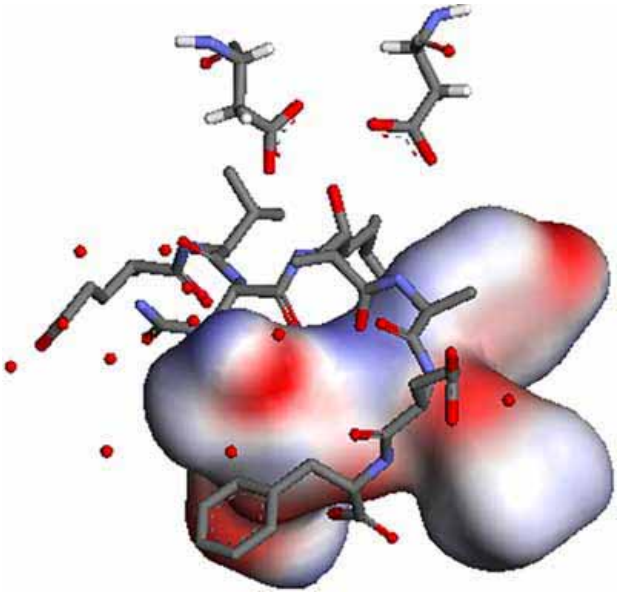

Fig. (2). BACE complexed to OM99-2 (8).

protease inhibitors from Renin and HIV protease programs, or cocktails thereof, had little inhibitory effect and gave misleading results. To this date, several reviews on secretase inhibition were published [67, 69-73]. And yet, potent non-peptidic inhibitors of β-secretase are still few. Several peptide-based inhibitors were patented or published immediately after the disclosure of BACE-inhibitor complex X-ray structures [67, 72-75] (Fig. **1** and **2** show fragments of a homodimeric structure). The active BACE1 used for co-crystallisation lacked the transmembrane and intracellular domains, and some flexible *N*-terminal regions were not resolved. The high affinity complex of Glu-Val-Asn-Ψ(Leu-Ala)-Ala-Glu-Phe (**8**, OM99-2, K_i = 1.6 nM) and β-secretase resulted in complete inhibition of β-secretase activity and allowed crystallisation and structure determination at 1.9 Å resolution (PDB: 1FKN, Fig. **1** and Fig. **2**) [67, 74-76]. The inhibitor is located in the active site as intended by design, and the hydroxyethylene is coordinated by four hydrogen bonds to the two catalytic aspartates. Further 10 hydrogen bonds are established between OM99-2 (**8**), the binding pocket and the flap region. Despite the analogies to other aspartic proteases, there are significant differences in the side chain preferences. S4, S3' are hydrophilic and readily accessible by water. The hydrophilic S4', which holds the phenylalanine, is located at the surface and contributes little to binding. The subsite specificity was revealed by the cleavage rates of combinatorial substrate mixtures and selective inhibitors. This resulted in Glu-Leu-Asp-Ψ(Leu-Ala)-Val-Glu-Phe (**9,** OM00-3, K_i = 0.31 nM), which is still the most potent inhibitor of β-secretase. The hydroxyl group of OM00-3 (**9**) is coordinated by the two active site aspartates Asp32 and Asp228 through four hydrogen bonds (PDB: 1M4H) [75, 77]. Although very similar to OM99-2 (**8,** Glu-Val-Asn-Ψ(Leu-Ala)-Ala-Glu-Phe), the P3, P2, and P2' residues are exchanged, resulting in a more linear and extended conformation at either end. The replacement of the P2' alanine by valine facilitates binding and allows re-orientation of the P3' glutamate and the P4' phenylalanine. This shifts the *C*-terminal residue towards the surface of the enzyme and exposes it to the solvent.

The crystal structure of free BACE (1SGZ) revealed a part of the flap to be locked in an "open" position [76]. The structure is essentially the same as BACE1 bound to an inhibitor, but the flap positions differ by 4.5 Å at the tips. The open position of the flap is stabilised by two intraflap hydrogen bonds and is anchored by a new hydrogen bond involving Tyr71 in a novel orientation. The resulting gorge may contribute to sequence and shape selection. A gatekeeper function was evident from the unusually small substituent Ala in P2' (**8**, 1FKN). Thr72 forms the narrowest point (6.5 Å in apo BACE) [248] between the flap and Arg235, Ser328, and Thr329 on the opposite side, and thus contributes to the specificity of BACE. This gatekeeper blocks the access of peptides carrying larger residues in this position, although pocket P1' provides more than enough space for a significantly larger residue [76]. The small interaction of the *C*-terminal end of the octapeptides OM99-2 (**8**) and OM00-3 (**9**) with the enzyme inspired the design of shorter peptidic inhibitors (**10**-**13**). Different peptidic inhibitors featuring the hydroxyethylene moiety and flanked by multitude of amino acid residues were published

A **B**

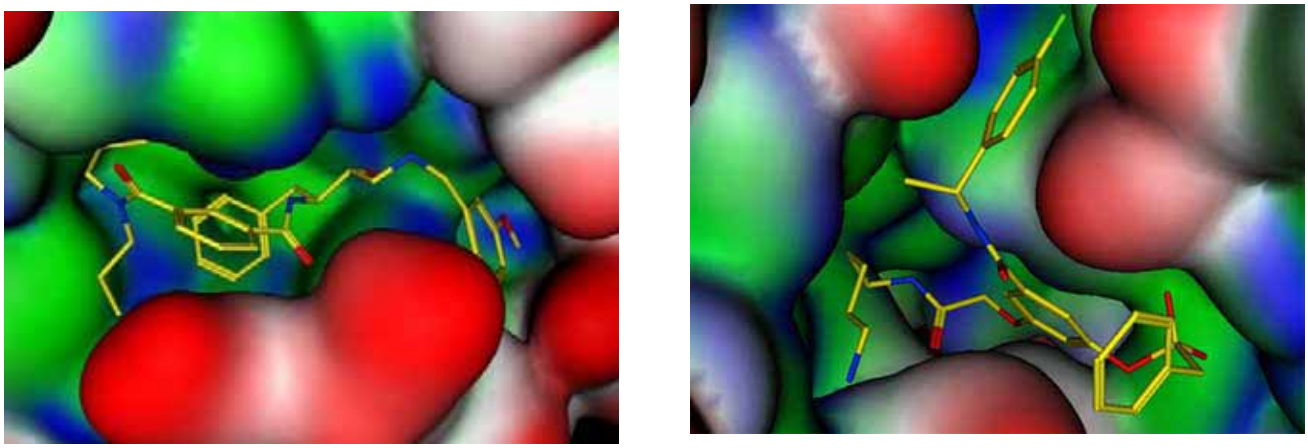

Fig. (3). (**a**) Isophthalamide 18 (yellow) and (**b**) resorcylate 27 (yellow) above the flap. MOE 2004.10 GaussConolly surface green: hydrophobic, blue: hydrophilic (PDB: 1W51, 1TQF).

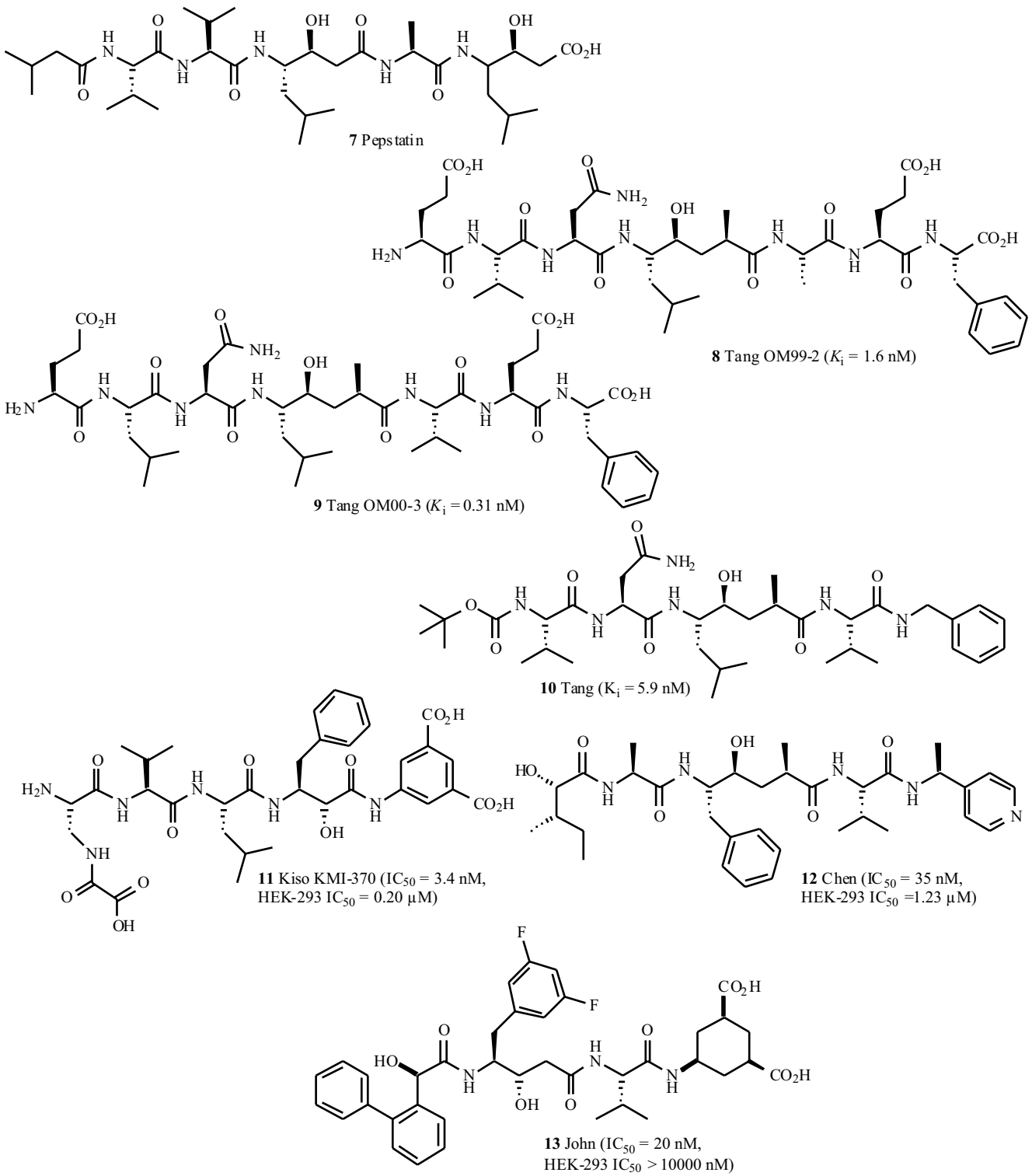

Scheme 4. BACE inhibitors I.

(Schemes **4** and **5**) [78-82]. Remarkably, the compact P1'-Ala of potent inhibitors has never been replaced by a sterically more demanding group.

Several scaffolds are known to provide inhibitors for aspartic proteases. Statines, norstatines, hydroxyethylamines and hydroxyethylureas can be employed as transition state mimetics, yet with dramatic differences in potency. The Kiso inhibitor **11** (KMI-370, IC_{50} = 3.4 nM) featured a short *C*-terminal dicarboxylic acid and displayed high activity *in vitro* and *in vivo* (BACE1-HEK293 cells EC_{50} = 0.20 μM) [83]. Chen *et al*. synthesised Ψ(Phe-Ala)-basedpentapeptide mimetics like **12** (IC_{50} = 35 nM) and came to similar conclusions [84, 85]. The SAR of these two series postulated a benzyl or a 3,5-difluorobenzyl residue to occupy the P1 position as realised in compound **13** [86, 87]. A good part of the peptidic heritage was replaced by an isophthalamide [88], which functions as the *N*-terminus in

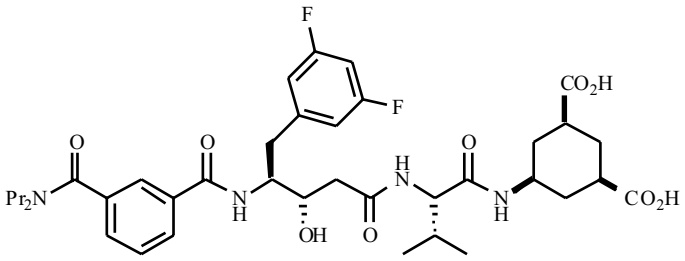

14 Elan (IC_{50} = 1 nM, HEK-293 IC_{50} = 1μM)

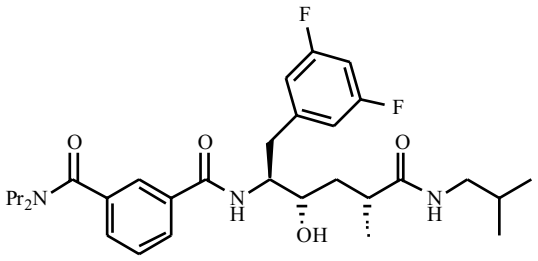

15 Elan (IC_{50} = 30 nM, HEK-293 IC_{50} = 3 μM)

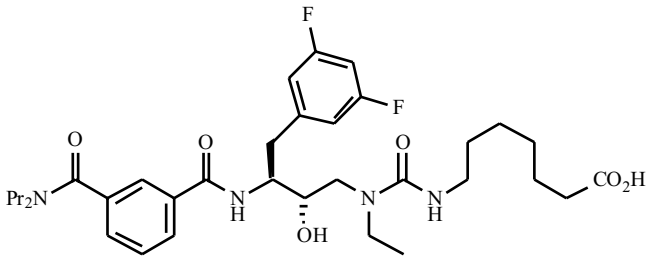

16 Elan

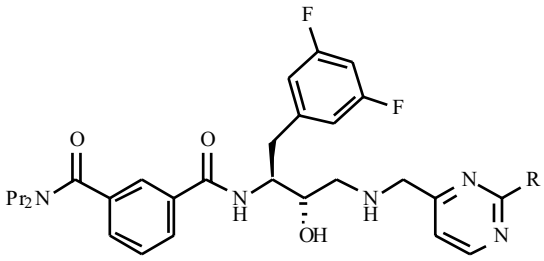

17 Elan

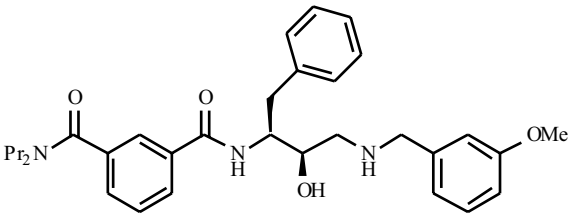

18 Astex (IC_{50} = 200 nM)

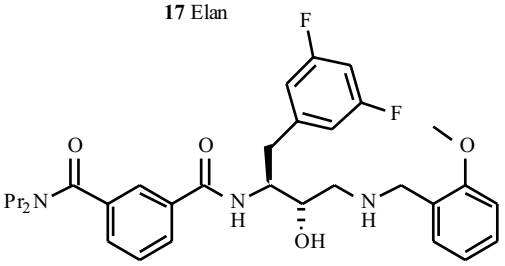

19 Elan

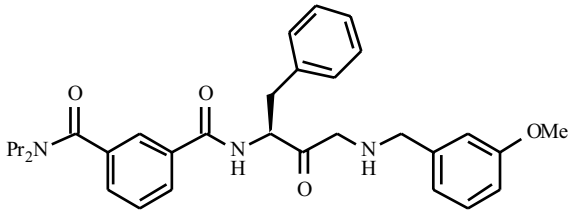

20 Takeda (IC_{50}= 99 nM)

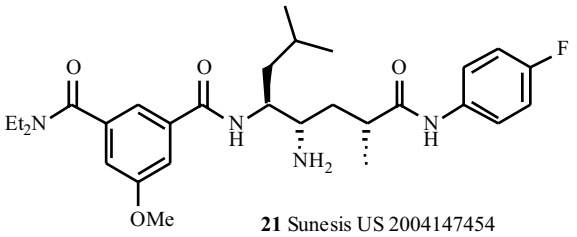

21 Sunesis US 2004147454

Scheme 5. BACE inhibitors II.

the compounds **14-21**. The switch from the statine core to the hydroxyethylene isoster allowed the replacement of the carboxylic acids by smaller groups, and resulted in the compact inhibitors (**16-19**) with reduced molecular mass and fewer hydrogen bond donors.

The Elan compounds (**13-19**) have lost a good part of their peptidic origin, which is mandatory to obtain sufficient oral absorption and blood brain barrier penetration [89, 90]. Significant information was revealed by a novel BACE complexed to a transition state mimetic [91]. Soaking of *apo* BACE crystals (PDB: 1W50) with small peptidomimetics, which were known to be moderate inhibitors in FRET or cellular assays, resulted in the incorporation of **18** in the active site (PDB: 1W51, Fig. **3a**). This peptide mimetic features the isophthalamide to mimic the S2-S4 section and was claimed to have an IC_{50} = 200 nM. Some 750 close analogues were revealed in patents by Takeda (**20**) [92], Glaxo [93], Upjohn Pharmacia, [94-96] Elan (**19**) [89, 97-99], Astex [100] and a Sunesis employee (**21**) [101]. But the amino alcohol **18** held a little surprise, despite the *R*-configuration of the alcohol, it was far more potent than its *S*-configured diastereomer or the parent ketone, and thus contradicted previous SAR of the absolute configuration. The neighbouring amine receives a proton from the catalytic Asp^{228} and places its benzyl substituent in the S2′ pocket. One of the *N*-propyl groups of the isophthalamide occupies the S3 pocket and is directed towards the phenyl ring in the S1 pocket. The phenyl rings in both the S1 and the S2' pocket interact with Tyr71. The *C*-terminal methoxyphenyl is positioned in the S2' pocket. This success in high-throughput crystallography enabled ASTEX to license out this programme to GSK in 2003.

Despite all efforts by the pharmaceutical companies and academic groups, non-peptidic leads for BACE inhibition are still few. The FRET assays of soluble BACE deliver false positive hits to such a degree, that it is mandatory to profile

potential hits in a reliable secondary assay, such as a radioligand displacement [102, 103]. This progress in assay development allowed to identify peptidic and non-peptidic leads. Takeda reported a tetraline (**22,** Scheme **6**), which is not an obvious scaffold for protease inhibition and is likely to stem from high-throughput screening efforts [104]. The activity is poor ($IC_{50} \geq 1$ μM) and the mode of action was not confirmed. Neurologic's diacid (**24**) [105] is unlikely to be an easy lead for AD. Latifolin (**23**), isolated from the heartwood of *Dalbergia sissoo*, was reported to inhibit the Aβ synthesis with an IC_{50} of 180 μM, again a rather weak and unsecured activity [106]. Vertex reported [107] the biphenylpiperazine (**25**) as BACE inhibitor (IC_{50} = 3 μM) and it was docked into the BACE structure by Park and Lee [108]. An unfortunate error improved it to 3 nM, which makes the outcome of this docking very questionable. Yet, similar biphenylated amines (**26**) were revealed by Actelion [109, 110]. MSD undertook the rational design [81, 111-113] of BACE inhibitors like many others [114-116].

More innovation was obtained by an *Automated Ligand Identification System* (ALIS): a novel resorcylic acid scaffold [117]. The amino pentyl derivative **27** was obtained after subtle modifications of the lead structure and displayed a moderate inhibition of BACE 1 (IC_{50} = 1.4 μM) and good selectivity towards cathepsin D (IC_{50} > 500 μM). A modified BACE 1 (K75A, E77A) was used for co-crystallisation with **27** (PDB: 1TQF, Fig. **3b**), which occupies the S1-S4 subsites. Quite unusually, the S' sites and the active site have no direct contact with the inhibitor. The acetamide is engaged in a hydrogen bond to the catalytic water, which is placed between the two aspartates. The 4-fluorophenyl moiety wedges the novel S3 subpocket open and the aminopentyl coils back into the S1 pocket. The S1 and S3 substituents may be linked together to result in macrolactams with reduced rotational freedom, the only way to improve activity [112]. Extension towards the active site, occupation of P1 by a phenyl group and placement of a cyclopropyl in P1' improved the inhibition to 11 nM for **29** and retained 500-fold selectivity towards cathepsin D [118]. The compound was co-crystallised with BACE, but there was no entry in the PDB by 11/2004. DeNovo reported several scaffolds and mimetics: sulfonamides, 1-piperazinylpropan-2-ols and the triazine **28**, which may offer additional imaging of Aβ fibrils [119-122].

γ-Secretase

Paradoxical: despite being the secretase reported first, the identity of γ-secretase was for a long time a subject debate and the detailed structure is still unknown. The close relation to the Notch pathway, which is important in embryonic development, became less hazy over the years.

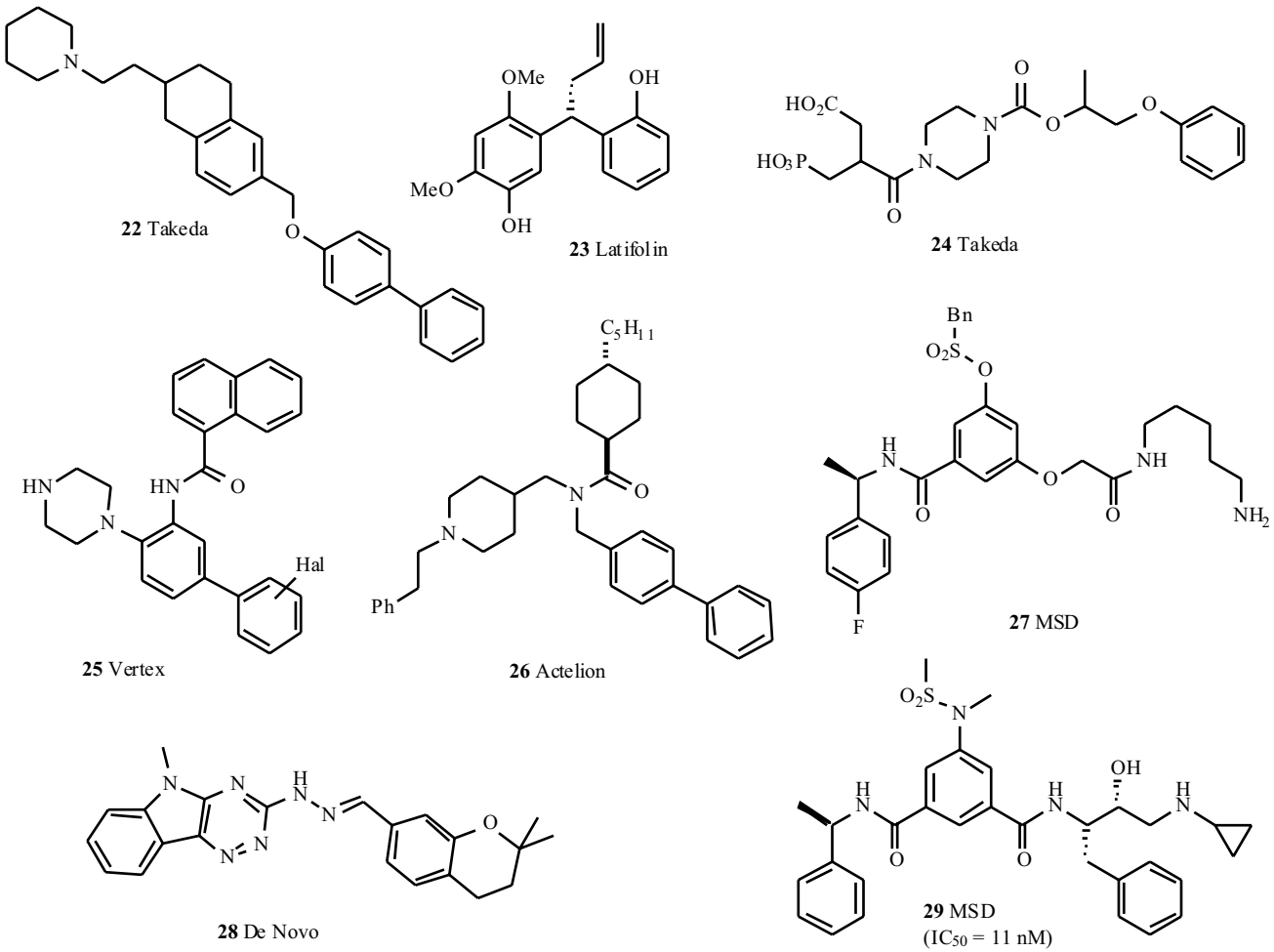

Scheme 6. Non-peptidic BACE inhibitors.

Notch 1, an integral membrane receptor, is processed by proteases upon ligand binding. The intramembranous cleavage is similar to the APP cleavage and requires PS1. The released intracellular domain migrates to the nucleus, where it finally activates Notch target genes [123]. The crossover to the Notch pathway hampered attempts towards PS-/- knockout animals, which do not pass the embryonic state, but embryonic stem cells may fill a part of the gap [124]. The intracellular trafficking of Notch in human CNS neurons is reduced by PS1 inhibitors, and results in dramatic changes in neurite morphology. Maybe the Notch dysregulation causes the neuritic dystrophy observed in AD brain tissue [125]. Several other substrates are known to be cleaved by γ-secretase, which seems to be the "proteasome of the membrane" [126]. The relevance of the presenilin co-factors: Pen-2, Aph-1, Nicastrin is well established [8], and even isoforms of these co-factors have been studied at detail [127]. The Nicastrin association to FAD was questioned recently [128]. Cell free γ-secretase assays are still an art, despite the progress in kinetics and feasibility [129]. Substrate optimisation was crucial for both β-secretase and γ-secretase assays [130, 131]. The localisation of the active site within the membrane and the cleavage within the membrane anchor of C99 turns γ-secretase inhibition into a rather slippery fish. Currently, there is only one related enzyme: the signal peptide peptidase, which shares a number of the features and problems, but is inserted into the membrane by 7 transmembrane helices [132]. A proposal for the arrangement of the transmembrane helices has been made, but it does not explain the observed cleavage pattern of APP [133]. Moreover, the importance of the cytoplasmic tail is not acknowledged in this model; two sequences of this tail are required for ER-retention and Nicastrin binding [134]. The active site of γ-secretase is known at some detail and the concerted action of all co-factors is still a subject of debate. The replacements of both Asp257 and Asp385 within the transmembrane regions of PS1 (and the analogue replacements in PS2) inhibit γ-secretase activity [135, 136]. Furthermore, both Asp modifications significantly inhibited the Notch pathway. The Notch pathway may be a druggable target on its own; however, applications in oncology were claimed already [137, 138].

γ-Secretase Inhibitors

Non-peptidic inhibitors of γ-secretase are known from the patents by Elan/Eli Lilly, Bristol Myers Squibb and DuPont. Peptidic PS1 inhibitors, like Merck's L-685,458 (**30**) [139] are still the most potent inhibitors and were patented [140] prior to publication in scientific journals [141, 142]. Lipophilic di- and tripeptides with bulky *N*-terminal protection are common inhibitors for γ-secretase and β-secretase. Lacking specificity and the inhibition of serine and cysteine proteases makes the use of these aldehydes rather cumbersome, because the general protease inhibition results in complex concentration activity

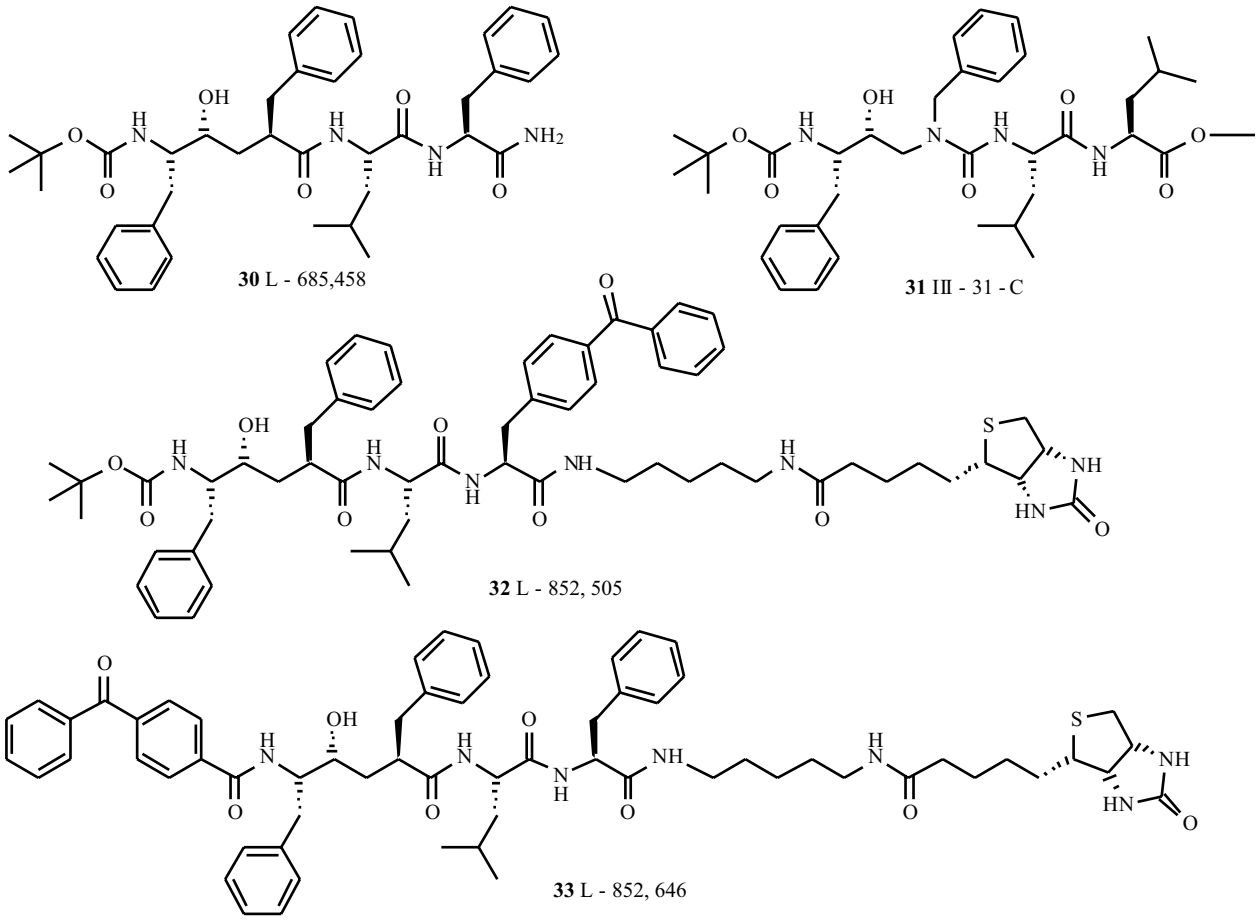

Scheme 7. γ-Secretase inhibitors I.

relationships. Obviously, this structural motif serves just a tool for assay development and labelling [143-150], e.g. difluoro ketones were used to block endoproteolysis of PS1 and to differentiate γ-secretase activity and Notch cleavage by selective modulation [151, 152]. The inhibition by several difluoro ketones supported the point mutation analysis and confirmed the phenylalanine scan of the APP transmembrane domain [133]. This scan strongly supported a unique α–helical presentation of the C99 fragment to the γ-secretase. Initial attempts of α-helix induction by α-amino isobutyric acid (Aib) were not convincing [153]. Yet, a surprising activity of an all D-tridecapeptide: Boc-VGAibVVIAibTV-AIbVIAib-OMe (cell free IC_{50} = 0.14 nM) was reported by Wolfe et al. recently [154, 155]. A more druglike tetrapeptide mimetic Boc-Ψ(*Phe*-Phe)-*Leu*-*Val*-OMe displayed a cellular IC_{50} of 0.4 μM [156].

A giant leap forward was obtained by the serendipitous identification of Merck's L-685,458 (**30,** Scheme **7**). The all-lipophilic sequence with 3 phenylalanines was somewhat anticipated, as several studies [133] had indicated the lipophilic binding pockets (P2, P1, P1', P2', even P4' and P7') in proximity to the cleavage site. The inversion of the hydroxyethylene moiety reduced the inhibition 270fold. Labelling studies were conducted with different non-radioactive probes, linking biotin and photoreactive fragments *N*- or *C*-terminally to the core structure to furnish L-852,505 (**32**) and L-852,646 (**33**). The biotin was introduced to facilitate the isolation and identification of the irreversibly labelled adducts via their streptavidin-enzyme linked conjugates. Both attachments of photoreactive benzophenones (L-852,646 (**33**), L-852,505 (**32**)) retained potent inhibition (IC_{50} < 1 nM for γ-secretase). Photolysis in the presence of solubilised γ-secretase provided a protein of 20 kD (L-852,505, **32**) after isolation on a biotin-specific streptavidin-agarose gel, followed by partial digestion. This 20 kD fragment was shown to be the C-terminal fragment of presenilin 1 (PS1-CTF) by specific antibodies. Binding to wild-type PS1 was negative in a control experiment, yet binding to the deletion construct PS1ΔE9, which lacks the cytosolic E9 loop, was positive [157]. Useful information resulted from the photolysis of L-852,646 (**33**) in the

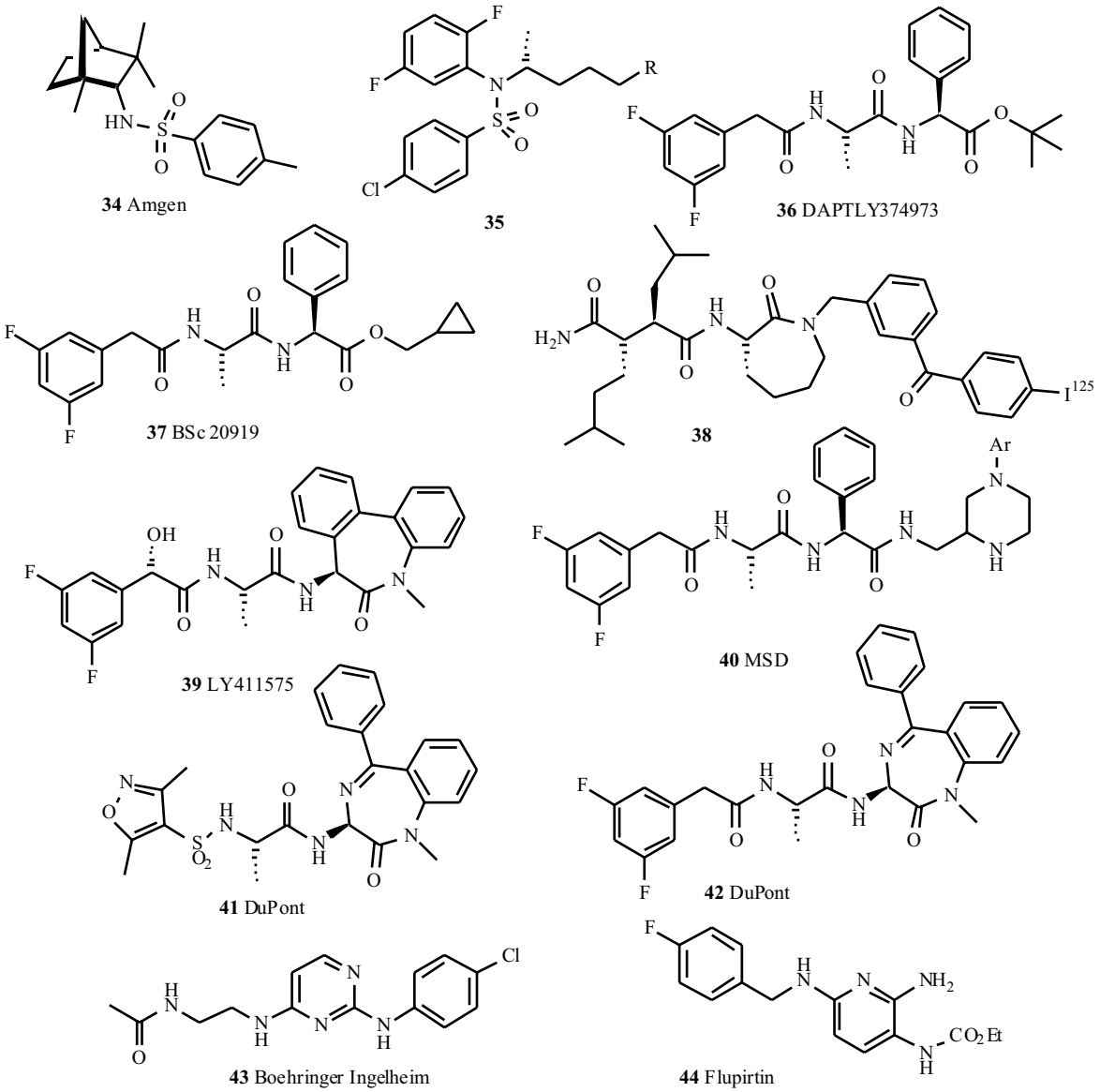

Scheme 8. γ-Secretase inhibitors II.

presence of solubilised γ-secretase. This resulted in the isolation of a 34 kD fragment, which was assigned to be an *N*-terminal fragment of PS1.

A similar transition-state motif, the hydroxyethylurea [158], was utilised for activity based affinity purification. The immobilisation of III-31-C (**31**, IC_{50} < 300 nM) on affi-gel 102 allowed isolation and identification of PS1-CTF, PS1-NTF and Nicastrin from solubilised γ-secretase preparations [159]. Initial attempts to free active γ-secretase from the affinity gel failed. This was probably due to the high binding affinity of III-31-C (**31**) to the target protein complex, and partially due to the deep and narrow binding site, which required strong denaturing conditions to break up the binding interactions. A delicate combination of Brij-35 and CHAPSO resulted in the isolation of active γ-secretase. The co-precipitation of the inhibited γ-secretase with its substrates C83 and C99 gave rise to speculations about additional binding sites, where the substrate is recognised prior to transfer to the active site. These speculations are in accordance with the observed promiscuous nature of the cleavage, as they assign the specific recognition to other domains.

To this day, very little structural information is available for the γ-secretase complex. Therefore, selective, non-peptidic γ-secretase inhibitors had to be provided by HTS efforts. Elan's DAPT **36** (HEK IC_{50} = 20 nM) was developed from a *N*-dichlorophenylalanine lead, and the phenylglycine and the difluoro phenylacetic acid are crucial for activity [160-162]. DAPT is not a prodrug, despite the labile tertiary butyl ester, which may be cleaved at the low pH of the gut. The even more labile cyclopropyl methyl ester **37** displayed similar activity [163]. Replacements of the ester by amides were tolerated, but primary alcohols were almost inactive [164]. The subcutaneous application to mice in a dosage of 100 mg/kg, resulted in a 50% reduction of cortical Aβ levels within 3 hours. A 40% Aβ reduction was observed at the dosage of 100 mg/kg orally, again after 3 hours, but no brain levels of DAPT were reported for the latter study. Moreover, there is evidence for the slow removal of tau lesions under DAPT treatment [165]. There were several reports of *in vivo* toxicity, mainly because DAPT effects the Notch pathway at higher levels (100-1000x) [166]. A biotinylated DAPT-based photoaffinity label (DAPT-BB) was used to investigate the competition of sulindac-*S* (**4**) and L-685,458 (**30**) for the active site of PS1. DAPT-BB binds to the PS1 CTF. There was no competitive replacement by sulindac-*S* up to 100 μM. The displacement of DAPT-BB by L-685,458 (**30**) depended on the CHAPSO concentration: full displacement at 0.25% CHAPSO, but only partial displacement at 1% [138]. Further improvements included the stereoselective placement of the hydroxyl group and the locked spatial arrangement of two phenyl rings in a caprolactam to result in **39** (LY411575, HEK IC_{50} < 1 nM), which is still the gold standard in the field. It halved plasma and cortical Aβ levels in young mice already at the oral dosage of 1 mg/kg. LY411575 (**39**) and a lesser active diastereomer were administered [167] orally to C57BL/6 and TgCRND8 APP mice for 15 days at 1-10 mg/kg per day and resulted in the reduction of Aβ levels. This was accompanied by atrophy of the thymus and deterioration of the intestinal epithelium. The Notch/APP selectivity was determined in cellular assays: $Aβ_{40}$ IC_{50} = 0.082 nM, Notch IC_{50} = 0.39 nM. This small toxicity window will be a crucial issue for clinical trials. Curiously, the Aβ lowering abilities of DAPT-like compounds are not effected by their sometimes poor blood brain barrier penetration. Thus, inhibition of APP processing in the periphery or enhanced clearance of peripheral Aβ by neprelysin [168-170] and other degrading enzymes [171] may hold a key for causal treatment.

Bristol Myers Squibb and Merck [172] disclosed 1000 derivatives of 4-Chloro-*N*-(2,5-difluorophenyl)-benzenesulfonamides **35**. 500 of these were reported to be very good inhibitors of γ-secretase activity. The activity clustered around the core structure **35**, with a wide variation of the substituent R to modulate bioavailability. Less active

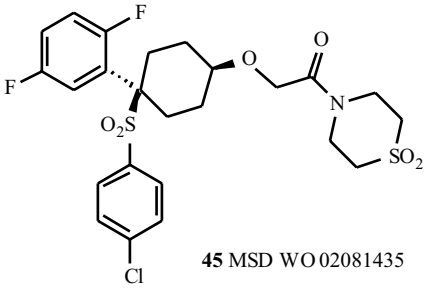

45 MSD WO 02081435

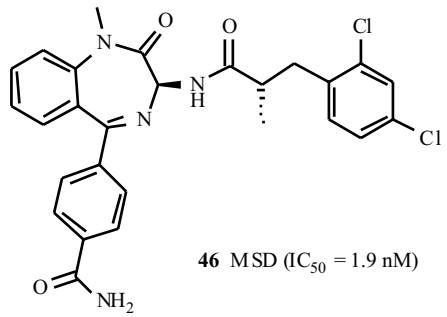

46 MSD (IC_{50} = 1.9 nM)

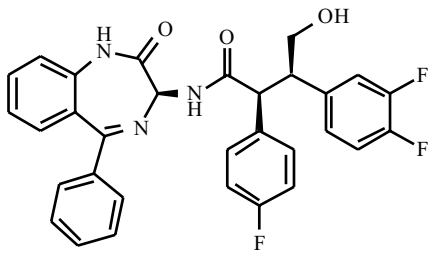

47 MSD (IC_{50} = 0.06 nM)

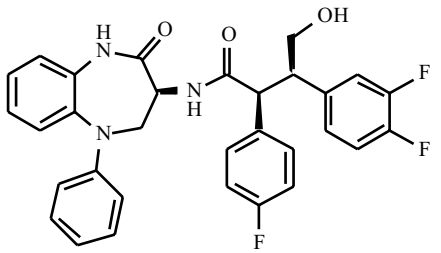

48 MSD (IC_{50} = 0.07 nM)

Scheme 9. γ-Secretase inhibitors III.

sulfonamides (**34**, IC_{50} = 2 μMol, Scheme **8**) were reported by Amgen and MSD, which featured similar bicycloalkane skeletons. They share the arylsulfonamide moiety with **35**, but lack the crucial *N*-alkyl extension [173, 174]. DuPont's hybrid structure **38** [175] bears both signatures of a dipeptide based SAR and the lead, which was identified from a matrix metalloproteinase (MMP) programme. Removal of the central amide bond of the parent dipeptide, the replacement of the hydroxamic acid by an amide and the introduction of a caprolactam provided good activity and removed some of the problems associated with dipeptide leads. The potent compounds (IC_{50}: 20-90 nM) were related to DAPT-like compounds and hybrids of the two series. The difluorophenacyl-caprolactam derivative **42**, stemming from a Scios/DuPont cooperation, proved to be the most potent compound (IC_{50} = 0.3 nM) [176].

DuPont Pharmaceuticals, which was taken over by Bristol-Myers Squibb, went on to elaborate the caprolactam motif and described a large number of derivatives in a patent family. Some effort was dedicated to modify the *N*-terminus, in order to avoid patent infringement of Elan patents and resulted in the oxazolylsulfonamide **41** [177, 178]. Another straightforward attempt to bypass Elan claims is present in a recent Merck series, which is generalised in compound **40.** Moreover, this series was claimed to be inactive on Notch signalling [179]. Several other compounds or claims exist for hybrid structures of **37** and **38**. A common feature is an aza-caprolactam, which places the phenyl groups in a defined, twisted arrangement. Additional residues can be attached to the amide, and the glycine is commonly exchanged for small spirocyclic amino acids or amide excision peptidomimetics. Unfortunately, activities for these compounds were not reported yet. Boehringer-Ingelheim [180, 181] disclosed diaminopyrimidines (**43**) as non-peptidic inhibitors of γ-secretase with an IC_{50} = 4 to 1000 nM. The single patent application is written in German and the most active compound is therefore hidden well. But the BI lead resembles flupirtin (**44**), which displayed beneficial effects on the cognitive function in humans [182]. MSD bypassed the BMS claims for sulfonamide (**35**) by introduction of a cyclohexyl linker (**45,** Scheme **9**). The seven-membered lactam re-appeared in several MSD structures (**46**-**48**) [183, 184], but the insufficient Notch selectivity put an end to the promising candidate **46** [185].

Nonsteroidal Anti-inflammatory Drugs (NSAIDS)

Negative outcomes have been reported for the non-steroidal anti-inflammatory drugs prednisone, diclofenac, rofecoxib and naproxen [6]. But promising results were obtained with some COX1 inhibitors [27], both *in vitro* and in a prospective, population-based cohort study of 6989 patients [28-30]. These convincing clinical results are still in need of a sound rational and experimental validation. The proof of concept is still missing, despite the rapid progress. Potential modes of action were hinted or reported several times, but there is much heat and little light: "Non-steroidal anti-inflammatory drugs may lower amyloidogenic $A\beta_{42}$" by inhibition of Rho/ROCK [31]. Yet, the Rho/ROCK inhibitors were applied at concentrations several magnitudes higher than the required IC_{50} for Rho/ROCK inhibition. In summary, just few NSAIDs (**3-6**, Scheme **2**) display the desired effect, and if they do so, they do it by modulation of γ-secretase. The active NSAIDs interfere with substrate recognition/cleavage and shift the Aβ cleavage to the $A\beta_{38}$ fragment. Any derivatisation of the NSAID's carboxylic acid results in loss of this activity or inversion of the $A\beta_{38}$ impact (unpublished results).

Flurbiprofen **3** (10 and 25 mg/kg/d) elicits non-selective reductions in both $A\beta_{1\text{-}40}$ and $A\beta_{1\text{-}42}$ plasma levels, and was found to be toxic. It produced small reductions in $A\beta_{1\text{-}40}$ in the cortex at 25 mg/kg/d, but did not affect Aβ levels in the hippocampus or CSF. Contrary to previous reports, sulindac sulfide (**4**) and ibuprofen (**6**) were found to be neither toxic nor efficacious at doses up to 50 mg/kg/d [32]. The striking discrepancies between these results and the previous reports by Eriksen [33] and Weggen [28, 29] may be explained by the different methods used to extract brain Aβ: alkaline guanidine solution versus 70% formic acid. The kinetics of Aβ formation in the presence of the two NSAIDs and the displacement of an active site directed inhibitor support allosteric, non-competitive modes of action of sulindac-*S* (**4**) and *R*-flurbiprofen (**3**) [34] at low concentrations. This results in selective inhibition of $A\beta_{42}$ production. However, both NSAIDs shift their mode of action from modulation to complete, non-selective inhibition of γ−secretase at high concentrations. This remarkable pharmacological behaviour may be explained by the stabilisation of dimeric or multimeric enzyme. Unfortunately, NSAID derivatives have escaped photolabelling techniques so far, although they are known to increase capture efficiency in affinity precipitation.

Vaccination

Immunisation therapies against Aβ hold high potential and are under investigation by several companies [35]. The most advanced companies in this field: Elan Corp plc and Wyeth-Ayerst Laboratories, suffered a setback of their joint clinical development of AN-1792 in March 2002 [36]. The phase IIa trials were abandoned after observation that 4 out of 372 patients displayed clinical signs consistent with inflammation in the central nervous system. The alarming and unexplained brain-shrinkage of 6% on average and the lack of cognitive improvement backed the decision to end the trial, but all patients were monitored until December 2002 [37, 38]. Unfortunately, just 13 patients were monitored afterwards, although a small group displayed significant improvements in brain volume and cognitive abilities [39]. These positive results suggest further studies with improved epitopes or different vaccination strategies. Aβ vaccination reduces not only extra- and intracellular Aβ accumulation, but is accompanied by the clearance of early tau pathology. The tau pathology is reduced by the proteasome and depends on tau phosphorylation. Hyperphosphorylated tau aggregates remained unaffected by this antibody treatment [40]. On the contrary, the clearance of tau aggregates was reported for immunotherapy and DAPT treatment. However, Aβ deposits were cleared within 3 days after injection, versus 5 days it took for the reduction of tau lesions [40].

Indirect Approaches- or: Do Our Souls Reside in Fat?

Lithium chloride was found [186] to reduce secreted Aβ levels in 3 different cell lines: COS7, CHO and HEK.

Unfortunately, lithium displays a small therapeutic window and the required concentrations of 1-5 mM are well above tolerated therapeutic plasma levels of 0.8-1.2 mM. The mediator of the lithium activity is likely to be a better target for drug development. A similar effect was observed [187] for kenpaullone (**49**, Scheme **10**), an unselective inhibitor of glycogen synthase kinase-3 (GSK3) [188]. Control experiments with other unselective inhibitors for the two forms of GSK3: GSK3α and GSK3β, suggested GSK3α to offer indirect modulation of γ-secretase, including Notch selectivity. These spectacular claims for GSK3α were backed up by siRNA knock-downs, but are contradicted by a reported involvement of GSK3β [189].

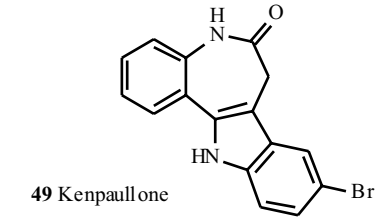

49 Kenpaullone

Scheme 10. Kenpaullone.

Brain cholesterol accounts for up to 25% of total body cholesterol and is turned over within a few months. Individuals on a high-cholesterol diet are at increased risk to develop AD, but the cholesterol brain levels were unaffected in animal models. Some cholesterol lowering drugs such as pravastatin and lovastatin, resulted in reduced risk for AD in retrospective trials. Paradoxically, prospective trials resulted in a rather confusing situation with contradicting outcome, most prospective trials failed to confirm a risk reduction for AD [190]. Simvastatin does not reduce risk and pravastatin exerts the effect regardless of the blood-brain barrier (BBB) crossing [190-193]. The answer is not simple; both simvastatin and lovastatin pass the BBB in the prodrug form, prior to hydrolysis to the active acids, and can be detected in the CSF. The rationale for this activity is still subject to debate, but three important observations may hold the clue for an explanation: 1.) hypercholesterolemia results in increased levels of extractable total Aβ in mice 2.) BACE1 was found to be associated with cholesterol stabilised rafts [194-197] in the plasma membrane and 3.) the activity of the benign α-secretase is inversely related to cholesterol levels [195]. The relevance of these different, yet concerted modes of actions remains to be established in humans, but transgenic mice respond to hyper-cholesterolemia by reduction of soluble Aβ [196]. The pleiotropic, non-lipid-related activities may be caused by the inhibition of the isoprenoid synthesis downstream of HMG-CoA reductase, interfering with RAS and thus cell signalling [50]. A specific inhibitor of squalene synthase can inhibit the cholesterol biosynthesis, but does not block the isoprenoid pathway leading to dolichol and ubiquinone. The potential of such inhibitors was published for the cholesterol-lowering BM15.766 (**50,** Scheme **11**), which resulted in halved Aβ brain loads. The plasma Aβ levels correlated well with the plasma cholesterol [197], but the brain cholesterol went down by a meagre 11-13%, which may be explained by uncorrected cholesterol determination. RPR107393 (**51**) and its *R*- and *S*-enantiomers are potent inhibitors of rat liver microsomal squalene synthase (IC_{50} = 0.6 to 0.9 nM) and modulate Aβ levels in transgenic mice [190]. The cholesterol acyltransferase ACAT modulates the generation of Aβ, and is thus a welcome addition for existing ACAT programmes [251, 252]. Most ACAT inhibitors were developed for cardiovascular therapies and still have to prove their clinical potential to treat AD.

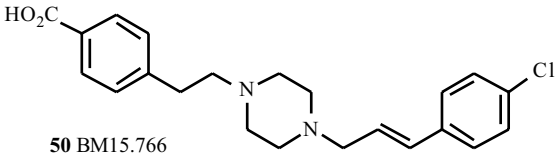

50 BM15.766

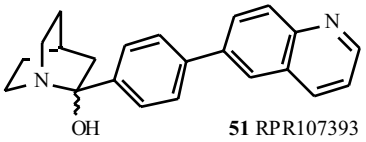

51 RPR107393

Scheme 11. Cholesterol lowering drugs with impact on Aβ levels.

Copper and Chelators

The copper enhanced Aβ associated toxicity stimulated investigations of dietary copper and copper homeostasis in mice and men [13, 198]. The initial hypothesis had to be revised, as increased copper levels (0.25 g $CuSO_4 \cdot 5\ H_2O$/L) in drinking water turned out to decrease Aβ levels in transgenic APP mice. A potential mode of action may be present in the reduced superoxide dismutase 1 activity. Metal chelators were frequently investigated to moderate copper levels in brain tissue, which were thought to be responsible for Aβ toxicity. However, in most *in vitro* studies, the copper concentrations required to observe the effect were magnitudes higher than found *in vivo*. Studies in 20 patients with clioquinol **52** (Scheme **12**), a metal chelator that crosses the blood-brain barrier readily and has similar affinity for zinc and copper ions, indicated interesting results.

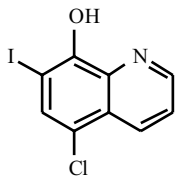

52 Clioquinol

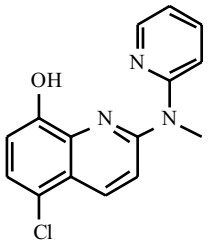

53 PBT1056

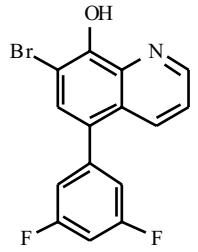

54

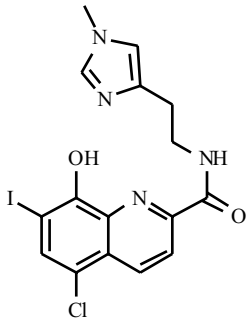

55 PBT1050

Scheme 12. Clioquinols.

But the lack of a control group in the study, left ample room for other explanations, e.g. inflammation stimulus [199, 200]. However, recent data from animal models support a benign impact of clioquinol on copper homeostasis. Clioquinol was found to mediate copper uptake and counteract copper efflux activities of APP [201]. The improved selectivity of the quinol towards copper was addressed by Prana Biotechnology [202], who submitted a multitude of clioquinol analogues to a catalase type assay in the presence of Aβ. Several inhibitors (**53-55**) were profiled in rats and the DMPK properties were communicated in a patent application.

Diagnostics - Markers for AD

Several genes and small molecules such as 24S-hydroxycholesterol, were previously linked to the age of onset and the severity of Alzheimer's disease [203-205]. Genetic factors are well established and reviewed: e.g. the ApoE e4 allele, which is a risk factor, but not a deterministic gene [206]. Currently, all these genes and their derived products, e.g. inflammatory proteins [207], do not fulfil the requirements for large scale diagnosis or medical imaging. Unfortunately, most of the promising, small molecules require sampling of cerebrospinal fluid (CSF) [208], which

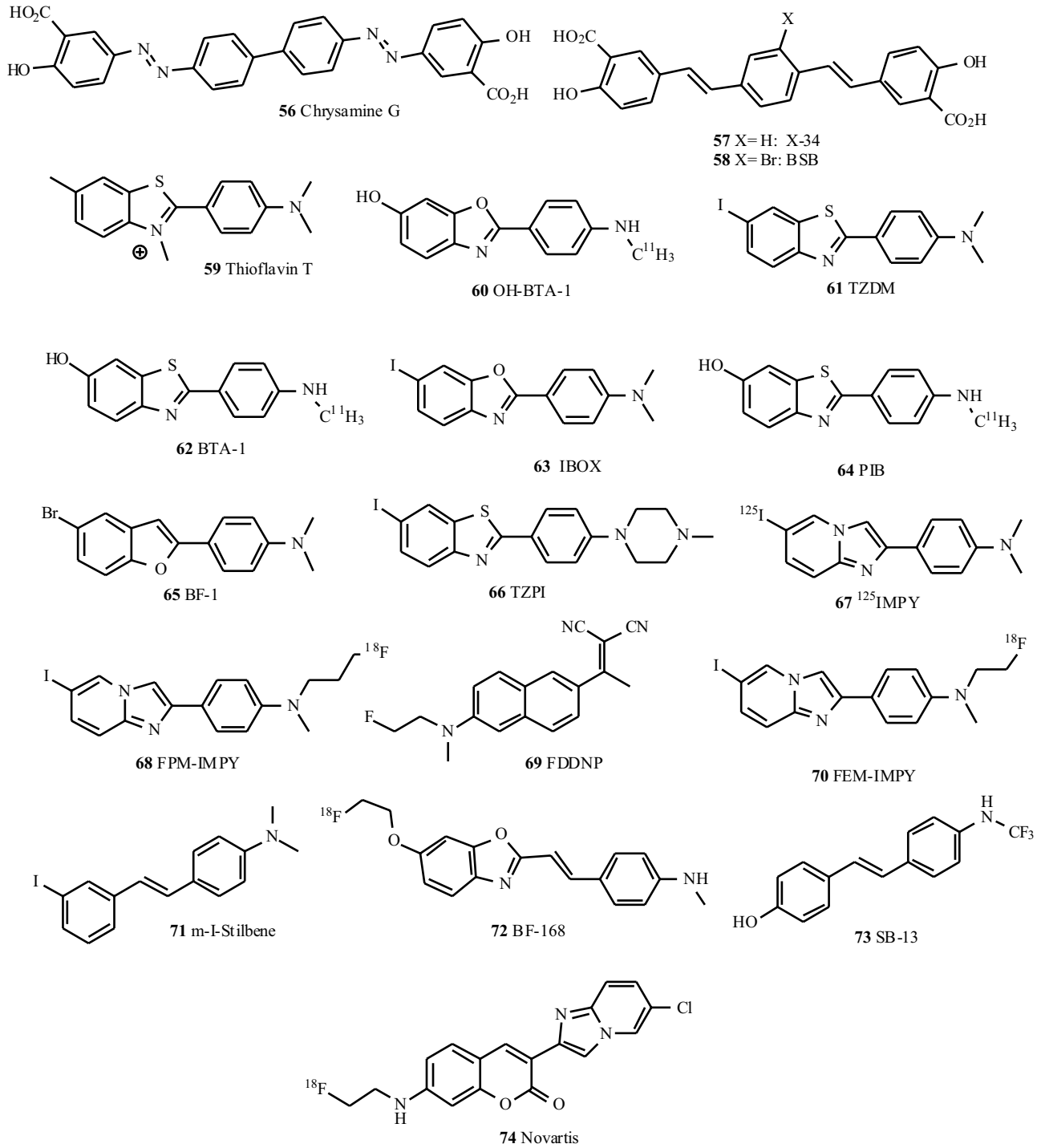

Scheme 13. AD imaging probes.

will be a major obstacle in clinical trials [209-214]. α7-nAChR levels correlate [215] to the Aβ levels, but the reliable sampling of indicative cells (e.g. olfactory neuroblasts) remains to be an issue. Congo red, which is known to stain amyloid deposits for several decades [216-218], stimulated the ongoing search for small markers of Aβ levels. Yet, the detailed mechanism of Congo red binding is still a subject of investigations [219-224]. Most amyloid binding dyes do not differentiate between the different aggregates of Aβ, PHF and PrP^{Sc}. This lack of selectivity is almost irrelevant for the development of aggregation inhibitors, but is a crucial issue for diagnostic markers. The Aβ deposits precede the formation of tau positive paired helical filaments, thus amyloid markers suitable for radio diagnostic of Alzheimer's disease have to be selective for just one of the proteins deposits, which accompany the pathology. Specifically designed compounds address the issue of improved brain penetration, and radioactive compounds were explored for non-invasive imaging: PET and SPECT. A technetium bipyridyl complex was reported in 1996, but was not taken up by other groups [225]. Chrysamine-G (**56,** Scheme **13**) [220] overcome some of the drawbacks of Congo red, particularly the poor BBB penetration. Furthermore, it indicated a promising inhibition of Aβ derived toxicity. X-34 (**57**), and its derivative BSB (**58**) were radiolabelled and profiled in rodents [226-229]. The pharmacokinetic properties and their mode of action justify the abbreviation BSB: beta sheet breaker. But styryl derivatives with improved properties [230] are available: SB-13 (**73**) [231] and BF-168 (**72**), which display sufficient fluorescence to be analysed in murine brain slices. Post-mortem incubation with human brain preparations of confirmed AD cases indicated unselective binding to Aβ deposits and neurofibrillary tangles. Thioflavin T (**59**, K_i = 750 to 2000 nM) does not pass the BBB, but several uncharged analogues with high affinity to Aβ oligomers do: IBOX (**63**) , BTA-1 (**62**, K_i = 2.8 nM) [232], 6OH-BTA-1 (**60**) [233, 234], PIB (Pittsburgh probe B, **64**, K_i = 7.6 nM), TZDM (**61**, K_i = 0.06-02 nM) [229], FDDNP (**69**) [235], ^{125}IMPY (**67**, K_i < 1.4 nM), FEM-IMPY (**70**, K_i = 40 nM) and FPM-IMPY (**68**, K_i = 8 nM) [236]. PIB (**64**) is probably the best documented probe and PIB load in cortical areas correlated inversely with cerebral glucose metabolism. However, the cognitive impairment and amyloid detection did not correlate well in patients (65 ± 10y) with mild dementia (Mini-Mental State Examination: 28-29). Moreover, the older control group (69 ± 7y) was identified as asymptomatic amyloid-positive [237].

This is in contrast to the post-mortem incubation with SB-13 (**73**), which displayed no *in vitro* labelling of the age matched controls [231]. FDDNP (**69**) binds to two sites on $Aβ_{40}$ fibrils with different affinity (K_D = 0.012 nM and 1.9 nM) [235] and was the second attempt to image the AD pathology in humans. The accumulation of FDDNP in human brains correlated with lower memory performance, and the brain residence time of the probe was greater in patients with AD than in control subjects [238]. All reported IMPYs pass the blood brain barrier rapidly after intravenous injection. The detailed synthesis suitable for different labels was published and further derivatives [236, 239, 240] are accessible by palladium mediated iodine/amine exchange. $^{123/125}$IMPY, ^{18}F-FEM-IMPY (**70**) and ^{18}F-FPM-IMPY display complex clearance patterns, which are characterised by polar and non-polar metabolites and substantial skull incorporation of ^{18}F by the latter two. Yet, the metabolism of the ^{18}F-FEM-IMPY was slower in rhesus monkey than in mouse [236]. The post-mortem incorporation of human brain sections of AD patients with ^{18}F-FEM-IMPY, resulted in displaceable uptake in grey matter and low non-specific binding in the white matter. Several of these markers are in advanced stages of development as AD radio diagnostics, despite their sometimes striking similarity to estrogen receptor [241, 242] ligands, which may effect the signal to noise ratio. Most of these compounds display excitation and emission between 340 and 440 nm, which differs from the fluorescence of Thioflavin T (450/480 nm) [243]. The Novartis probe (**74**) [244, 250] resembles the dye *Disperse Yellow 332* and introduces a fluorescent coumarin to the Aβ ligand. This will aid to relate cold imaging of brain slices to PET or SPECT images, thus, will improve image calibration and validation. The affinity of these compounds to Aβ fibrils is uniformly high in the nanomolar range (K_D =0.2 to 10 nM) and selectivity versus tau PHFs is usually poor, except for PIB (**64**) [232, 245]. But these values are misleading in the absence of a well-defined target and the high number of binding sites per fibril. The whole research area was moved to solid ground by the identification of three distinctly different binding sites: BS1-3 for Thioflavin T analogues. A GlaxoSmithKline team [243] accomplished a formidable task and evaluated several known compounds in fluorescence based assays. They determined the highest affinities to relate to the low capacity BS3, which is present per every 300 Aβ peptides. The BS1 and BS2 binding sites are far more abundant (1 per every 4 or 30 Aβ) and are characterised by similar affinity and partial overlap between BS1 and BS2. Certain markers: TZDM, TZPI (**66**, K_D = 0.13 nM) [229] and BF-1 (**65**, K_D = 1.6 nM) [229] display selectivity for BS2. The structural discriminator for selectivity was assigned to the halogen substituent. The authors concluded that improved PET probes may be available in BS2 targeting ligands, because they will display the highest sensitivity for Aβ.

OUTLOOK

Despite the tremendous progress in the field, a γ-secretase inhibitor, free of Notch activity is still in utter demand. The selective inhibition of γ-secretase by NSAIDs is pointing in the right direction: allosteric modulation of the active site, which can be identified by additional cleavage sites mediated by PS1 [246]. Confirmed, non-peptidic β-secretase inhibitors are few and still have to reveal their true potential. Several compounds and vaccinations are entering phase II clinical trials and demand improved AD diagnostics. Actually, the vaccination may outpace the other therapies on the way to market. Dietary copper is unlikely to be a remedy for late stage AD, but may offer inexpensive prevention.

ACKNOWLEDGEMENTS

B.S., H.B. and R.N. thank the DFG SPP1085 SCHM1012-3-1/2 and the EU contract LSHM-CT-2003-503330 (APOPIS) for support of this work.

REFERENCES

[1] WHO, The World Health Report 2001 Mental Health: New Understanding, New Hope.

[2] Polvikoski, T.; Sulkava, R.; Myllykangas, L.; Notkola, I. L.; Niinisto, L.; Verkkoniemi, A.; Kainulainen, K.; Kontula, K.; Perez-Tur, J.; Hardy, J.; Haltia, M. *Neurology* **2001,** *56*, 1690.

[3] Gil Gregorio, P.; Ramirez Diaz, S. P.; Ribera Casado, J. M. *J. Nutr. Health Aging* **2003,** *7*, 304.

[4] Thorsett, E. D.; Latimer, L. H. *Curr. Opin. Chem. Biol.* **2000,** *4*, 377–382.

[5] Grant, W. B. *J. Alzheimer's Dis.* **1999,** *1*, 197.

[6] Cummings, J. L. *N. Engl. J. Med.* **2004,** *351*, 56.

[7] Chou, K.-C. *J. Proteome Res.* **2004**, *3*, 1969.

[8] Mattson, M. P. *Nature* **2004,** *430*, 631.

[9] Czech, C.; Adessi, C. *Curr. Neuropharmacol.* **2004,** *2*, 295.

[10] Mandelkow, E.-M.; Mandelkow, E. *Trends Cell Biol.* **1998,** *8*, 425.

[11] Augustinack, J. C.; Schneider, A.; Mandelkow, E.-M.; Hyman, B. T. *Acta Neuropathologica* **2002,** *103*, 26.

[12] Ritchie, C. W.; Bush, A. I.; Mackinnon, A.; Macfarlane, S.; Mastwyk, M.; MacGregor, L.; Kiers, L.; Cherny, R.; Li, Q. X.; Tammer, A.; Carrington, D.; Mavros, C.; Volitakis, I.; Xilinas, M.; Ames, D.; Davis, S.; Beyreuther, K.; Tanzi, R. E.; Masters, C. L. *Arch. Neurol.* **2003,** *60*, 1685.

[13] Bush, A. I.; Masters, C. L.; Tanzi, R. E. *PNAS* **2003**, 11193.

[14] Altmann, P. *Alum. Alzheimer's Dis.* **2001**, 1.

[15] Fischer, F.; Matthisson, M.; Herrling, P. *Neurodegenerative Diseases* **2004,** *1*, 50.

[16] Kwon, M.-O.; Fischer, F.; Matthisson, M.; Herrling, P. *Neurodegenerative Diseases* **2004,** *1*, 113.

[17] Luond, R. M.; Banziger, M.; Frey, P. Preparation of piperidine and piperazine derivatives as inhibitors of the Aβ fibril formation. WO 0047571, **2000**.

[18] Goldsbury, C. S.; Wirtz, S.; Muller, S. A.; Sunderji, S.; Wicki, P.; Aebi, U.; Frey, P. *J. Struct. Biol.* **2000,** *130*, 217.

[19] Howlett, D. R.; Perry, A. E.; Godfrey, F.; Swatton, J. E.; Jennings, K. H.; Spitzfaden, C.; Wadsworth, H.; Wood, S. J.; Markwell, R. E. *Biochem. J.* **1999,** *340*, 283.

[20] Courtney, C.; Farrell, D.; Gray, R.; Hills, R.; Lynch, L.; Sellwood, E.; Edwards, S.; Hardyman, W.; Raftery, J.; Crome, P.; Lendon, C.; Shaw, H.; Bentham, P. *Lancet* **2004,** *363*, 2105.

[21] Jacobsen, J. S. *Curr. Top. Med. Chem.* **2002,** *2*, 343.

[22] Ikeda, S.; Yamada, Y.; Ikegami, N. *Dementia Geriatr. Cognit. Disord.* **2002,** *13*, 33.

[23] Carlson, M. C.; Brandt, J.; Steele, C.; Baker, A.; Stern, Y.; Lyketsos, C. G. *J. Gerontol. A Biol. Sci. Med. Sci.* **2001,** *56*, M567.

[24] Schneider, L. S. *The Lancet* **2004,** *363*, 2100.

[25] AD2000Collaborative Group. *The Lancet* **2004,** *363*, 2105.

[26] Witt, A.; Macdonald, N.; Kirkpatrick, P. *Nat. Rev. Drug Discov.* **2004,** *3*, 109.

[27] Serradji, N.; Bensaid, O.; Martin, M.; Kan, E.; Dereuddre-Bosquet, N.; Redeuilh, C.; Huet, J.; Heymans, F.; Lamouri, A.; Clayette, P.; Chang Zhi Dong; Dormont, D.; Godfroid, J.-J. *J. Med. Chem.* **2004**, *47*, 6410.

[28] Weggen, S.; Eriksen, J. L.; Das, P.; Sagi, S. A.; Wang, R.; Pietrizik, C. U.; Findlay, K. A.; Smith, T. E.; Murphy, M. P.; Bulter, T.; Kang, D. E.; Marquez-Sterling, N.; Golde, T. E.; Koo, E. H. *Nature* **2001,** *414*, 212.

[29] Weggen, S.; Eriksen, J. L.; Sagi, S. A.; Pietrzik, C. U.; Golde, T. E.; Koo, E. H. *J. Biol. Chem.* **2003,** *278*, 30748.

[30] in 't Veld, B. A.; Ruitenberg, A.; Hofman, A.; Launer, L. J.; van Duijn, C. M.; Stijnen, T.; Breteler, M. M. B.; Stricker, B. H. C. *N. Engl. J. Med.* **2001,** *345*, 1515.

[31] Zhou, Y.; Su, Y.; Li, B.; Liu, F.; Ryder, J. W.; Wu, X.; Gonzalez-DeWhitt, P. A.; Gelfanova, V.; Hale, J. E.; May, P. C.; Paul, S. M.; Ni, B. *Science* **2003,** *302*, 1215.

[32] Lanz, T. A.; Fici, G. J.; Merchant, K. M. *J. Pharm. Exp. Therapeutics* **2004,** *309*, 49.

[33] Eriksen, J. L.; Sagi, S. A.; Smith, T. E.; Weggen, S.; Das, P.; McLendon, D. C.; Ozols, V. V.; Jessing, K. W.; Zavitz, K. H.; Koo, E. H.; Golde, T. E. *J. Clin. Investigation* **2003,** *112*, 440.

[34] Beher, D.; Clarke, E. E.; Wrigley, J. D. J.; Martin, A. C. L.; Nadin, A.; Churcher, I.; Shearman, M. S. *J. Biol. Chem.* **2004,** *279*, 43419.

[35] Bachmann, M. F.; Tissot, A.; Ortmann, R.; Lueoend, R.; Staufenbiel, M.; Frey, P. Vaccine compositions containing amyloid β1-6 antigen epitopes conjugated with virus-like particles. WO 2004016282, **2004**.

[36] Schenk, D.; Games, D.; Seubert, P. *Neurosci. News* **2000,** *3*, 46.

[37] Nicoll, J. A.; Wilkinson, D.; Holmes, C.; Steart, P.; Markham, H.; Weller, R. O. *Nat. Med.* **2003,** *9*, 448.

[38] Greenberg, S. M.; Bacskai, B. J.; Hyman, B. T. *Nat. Med.* **2003,** *9*, 389.

[39] Abbott, A. *Nature* **2004,** *430*, 715.

[40] Oddo, S.; Billings, L.; Kesslak, J. P.; Cribbs, D. H.; LaFerla, F. M. *Neuron* **2004,** *43*, 321.

[41] Saunders, A. M. *Pharmacogenomics* **2001,** *2*, 239.

[42] Holmes, C. *Br. J. Psychiatry* **2002,** *180*, 131.

[43] Tanzi, R. E.; Bertram, L. *Neuron* **2001,** *32*, 181.

[44] Hardy, J. *PNAS* **1997,** *94*, 2095.

[45] Hardy, J.; Myers, A.; Wavrant-De Vrieze, F. *Neurodegenerative Diseases* **2004,** *1*, 213.

[46] Bertram, L.; Tanzi, R. E. *J. Mol. Neurosci.* **2001,** *17*, 127.

[47] Fraser, P. E.; Yang, D.-S.; Yu, G.; Lévesque, L.; Nishimura, M.; Arawak, S.; Serpell, L. C.; Rogaev, E.; George-Hyslop, P. S. *Biochim. Biophys. Acta (BBA) - Molecular Basis of Disease* **2000,** *1502*, 1.

[48] Janus, C.; Westaway, D. *Physiol. Behav.* **2001,** *73*, 873.

[49] Schmitz, C.; Rutten Bart, P. F.; Pielen, A.; Schafer, S.; Wirths, O.; Tremp, G.; Czech, C.; Blanchard, V.; Multhaup, G.; Rezaie, P.; Korr, H.; Steinbusch Harry, W. M.; Pradier, L.; Bayer Thomas, A. *Am. J. Pathology* **2004,** *164*, 1495.

[50] Eckert, G. P.; Kirsch, C.; Leutz, S.; Wood, W. G.; Muller, W. E. *Pharmacopsychiatry* **2003,** *36 Suppl 2*, S136.

[51] Moss, M. L.; White, J. M.; Lambert, M. H.; Andrews, R. C. *Drug Discov. Today* **2001,** *6*, 417.

[52] Kinoshita, A.; Whelan, C. M.; Smith, C. J.; Berezovska, O.; Hyman, B. T. *J. Neurochemistry* **2002,** *82*, 839.

[53] Kinoshita, A.; Whelan, C. M.; Berezovska, O.; Hyman, B. T. *J. Biol. Chem.* **2002,** *277*, 28530.

[54] Soto, C. *Mol. Med. Today* **1999,** 5, 343.

[55] Kayed, R.; Glabe, C. G. Immunogens and corresponding antibodies specific for high molecular weight aggregation intermediates common to amyloids formed from proteins of differing sequence. WO 2004024090, **2004**.

[56] Kayed, R.; Head, E.; Thompson, J. L.; McIntire, T. M.; Milton, S. C.; Cotman, C. W.; Glabe, C. G. *Science* **2003,** *300*, 486.

[57] Capell, A.; Steiner, H.; Willem, M.; Kaiser, H.; Meyer, C.; Walter, J.; Lammich, S.; Multhaup, G.; Haass, C. *J. Biol. Chem.* **2000,** *275*, 30849.

[58] Marcinkeviciene, J.; Luo, Y.; Graciani, N. R.; Combs, A. P.; Copeland, R. A. *J. Biol. Chem.* **2001,** *276*, 23790.

[59] Leung, D.; Abbenante, G.; Fairlie, D. P. *J. Med. Chem.* **2000,** *43*, 305.

[60] Farzan, M.; Schnitzler, C. E.; Vasilieva, N.; Leung, D.; Choe, H. *PNAS* **2000,** *97*, 9712.

[61] Yan, R.; Munzner, J. B.; Shuck, M. E.; Bienkowski, M. J. *J. Biol. Chem.* **2001,** *276*, 34019.

[62] Westmeyer, G. G.; Willem, M.; Lichtenthaler, S. F.; Lurman, G.; Multhaup, G.; Assfalg-Machleidt, I.; Reiss, K.; Saftig, P.; Haass, C. *J. Biol. Chem.* **2004**, 279, 53205.

[63] Fischer, F.; Molinari, M.; Bodendorf, U.; Paganetti, P. *J. Neurochem.* **2002,** *80*, 1079.

[64] Luo, Y.; Bolon, B.; Kahn, S.; Bennett, B. D.; Babu-Khan, S.; Denis, P.; Fan, W.; Kha, H.; Zhang, J.; Gong, Y.; Martin, L.; Louis, J.-C.; Yan, Q.; Richards, W. G.; Citron, M.; Vassar, R. *Nat. Neurosci.* **2001,** *4*, 231.

[65] Vassar, R. *J. Mol. Neurosci.* **2001,** *17*, 157.

[66] Gruninger-Leitch, F.; Schlatter, D.; Kung, E.; Nelbock, P.; Dobeli, H. *J. Biol. Chem.* **2002,** *277*, 4687.

[67] Roggo, S. *Curr. Top. Med. Chem.* **2002,** *2*, 359.

[68] Dominguez, D. I.; Hartmann, D.; De Strooper, B. **2004,** *1*, 168.

[69] Wolfe, M. S.; Haass, C. *J. Biol. Chem.* **2001,** *276*, 5413.

[70] Ishiura, S. *Dementia Jpn.* **2000,** *14*, 236.

[71] Citron, M. *Trends Pharmacol. Sci.* **2004,** 25, 92.

[72] Varghese, J.; Beck, J. P.; Bienkowski, M. J.; Sinha, S.; Heinrikson, R. L. *J. Med. Chem.* **2003,** *46*, 4625.

[73] Schmidt, B. *ChemBioChem* **2003,** *4*, 366.

[74] Hong, L.; Koelsch, G.; Lin, X.; Wu, S.; Terzyan, S.; Ghosh, A. K.; Zhang, X. C.; Tang, J. *Science* **2000,** *290*, 150.

[75] Hong, L.; Turner, R. T. III.; Koelsch, G.; Shin, D.; Ghosh, A. K.; Tang, J. *Biochemistry* **2002,** *41*, 10963.

[76] Hong, L.; Tang, J. *Biochemistry* **2004,** *43*, 4689.

[77] Hong, L.; Turner, I. R. T.; Koelsch, G.; Ghosh, A. K.; Tang, J. *Biochem. Soc. Trans.* **2002,** *30*, 530.
[78] Tung, J. S.; Davis, D. L.; Anderson, J. P.; Walker, D. E.; Mamo, S.; Jewett, N.; Hom, R. K.; Sinha, S.; Thorsett, E. D.; John, V. *J. Med. Chem.* **2002,** *45*, 259.
[79] Shuto, D.; Kasai, S.; Kimura, T.; Liu, P.; Hidaka, K.; Hamada, T.; Shibakawa, S.; Hayashi, Y.; Hattori, C.; Szabo, B.; Ishiura, S.; Kiso, Y. *Bioorg. Med.Chem. Lett.* **2003,** *13*, 4273.
[80] Tamamura, H.; Kato, T.; Otaka, A.; Fujii, N. *Org. Biomol. Chem.* **2003,** *1*, 2468.
[81] Brady, S. F.; Singh, S.; Crouthamel, M.-C.; Holloway, M. K.; Coburn, C. A.; Garsky, V. M.; Bogusky, M.; Pennington, M. W.; Vacca, J. P.; Hazuda, D.; Lai, M.-T. *Bioorg. Med. Chem. Lett.* **2004,** *14*, 601.
[82] Ghosh, A. K.; Bilcer, G.; Harwood, C.; Kawahama, R.; Shin, D.; Hussain, K. A.; Hong, L.; Loy, J. A.; Nguyen, C.; Koelsch, G.; Ermolieff, J.; Tang, J. *J. Med. Chem.* **2001,** *44*, 2865.
[83] Kimura, T.; Shuto, D.; Kasai, S.; Liu, P.; Hidaka, K.; Hamada, T.; Hayashi, Y.; Hattori, C.; Asai, M.; Kitazume, S.; Saido, T. C.; Ishiura, S.; Kiso, Y. *Bioorg. Med. Chem. Lett.* **2004,** *14*, 1527.
[84] Chen, S.-H.; Lamar, J.; Guo, D.; Kohn, T.; Yang, H.-C.; McGee, J.; Timm, D.; Erickson, J.; Yip, Y.; May, P.; McCarthy, J. *Bioorg. Med. Chem. Lett.* **2004,** *14*, 245.
[85] Lamar, J.; Hu, J.; Bueno, A. B.; Yang, H.-C.; Guo, D.; Copp, J. D.; McGee, J.; Gitter, B.; Timm, D.; May, P.; McCarthy, J.; Chen, S.-H. *Bioorg. Med.Chem. Lett.* **2004,** *14*, 239.
[86] Hu, B.; Fan, K. Y.; Bridges, K.; Chopra, R.; Lovering, F.; Cole, D.; Zhou, P.; Ellingboe, J.; Jin, G.; Cowling, R.; Bard, J. *Bioorg. Med. Chem. Lett.* **2004,** *14*, 3457.
[87] Hom, R. K.; Fang, L. Y.; Mamo, S.; Tung, J. S.; Guinn, A. C.; Walker, D. E.; Davis, D. L.; Gailunas, A. F.; Thorsett, E. D.; Sinha, S.; Knops, J. E.; Jewett, N. E.; Anderson, J. P.; John, V. *J. Med. Chem.* **2003,** *46*, 1799.
[88] Hom, R. K.; Gailunas, A. F.; Mamo, S.; Fang, L. Y.; Tung, J. S.; Walker, D. E.; Davis, D.; Thorsett, E. D.; Jewett, N. E.; Moon, J. B.; John, V. *J. Med. Chem.* **2004,** *47*, 158.
[89] Maillaird, M.; Hom, C.; Gailunas, A.; Jagodzinska, B.; Fang, L. Y.; John, V.; Freskos, J. N.; Pulley, S. R.; Beck, J. P.; Tenbrink, R. E. Preparation of substituted amines to treat Alzheimer's disease. WO 200202512, **2002**.
[90] Beck, J. P.; Gailunas, A.; Hom, R.; Jagodzinska, B.; John, V.; Maillaird, M. Compounds to treat alzheimer's disease. WO 0202520, **2002**.
[91] Patel, S.; Vuillard, L.; Cleasby, A.; Murray, C. W.; Yon, J. *J. Mol. Biol.* **2004,** *343*, 407.
[92] Uchikawa, O.; Aso, K.; Koike, T.; Tarui, N.; Hirai, K. Preparation of benzamide derivatives as β-secretase inhibitors. WO 2004014843, **2004**.
[93] Demont, E. H.; Faller, A.; MacPherson, D. T.; Milner, P. H.; Naylor, A.; Redshaw, S.; Stanway, S. J.; Vesey, D. R.; Walter, D. S. Preparation of hydroxyethylamine derivatives for the treatment of Alzheimer's disease. WO 2004050619, **2004**.
[94] Pulley, S. R.; Beck, J. P.; Tenbrink, R. E.; Jacobs, J. S. Preparation of macrocycles useful in the treatment of Alzheimer's disease. WO 2002100399, **2002**.
[95] Reeder, M. R. Processes for the synthesis of amino acid-related benzyl epoxides used in the production of pharmaceutical agents. WO 2002085877, **2002**.
[96] Tenbrink, R.; Maillard, M.; Warpehoski, M. Preparation of substituted hydroxyethyl-amines as β-secretase inhibitors. WO 0350073, **2003**.
[97] Fang, L. Y.; Hom, R.; John, V.; Maillaird, M. Preparation of substituted amines for treating Alzheimer's disease. WO 0202505, **2002**.
[98] Fang, L. Y.; John, V. Compounds to treat Alzheimer's disease. WO 0202506, **2002**.
[99] Fobian, Y. M.; Freskos, J. N.; Jagodzinska, B. A preparation of 1,3-diamino-2-hydroxypropane derivatives as β-secretase enzyme inhibitors. WO 2004022523, **2004**.
[100] Vuillard, L. M. M.; Patel, S. J.; Yon, J. R.; Cleasby, A.; Hamilton, B. J.; Shah, A. Crystal structure of human β-secretase mutants and drug discovery applications. WO 2004011641, **2004**.
[101] Yang, W. Preparation of amino carboxamide derivatives as aspartyl protease inhibitors. WO 2004147454, **2004**.
[102] Brockhaus, M.; Doebeli, H.; Grueninger, F.; Huguenin, P.; Kitas, E. A.; Nelboeck-Hochstetter, P. Fluorescence and competitive radioligand binding assays for identifying β-secretase inhibitors and for screening agents for treatment of Alzheimer's disease and cerebrovascular amyloidosis. US 2003125257, **2003**.
[103] Brockhaus, M.; Doebeli, H.; Grueninger, F.; Huguenin, P.; Kitas, E. A.; Nelboeck-Hochstetter, P. Assay for identifying beta secretase inhibitors. US 20030125257, **2003**.
[104] Miyamoto, M.; Matsui, J.; Fukumoto, H.; Tarui, N. Preparation of 2-[2-amino- or 2-(N-heterocyclyl)ethyl]-6-(4-biphenylylmethoxy)-tetralin derivatives as β secretase inhibitors. WO 0187293, **2001**.
[105] Qiao, L.; Etcheberrigaray, R. Preparation of phosphinylmethyl and phosphorylmethyl succinic and glutaric acid analogs as β-secretase inhibitors useful in the treatment of Alzheimer's disease. WO 2002096897, **2002**.
[106] Ramakrishna, N. V. S.; Kumar, E. K. S. V.; Kulkarni, A. S.; Jain, A. K.; Bhat, R. G.; Parikh, S.; Quadros, A.; Deuskar, N.; Kalakoti, B. S. *Indian J. Chem., Sect. B: Org. Chem. Incl. Med. Chem.* **2001,** *40B*, 539.
[107] Bhisetti, G. R.; Saunders, J. O.; Murcko, M. A.; Lepre, C. A.; Britt, S. D.; Come, J. H.; Deninger, D. D.; Wang, T. Preparation of β-carbolines and other inhibitors of BACE-1 aspartic proteinase useful against Alzheimer's and other BACE-mediated diseases. WO 2002088101, **2002**.
[108] Park, H.; Lee, S. *J. Am. Chem. Soc.* **2003,** *125*, 16416.
[109] Boss, C.; Bur, D.; Fischli, W.; Jenck, F.; Weller, T. Preparation of piperidines for the treatment of central nervous system disorders. WO 2004009549, **2004**.
[110] Boss, C.; Bur, D.; Fischli, W.; Jenck, F.; Weller, T. Preparation of substituted 3- and 4-(aminomethyl)piperidines for use as β-secretase inhibitors in the treatment of Alzheimer's disease. WO 2004002483, **2004**.
[111] Coburn, C. A.; Stachel, S. J.; Vacca, J. P. Preparation of phenylcarboxamide derivatives as β-secretase inhibitors for the treatment of Alzheimer's disease. WO 2004043916, **2004**.
[112] Coburn, C. A.; Stachel, S. J.; Vacca, J. P. Preparation of macrocyclic β-secretase inhibitors for treatment of Alzheimer's disease. WO 2004062625, **2004**.
[113] Holloway, M. K.; Culberson, J. C.; Shpungin, J.; Munshi, S.; Coburn, C. A.; Stachel, S. J.; Jones, K. G.; Loutzenhiser, E.; Gregro, A. R.; Lai, M.-T.; Crouthamel, M.-C.; Pietrak, B. L. *Abstracts of Papers, 228th ACS National Meeting, Philadelphia, PA, United States, August 22-26, 2004* **2004**.
[114] Rajamani, R.; Reynolds, C. H. *Bioorg. Med. Chem. Lett.* **2004,** *14*, 4843.
[115] Rajamani, R.; Reynolds, C. H. *J. Med. Chem.* **2004,** *47*, 5159.
[116] Tounge, B. A.; Reynolds, C. H. *J. Med. Chem.* **2003,** *46*, 2074.
[117] Coburn, C. A.; Stachel, S. J.; Li, Y.-M.; Rush, D. M.; Steele, T. G.; Chen-Dodson, E.; Holloway, M. K.; Xu, M.; Huang, Q.; Lai, M.-T.; DiMuzio, J.; Crouthamel, M.-C.; Shi, X.-P.; Sardana, V.; Chen, Z.; Munshi, S.; Kuo, L.; Makara, G. M.; Annis, D. A.; Tadikonda, P. K.; Nash, H. M.; Vacca, J. P. *J. Med. Chem.* **2004**, *47*, 6117.
[118] Stachel, S. J.; Coburn, C. A.; Steele, T. G.; Jones, K. G.; Loutzenhiser, E. F.; Gregro, A. R.; Rajapakse, H. A.; Lai, M.-T.; Crouthamel, M.-C.; Xu, M.; Tugusheva, K.; Lineberger, J. E.; Pietrak, B. L.; Espeseth, A. S.; Shi, X.-P.; Chen-Dodson, E.; Holloway, M. K.; Munshi, S.; Simon, A. J.; Kuo, L.; Vacca, J. P. *J. Med. Chem.* **2004**, *47*, 6447.
[119] Willems, H. Preparation of piperazines as β-amyloid converting enzyme (BACE) inhibitors for the treatment of Alzheimer's disease. WO 2004020422, **2004**.
[120] Willems, H.; Gordon, R. Protected amino acid derivatives for the treatment of Alzheimer's disease. GB 2392443, **2004**.
[121] Willems, H.; Harris, W.; John, D. E. A preparation of triazinoindole derivatives as inhibitors of β-secretase (BACE), useful in the treatment of Alzheimer's disease. WO 2004063196, **2004**.
[122] Willems, H.; Harris, W. H. Preparation of N-sulfonyl amino acid derivatives for the treatment of Alzheimer's disease. WO 2004020402, **2004**.
[123] De Strooper, B.; Annaert, W. *J. Cell Biol.* **2001,** *152*, F17.
[124] Herreman, A.; Serneels, L.; Annaert, W.; Collen, D.; Schoonjans, L.; Strooper, B. D. *Nat. Cell Biol.* **2000,** *2*, 461.
[125] Figueroa, D. J.; Morris, J. A.; Ma, L.; Kandpal, G.; Chen, E.; Li, Y. M.; Austin, C. P. *Neurobiol. Dis.* **2002,** *9*, 49.
[126] Kopan, R.; Ilagan, M. X. G. *Nat. Rev. Mol. Cell Biol.* **2004,** *5*, 499.
[127] Shirotani, K.; Edbauer, D.; Prokop, S.; Haass, C.; Steiner, H. *J. Biol. Chem.* **2004**, *279*, 41340.

[128] Cousin, E.; Hannequin, D.; Mace, S.; Dubois, B.; Ricard, S.; Genin, E.; Brun, C.; Chansac, C.; Pradier, L.; Frebourg, T.; Brice, A.; Campion, D.; Deleuze, J.-F. *Neurosci. Lett.* **2003,** *353*, 153.
[129] Edbauer, D.; Winkler, E.; Regula, J. T.; Pesold, B.; Steiner, H.; Haass, C. *Nat. Cell Biol.* **2003,** *5*, 486.
[130] Turner, R. T.; Loy, J. A.; Nguyen, C.; Devasamudram, T.; Ghosh, A. K.; Koelsch, G.; Tang, J. *Biochemistry* **2002,** *41*, 8742.
[131] Farmery, M. R.; Tjernberg, L. O.; Pursglove, S. E.; Bergman, A.; Winblad, B.; Naslund, J. *J. Biol. Chem.* **2003,** *278*, 24277.
[132] Weihofen, A.; Binns, K.; Lemberg, M. K.; Ashman, K.; Martoglio, B. *Science* **2002,** *296*, 2215.
[133] Lichtenthaler, S. F.; Wang, R.; Grimm, H.; Uljon, S. U.; Masters, C. L.; Beyreuther, K. *PNAS* **1999,** *96*, 3053.
[134] Kaether, C.; Capell, A.; Edbauer, D.; Winkler, E.; Novak, B.; Steiner, H.; Haass, C. *EMBO J.* **2004**, *23*, 4738.
[135] Wolfe, M. S.; Xia, W.; Ostaszewski, B. L.; Diehl, T. S.; Kimberly, W. T.; Selkoe, D. J. *Nature* **1999,** *398*, 513.
[136] Kimberly, W. T.; Xia, W.; Rahmati, T.; Wolfe, M. S.; Selkoe, D. J. *J. Biol. Chem.* **2000,** *275*, 3173.
[137] Paris, D.; Mullan, M. J. Anti-angiogenic and anti-tumoral properties of beta and gamma secretase inhibitors. WO 2004073630, **2004**.
[138] Kan, T.; Tominari, Y.; Rikimaru, K.; Morohashi, Y.; Natsugari, H.; Tomita, T.; Iwatsubo, T.; Fukuyama, T. *Bioorg. Med. Chem. Lett.* **2004,** *14*, 1983.
[139] Shearman, M. S.; Beher, D.; Clarke, E. E.; Lewis, H. D.; Harrison, T.; Hunt, P.; Nadin, A.; Smith, A. L.; Stevenson, G.; Castro, J. L. *Biochemistry* **2000,** *39*, 8698.
[140] Nadin, A. J.; Stevenson, G. I. Preparation of peptides as γ-secretase inhibitors. WO 0177144, **2001**.
[141] Nadin, A.; Owens, A. P.; Castro, J. L.; Harrison, T.; Shearman, M. S. *Bioorg. Med. Chem. Lett.* **2003,** *13*, 37.
[142] Nadin, A.; López, J. M. S.; Neduvelil, J. G.; Thomas, S. R. *Tetrahedron* **2001,** *57*, 1861.
[143] Moore, C. L.; Leatherwood, D. D.; Diehl, T. S.; Selkoe, D. J.; Wolfe, M. S. *J. Med. Chem.* **2000,** *43*, 3434.
[144] Wolfe, M. S. *J. Mol. Neurosci.* **2001,** *17*, 199.
[145] Campbell, W. A.; Iskandar, M. K.; Reed, M. L.; Xia, W. *Biochemistry* **2002,** *41*, 3372.
[146] Petit, A.; Bihel, F.; Alves da Costa, C.; Pourquie, O.; Checler, F.; Kraus, J.-L. *Nat. Cell Biol.* **2001,** *3*, 507.
[147] Zhang, L.; Song, L.; Terracina, G.; Liu, Y.; Pramanik, B.; Parker, E. *Biochemistry* **2001,** *40*, 5049.
[148] Berezovska, O.; Jack, C.; McLean, P.; Aster, J. C.; Hicks, C.; Xia, W.; Wolfe, M. S.; Kimberly, W. T.; Weinmaster, G.; Selkoe, D. J.; Hyman, B. T. *J. Neurochem.* **2000,** *75*, 583.
[149] Wolfe, M. S.; Xia, W.; Moore, C. L.; Leatherwood, D. D.; Ostaszewski, B.; Rahmati, T.; Donkor, I. O.; Selkoe, D. J. *Biochemistry* **1999,** *38*, 4720.
[150] Wolfe, M. S.; Citron, M.; Diehl, T. S.; Xia, W.; Donkor, I. O.; Selkoe, D. J. *J. Med. Chem.* **1998,** *41*, 6.
[151] Doerfler, P.; Shearman, M. S.; Perlmutter, R. M. *PNAS* **2001,** *98*, 9312.
[152] Roncarati, R.; Sestan, N.; Scheinfeld, M. H.; Berechid, B. E.; Lopez, P. A.; Meucci, O.; McGlade, J. C.; Rakic, P.; D'Adamio, L. *PNAS* **2002,** *99*, 7102.
[153] Das, C.; Wolfe, M. S.; Tsai, J.-Y.; Diehl, T. S. Abstracts of Papers, 223rd ACS National Meeting, Orlando, FL, United States, April 7-11, 2002 **2002**, MEDI.
[154] Wolfe, M. S. Helical peptidomimetics as inhibitors of β-amyloid production, and therapeutic use thereof. WO 2003068168, **2003**.
[155] Bihel, F.; Das, C.; Bowman, M. J.; Wolfe, M. S. *J. Med. Chem.* **2004,** *47*, 3931.
[156] Bakshi, P.; Wolfe, M. S. *J. Med. Chem.* **2004**, *47*, 6485.
[157] McLendon, C.; Xin, T.; Ziani-Cherif, C.; Murphy, M. P.; Findlay, K. A.; Lewis, P. A.; Pinnix, I.; Sambamurti, K.; Wang, R.; Fauq, A.; Golde, T. E. *FASEB* **2000,** *14*, 2383.
[158] Castro Pineiro, J. L.; Smith, A. L.; Stevenson, G. I. γ-Secretase inhibitors for treatment or prevention of Alzheimer's disease. WO 0166564, **2001**.
[159] Esler, W. P.; Kimberly, W. T.; Ostaszewski, B. L.; Ye, W.; Diehl, T. S.; Selkoe, D. J.; Wolfe, M. S. *PNAS* **2002,** *99*, 2720.
[160] Dovey, H. F.; John, V.; Anderson, J. P.; Chen, L. Z.; De Saint Andrieu, P.; Fang, L. Y.; Freedman, S. B.; Folmer, B.; Goldbach, E.; Holsztynska, E. J.; Hu, K. L.; Johnson-Wood, K. L.; Kennedy, S. L.; Kholodenko, D.; Knops, J. E.; Latimer, L. H.; Lee, M.; Liao, Z.; Lieberburg, I. M.; Motter, R. N.; Mutter, L. C.; Nietz, J.; Quinn, K. P.; Sacchi, K. L.; Seubert, P. A.; Shopp, G. M.; Thorsett, E. D.; Tung, J. S.; Wu, J.; Yang, S.; Yin, C. T.; Schenk, D. B.; May, P. C.; Altstiel, L. D.; Bender, M. H.; Boggs, L. N.; Britton, T. C.; Clemens, J. C.; Czilli, D. L.; Dieckman-McGinty, D. K.; Droste, J. J.; Fuson, K. S.; Gitter, B. D.; Hyslop, P. A.; Johnstone, E. M.; Li, W. Y.; Little, S. P.; Mabry, T. E.; Miller, F. D.; Ni, B.; Nissen, J. S.; Porter, W. J.; Potts, B. D.; Reel, J. K.; Stephenson, D.; Su, Y.; Shipley, L. A.; Whitesitt, C. A.; Yin, T.; Audia, J. E. *J. Neurochem.* **2001,** *76*, 173.
[161] Audia, J. E.; Britton, T. C.; Droste, J. J.; Folmer, B. K.; Huffman, G. W.; John, V.; Latimer, L. H.; Mabry, T. E.; Nissen, J. S.; Porter, W. J.; Reel, J. K.; Thorsett, E. D.; Tung, J. S.; Eid, C. N.; Scott, W. L. Preparation of N-(phenylacetyl)di- and tripeptide derivatives for inhibiting β-amyloid peptide release. WO 9822494, **1998**.
[162] Audia, J. E.; Britton, T. C.; Droste, J. J.; Folmer, B. K.; Huffman, G. W.; Varghese, J.; Latimer, L. H.; Mabry, T. E.; Nissen, J. S.; Porter, W. J.; Reel, J. K.; Thorsett, E. D.; Tung, J. S.; Wu, J.; Eid, C. N.; Scott, W. L. Methods and compounds for inhibiting β-amyloid peptide release and/or its synthesis. US 6191166, **2001**.
[163] Larbig, G.; Zall, A.; Schmidt, B. *Helvetica Chimica Acta* **2004,** *87*, 2334.
[164] Garofalo, A. W.; Wone, D. W. G.; Phuc, A.; Audia, J. E.; Bales, C. A.; Dovey, H. F.; Dressen, D. B.; Folmer, B.; Goldbach, E. G.; Guinn, A. C.; Latimer, L. H.; Mabry, T. E.; Nissen, J. S.; Pleiss, M. A.; Sohn, S.; Thorsett, E. D.; Tung, J. S.; Wu, J. *Bioorg. Med. Chem. Lett.* **2002,** *12*, 3051–3053.
[165] Hutton, M.; Lewis, J.; Dickson, D.; Yen, S. H.; McGowan, E. *Trends Mol. Med.* **2001,** *7*, 467.
[166] Hadland, B. K.; Manley, N. R.; Su, D.-M.; Longmore, G. D.; Moore, C. L.; Wolfe, M. S.; Schroeter, E. H.; Kopan, R. *PNAS* **2001,** *98*, 7487.
[167] Wong, G. T.; Manfra, D.; Poulet, F. M.; Zhang, Q.; Josien, H.; Bara, T.; Engstrom, L.; Pinzon-Ortiz, M.; Fine, J. S.; Lee, H.-J. J.; Zhang, L.; Higgins, G. A.; Parker, E. M. *J. Biol. Chem.* **2004,** *279*, 12876.
[168] Iwata, N.; Tsubuki, S.; Takaki, Y.; Shirotani, K.; Lu, B.; Gerard, N. P.; Gerard, C.; Hama, E.; Lee, H.-J.; Saido, T. C. *Science* **2001,** *292*, 1550.
[169] Iwata, N.; Tsubuki, S.; Takaki, Y.; Watanabe, K.; Sekiguchi, M.; Hosoki, E.; Kawashima-Morishima, M.; Lee, H.-J.; Hama, E.; Sekine-Aizawa, Y.; Saido, T. C. *Nat. Med.* **2000,** *6*, 143.
[170] Iwata, N.; Saido, T. C. *Dementia Jpn.* **2000,** *14*, 80.
[171] Abraham, C. R.; McGraw, W. T.; Slot, F.; Yamin, R. *Ann. N. Y. Acad. Sci.* **2000,** *920*, 245.
[172] Smith, D. W.; Munoz, B.; Srinivasan, K.; Bergstrom, C. P.; Chaturvedula, P. V.; Deshpande, M. S.; Keavy, D. J.; Lau, W. Y.; Parker, M. F.; Sloan, C. P.; Wallace, O. B.; Wang, H. H. Preparation of sulfonamide derivs. as amyloidβ production inhibitors useful in treating or preventing diseases related to Aβ. WO 0050391, **2000**.
[173] Rishton, G. M.; Retz, D. M.; Tempest, P. A.; Novotny, J.; Kahn, S.; Treanor, J. J. S.; Lile, J. D.; Citron, M. *J. Med. Chem.* **2000,** *43*, 2297.
[174] Belanger, P. C.; Collins, I. J.; Hannam, J. C.; Harrison, T.; Lewis, S. J.; Madin, A.; McIver, E. G.; Nadin, A. J.; Neduvelil, J. G.; Shearman, M. S.; Smith, A. L.; Sparey, T. J.; Stevenson, G. I.; Teall, M. R. Synthesis of sulfonamido-substituted bridged bicycloalkyl derivatives as γ-secretase inhibitors. WO 0170677, **2001**.
[175] Olson, R. E.; Maduskuie, T. P.; Thomas, L. A. Preparation of succinoylamino-azepinones and related compounds as inhibitors of Aβ-peptide production. WO 0007995, **2000**.
[176] Seiffert, D.; Bradley, J. D.; Rominger, C. M.; Rominger, D. H.; Yang, F.; Meredith, J. E. Jr.; Wang, Q.; Roach, A. H.; Thompson, L. A.; Spitz, S. M.; Higaki, J. N.; Prakash, S. R.; Combs, A. P.; Copeland, R. A.; Arneric, S. P.; Hartig, P. R.; Robertson, D. W.; Cordell, B.; Stern, A. M.; Olson, R. E.; Zaczek, R. *J. Biol. Chem.* **2000,** *275*, 34086.
[177] Thompson, L. A.; Han, A. Q. Preparation of amino lactam sulfonamides as inhibitors of Aβ-protein production. WO 0127108, **2001**.
[178] Thompson, L. A. Amino lactam sulfonamides as inhibitors of Aβ protein production. WO 0127091, **2001**.
[179] Teall, M. R. γ-secretase inhibitors. Us 20020013315, **2002**.
[180] Fuchs, K.; Romig, M.; Mendla, K.; Briem, H.; Fechteler, K. Preparation of novel imidazopyridines as β-amyloid formation inhibitors. WO 2002014313, **2002**.

[181] Himmelsbach, F.; Fuchs, K.; Briem, H.; Fechteler, K.; Kostka, M.; Dorner-Ciossek, C.; Bornemann, K.; Klinder, K. Preparation of diaminopyrimidines as inhibitors of β-amyloid formation or its release. WO 2003032994, **2003**.

[182] Otto, M.; Cepek, L.; Ratzka, P.; Doehlinger, S.; Boekhoff, I.; Wiltfang, J.; Irle, E.; Pergande, G.; Ellers-Lenz, B.; Windl, O.; Kretzschmar, H. A.; Poser, S.; Prange, H. *Neurology* **2004,** *62*, 714.

[183] Churcher, I.; Williams, S.; Kerrad, S.; Harrison, T.; Castro, J. L.; Shearman, M. S.; Lewis, H. D.; Clarke, E. E.; Wrigley, J. D.; Beher, D.; Tang, Y. S.; Liu, W. *J. Med. Chem.* **2003,** *46*, 2275.

[184] Churcher, I.; Ashton, K.; Butcher, J. W.; Clarke, E. E.; Harrison, T.; Lewis, H. D.; Owens, A. P.; Teall, M. R.; Williams, S.; Wrigley, J. D. *Bioorg. Med. Chem. Lett.* **2003,** *13*, 179.

[185] Lewis, H. D.; Perez Revuelta, B. I.; Nadin, A.; Neduvelil, J. G.; Harrison, T.; Pollack, S. J.; Shearman, M. S. *Biochemistry* **2003,** *42*, 7580.

[186] Sun, X.; Sato, S.; Murayama, O.; Murayama, M.; Park, J. M.; Yamaguchi, H.; Takashima, A. *Neurosci. Lett.* **2002,** *321*, 61.

[187] Phiel, C. J.; Wilson, C. A.; Lee, V. M.; Klein, P. S. *Nature* **2003,** *423*, 435.

[188] Cohen, P.; Goedert, M. *Nat. Rev. Drug Discov.* **2004,** *3*, 479.

[189] Ryder, J.; Su, Y.; Liu, F.; Li, B.; Zhou, Y.; Ni, B. *Biochem. Biophys. Res. Commun.* **2003,** *312*, 922.

[190] Eckert, G. P.; Wood, W. G.; Müller, W. E. *J. Neural. Transm.* **2004**, *in press*.

[191] Cucchiara, B.; Kasner, S. E. *J. Neurol. Sci.* **2001,** *187*, 81.

[192] Fassbender, K.; Simons, M.; Bergmann, C.; Stroick, M.; Lutjohann, D.; Keller, P.; Runz, H.; Kuhl, S.; Bertsch, T.; Von Bergmann, K.; Hennerici, M.; Beyreuther, K.; Hartmann, T. *PNAS* **2001,** *98*, 5856.

[193] Simons, M.; Keller, P.; Dichgans, J.; Schulz, J. B. *Neurology* **2001,** *57*, 1089.

[194] Riddell, D. R.; Christie, G.; Hussain, I.; Dingwall, C. *Curr. Biol.* **2001,** *11*, 1288.

[195] Kojro, E.; Gimpl, G.; Lammich, S.; Marz, W.; Fahrenholz, F. *PNAS* **2001,** *98*, 5815.

[196] George, A. J.; Holsinger, R. M. D.; McLean, C. A.; Laughton, K. M.; Beyreuther, K.; Evin, G.; Masters, C. L.; Li, Q.-X. *Neurobiol. Dis.* **2004,** *16*, 124.

[197] Refolo, L. M.; Pappolla, M. A.; LaFrancois, J.; Malester, B.; Schmidt, S. D.; Thomas-Bryant, T.; Tint, G. S.; Wang, R.; Mercken, M.; Petanceska, S. S.; Duff, K. E. *Neurobiol. Dis.* **2001,** *8*, 890.

[198] Bayer, T. A.; Schaefer, S.; Simons, A.; Kemmling, A.; Kamer, T.; Tepest, R.; Eckert, A.; Schuessel, K.; Eikenberg, O.; Sturchler-Pierrat, C.; Abramowski, D.; Staufenbiel, M.; Multhaup, G. *PNAS* **2003,** *100*, 14187.

[199] Regland, B.; Lehmann, W.; Abedini, I.; Blennow, K.; Jonsson, M.; Karlsson, I.; Sjoegren, M.; Wallin, A.; Xilinas, M.; Gottfries, C.-G. *Dement. Geriatr. Cog. Disord.* **2001,** *12*, 408.

[200] Melov, S. *Trends. Neurosci.* **2002,** *25*, 121.

[201] Treiber, C.; Simons, A.; Strauss, M.; Hafner, M.; Cappai, R.; Bayer, T. A.; Multhaup, G. *J. Biol. Chem.* **2004**, *279*, 51958.

[202] Barnham, K. J.; Gautier, E. C. L.; Kok, G. B.; Krippner, G. Preparation of 8-hydroxy-quinolines for treatment of neurological conditions. WO 2004007461, **2004**.

[203] Khachaturian, Z. S. *Neurobiol. Aging.* **2002,** *23*, 509.

[204] Papassotiropoulos, A.; Hock, C. *Neurobiol. Aging* **2002,** *23*, 513.

[205] Papassotiropoulos, A.; Lutjohann, D.; Bagli, M.; Locatelli, S.; Jessen, F.; Buschfort, R.; Ptok, U.; Bjorkhem, I.; von Bergmann, K.; Heun, R. *J. Psychiatr. Res.* **2002,** *36*, 27.

[206] Boss, M. A. *Biochim. Biophysica Acta* **2000,** 1502, 188.

[207] Teunissen, C. E.; de Vente, J.; Steinbusch, H. W.; De Bruijn, C. *Neurobiol. Aging* **2002,** *23*, 485.

[208] Klunk, W. E. *Neurobiol. Aging* **2002,** *23*, 517.

[209] Kawarabayashi, T.; Younkin, L. H.; Saido, T. C.; Shoji, M.; Ashe, K. H.; Younkin, S. G. *J. Neurosci.* **2001,** *21*, 372.

[210] Couderc, R. *Ann. Biol. Clin.* **2000,** *58*, 581.

[211] Montine, T. J.; Kaye, J. A.; Montine, K. S.; McFarland, L.; Morrow, J. D.; Quinn, J. F. *Arch. Pathol. Lab. Med.* **2001,** *125*, 510.

[212] Pratico, D.; Clark, C. M.; Lee, V. M. Y.; Trojanowski, J. Q.; Rokach, J.; FitzGerald, G. A. *Ann. Neurol.* **2000,** *48*, 809.

[213] Pratico, D.; Clark, C. M.; Liun, F.; Lee, V. Y.; Trojanowski, J. Q. *Arch. Neurol.* **2002,** *59*, 972.

[214] Ripova, D.; Strunecka, A. *Physiol. Res. (Prague, Czech Repub.)* **2001,** *50*, 119.

[215] Lee, D. H. S.; Reitz, A. B.; Plata-Salaman, C. R.; Wang, H.-Y. Method of diagnosing neurodegenerative disease. WO 0140261, **2001**.

[216] Gupta-Bansal, R.; Brunden, K. R. *J. Neurochem.* **1998,** *70*, 292.

[217] Ashburn, T.; Hogyu, T. H.; McGuinness, B. F.; Lansbury, Jr. P. T. *Chem. Biol.* **1996,** *3*, 351.

[218] Probst, A.; Heitz, P. U.; Ulrich, J. *Virchows Archiv. A, Pathol. Anat. Histol.* **1980,** *388*, 327.

[219] Klunk, W. E.; Debnath, M. L.; Pettegrew, J. W. *Neurobiol. Aging* **1994,** *15*, 691.

[220] Klunk, W. E.; Debnath, M. L.; Koros, A. M. C.; Pettegrew, J. W. *Life Sci.* **1998,** *63*, 1807.

[221] Klunk, W. E.; Pettegrew, J. W.; Mathis, C. A. Jr. Azo compounds for the *antemortem* diagnosis of Alzheimer's disease and *in vivo* imaging and prevention of amyloid deposition. WO 9634853, **1996**.

[222] Klunk, W. E.; Pettegrew, J. W.; Mathis, C. A. Jr. Alkyl, alkenyl and alkynyl Chrysamine G derivatives for the *antemortem* diagnosis of Alzheimer's disease and *in vivo* imaging and prevention of amyloid deposition. WO 9847969, **1998**.

[223] Klunk, W. E.; Pettegrew, J. W.; Mathis, C. A. Jr. Compounds for the antemortem diagnosis of Alzheimer's disease and *in vivo* imaging and prevention of amyloid deposition. WO 9924394, **1999**.

[224] Klunk, W. E.; Wang, Y.; Huang, G.-F.; Debnath, M. L.; Holt, D. P.; Mathis, C. A. *Life Sci.* **2001,** *69*, 1471.

[225] Han, H.; Cho, C.-G.; Lansbury, P. T. Jr. *J. Am. Chem. Soc.* **1996,** *118*, 4506.

[226] Link, C. D.; Johnson, C. J.; Fonte, V.; Paupard, M. C.; Hall, D. H.; Styren, S.; Mathis, C. A.; Klunk, W. E. *Neurobiol. Aging* **2001,** *22*, 217.

[227] Caltech; Magnetic resonance imaging agents for *in vivo* labeling and detection of amyloid deposits. WO 028441, **2002**.

[228] Skovronsky, D. M.; Zhang, B.; Kung, M.-P.; Kung, H. F.; Trojanowski, J. Q.; Lee, V. M.-Y. *PNAS* **2000,** *97*, 7609–7614.

[229] Zhuang, Z. P.; Kung, M. P.; Hou, C.; Skovronsky, D. M.; Gur, T. L.; Ploessl, K.; Trojanowski, J. Q.; Lee, V. M. Y.; Kung, H. F. *J. Med. Chem.* **2001,** *44*, 1905.

[230] Okamura, N.; Suemoto, T.; Shimadzu, H.; Suzuki, M.; Shiomitsu, T.; Akatsu, H.; Yamamoto, T.; Staufenbiel, M.; Yanai, K.; Arai, H.; Sasaki, H.; Kudo, Y.; Sawada, T. *J. Neurosci.* **2004,** *24*, 2535.

[231] Kung, M.-P.; Hou, C.; Zhuang, Z.-P.; Skovronsky, D.; Kung, H. F. *Brain Res.* **2004,** *1025*, 98.

[232] Mathis, C. A.; Wang, Y.; Holt, D. P.; Huang, G. F.; Debnath, M. L.; Klunk, W. E. *J. Med. Chem.* **2003,** *46*, 2740.

[233] Wilson, A. A.; Garcia, A.; Chestakova, A.; Kung, H.; Houle, S. *J. Labelled Comp. Radiopharm.* **2004,** *47*, 679.

[234] Wang, Y.; Klunk, W. E.; Debnath, M. L.; Huang, G.-F.; Holt, D. P.; Li, S.; Mathis, C. A. *J. Mol. Neurosci.* **2004,** *24*, 55.

[235] Agdeppa, E. D.; Kepe, V.; Liu, J.; Flores-Torres, S.; Satyamurthy, N.; Petric, A.; Cole, G. M.; Small, G. W.; Huang, S.-C.; Barrio, J., *J. Neurosci.* **2001,** *21*, RC189/1.

[236] Cai, L.; Chin, F. T.; Pike, V. W.; Toyama, H.; Liow, J.-S.; Zoghbi, S. S.; Modell, K.; Briard, E.; Shetty, H. U.; Sinclair, K.; Donohue, S.; Tipre, D.; Kung, M.-P.; Dagostin, C.; Widdowson, D. A.; Green, M.; Gao, W.; Herman, M. M.; Ichise, M.; Innis, R. B. *J. Med. Chem.* **2004,** *47*, 2208.

[237] Klunk, W. E.; Engler, H.; Nordberg, A.; Wang, Y.; Blomqvist, G.; Holt, D. P.; Bergstrom, M.; Savitcheva, I.; Huang, G.-f.; Estrada, S.; Ausen, B.; Debnath, M. L.; Barletta, J.; Price, J. C.; Sandell, J.; Lopresti, B. J.; Wall, A.; Koivisto, P.; Antoni, G.; Mathis, C. A.; Langstrom, B. *Ann. Neurol.* **2004,** *55*, 306.

[238] Shoghi-Jadid, K.; Small, G. W.; Agdeppa, E. D.; Kepe, V.; Ercoli, L. M.; Siddarth, P.; Read, S.; Satyamurthy, N.; Petric, A.; Huang, S. C.; Barrio, J. R. *Am. J. Geriatr. Psychiatry* **2002,** *10*, 24.

[239] Enguehard, C.; Allouchi, H.; Gueiffier, A.; Buchwald, S. L. *J. Org. Chem.* **2003,** *68*, 4367.

[240] Enguehard, C.; Allouchi, H.; Gueiffier, A.; Buchwald, S. L. *J. Org. Chem.* **2003,** *68*, 5614.

[241] Manas, E. S.; Unwalla, R. J.; Xu, Z. B.; Malamas, M. S.; Miller, C. P.; Harris, H. A.; Hsiao, C.; Akopian, T.; Hum, W.-T.; Malakian, K.; Wolfrom, S.; Bapat, A.; Bhat, R. A.; Stahl, M. L.; Somers, W. S.; Alvarez, J. C. *J. Am. Chem. Soc.* **2004**, *126*, 15106.

[242] Barlaam, B.; Bernstein, P.; Dantzman, C.; Warwick, P. Preparation of benzoxazoles and benzothiazoles as selective ligands for human β-estrogen receptor. WO 2002051821, **2002**.

[243] Lockhart, A.; Ye, L.; Judd, D. B.; Merritt, A. T.; Lowe, P.; Morgenstern, J. L.; Hong, G.; Gee, A. D.; Brown, J. *J. Biol. Chem.* **2004**, 10.1074/jbc.M41205620.

[244] Auberson, Y. Coumarines useful as biomarkers. WO 03074519, **2003**.

[245] Klunk, W. E.; Wang, Y.; Huang, G. F.; Debnath, M. L.; Holt, D. P.; Shao, L.; Hamilton, R. L.; Ikonomovic, M. D.; DeKosky, S. T.; Mathis, C. A. *J. Neurosci.* **2003,** *23*, 2086.

[246] Zhao, G.; Mao, G.; Tan, J.; Dong, Y.; Cui, M.-Z.; Seong-Hun, K.; Xu, X. *J. Biol. Chem.* **2004**, 279, 50647.

[247] McLean, C. A.; Cherny, R. A.; Fraser, F. W.; Fuller, S. J.; Smith, M. J.; Beyreuther, K.; Bush, A. I.; Masters, C. L. *Ann. Neurol.* **1999**, *46*, 860.

[248] apo: The protein component of an enzyme that is separable from the prosthetic group but that requires the prosthetic group to form the functioning holoenzyme.

[249] Confaloni, A.; Terreni, L.; Piscopo, P.; Crestini, A.; Campeggi, L. M.; Frigerio, C. S.; Blotta, I.; Perri, M.; Di Natale, M.; Maletta, R.; Marcon, G.; Franceschi, M.; Bruni, A. C.; Forloni, G.; Cantafora, A. *Neurosci. Lett.* **2003**, *353*, 61.

[250] Hunger, K. In *Industrial Dyes*, Wiley-VCH **2004**, Weinheim. pp. 141

[251] Puglielli, L.; Konopka, G.; Pack-Chung, E.M.; Ingano, L. A. M.; Berezovska, O.; Hyman, B. T.; Chang Ta, Y.; Tanzi, R.E.; Kovacs, D. M. *Nat. Cell Biol.* **2001***, 3,* 905.

[252] Puglielli, L.; Ellis, B. C.; Ingano, L. A. M.; Kovacs, D. M. *J. Mol. Neurosci.* **2004**, *24*, 93.

Original Paper

Neurodegenerative Diseases

Neurodegenerative Dis 2006;3:290–297
DOI: 10.1159/000095269

Modulators and Inhibitors of γ- and β-Secretases

Boris Schmidt Stefanie Baumann Rajeshwar Narlawar Hannes A. Braun Gregor Larbig

Clemens Schöpf Institute for Organic Chemistry and Biochemistry, TU Darmstadt, Darmstadt, Germany

Key Words
Alzheimer's disease · Secretase · Aspartic protease · BACE inhibitors · Presenilin

Abstract
Most gene mutations associated with Alzheimer's disease point to the metabolism of amyloid precursor protein as a potential cause. The β- and γ-secretases are two executioners of amyloid precursor protein processing resulting in amyloid-β. Significant progress has been made in the selective inhibition of both proteases, regardless of structural information for γ-secretase. Several peptidic and nonpeptidic leads were identified for both targets.

Introduction

Alzheimer's disease (AD) is the most common progressive, irreversible dementia with neither definitely assigned cause nor an available causal therapy. The symptoms of the disease include memory loss, confusion, impaired judgment, personality changes, disorientation, and loss of language skills [1]. A hallmark of AD is the accumulation of extracellular amyloidic plaques in the brain. The β-amyloid (Aβ) peptide, which is the major constituent of these amyloid plaques, performs a central role in the neuropathology of AD. The Aβ peptides, which differ in length from 38 to 42 amino acids, are generated from the amyloid precursor protein (APP) by two aspartic proteases: β-secretase and γ-secretase (fig. 1). Both secretases are rather promiscuous, they have multiple substrates and cause several distinctly different cleavages of APP. The membrane localization of both enzymes is crucial for selectivity, as cell-free conditions shift the cleavage pattern or result in additional cleavage sites. Usually 90% of APP is degraded by the benign α-secretase pathway, and a mere 10% of APP is degraded by the consecutive cleavages of β- and γ-secretases to result in the build-up of extracellular Aβ deposits. Neither the pathological consequences of deposited or soluble Aβ are established beyond doubt, nor does plaque formation adequately correlate to the progress of AD. A definite proof of the Aβ hypothesis is still missing for humans.

BACE Inhibitors

Several reviews on BACE inhibition summarize the biology and chemical concepts [2–6]. The majority of potent inhibitors are still peptide-based transition state analogues. Hydroxyethylenes, statins, norstatins, bisstatins, hydroxyethylamines and hydroxyethylureas were employed. The hydroxyethylenes delivered the first highly potent inhibitors. Their subsite specificity was revealed by the cleavage rates of substrate mixtures and selective inhibitors, resulting in the design of the heptapeptides

KARGER

Fax +41 61 306 12 34
E-Mail karger@karger.ch
www.karger.com

1660–2854/06/0035–0290$23.50/0

Accessible online at:
www.karger.com/ndd

Boris Schmidt
Clemens Schöpf Institute for Organic Chemistry and Biochemistry
TU Darmstadt, Petersenstrasse 22
DE–64287 Darmstadt (Germany)
Tel. +49 6151 163 075, Fax +49 6151 163 278, E-Mail Schmidt_Boris@t-online.de

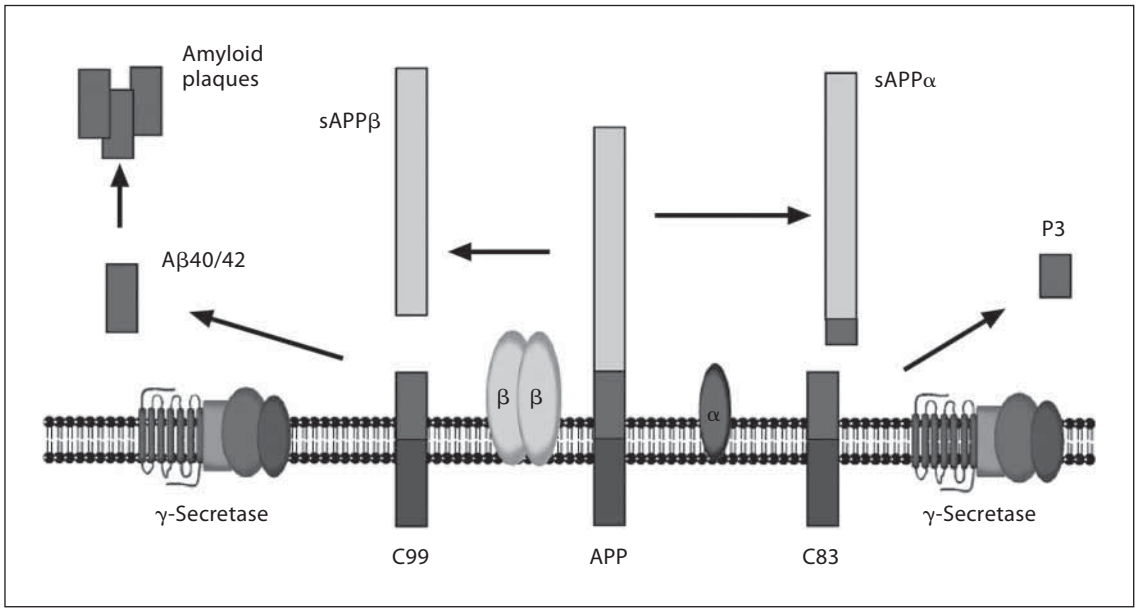

Fig. 1. Processing of APP by secretases.

Glu-Val-Asn-Ψ(Leu-Ala)-Ala-Glu-Phe (1, OM99-2, K_i = 1.6 nM, fig. 2) and Glu-Leu-Asp-Ψ(Leu-Ala)-Val-Glu-Phe (2, OM00-3, K_i = 0.31 nM) [7]. The two inhibitors allowed co-crystallization with BACE and structure determination at 1.9 Å and 2.1 Å, respectively (PDB: OM99-2, 1FKN; OM00-3, 1M4H) [8]. The hydroxyethylenes are coordinated by four hydrogen bonds to the two catalytic aspartates. Essentially, the structure of the enzyme and the backbone conformations from P_3 to P_2' are the same, although they differ in side-chain orientation in several subsites.

The introduction of the isophthalamide was an important step towards less peptidic compounds 3–6 (fig. 2), which is mandatory to obtain sufficient oral absorption and blood-brain barrier penetration [9]. We adopted this moiety for our BACE inhibitor program utilizing our novel methodology for iodomethanols [10]. This resulted in the stereoselective synthesis of an advanced intermediate 7. Opening of the epoxide with benzylamines furnished a series of hydroxyethylene isosters (fig. 3), which were tested in collaboration with M. Willem, LMU München, and F. Hoffmann-La Roche, Basel. Almost all compounds displayed poor activity; we attribute this to the wrong S-stereochemistry of the hydroxyl group. However, the epoxide 7 turned out to be an irreversible inhibitor of BACE; the irreversibility is apparent from the time dependence of the inhibition. Unfortunately, the compound displays poor activity in cellular assays; this may be due to rapid degradation by other proteases, which in turn is an indicator of lacking selectivity [10]. We currently revise our synthesis to obtain the necessary diastereomers.

Despite all efforts in the development of BACE-1 inhibitors, two major hurdles have hampered progress: blood-brain barrier permeability and oral bioavailability. To overcome these problems, novel nonpeptidic lead structures are of great interest. For several years, there were few structures, usually with an obscure mode of action [11, 12]. However, detailed activities were reported by A. Simon for 12 at the Alzheimer/Parkinson conference in Sorrento, March 2005 (IC_{50} = 15 nM BACE-1, IC_{50} = 230 nM BACE-2, IC_{50} = 7,620 nM cathepsin D, $T_{1/2} \sim$ 2.1 h, clearance 76 ml/min/kg, V_{diss} 7.2 l/kg). Furthermore, the compound did not pass the blood-brain barrier in mice. A proof of concept was attempted via intracerebroventricular dosage (7.5 mg/kg/day) for 14 days. $A\beta_{40}$ was reduced by 47% at the end of the trial [13]. A compound with improved properties was reported recently [14].

Acylated tetronic and tetramic acids have been investigated as aspartic protease inhibitors before [15]. This was due to their similarity to Tipranavir, an active site inhibitor of the HIV-1 aspartic protease. Co-crystallization with the HIV-1 protease and structure determination revealed that the acidic hydroxyl of Tipranavir interacts with the catalytic aspartates [16]. The more compact

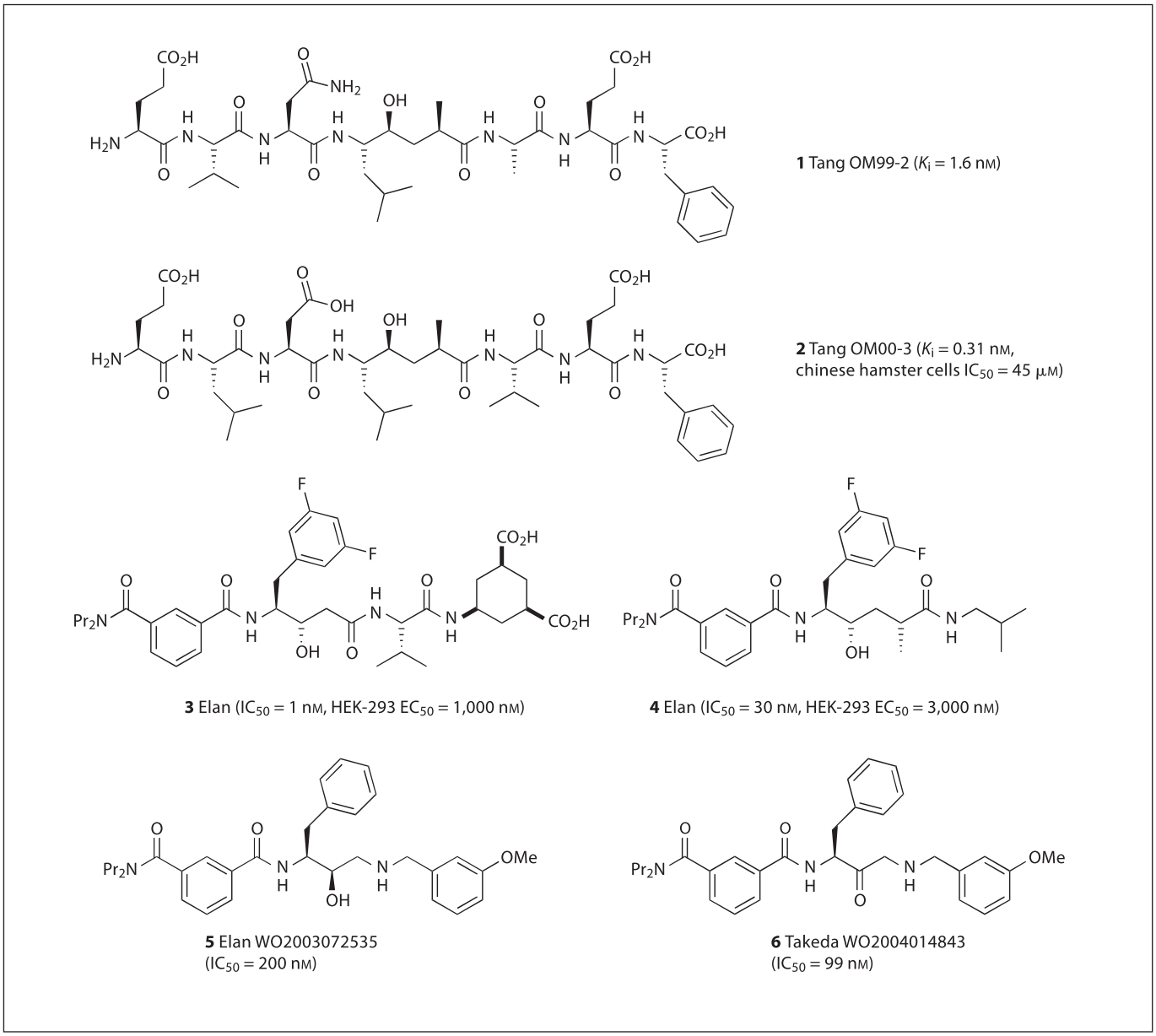

Fig. 2. BACE inhibitors I.

tetronates and tetramic acids may adopt a similar orientation in the active site, placing their substituents into lipophilic pockets. At the time we started the synthetic program on tetronic and tetramic acids, researchers from F. Hoffmann-La Roche identified a broad series of tetronic and tetramic acids with BACE inhibitor activity (13, IC_{50} = 11 μM) [17]. We explored several synthetic strategies in solution and on polymeric supports. A cyclization/cleavage strategy allowed to introduce diversity and resulted in more than 70 derivatives. The compounds 14–17 (fig. 4) were tested in collaboration with F. Hoffmann-La Roche, Basel, and M. Willem at the LMU, München. However, the activities were moderate at best. The removal of the acyl substituent or the replacement by a sulfoxide reduced the activity (IC_{50} > 200 μM) in FRET assays on isolated BACE-1 dramatically. The compounds were inactive in a radio ligand displacement assay against an active site-directed inhibitor. Furthermore, they displayed very poor inhibition in cellular assays, which points at a weak allosteric mode of action [18].

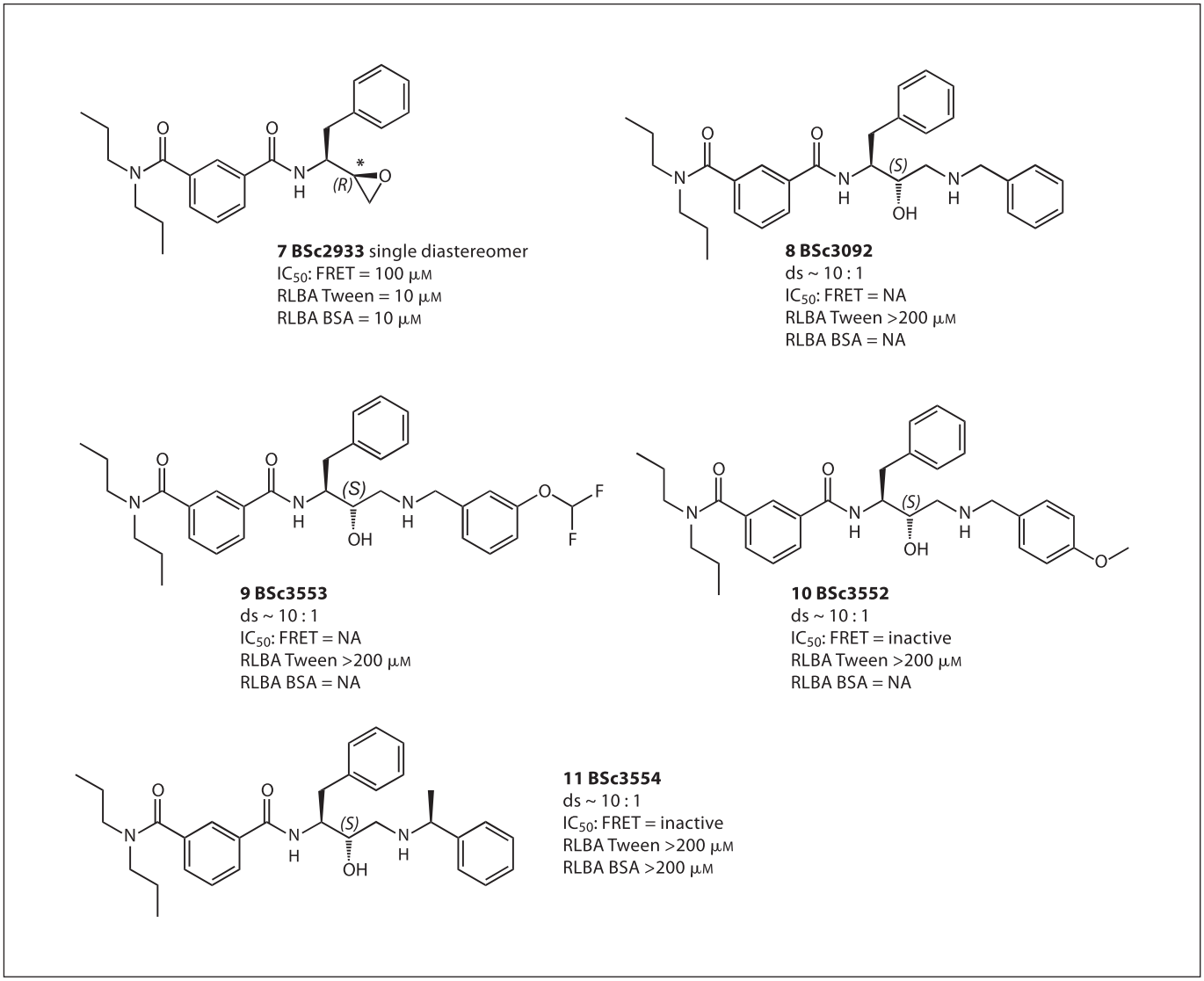

Fig. 3. BACE inhibitors II.

γ-Secretase Inhibitors

Special features of the γ-secretase complex hinder crystallization and thus crystallographic analysis of the enzyme, which is a major obstacle for structure-based drug design. Furthermore, the information available on inhibitor-binding sites is still limited. Therefore, all selective, nonpeptidic γ-secretase inhibitors had to be provided by high throughput screening efforts. Peptidic PS1 inhibitors, like Merck's L-685,458 (18, IC_{50} = 17 nM) (fig. 5), are potent inhibitors [19]. The all-lipophilic sequence with 3 phenylalanines was somewhat anticipated, as several studies had indicated the lipophilic binding pockets (P_2, P_1, P_1', P_2', even P_4' and P_7') in proximity to the cleavage site [20]. It was suggested that compound 18 acts as a direct transition-state analogue of the Aβ 1–40 and 1–42 cleavage sites. Elan's semipeptidic γ-secretase inhibitor DAPT (19, IC_{50} = 20 nM) was developed from an N-dichlorophenylalanine lead. Structure activity relationships studies revealed phenylglycine and difluorophenylacetic acid to be crucial for activity [21]. DAPT has demonstrated robust efficacy in vivo at relatively high doses. Several preclinical studies revealed in vivo toxicity, because DAPT affects the Notch pathway at higher levels (100- to 1,000-fold) [22]. We speculated in 2002 that DAPT may be binding in close contact to the aspartic ac-

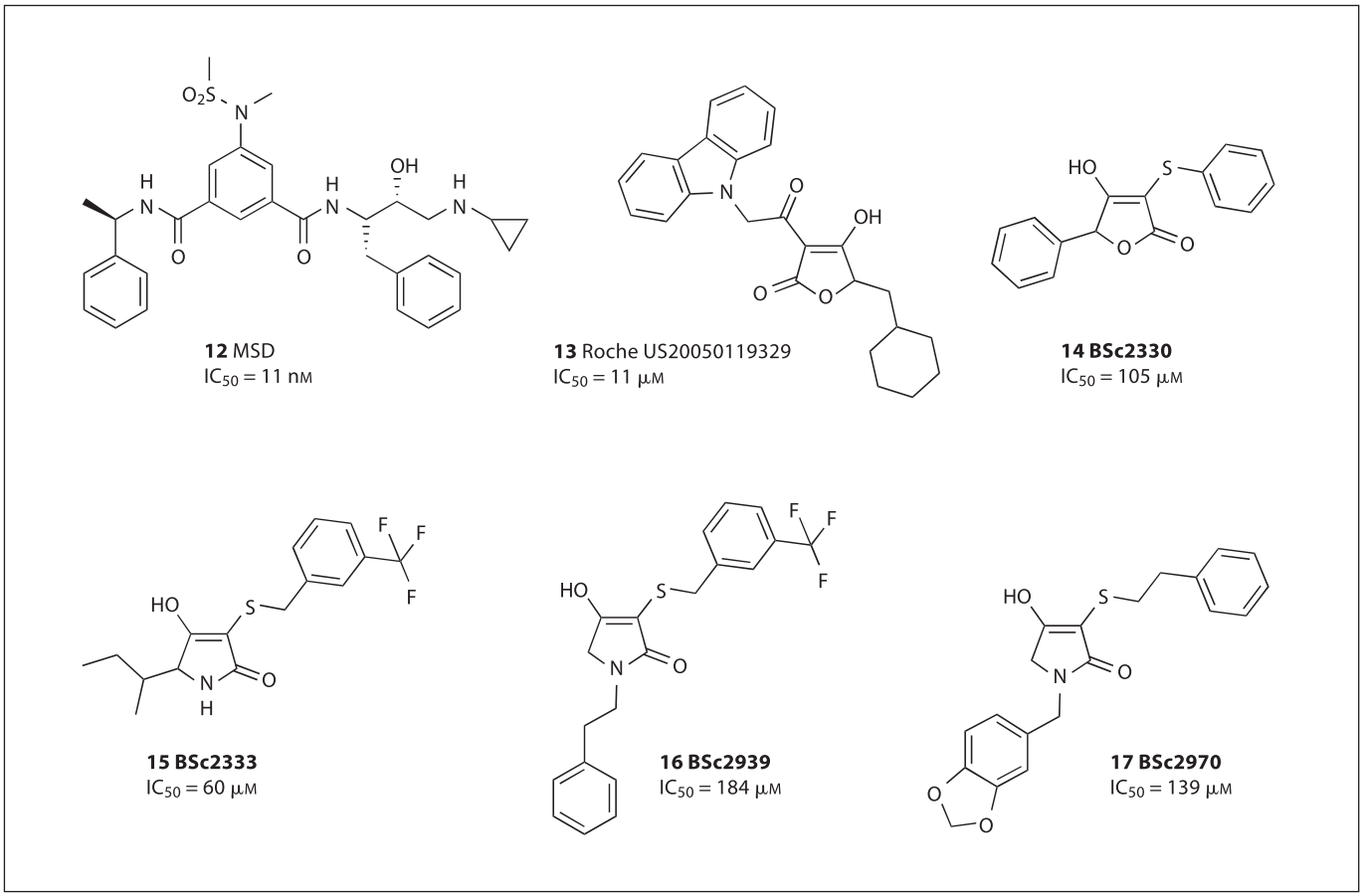

Fig. 4. Nonpeptidic BACE inhibitors.

ids of the active site and developed a series of acid-labile DAPT analogues. The compounds were intended to result in H^+ catalyzed fragmentation and reactive cationic intermediates. Some of the DAPT analogues were indeed potent inhibitors, but none of the compounds displayed the predicted time-dependent inhibition in the assays of C. Haass and H. Steiner, LMU München. We concluded that there is no irreversible inhibition by these pH sensors [23]. The difluorophenylacetyl moiety in DAPT can be replaced by 5-bromopyridin-3-ylacetyl without loss of activity. Methylation of the pyridine results in membrane-blocked DAPT analogues; these were evaluated in the reconstituted γ-secretase assay (C. Haass, H. Steiner, LMU München) and cellular assays (K. Baumann, M. Brockhaus, F. Hoffmann-La Roche, Basel). All compounds displayed activity in the reconstituted assay, yet at a varying degree. The quaternized, membrane-blocked compounds lacked activity in the cellular assay. The analysis of these compounds is ongoing. In the meantime, we moved on to immobilize DAPT analogue esters on affigel (Biorad) by 3 different linkers of varying length. One of the linkers included a photolabile nitrobenzyl ester to allow a mild cleavage without denaturation of the assembled complex. However, all affinity gels displayed high and unspecific background binding, the isolation of active γ-secretase by these gels was unsuccessful.

The γ-secretase inhibitors must reduce Aβ production sufficiently to alleviate the cause of AD, but must not totally abolish either its production or the processing of other proteins, which have important roles in neuronal structure and function. Several substrates must be considered in addition to APP and Notch: the Notch ligands Delta and Jagged, apoER2 lipoprotein receptor, the low-density lipoprotein receptor-related protein, ErbB4 receptor tyrosine kinase, CD44, p75 neurotrophin and β-subunits of voltage-gated sodium channels. The important issue is: are there γ-secretase inhibitors that reduce APP processing without generating an unacceptable side

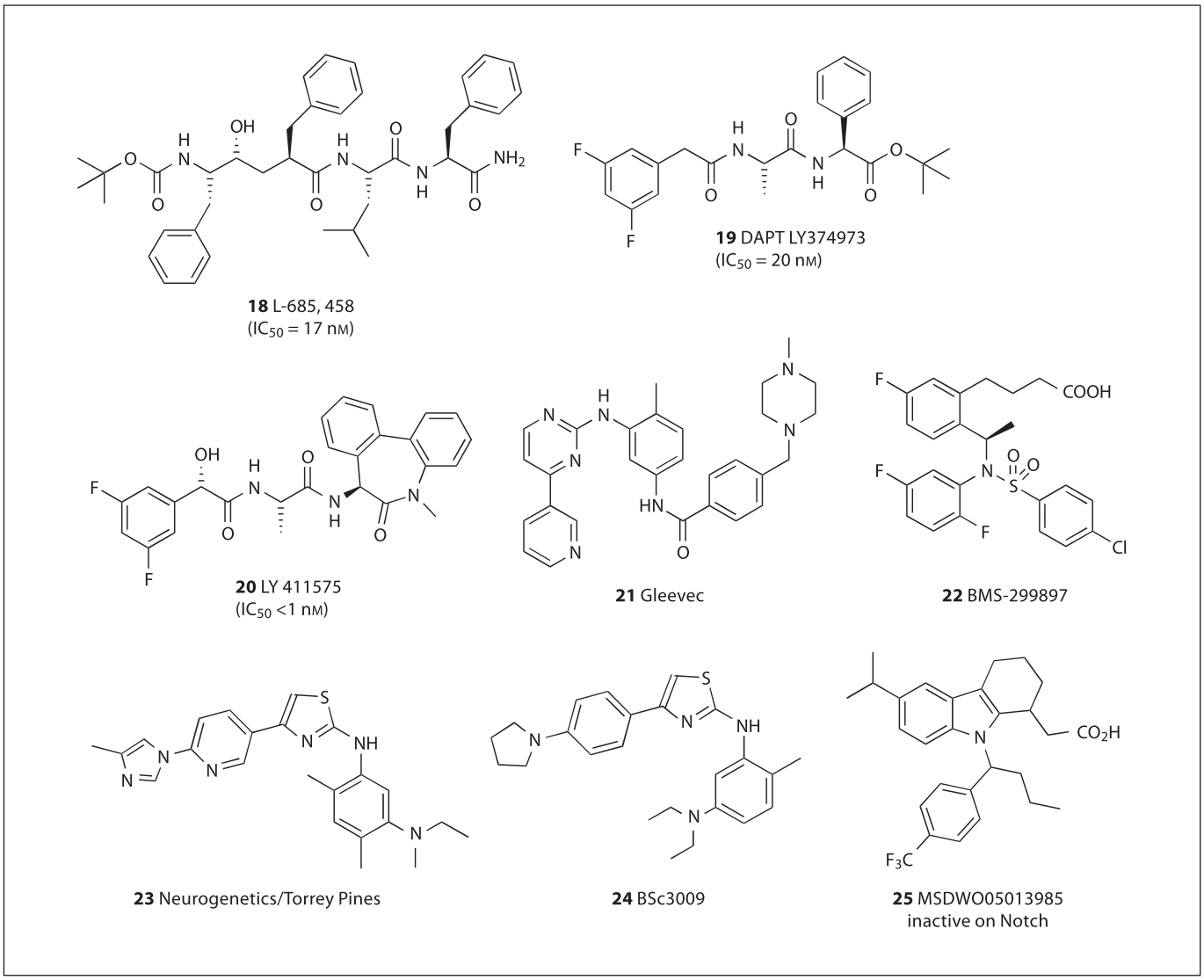

Fig. 5. Inhibitors and modulators of γ-secretase.

effect? Gleevec (21) inhibits Aβ production but not Notch cleavage [24]. IC_{50} values for $A\beta_{40}$, $A\beta_{42}$ and AICD were recently reported to be ~75 μM. The generation of NICD-Flag was not inhibited, even at >10-fold concentrations.

Selected nonsteroidal anti-inflammatory drugs (NSAIDs) reduce Aβ production without affecting alternative cleavages [25, 26]. The mechanisms of different γ-secretase inhibitors were explored in detail [27, 28]. Most of these bind directly to the active site or alter it through an allosteric interaction. Torrey Pines Pharmaceuticals disclosed a large number of aminothiazol-derivatives (23) with $A\beta_{42}/A\beta_{40}$-lowering activity at a concentration of about 30 μM [29]. Approximately 60 of these structures were claimed to display modulation of γ-secretase (activity < 0.2 μM). We decided to synthesize compound 24 and to evaluate it in collaboration with C. Haass and Hoffman-La Roche, Basel. The substance did not display modulation but inhibition: $EC_{50}(A\beta_{38})$ = 1.5 μM, $IC_{50}(A\beta_{40})$ = 1.8 μM, $IC_{50}(A\beta_{42})$ = 1.6 μM. A selective γ-secretase modulator (25) was reported by Merck Sharp & Dohme [30]; the carboxylic acid seems to be relevant for the desired ratio of $A\beta_{38}/A\beta_{40}/A\beta_{42}$. This modulation is distinctly different from inhibition as the total Aβ load may be unaffected. This was observed for several NSAIDs and is unrelated to COX1 inhibition [25]. Some COX1 inhibitors are suitable candidates to improve their ini-

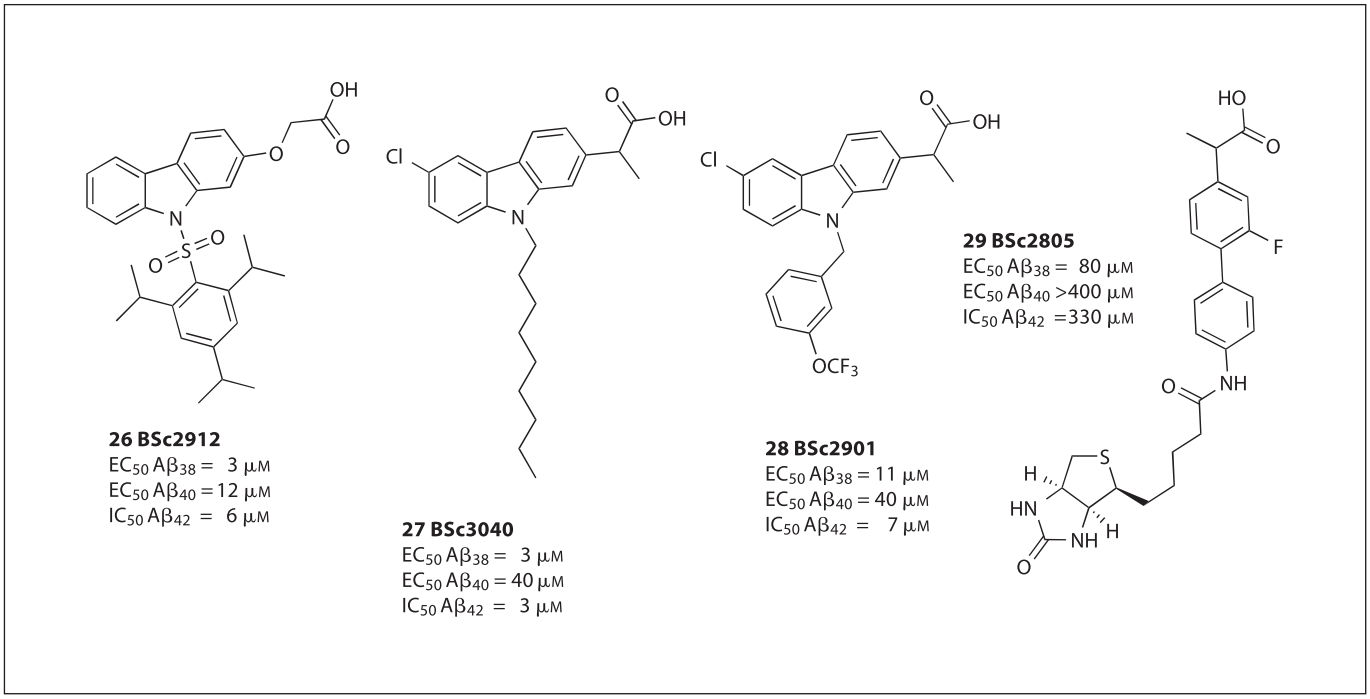

Fig. 6. NSAID-derived γ-secretase modulators.

tially weak activity. The analogy of BMS-299897 to COX1 inhibitors inspired us to explore derivatives of commercial NSAIDs: sulindac, flurbiprofen, ibuprofen, indomethacin, diclofenac, naproxen, carprofen, ketoprofen, and diflunisal. We prepared more than 150 derivatives, initially esters and amides of the parent carboxylic acids and identified several full γ-secretase inhibitors. The veratryl amides obtained from sulindac and diclofenac caused reduction of $A\beta_{38}$, $A\beta_{40}$ and $A\beta_{42}$ in cellular assays (IC_{50} 10–50 μM). However, some amides and esters displayed 'inverse' NSAID properties: $A\beta_{38}$ levels decreased, whereas $A\beta_{40}$ and $A\beta_{42}$ levels increased in cellular assays. γ-Secretase modulation was observed as the third mode of action: $A\beta_{38}$ increased, whereas $A\beta_{40}$ and $A\beta_{42}$ decreased in cellular assays. A structure-activity relationship is already apparent: the carboxylic acid is strictly required, and a lipophilic substituent branching out from the core structure improves the activity 10- to 100-fold. The scaffold can either derive from carprofen or carbazole. The lipophilic branch can be attached by alkylation or by sulfonylation of the aniline. The best cores have been attached to biotinylated, photoreactive linkers to result in 5 biotinylated compounds (just one example is provided in figure 6). However, these compounds turned out to be unsuitable baits for the γ-secretase complex, although some displayed significant modulation of γ-secretase activity. They resulted in unspecific binding or no detectable binding at all. A robust bait for the successful pull-down of the binding domain within γ-secretase is still unknown.

Outlook

The availability of peptidic and peptidomimetic inhibitors for β- and γ-secretase inhibitors, both as tool and lead structures, made a huge impact on the research area. But these potent peptidomimetics come with costly price tags: oral availability, cost of goods and blood-brain barrier penetration impose severe obstacles on drug development. Despite the extremely rapid progress in the field, there are no reports of brain penetrating secretase inhibitors in phase II or III (02/2006). The only γ-secretase inhibitor in phase I has a red flag associated with it. This is due to its impact on the Notch pathway. The selective modulation of γ-secretase by NSAIDs is pointing in the right direction: allosteric modulation of the active site, which can be identified by additional cleavage sites of presenilin-1.

Collaborations within the German Research Foundation Priority Program 1085

A ligand-based approach to Tau aggregation inhibitors was conducted in collaboration with the participant E. Mandelkow, Hamburg. A manuscript was submitted (30/01/06).

β-Secretase inhibitors, γ-secretase inhibitors and modulators, 20S proteasome inhibitors and targeted screening collections were supplied to R. Baumeister, C. Haass, T. Hartmann, U. Müller, G. Multhaup , J. Walter, S. Weggen, M. Willem. This resulted in 6 publications [2, 3, 10, 31–33] and 1 patent application (not yet published).

Acknowledgements

The authors thank the DFG (SPP1085 SCHM1012-3-1/2) and the EU (contract LSHM-CT-2003-503330; APOPIS) for support. We thank K. Baumann, M. Brockhaus and C. Czech (all at F. Hoffmann-La Roche, Basel) for biological assays, valuable input and long discussions.

References

1 WHO: The World Health Report 2001 Mental Health: New Understanding, New Hope. Geneva, WHO, 2001.

2 Schmidt B: Aspartic proteases involved in Alzheimer's disease. Chembiochem 2003;4:366–378.

3 Schmidt B, Baumann S, Braun HA, Larbig G: Inhibitors and modulators of β- and γ-secretase. Curr Top Med Chem 2006;6:377–392.

4 Schmidt B, Braun HA, Narlawar R: Drug development and PET-diagnostics for Alzheimer's disease. Curr Med Chem 2005;12:1677–1695.

5 Roggo S: Inhibition of BACE, a promising approach to Alzheimer's disease therapy. Curr Top Med Chem 2002;2:359–370.

6 John V, Beck JP, Bienkowski MJ, Sinha S, Heinrikson RL: Human β-secretase (BACE) and BACE inhibitors. J Med Chem 2003;46:4625–4630.

7 Ghosh AK, Hong L, Tang J: β-Secretase as a therapeutic target for inhibitor drugs. Curr Med Chem 2002;9:1135–1144.

8 Hong L, Turner RT III, Koelsch G, Shin D, Ghosh AK, Tang J: Crystal structure of memapsin 2 (β-secretase) in complex with an inhibitor OM00-3. Biochemistry 2002;41:10963–10967.

9 Maillaird M, Hom C, Gailunas A: Preparation of substituted amines to treat Alzheimer's disease. WO 200202512, 2002.

10 Braun HA, Meusinger R, Schmidt B: 2-Iodoethanols from aldehydes, diiodomethane and isopropylmagnesium chloride. Tet Lett 2005;46:2551–2554.

11 Miyamoto M, Matsui J, Fukumoto H, Tarui N: Preparation of 2-[2-amino- or 2-(N-heterocyclyl)ethyl]-6-(4-biphenylyl-methoxy)-tetralin derivatives as β-secretase inhibitors. WO 0187293, 2001.

12 Ramakrishna NVS, Kumar EKSV, Kulkarni AS: Screening of natural products for new leads as inhibitors of b-amyloid production: Latifolin from Dalbergia sissoo. Indian J Chem 2001;40B:539–540.

13 Barrow JC, Coburn CA, Nantermet PG: Preparation of phenylamides and pyridylamides as 1-secretase inhibitors. WO2005065195, 2005.

14 Stachel SJ, Coburn CA, Steele TG, et al: Conformationally biased P3 amide replacements of beta-secretase inhibitors. Bioorg Med Chem Lett 2006;16:641–644.

15 Yehia NA, Antuch W, Beck B, et al: Novel nonpeptidic inhibitors of HIV-1 protease obtained via a new multicomponent chemistry strategy. Bioorg Med Chem Lett 2004;14:3121–3125.

16 Thaisrivongs S, Strohbach JW: Structure-based discovery of tipranavir disodium (PNU-140690E): a potent, orally bioavailable, nonpeptidic HIV protease inhibitor. Biopolymers 1999;51:51–58.

17 Godel T, Hilpert H, Humm R: Preparation of tetronic and tetramic acids as beta-secretase inhibitors. WO 2005119329, 2005.

18 Larbig G, Schmidt B: Synthesis of tetramic and tetronic acid as beta-secretase inhibitors. J Comb Chem 2006;8:480–490.

19 Shearman MS, Beher D, Clarke EE, et al: L-685,458, an aspartyl protease transition state mimic, is a potent inhibitor of amyloid beta-protein precursor gamma-secretase activity. Biochemistry 2000;39:8698–8704.

20 Lichtenthaler SF, Wang R, Grimm H, Uljon SU, Masters CL, Beyreuther K: Mechanism of the cleavage specificity of Alzheimer's diseases γ-secretase identified by phenylalanine-scanning mutagenesis of the transmembrane domain of the amyloid precursor protein. PNAS 1999;96:3053–3058.

21 Dovey HF, John V, Anderson JP, et al: Functional γ-secretase inhibitors reduce b-amyloid peptide levels in brain. J Neurochem 2001;76:173–181.

22 Geling A, Steiner H, Willem M, Bally-Cuif L, Haass C: A γ-secretase inhibitor blocks Notch signaling in vivo and causes a severe neurogenic phenotype in zebrafish. EMBO Rep 2002;3:688–694.

23 Larbig G, Zall A, Schmidt B: Inhibitors designed for presenilin 1 utilizing by means of aspartic acid activation. Helv Chim Acta 2004;87:2334–2340.

24 Netzer WJ, Dou F, Cai D, et al: Gleevec inhibits beta-amyloid production but not Notch cleavage. PNAS 2003;100:12444–12449.

25 Weggen S, Eriksen JL, Das P, et al: A subset of NSAIDs lower amyloidogenic Aβ42 independently of cyclooxygenase activity. Nature 2001;414:212–216.

26 Lanz TA, Fici GJ, Merchant KM: Lack of specific amyloid-beta(1–42) suppression by nonsteroidal anti-inflammatory drugs in young, plaque-free Tg2576 mice and in guinea pig neuronal cultures. J Pharmacol Exp Ther 2005;312:399–406.

27 Beher D, Clarke EE, Wrigley JD, et al: Selected non-steroidal anti-inflammatory drugs and their derivatives target gamma-secretase at a novel site. Evidence for an allosteric mechanism. J Biol Chem 2004;279:43419–43426.

28 Kornilova AY, Das C, Wolfe MS: Differential effects of inhibitors on the γ-secretase complex. J Biol Chem 2003;278:16470–16473.

29 Cheng S, Comer DD, Mao L, Balow GP, Pleynet D: Aryl compounds and uses in modulating amyloid β. WO 2004110350, 2004.

30 Beher D, Bettati M, Checksfield GD: Preparation of tetrahydrocarbazole-1-alkanoic acids for the treatment of Alzheimer's disease and related conditions. WO 2005013985, 2005.

31 Schmidt B, Ehlert DK, Braun HA: E-1,2-dichlorovinyl ethers as irreversible protease inhibitors. Tet Lett 2004;45:1751–1753.

32 Braun HA, Umbreen S, Groll M, et al: Tripeptide mimetics inhibit the 20 S proteasome by covalent bonding to the active threonines. J Biol Chem 2005;280:28394–28401.

33 Schmidt B, Siegler A: Aspartic proteases involved in Alzheimer's disease; in Schmuck C, Wennemers H (eds): Highlights in Bioorganic Chemistry. Weinheim, Wiley-VCH, 2004, pp 262–276.

Inhibitors and Modulators of β- and γ-Secretase

Boris Schmidt*, Stefanie Baumann, Hannes A. Braun and Gregor Larbig

Clemens Schöpf-Institute for Organic Chemistry and Biochemistry, TU Darmstadt, Petersenstrasse 22, D-64287 Darmstadt, Germany

Abstract: Most gene mutations associated with Alzheimer's disease point to the metabolism of amyloid precursor protein as potential cause. The β- and γ-secretases are two executioners of amyloid precursor protein processing resulting in amyloid β. Significant progress has been made in the selective inhibition of both proteases, regardless of structural information for γ-secretase. Several peptidic and non-peptidic leads were identified and first drug candidates are in clinical trials. This review focuses on the developments since 2003.

Keywords: Alzheimer's disease, secretase, aspartic protease, inhibitor, presenilin.

INTRODUCTION

Alzheimer's disease (AD) is the most common progressive, irreversible dementia with neither definitely assigned cause nor an available causal therapy. The symptoms of the disease include memory loss, confusion, impaired judgment, personality changes, disorientation, and loss of language skills Furthermore, it is always fatal [1]. More than 4.5 million Americans are struck by Alzheimer's disease and this number may increase to 14 million by 2050. Approximately 350,000 new cases of Alzheimer's disease are diagnosed each year and 59,000 patients die of it in the US alone. A hallmark of Alzheimer's disease is the accumulation of extracellular amyloidic plaques in the brain [2-3]. The β-amyloid (Aβ) peptide, which is the major constituent of these amyloid plaques, performs a central role in the neuropathology of AD. The Aβ peptides, which differ in length from 38 to 42 amino acids, are generated from the amyloid precursor protein (APP) by two aspartic proteases: β-secretase and γ-secretase (Fig **1**). Both secretases are rather promiscuous, they have a multiple substrates and cause several distinctly different cleavages of APP. The membrane localisation of both enzymes is crucial for selectivity, as cell free conditions shift the cleavage pattern or result in additional cleavage sites. Usually 90% of the APP is degraded by the benign α-secretase pathway, and a mere 10% of APP are degraded by the consecutive cleavages of β- and γ-secretase to result in the build up of extracellular Aβ deposits. The contribution of these deposits to AD is still subject to debate. Neither the pathological consequences of deposited or soluble Aβ are established beyond doubt, nor does plaque formation adequately correlate to the progress of AD. A definite proof of the Aβ hypothesis is still missing for humans.

ESTABLISHED THERAPIES AND NOVEL APPROACHES

More than 50 compounds are in development to treat AD [4-5]. They target a whole range of known receptors and enzymes: GSK-3, PDE 4, and muscarinic M1 amongst others. Several acetylcholine (nACh) modulators, acetylcholinesterase (AchE) inhibitors, *N*-methyl-*D*-aspartate (NMDA) modulators, 5-hydroxytryptamine (5-HT) agonists and vaccination projects are in advanced stages of research or clinical development. The approved nAChE inhibitors and Vitamin E or combinations thereof have been marketed as therapies for AD. Unfortunately, recent clinical studies did not confirm benefits superior to placebo for vitamin E in mild cognitive impairment. Donepezil, an approved AChE inhibitor, slowed the AD progress in the first 12 months of treatment, but not in the following two years [6].

Some cholesterol lowering drugs such as pravastatin and lovastatin resulted in reduced risk for AD in retrospective trials. Paradoxically, prospective trials resulted in a contradicting outcome, and failed to confirm a risk reduction for AD. The rationale for this activity was subject to debate, but three observations suggested an explanation:

1). hypercholesterolemia is accompanied by increased levels of extractable total Aβ

2). β-secretase is associated to cholesterol stabilized rafts in the plasma membrane and

3). activity of the benign α-secretase is inversely related to cholesterol levels [7-9].

This hinted at a connection of AD pathology and cholesterol levels. The missing link turned out to be the regulation of cholesterol metabolism by amyloid β, which modifies the *de novo* cholesterol synthesis *via* 3-hydroxy-3-methylglutaryl-CoA reductase (HMGR) inhibition [10].

The early rush on fibril formation inhibition resulted in a number of potent inhibitors thereof. However, the activities were confined to *in vitro* experiments or limited by poor drug metabolism and pharmacokinetic (DMPK) properties, which excluded further development. Several drug candidates were tested in transgenic mice, but convincing data were not reported for humans. Furthermore, the view on Aβ toxicity has changed dramatically. Plaques were seen as the culprit and their removal was a therapeutic goal until 2001. Now, soluble Aβ and early oligomers have to take the

*Address correspondence to this author at the Clemens Schöpf-Institute for Organic Chemistry and Biochemistry, TU Darmstadt, Petersenstrasse 22, D-64287 Darmstadt, Germany; E-mail: Schmidt_Boris@t-online.de

1568-0266/06 $50.00+.00

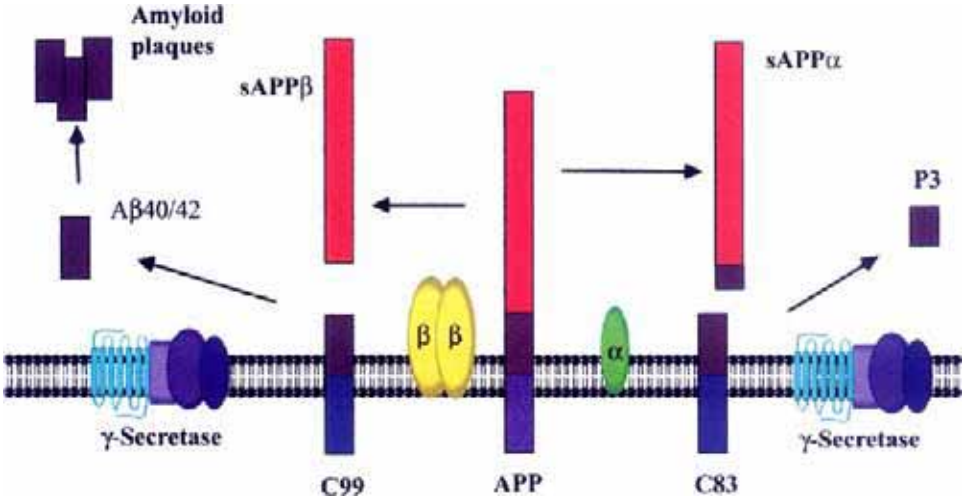

Fig. (1). Processing of APP by secretases.

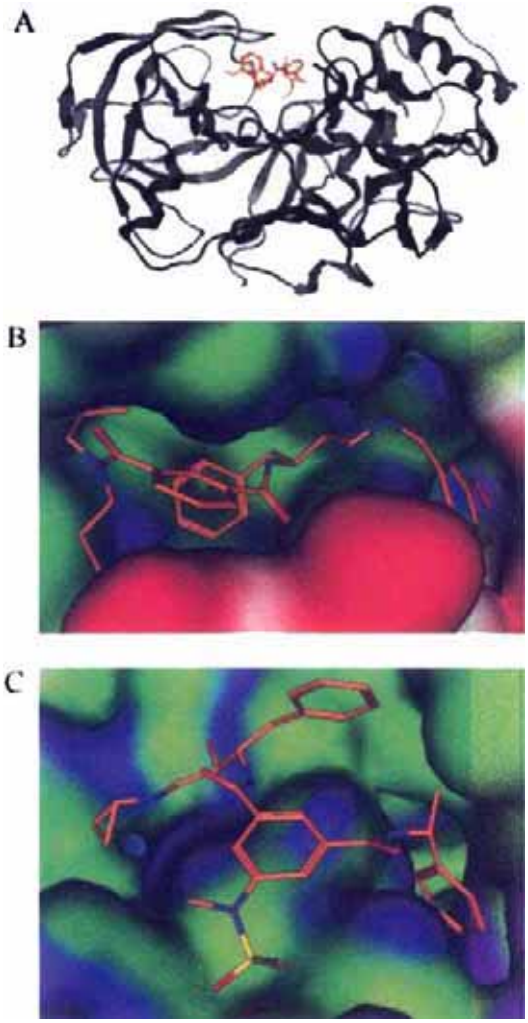

Fig. (2). (**a**) BACE complexed to **13** (PDB: 1W51). (**b**) Compound **13** in BACE above the flap (PBD: 1W51). (**c**) Sulfonamide **33** in BACE with the flap removed (PDB: 2B8L). MOE 2004.10 GaussConolly surface, green: hydrophobic, blue: hydrophilic.

blame for the Aβ associated effects. Thus mature Aβ plaques may rather rest in peace.

β-SECRETASE (BACE)

BACE-1 seemed to be an ideal target for drug development, because APP was the only known substrate. This scenario has changed substantially over the last two years, when amyloid precursor-like proteins (APLP1 and APLP2) and other substrates were reported [11]. However, these substrates can actually improve drug development as they can be utilized to identify BACE modifiers [12]. β-Secretase was identified as an aspartic protease long before selective inhibitors became available [13]. The key feature of an aspartic protease was confirmed early: the flexible flap region, which is crucial for substrate docking. The kinetics of statine-based inhibitors revealed a two state mechanism with structural reorganisation and activity modulation [14]. The two states: open and closed, contribute to selectivity and activity of the enzyme [15]. The flexibility of free and inhibitor bound BACE was investigated *in silico* and revealed several novel aspects of BACE, which are useful for structure-based, computer-aided inhibitor design [16]. The protonation states of the two active site residues Asp32 and Asp228 were calculated by several groups with different results [16-19]. Two β-secretases are known: BACE-1 (ASP2 or memapsin 2) and BACE-2 (ASP1 or memapsin 1) with high homology, yet subtle differences in the active site and an additional disulfide bridge for BACE-1 [20]. BACE-2 causes additional cleavages close to Phe20, which are reminiscent of α-secretase activity [21, 22]. BACE-1 is anchored to the membrane *via* its transmembrane domain (455-480) and may be active as a dimer [23]. BACE-1 has a propeptide domain, which is cleaved by furin-like proteases to form mature enzyme. The C-terminal transmembrane domain of BACE-1 is not strictly required for activity, but the localization of both enzyme and substrate in the same membrane enhances kinetics and specificity. The C-terminal truncation influences enzyme kinetics even in the absence of membranes. BACE-1 maturation requires cysteine bridge formation (Cys216/Cys420, Cys278/Cys443, Cys330/Cys380), *N*-glycosylation and propeptide removal. Cysteine

mutants undergo impaired maturation, but retain catalytic activity. The Cys330/Cys380 bridge was found to be the most important [4]. Crucial for assay development and animal models: BACE-1 -/- knockout mice are fertile and healthy, and display reduced Aβ levels [24]. Selectivity issues arise from other aspartic proteases, and the homologous BACE-2, which displays a less pathogenic APP cleavage pattern and a distinctly different localization [25-26]. The Aβ protein is released by a subsequent proteolysis at Val711-Ile712 or Ala713-Thr714 by the intramembrane protease: γ-secretase, resulting in $Aβ_{40}$ and $Aβ_{42}$. A detailed analysis of BACE distribution, structure, species variation, degradation and properties was published [27]. There is a ligand binding pocket within the catalytic domain of BACE that is distinct from the enzymatic active site [28]. Peptides binding to this exosite can inhibit proteolysis of APP in BACE (e.g. Ac-ALYPYFLPISAK-NH_2, IC_{50} = 1.3 μM). However, BACE inhibition is not the only way to modulate the BACE dependent APP cleavage. High levels of ceramide or improved raft association can extend the half-life of BACE-1 to 16 h [29]. Modest overexpression of BACE resulted in an enhanced amyloid deposition, while a high overexpression decreased amyloid deposition and altered the subcellular localization of BACE cleavage [30].

BACE INHIBITORS

Several reviews on secretase inhibition of BACE have been published [27, 31-34]. The majority of potent inhibitors are still peptide-based transition state analogues. Hydroxyethylenes, statines, norstatines, bis-statines, hydroxyethylamines and hydroxyethylureas were employed. The hydroxyethylenes delivered the first highly potent inhibitors. Their subsite specificity was revealed by the cleavage rates of combinatorial substrate mixtures and selective inhibitors, resulting in the design of the heptapeptides Glu-Val-Asn-Ψ(Leu-Ala)-Ala-Glu-Phe (**1** ,OM99-2, K_i = 1.6 nM, Scheme **1**) and Glu-Leu-Asp-Ψ(Leu-Ala)-Val-Glu-Phe (**2**, OM00-3, K_i = 0.31 nM) [35-37]. The two Tang-Ghosh inhibitors allowed co-crystallisation with BACE and structure determination at 1.9 Å and 2.1 Å, respectively (PDB: OM99-2, 1FKN; OM00-3, 1M4H) [38-40]. The inhibitors are located in the active site as intended by design. The hydroxyethylenes are coordinated by four hydrogen bonds to the two catalytic aspartates. Essentially, the structure of the enzyme and the backbone conformations from P_3 to P_2' are the same, although they differ in sidechain configurations of several subsites. In OM00-3, the P_3, P_2, and P_2' residues have been replaced. However, it is the P_4 Glu of OM00-3 that resides in a new S_4 pocket and the P_3' and P_4' residues are more extended, leading to a more linear conformation at both ends of OM00-3 compared to OM99-2. In the latter complex, a hydrogen bond from the P_4 Glu to the P_2 Asn is more favourable than to the P_2 Asp in OM00-3. This hydrogen bond and resulting interactions inspired the design of a novel inhibitors with low nanomolar potencies comprising a 14- to 16-membered P_2-cycloamide-urethane [41]. A protein-ligand X-ray structure of compound **3** bound to memapsin 2 was prepared (resolution 2.8 Å, PDB: 1XS7).

The crystal structure of free BACE (1SGZ) revealed a flap segment to be locked in an "open" position [42]. The structure is essentially the same as BACE-1 bound to an inhibitor, but the flap positions differ by 4.5 Å at the tips. The open position of the flap is stabilized by two intraflap hydrogen bonds and is anchored by a new hydrogen bond involving Tyr71 in a novel orientation. The resulting gorge may contribute to sequence and shape selection. A gatekeeper function was evident from the unusually small substituent Ala in P2' (**1**, 1FKN). Thr72 forms the narrowest point (6.5 Å in apo BACE) between the flap and Arg235, Ser328, and Thr329 on the opposite side and thus contributes to the specificity of BACE. This gatekeeper blocks the access of peptides carrying larger residues in this position, although pocket P_1' provides more than enough space for a significantly larger residue. Simulations suggest that BACE inhibitors should make use of both the open-flap and the closed-flap conformation, including different hydrogen bonds to Tyr71 [16].

Another inhibitor Lys-Thr-Glu-Glu-Ile-Ser-Glu-Val-Asn-(statine)-Val-Ala-Glu-Phe (P10-P4'StatVal, K_i = 40 nM, PDB: 1XN3) was co-crystallised with BACE [43]. The crystal structure revealed that the active cleft can accommodate at least three additional residues P_5-P_7 at the N-terminus. The residue preference of the new subsites and their influence on the hydrolytic activity of BACE were examined. An inhibitor Arg-Glu-Trp-Trp-Ser-Glu-Val-Asn-L*A-Ala-Glu-Phe (hydroxyethylene isostere, OM03-4) with a K_i-value of 0.03 nM was co-crystallized with BACE (PDB: 1XN2).

The small interactions of the C-terminal ends of OM99-2 and OM00-3 co-crystallised with BACE indicated a possible reduction without loss of activity. This was realised in the cyclic urethanes and further acyclic derivatives (**4**), yet with different degrees of success [44-47]. Hanessian *et al.* designed inhibitor **5** (IC_{50} = 0.039 μM) with a cyclopentane ring fused to the hydroxyethylene portion and a short Ala-terminus [48]. Chen *et al*. synthesised mimetics based on the Ψ(Phe-Ala) hydroxyethylene such as **6** and arrived at similar conclusions [49, 50]. Kiso *et al*. started from large hydroxymethylcarbonyl isosteres [51]. Inhibitor **7a** (KMI-370, IC_{50} = 3.4 nM) features a short dicarboxylic acid and displayed high activity *in vitro* and *in vivo* (BACE HEK293 cells IC_{50} = 0.20 μM) [52]. The tetrazole **7b** is a bioisostere of **7a** and exhibits similar activity and improved stability [53]. In the "Kiso" and the "Chen" series benzyl groups occupy the P_1 position. The introduction of a 3,5-difluorobenzyl to the S_1 pocket and non-peptidic N-termini made a further chain reduction possible, e.g. compound **8**. The asparagine replacements to the P_2-P_3 region deleted the peptidic character of the N-terminus, as realised in compound **9** by Elan [54-55].

The introduction of the isophthalamide was an important step towards less peptidic compounds **10**-**15** (Scheme **2**), which is mandatory to obtain sufficient oral absorption and blood brain barrier penetration [56, 57]. The modification also enabled further reduction of the C-terminus and utilization of different transition state isosteres. Significant information was revealed by a novel crystal structure of BACE complexed to hydroxyethylamine **13** [58- 59]. Soaking of *apo* BACE crystals (PDB: 1W50) with small peptidomimetics, which were known to be moderate inhibitors in FRET or cellular assays, resulted in the

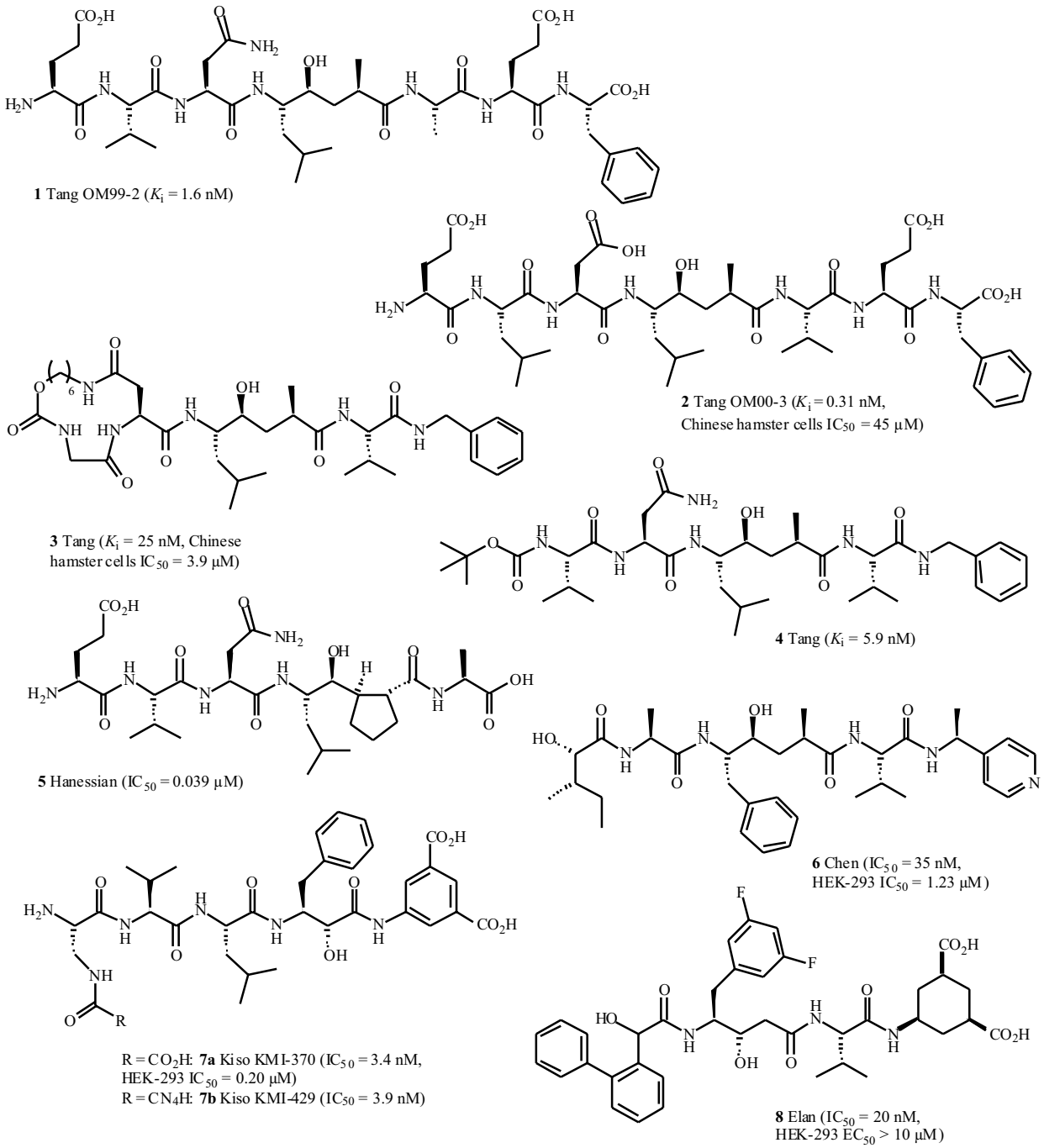

Scheme 1. BACE inhibitors I.

incorporation of **13** in the active site (PDB: 1W51, Fig. **2a, 2b**). The inhibitor features the isophthalamide to mimic the S_2-S_3 section and was claimed to have an IC_{50} = 200 nM, although the secondary alcohol is *R*-configured and thus has a different stereochemistry compared to other BACE transition state mimetics. The secondary amine and secondary alcohol recognise the active site aspartates in an unusual fashion. The neighbouring amine receives a proton from the catalytic Asp228 and places its 3-methoxy benzyl substituent in the S_2' pocket. One of the *N*-propyl groups of the isophthalamide occupies the S_3 pocket and is directed towards the phenyl ring in the S_1 pocket. The phenyl rings in both the S_1 and the S_2' pocket interact with Tyr71 of the flap in a T-shaped stacking. Some 750 close analogues of **13** were revealed in patents by Takeda (**14**) [60], Glaxo [61], Upjohn Pharmacia [62-64], Elan [56, 65-68] and a Sunesis employee (**15**) [69]. A series of inhibitors by Bristol-Myers Squibb makes use of benzylic hydroxyethylamines (**16**, IC_{50} < 0.1 μM), but rely on more peptidic scaffolds, some of these compounds display good activity [70].

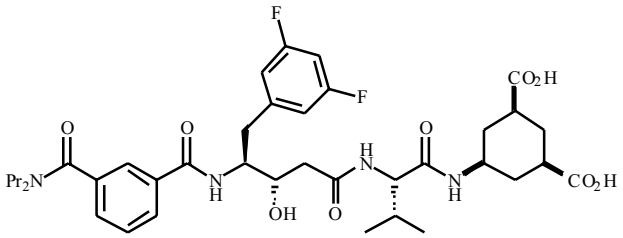

9 Elan (IC_{50} = 1 nM, HEK-293 EC_{50} = 1000 nM)

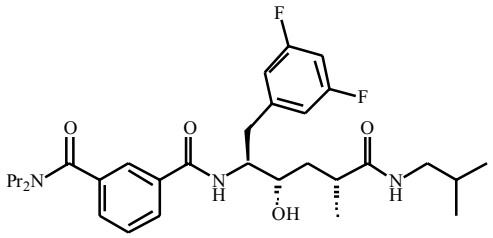

10 Elan (IC_{50} = 30 nM, HEK-293 EC_{50} = 3000 nM)

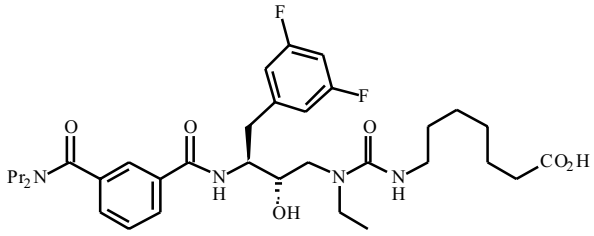

11 Elan WO2002002520

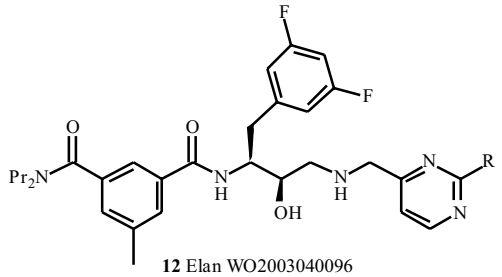

12 Elan WO2003040096

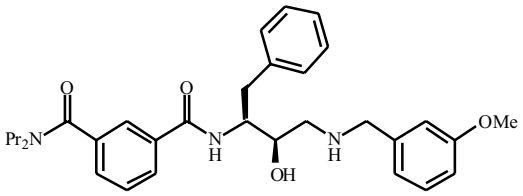

13 Elan WO2003072535
(IC_{50} = 200 nM)

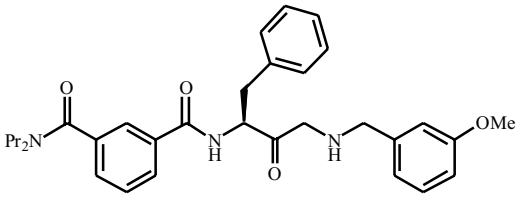

14 Takeda WO2004014843
(IC_{50} = 99 nM)

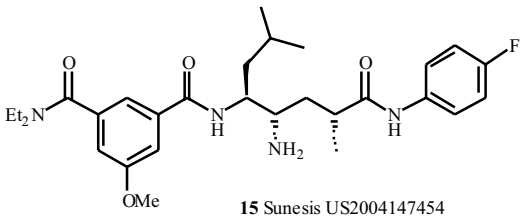

15 Sunesis US2004147454

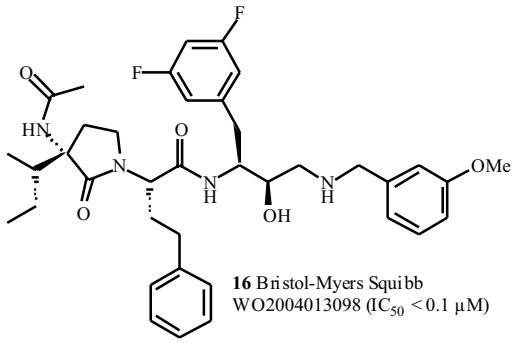

16 Bristol-Myers Squibb
WO2004013098 (IC_{50} < 0.1 μM)

Scheme 2. BACE inhibitors II.

Schering-Plough filed patent applications based on isophthalamide bioisosteres and derivatives such as **17** (IC_{50} = 1.4 nM) and **18** (IC_{50} = 1 nM) with isophthalide replacement by a multitude of other groups, e.g. 5- and 6-membered cyclic ureas or lactams (Scheme **3**) [71]. For the most part, the C-terminus is a substituted piperazine or piperazinone. Elan filed additional patents on BACE inhibitors: dipeptides and a number of smaller inhibitors were claimed (**19**, **20**) [72-74]. In two Elan patents, the inhibitors have neither a P_2 nor a P_3 substituent and the N-terminus is formed by an acetyl group only (**21**, **22**) [75-78]. The bicyclic inhibitor **23** has a low nanomolar IC_{50} in both the cell free and the cellular assay. It displays an oral bioavailability of 15%, a relative brain uptake (brain / plasma, 60 min) of 3.5 and an efficacy (efficacy = {1-(total Aβ concentration in tissue of dose group / total Aβ concentration in tissue of vehicle control)}x100%, at 100 mg / kg) for the cortex and the plasma of 47% and 63%, respectively. There are even smaller inhibitors of BACE (**24**, **25**), but **25** exhibits no selectivity toward cathepsin D (IC_{50}(CatD) / IC_{50}(BACE) = 1.1) [79]. Novartis created small inhibitors based on the original hydroxyethylene core [80-82]. The central portion is flanked by a very short alkyl residue at the C-terminus and a 14-membered macrocyclus at the N-terminus incorporating a fragment of the hydroxyethylene and an isophthalamide derivative (**26**), mimicking the P_1-P_3 residues.

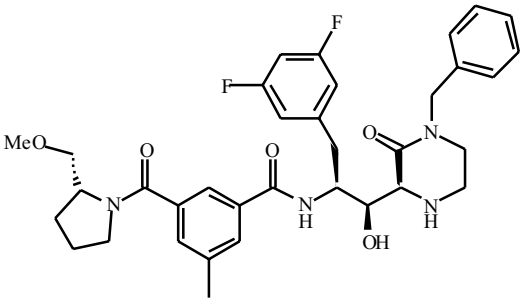

17 Schering-Plough WO2005016876
(IC_{50} = 1.4 nM)

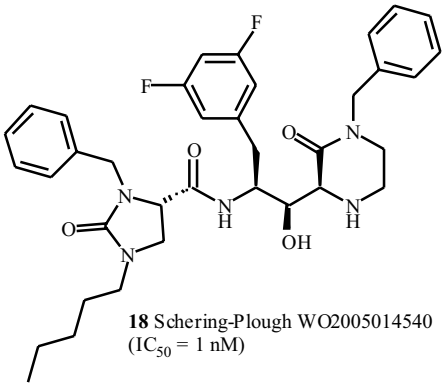

18 Schering-Plough WO2005014540
(IC_{50} = 1 nM)

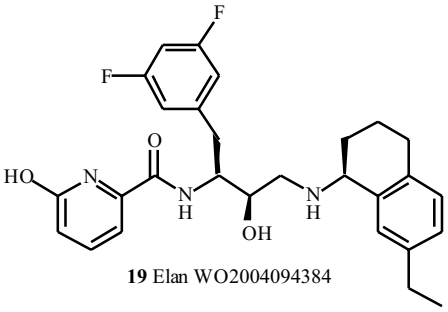

19 Elan WO2004094384

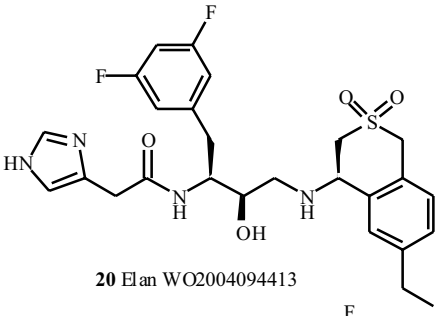

20 Elan WO2004094413

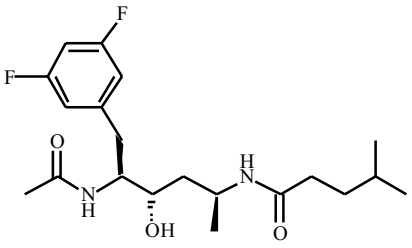

21 Elan WO2005042472

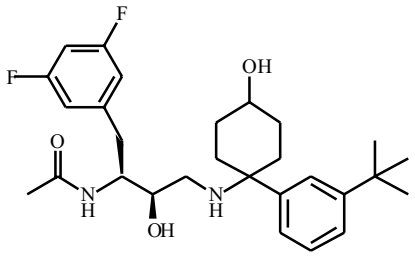

22 Elan WO2005070407

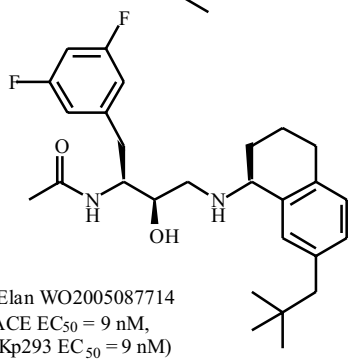

23 Elan WO2005087714
(BACE EC_{50} = 9 nM,
HEKp293 EC_{50} = 9 nM)

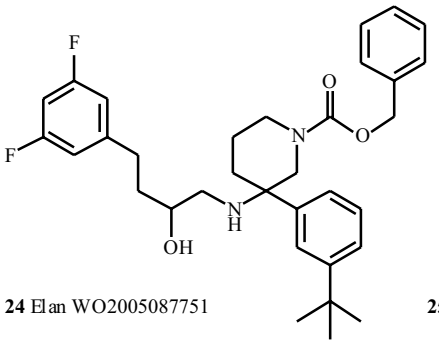

24 Elan WO2005087751

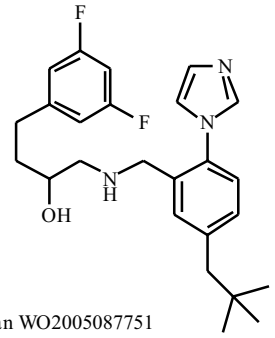

25 Elan WO2005087751

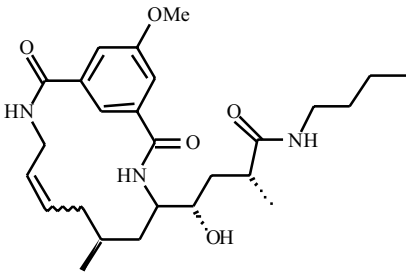

26 Novartis WO2005049585

Scheme 3. BACE inhibitors III.

Despite all efforts in the development of BACE-1 inhibitors, two major hurdles have hampered progress: blood-brain barrier permeability and oral bioavailability. To overcome these problems novel non-peptidic lead structures are of great interest. For several years, there were just few structures, usually with an obscure mode of action [83, 84]. Fluorescence resonance energy transfer (FRET) assays of soluble BACE delivered false positive hits to such a degree, that it was mandatory to profile potential hits in a reliable secondary assay, such as a radioligand displacement assay [85]. Vertex reported the biphenylpiperazine (**27**) as BACE inhibitor (IC_{50} = 3 μM, Scheme **4**) [86] and it was docked into the BACE structure by Park and Lee [17]. An unfortunate error improved it to 3 nM, which makes the outcome of this docking questionable. Yet, Actelion Pharmaceuticals revealed similar biphenylated amines (**28**) [87, 88].

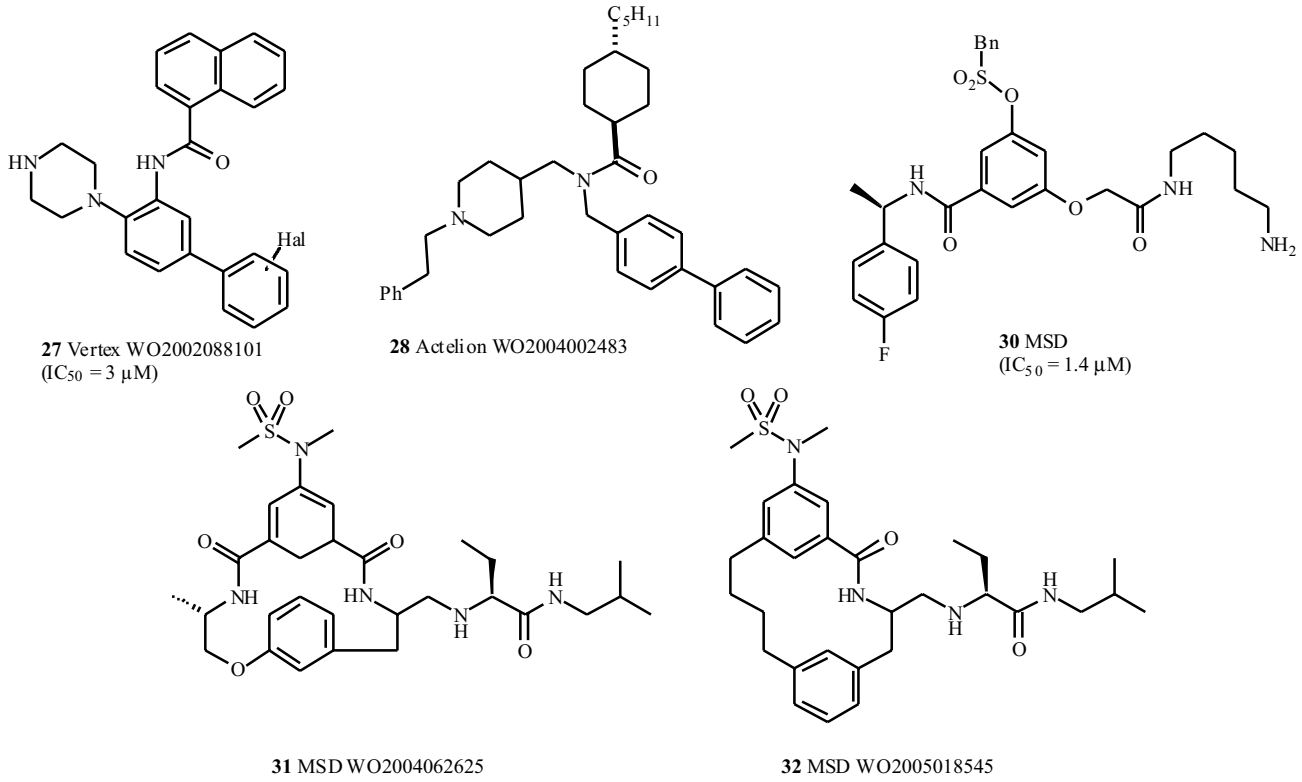

Scheme 4. Non-peptidic BACE inhibitors I.

The *Automated Ligand Identification System* (ALIS) [89] enabled MSD researchers to discover a novel resorcylic acid scaffold as reversible and selective BACE-1 inhibitor [90]. Further modifications lead to an aminopentyl derivative (**29**), which displays moderate inhibition of BACE-1 (IC_{50} = 1.4 μM) and a good selectivity towards cathepsin D (IC_{50} > 500 μM). Examination of an enzyme/inhibitor complex, which was obtained by using a modified BACE-1 (K75A, E77A) for co-crystallisation with **29** (PDB: 1TQF), revealed that the compound occupies the S_4 to S_1 subsites and does not have any interaction with the "prime side" of the enzyme. Most notably, the active site has no direct contact with the inhibitor. The acetamide is engaged in a hydrogen bond to the catalytic water, which is placed between the two aspartates as observed for the apo crystal structures of other aspartic proteases [90]. A novel S_3^{sp} subpocket was identified which is created by the orientation of the p-fluorophenyl ring towards the S_3 site. Another notable finding is that the terminal aminopentyl residue coils back into the S_1 pocket – a discovery that inspired the design of macrocycles (**31**, **32**) in which the P_1 and P_3 substituents are linked together increasing the activity by reduction of rotational freedom [91, 92].

Further development focused on the direct interaction with the catalytic aspartates, which is assumed to enhance activity. The hydroxylamine motif connected to an isophthalamide backbone improved the inhibition to 11 nM (**33**) and retained 500fold selectivity towards cathepsin D (Scheme **5**) [93]. The direct two-pronged interaction - wherein the hydroxyl functionality of the inhibitor engages Asp32, while the protonated α-amino group simultaneously contacts Asp228 – contributes to the increased potency. The occupation of the S_1 subsite and placement of a cyclopropyl, which is oriented toward the S_1' site of the enzyme, may have improved the inhibition further. The variation of the P_1' substituent exerts influence on cell permeability only. The compound was co-crystallised with BACE and the structure was deposited in the PDB recently (2B8L, Fig. **2c**). Slightly different activities were reported by A. Simon for **33** at the Alzheimer / Parkinson conference in Sorrento, March 2005 (IC_{50} = 15 nM BACE-1, IC_{50} = 230 nM BACE-2, IC_{50} = 7620 nM cathepsin D, $T_{1/2}$ ~ 2.1 hr, clearance 76 ml/min/kg, V_{diss} 7.2 l/kg). Furthermore, the compound did not pass the blood brain barrier in mice. A proof of concept was attempted *via* intracerebroventricular (ICV) dosage (7.5 mg/kg/d) for 14 days. $A\beta_{40}$ was reduced by 47% at the end of the trial. Several recent patents focus on the diversification of the side chains. Yet, there are no hints of an activity enhancement [94-98]. The Glaxo compound **34** features the same N-terminus, a similar transition state isostere, and a sulfonamide in the same position as the MSD compound, but all features are now locked in a tricyclic indolic ring system. Compound **34** has an activity (IC_{50}) of less than 1 μM in the Asp-2 inhibitory assay and more than 100fold selectivity for BACE over cathepsin D [99]. DeNovo reported several other scaffolds and mimetics: sulfonamides, 1-piperazinylpropan-2-ols and the triazine **35**, which may be useful for Aβ fibril imaging [100-103]. Researchers from Hoffmann-La Roche described a broad series of tetronic and tetramic acids with BACE inhibitor

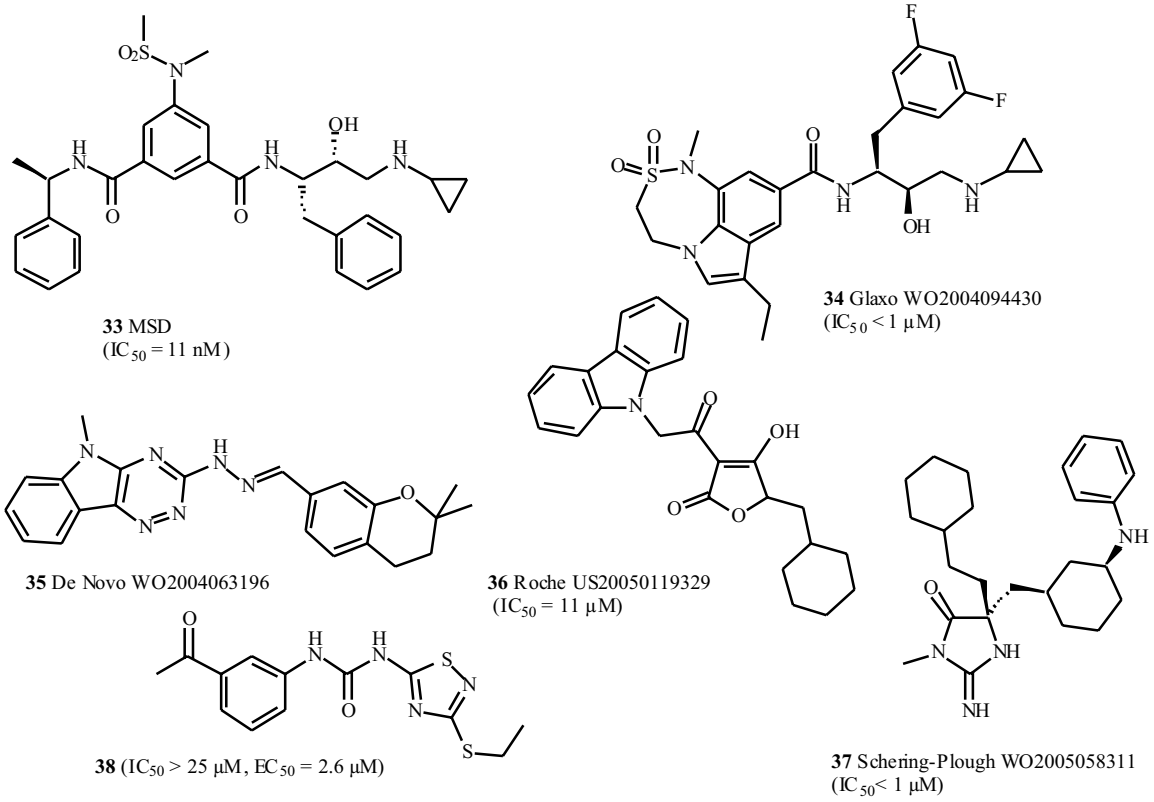

Scheme 5. Non-peptidic BACE inhibitors II.

activity (**36**, IC_{50} = 11 μM) [104]. Acylated tetronic and tetramic acids have been investigated as aspartic protease inhibitors before [105]. This was due to their similarity to Tipranavir, an active site inhibitor of the HIV-1 aspartic protease. Co-crystallisation with the HIV-1 protease and structure determination revealed that the acidic hydroxyl of Tipranavir interacts with the catalytic aspartates [106]. The more compact tetronates and tetramic acids may adopt a similar orientation in the active site, placing their substituents into lipophilic pockets. The removal of the acyl substituent or the replacement by a sulfoxide reduced the activity (IC_{50} > 200 μM) in FRET assays on isolated BACE1 [107].

Schering-Plough revealed 2-iminoimidazolidin-4-ones (**37**, IC_{50} < 1 μM) as BACE-1 inhibitors [108]. The same scaffold was described as potent inhibitor for cathepsin D – a limiting factor for the progression of that substance class into drug development.

A fragment-based docking procedure followed by substructure search was used to identify the phenyl-ureathiadiazole **38** (IC_{50} > 25 μM BACE-1, EC_{50} = 2.6 μM Aβ) [71]. The rigid conformation of BACE-1 in its complex with OM00-3 inhibitor (PDB: 1M4H) was used for the docking of **38** into the active site, resulting in the prediction of two binding modes. The two NH groups are involved in hydrogen bonds with one of the two catalytic aspartates. The S_1 pocket is occupied by the phenyl group and the ethylthioether is oriented toward the S_2' site of the enzyme. In the alternative binding mode, the two NH groups of the urea are involved in hydrogen bonds with Asp228 instead of Asp32. The overall orientation is flipped end-to-end. The phenyl group now occupies the S_1' subsite and the ethylthioether reaches into the S_1 pocket.

γ-SECRETASE

Paradoxical: despite being the secretase reported first, the identity of γ-secretase was subject to debate for a long time and the exact topology is still insecure. Now, it is well established that the γ-secretase is a high molecular weight protein complex composed of presenilin (PS) 1 or 2, nicastrin, Aph-1, and Pen-2 [109-113]. There is increasing evidence that PS – a polytopic transmembrane (TM) protein of ~50 kDa with 10 hydrophobic domains (HD) - forms the catalytic component of the γ-secretase complex [114-116], but presenilins alone are not sufficient to mediate enzyme activity [117, 118]. The active site of γ-secretase is known at some detail and the concerted action of all co-factors is still subject to debate. The inhibition by peptidomimetic transition-state analogues pointed to an aspartyl protease at work [118]. Following this assumption, the sequence analysis of presenilin revealed two likely candidates: Asp-257 and Asp-385 [115]. The ten HD may all cross the membrane, but it is still a controversial issue. The prevalent view until 2003 held that PS has an eight TM domain organization. A significant difference for this arrangement was reported recently. The introduction of glycosylation sites in PS1 revealed 9 TM domains, with the N-terminus and the large hydrophilic loop located in the cytosol, and the C-terminus in the ER lumen or extracellular [119]. Domain

swap experiments indicated two domains within the TM1, which affect presenilinase and γ-secretase activity differently. These TM1 mutants did not bind to the transition state mimetic Merck C [120], indicating a conformational change resulting in loss or reduction of catalytic activity [121].

In addition to βAPP, several other substrates are known to be cleaved by γ-secretase, which seems to be the "proteasome of the membrane" [122]. Generally, such multiple substrates increase the risk for toxic side effects by γ-secretase inhibition. In fact, the close relation to the Notch pathway, which is important in embryonic development, makes the γ-secretase a rather challenging and risky drug target. The crossover to the Notch pathway hampered attempts towards PS -/- knockout animals, which did not pass the embryonic state, but embryonic stem cells may fill part of the gap [123]. The intracellular trafficking of Notch in human CNS neurons is reduced by PS1 inhibitors, and results in dramatic changes in neurite morphology. A great task will be the determination of a therapeutic window between efficacy and any unacceptable toxicity [43]. Similar IC_{50}s for the competing cleavages of Notch and C99 do not rule out a safe application per se, as a 10% reduction in $A\beta_{42}$ production is regarded as the therapeutic goal. And indeed, a first compound with moderate Notch selectivity is in human trials [153].

γ-SECRETASE INHIBITORS

Special features of the γ-secretase complex hinder crystallisation and thus crystallographic analysis of the enzyme, which is a major obstacle for structure-based drug design. Furthermore, the information available on inhibitor binding sites is still limited. Therefore, all selective, non-peptidic γ-secretase inhibitors had to be provided by high throughput screening (HTS) efforts. Peptidic PS1 inhibitors, like Merck's L-685,458 (**39**, IC_{50} = 17 nM) are potent inhibitors and were patented prior to publication in scientific journals [124, 125]. The all-lipophilic sequence with 3 phenylalanines was somewhat anticipated, as several studies had indicated the lipophilic binding pockets (P_2, P_1, P_1', P_2', even P_4' and P_7') in proximity to the cleavage site [10]. It was suggested that compound **39** acts as a direct transition-state analogue of the Aβ (1-40) and (1-42) cleavage sites (Scheme **6**). The two des-hydroxy analogues displayed reduced inhibition (270fold) [124]. The core structure of **39** was linked to biotin and photoreactive fragments N- or C-terminally leading to L-852,505 (**41**) and L-852,646 (**42**), which were suitable for labelling studies. Despite the attachment of the photoreactive benzophenones, **41** and **42** retained potent inhibition (IC_{50} < 1 nM for γ-secretase). Biotin was used to facilitate the isolation and identification of the reversibly labelled adducts *via* their streptavidin-enzyme linked conjugates. Photolysis in the presence of solubilised γ-secretase and isolation on a biotin-specific streptavidin-agarose gel provided a protein of 20 kD linked to L-852,505 (**41**). This fragment was shown to be the C-terminal fragment of PS1 (PS1-CTF) by specific antibodies. In a control experiment, the binding of **41** to wild type PS1 was negative. However, the binding to the deletion construct PS1ΔE9, which lacks the cytosolic E9 loop, was positive [126]. Useful information resulted from the photolysis of L-852,646 (**42**) in the presence of solubilised γ-secretase. This resulted in the isolation of a 34 kD fragment, which was assigned to be an N-terminal fragment of PS1. A similar transition-state motif, the hydroxyethylurea **40** [127], was utilised for activity based affinity purification. The immobilisation of III-31-C (**40**, IC_{50} < 300 nM) on affigel 102 allowed isolation and identification of PS1-CTF, PS1-NTF and Nicastrin from solubilised γ-secretase preparations[128]. Initial attempts to free active γ-secretase from the affinity gel failed. This was probably due to the high binding affinity of III-31-C (**40**) to the target protein complex, and partially due to the deep and narrow binding site, which required strong denaturing conditions to break up the binding interactions. Yet, a delicate combination of Brij-35 (polyoxyethyl lauryl ether 30% aq. solution) and CHAPSO (3-(cyclohexylamino)-2-hydroxy-1-propanesulfonic acid) resulted in the isolation of active γ-secretase. The co-precipitation of the inhibited γ-secretase with its substrates C83 and C99 gave rise to speculations about additional binding sites, where the substrate is recognised prior to transfer to the active site. These speculations are in accor-dance with the observed promiscuous nature of the cleavage, as they assign the specific recognition to other domains. Elan's semi-peptidic γ-secretase inhibitor DAPT (**43**, IC_{50} = 20 nM) was developed from a *N*-dichlorophenylalanine lead. Structural activity relationships (SAR) studies revealed the phenylglycine and the difluoro phenylacetic acid to be crucial for activity [129, 130]. DAPT has demonstrated robust efficacy *in vivo* at relatively high doses. The subcutaneous application to mice in a dosage of 100 mg/kg resulted in a 50% reduction of cortical Aβ levels within 3 hours. A 40% Aβ reduction was observed at the dosage of 100 mg/kg orally, again after 3 hours, but no brain levels of DAPT were reported for the latter study [131]. Several preclinical studies revealed *in vivo* toxicity, because DAPT affects the Notch pathway at higher levels (100 – 1000fold) [132, 133]. These are negative news for future development.

Extensive *in vivo* studies have been carried out with the more potent analogue LY-411575 (**44a**). A stereoselective placement of the hydroxyl group and the locked spatial arrangement of two phenyl rings in a caprolactam increased the activity 20fold (**44a**, IC_{50} < 1 nM). Upon oral dosing of 1 mg/kg in 3 to 5 month-old Tg2576 mice, LY-411575 (**44a**) halved plasma and cortical Aβ levels within 3 hours [134]. A lesser active diastereomer was administered orally to C57BL/6 and TgCRND8 APP mice for 15 days at 1-10 mg/kg per day and resulted in the reduction of Aβ levels [135]. This was accompanied by atrophy of the thymus and deterioration of the intestinal epithelium. The Notch/APP selectivity was determined in cellular assays: $A\beta_{40}$ IC_{50} = 0.082 nM, Notch IC_{50} = 0.39 nM. This small toxicity window and the high potency made DAPT and **44a** unlikely candidates to enter clinical trials. Nevertheless, E. Siemers *et al*. went on and reported the first phase I study of the γ-secretase inhibitor **44b**, which is less potent than **44a** [136]. The oral application of LY450139 (**44b**) to healthy volunteers resulted in reduced plasma levels of $A\beta_{total}$ to 74.3% of the initial baseline at 40 mg/d after 14 days. The sampling time point was crucial, as a single dose results in reduction of $A\beta_{total}$ for 1-3 h and a dramatic overshoot between 5 and 24 h post dosage. However, cerebrospinal

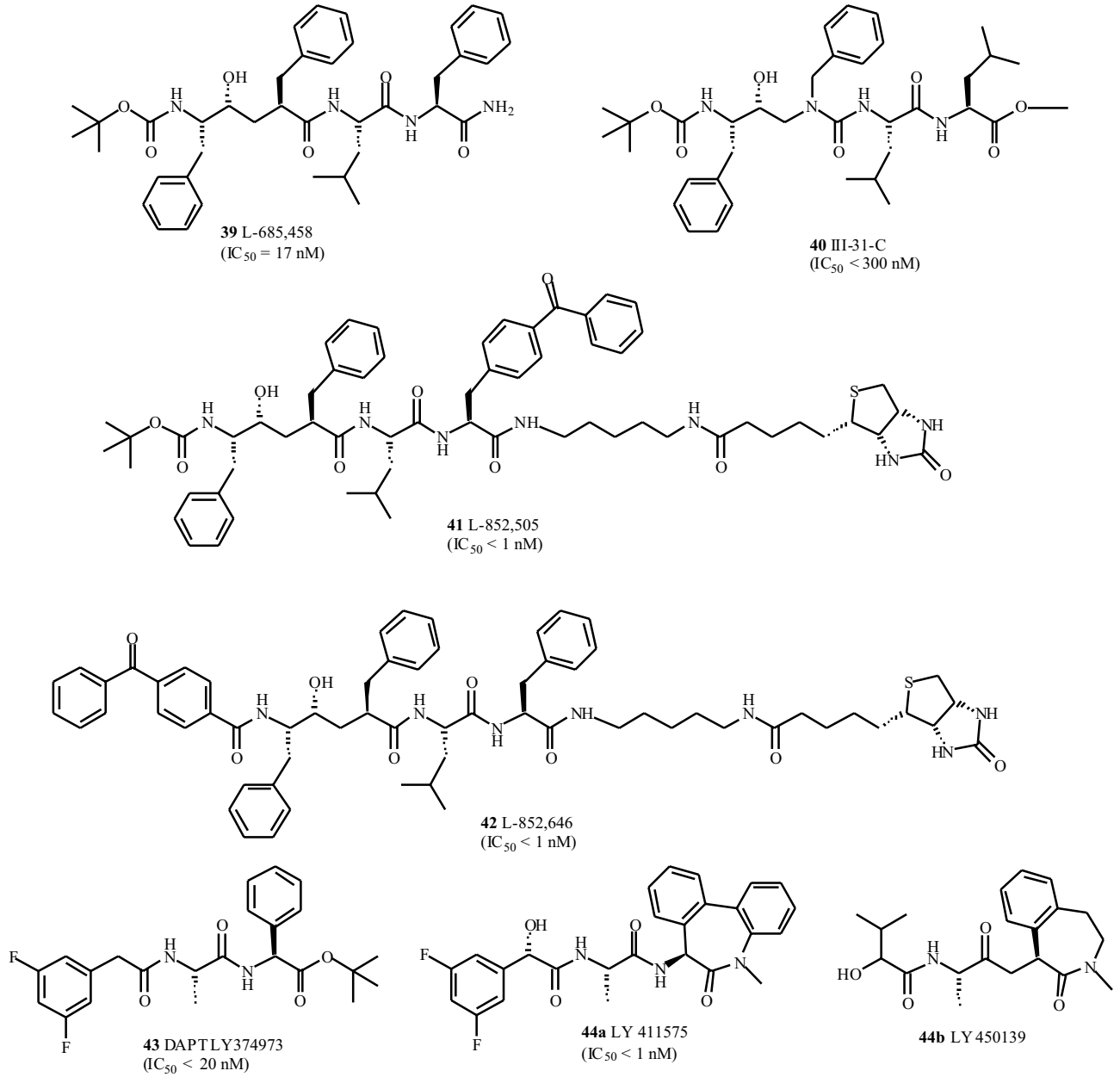

Scheme 6. γ-Secretase inhibitors I.

fluid (CSF) levels were constant. LY450139 (**44b**) is claimed to be mildly selective for γ-secretase cleavage over the Notch pathway,

DuPont Pharmaceuticals and Scios described a highly potent difluorophenacyl-caprolactam derivative (**45**, IC_{50} = 0.3 nM) [137]. Bristol-Meyers Squibb assumed DuPont, and continued to elaborate this caprolactam motif. As a result, a large number of derivatives were described. Some efforts were dedicated to modify the N-terminus to create non-infringing structures to the Elan patent. The synthesis of oxazolylsulfonamide **46** [138] is one such example.

The γ-secretase inhibitors must reduce Aβ production sufficiently to alleviate the cause of AD, but neither abolish totally its production nor the processing of other proteins, which have important roles in neuronal structure and function [139]. Several substrates must be considered in addition to APP and Notch: the Notch ligands Delta and Jagged, apoER2 lipoprotein receptor, the low density lipoprotein receptor-related protein, ErbB4 receptor tyrosine kinase, CD44, p75 neurotrophin and β subunits of voltage-gated sodium channels [140-141]. The important issue is: are there γ-secretase inhibitors, which reduce APP processing without generating an unacceptable side effect? Gleevec (**47**) inhibits Aβ production but not Notch cleavage (Scheme **7**) [142]. Recently, Fraering *et al.* reported IC_{50} values for $A\beta_{40}$, $A\beta_{42}$ and AICD of ~75 μM. Generation of NICD-Flag was not inhibited, even at >10-fold concentrations. The authors proposed a potential nucleotide-binding domain on γ-secretase, because ATP was able to rescue the γ-secretase

activity inhibited by a Gleevec formulation. There is strong support for this hypothesis: γ-secretase binds to ATP-acrylamide resin through the γ-phosphate [143]. Furthermore, selected nonsteroidal anti-inflammatory drugs reduce Aβ production without affecting alternative cleavages [124]. Isocoumarin inhibitors (JLK inhibitors) do not inhibit the E-cadherin processing, BACE-1/2, α-secretase, the proteasome and GSK2β kinase [144]. BMS-299897 (**48**) displayed a 15-fold lower IC_{50} value for APP than Notch-1-cleavage *in vitro* (HEK293 cells, APP IC_{50}: 7.1 nM, Notch IC_{50}: 105.9 nM) [43]. 2,3-Benzodiazepin-4-diones were designed as peptidomimetic inhibitors for γ-secretase [145]. The oral administration of these triamides in Tg2675 βAPP-Swedish transgenic mice resulted in a 15% reduction of CNS Aβ levels. Wolfe *et al.* explored the mechanisms of different γ-secretase inhibitors at detail [146]. Most of these bind directly to the active site or alter it through an allosteric interaction. Some inhibitors, e.g. the isocoumarins and the *Aib*-containing helical peptides, do not block Aβ production by affecting the active site of the protease, thus they do not target γ-secretase directly. Signal Peptide Peptidase SPP inhibitors can inhibit γ-secretase too, showing that SPP and γ-secretase have similar active sites and are likely to share the proteolytic mechanism [147].

Neurogenetics (now Torrey Pines Pharmaceuticals) disclosed a large number of aminothiazol-derivatives (**49**) with $Aβ_{42}/Aβ_{40}$-lowering activity at a concentration of about 30 μM [148]. The compounds derived from α-halogenated ketones and appropriate thioureas or ureas. Approximately 60 of these structures were claimed to display very good inhibition (activity < 0.2 μM). Compound **50** displayed similar activity ($EC_{50}(Aβ_{38})$ = 1.5 μM, $IC_{50}(Aβ_{40})$ = 1.8 μM, $IC_{50}(Aβ_{42})$ = 1.6 μM) [unpublished data]. The substituted thiazolamides (**51**), which resemble the Torrey Pines compounds, were coupled to a redox chemical delivery system (RCDS) and may feature enhanced pharmacokinetic properties [149]. A dihydropyridine RCDS was introduced to improve the blood brain barrier (BBB) permeation. The tested compounds exhibited EC_{50} values ranging from 0.1 to 1.0 μM in cell free assays. Compound **51** displayed an EC_{50} value of 0.2 μM in cellular assays using APP transfected HEK 293 cells.

The Elan patent application [149] reported three general synthetic schemes and about 700 tabulated examples. Selected *N*-(oxoazepanyl) benzenesulfonamides showed promising activities, for example, compound **52** inhibited γ-secretase with an IC_{50} within the range of 0.1-25 nM.

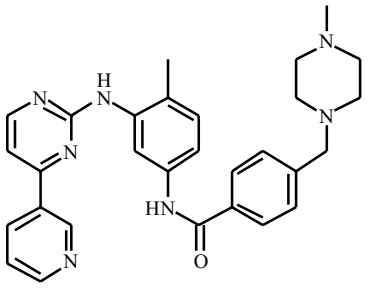

47 Gleevec

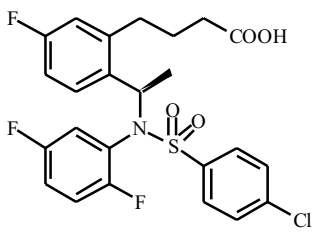

48 BMS-299897

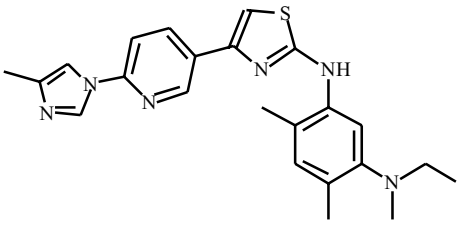

49 Neurogenetics/Torrey Pines

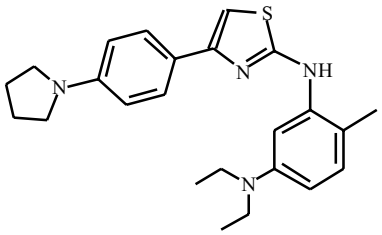

50 BSc3009

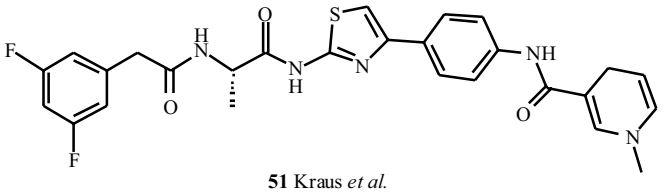

51 Kraus *et al.*

Scheme 7. γ-Secretase inhibitors II.

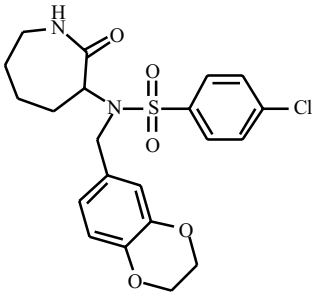

52 Elan WO2005042489
(IC_{50} = 0.1-25 nM)

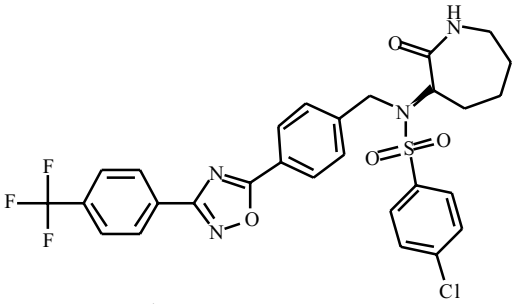

53 Elan WO2005042489

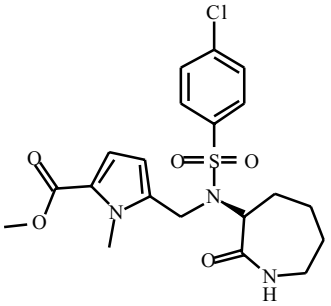

54 Elan WO2005042489

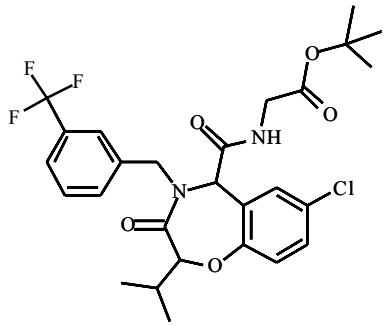

55 Roche US20040235819
(IC_{50} = 0.18)

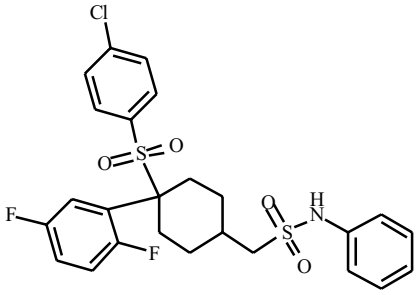

56 Merck WO2004031130
(ED_{50} < 1 μM)

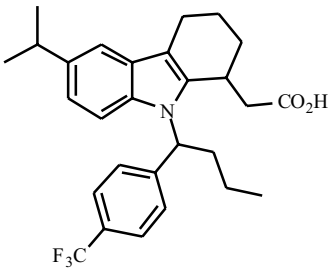

57 MSDWO05013985
inactive on Notch

Scheme 8. γ-Secretase inhibitors III.

However, the activities of compound **53** and **54** are unknown (or not reported).

Roche´s 1,4-benzoxazepin-3-one (**55**) was prepared by a cyclocondensation of (formylaryloxy)alkanoic acid, amine and isonitrile [151]. Compound **55** inhibited γ-secretase with an IC_{50} value of 0.18 (no units given). Additionally, Roche presented malonamide derivatives, where some compounds display IC_{50} values of < 1.0 μM [152]. The aryl cyclohexyl sulfone (**56**) [153], developed by Merck, inhibits the processing of APP by γ-secretase with ED_{50} values of < 1 μM. Eli Lilly optimized the series of dipeptides to challenge the amyloid hypothesis in a clinical setting [154]. Vlaams Interuniversitair Instituut disclosed peptides deriving from APP that specifically inhibit the γ-secretase cleavage without affecting the cleavage of Notch [155]. Their most potent inhibitor, the peptide D7 having the amino acid sequence VVIATVIVITLVMLK-TP inhibits γ–secretase activity up to 60-40% at a concentration of 1.5 μM. D7 did not affect S3-cleavage within the transmembrane domain of Notch.

A selective γ-secretase modulator (**57**) was reported by MSD [156], the carboxylic acid seems to be important to achieve the desired ratio of $A\beta_{38}/A\beta_{40}/A\beta_{42}$. This modulation is distinctly different from inhibition as the total Aβ load may be unaffected. This was observed for several NSAIDs and is unrelated to cyclooxygenase 1 (COX1) inhibition [157]. Some COX1 inhibitors are suitable candidates to enhance the initially weak activity.

OUTLOOK

The early availability of peptidic and peptidometimetic inhibitors for β- and γ-secretase inhibitors, both a tools and as lead structures, made a huge impact on the research area.

These potent peptidomimetics come with costly price tags: oral availability, cost of goods and blood brain barrier penetration impose severe obstacles on drug development. The lessons learned in the renin and HIV programmes certainly paid off, but the BBB issue multiplied the tasks for the medicinal chemists. There is a rigorous trend in most patent families founding on peptidomimetics leads to reduce the peptidic heritage as much as possible. BACE HTS assays provided very few non-peptidic scaffolds, but *in silico* screens were able to identify scaffolds with the desired properties. On the contrary, HTS on γ-secretase provided plenty of non-peptidic leads, but most of these are γ-secretase inhibitors, not modulators. Several compounds are close to enter phase I or phase II clinical trials. Despite the extremely rapid progress in the field, there are no reports of brain penetrating secretase inhibitors in phase II or III (Dec. 2005). The reported γ-secretase inhibitor in phase I has a red flag associated to it, this is due to its impact on the Notch pathway. The selective modulation of γ-secretase by nonsteroidal anti-inflammatory drugs (NSAIDs) is pointing in the right direction: allosteric modulation of the active site, which can be identified by additional cleavage sites of presenilin 1 (PS1). However, the required concentrations of most NSAIDs are well above safe levels. The differences of enantiomeric NSAIDs on COX1 inhibition provide an opportunity for drug development. Both enantiomers of flurbiprofen modulate γ-secretase, and the *S*-enantiomer of flurbiprofen, which is inactive on COX1 inhibition, is in development to treat AD. β-Secretase inhibitors do lower Aβ levels in mice, but there are no data on clinical trials available to the general public. The ultimate proof of concept for both secretases has not been revealed yet.

ACKNOWLEDGEMENT

B.S., H.A.B., S.B. and G.L. thank the DFG SPP1085 SCHM1012-3-1/2 and the EU contract LSHM-CT-2003-503330 (APOPIS) for support of this work.

REFERENCES

[1] WHO, The World Health Report 2001 Mental Health: New Understanding, New Hope. **2001**.
[2] Selkoe, D. *J. Physiol. Rev.* **2001,** *81,* 741.
[3] Selkoe, D. J. *J. Alzheimer's Dis.* **2001,** *3,* 75.
[4] Fischer, F.; Molinari, M.; Bodendorf, U.; Paganetti, P. J. Neurochem. **2002,** *80,* 1079.
[5] Kwon, M.-O.; Fischer, F.; Matthisson, M.; Herrling, P. *Neurodegenerative Dis.* **2004,** *1,* 113.
[6] Petersen, R. C.; Thomas, R. G.; Grundman, M.; Bennett, D.; Doody, R.; Ferris, S.; Galasko, D.; Jin, S.; Kaye, J.; Levey, A.; Pfeiffer, E.; Sano, M.; van Dyck, C. H.; Thal, L. *J. New England J. Med.* **2005,** *352,* 2379.
[7] Riddell, D. R.; Christie, G.; Hussain, I.; Dingwall, C. *Curr. Biol.* **2001,** *11,* 1288.
[8] Kojro, E.; Gimpl, G.; Lammich, S.; Marz, W.; Fahrenholz, F. *PNAS* **2001,** *98,* 5815.
[9] Refolo, L. M.; Sambamurti, K.; Efthimiopoulos, S.; Pappolla, M. A.; Robakis, N. K. *J. Neurosci. Res.* **1995,** *40,* 694.
[10] Lichtenthaler, S. F.; Wang, R.; Grimm, H.; Uljon, S. N.; Masters, C. L.; Beyreuther, K. *Proc. Natl. Acad. Sci. USA* **1999,** *96,* 3053.
[11] Li, Q.; Südhof, T. C. *J. Biol. Chem.* **2004,** *279,* 10542.
[12] Thomas C. Südhof; Li, Q. Fusion proteins with secretase cleavage specificity and therapeutic use for Alzheimer's disease. US2005112696, **2005**.
[13] Capell, A.; Steiner, H.; Willem, M.; Kaiser, H.; Meyer, C.; Walter, J.; Lammich, S.; Multhaup, G.; Haass, C. *J. Biol. Chem.* **2000,** *275,* 30849.
[14] Marcinkeviciene, J.; Luo, Y.; Graciani, N. R.; Combs, A. P.; Copeland, R. A. *J. Biol. Chem.* **2001,** *276,* 23790.
[15] Leung, D.; Abbenante, G.; Fairlie, D. P. *J. Med. Chem.* **2000,** *43,* 305.
[16] Gorfe, A. A.; Caflisch, A. *Structure* (*Camb*) **2005,** *13,* 1487.
[17] Park, H.; Lee, S. *J. Am. Chem. Soc.* **2003,** *125,* 16416.
[18] Rajamani, R.; Reynolds, C. H. *J. Med. Chem*. **2004,** *47,* 5159.
[19] Polgar, T.; Keserue, G. M. *J. Med. Chem.* **2005,** *48,* 3749.
[20] Chou, K. C. *J. Proteome Res.* **2004,** *3,* 1069.
[21] Farzan, M.; Schnitzler, C. E.; Vasilieva, N.; Leung, D.; Choe, H. *Proc. Natl. Acad. Sci. USA* **2000,** *97,* 9712.
[22] Yan, R.; Munzner, J. B.; Shuck, M. E.; Bienkowski, M. J. *J. Biol. Chem.* **2001,** *276,* 34019.
[23] Westmeyer, G. G.; Willem, M.; Lichtenthaler, S. F.; Lurman, G.; Multhaup, G.; Assfalg-Machleidt, I.; Reiss, K.; Saftig, P.; Haass, C. *J. Biol. Chem.* **2004,** *279,* 53205.
[24] Luo, Y.; Bolon, B.; Kahn, S.; Bennett, B. D.; Babu-Khan, S.; Denis, P.; Fan, W.; Kha, H.; Zhang, J.; Gong, Y.; Martin, L.; Louis, J. C.; Yan, Q.; Richards, W. G.; Citron, M.; Vassar, R. *Nat. Neurosci.* ***2001*****,** *4,* 231.
[25] Vassar, R. J. Mol. Neurosci. **2001,** *17,* 157.
[26] Gruninger-Leitch, F.; Schlatter, D.; Kung, E.; Nelbock, P.; Dobeli, H. *J. Biol. Chem.* **2002,** *277,* 4687.
[27] Roggo, S. *Curr. Top. Med. Chem.* **2002,** *2,* 359.
[28] Kornacker, M. G.; Lai, Z.; Witmer, M.; Ma, J.; Hendrick, J.; Lee, V. G.; Riexinger, D. J.; Mapelli, C.; Metzler, W.; Copeland, R. A. *Biochemistry* **2005,** *44,* 11567.
[29] Dominguez, D.-I.; Hartmann, D.; De Strooper, B. *Neurodegenerative Diseases* **2004,** *1,* 168.
[30] Lee, E. B.; Zhang, B.; Liu, K.; Greenbaum, E. A.; Doms, R. W.; Trojanowski, J. Q.; Lee, V. M. Y. *J. Cell. Biol.* **2005,** *168,* 291.
[31] Ishiura, S. *Dementia Jpn.* **2000,** *14,* 236.
[32] Citron, M. *Trends Pharmacol. Sci.* **2004,** *25,* 92.
[33] Schmidt, B. *ChemBioChem* **2003,** *4,* 366.
[34] John, V.; Beck, J. P.; Bienkowski, M. J.; Sinha, S.; Heinrikson, R. L. *J. Med. Chem.* **2003,** *46,* 4625.
[35] Ghosh, A. K.; Hong, L.; Tang, J. *Curr. Med. Chem.* **2002,** *9,* 1135.
[36] Ghosh, A. K.; Shin, D.; Downs, D.; Koelsch, G.; Lin, X.; Ermolieff, J.; Tang, J. *J. Am. Chem. Soc.* **2000,** *122,* 3522.
[37] Turner, R. T., 3rd; Koelsch, G.; Hong, L.; Castanheira, P.; Ermolieff, J.; Ghosh, A. K.; Tang, J. *Biochemistry* **2001,** *40,* 10001.
[38] Hong, L.; Turner, R. T., 3rd; Koelsch, G.; Ghosh, A. K.; Tang, J. *Biochem. Soc. Trans.* **2002,** *30,* 530.
[39] Hong, L.; Koelsch, G.; Lin, X.; Wu, S.; Terzyan, S.; Ghosh, A. K.; Zhang, X. C.; Tang, J. *Science* **2000,** *290,* 150.
[40] Hong, L.; Turner, R. T., 3rd; Koelsch, G.; Shin, D.; Ghosh, A. K.; Tang, J. *Biochemistry* **2002,** *41,* 10963.
[41] Ghosh, A. K.; Devasamudram, T.; Hong, L.; DeZutter, C.; Xu, X.; Weerasena, V.; Koelsch, G.; Bilcer, G.; Tang, J. Bioorg. Med. Chem. Lett. **2005,** *15,* 15.
[42] Hong, L.; Tang, J. *Biochemistry* **2004,** *43,* 4689.
[43] Barten, D. M.; Guss, V. L.; Corsa, J. A.; Loo, A.; Hansel, S. B.; Zheng, M.; Munoz, B.; Srinivasan, K.; Wang, B.; Robertson, B. J.; Polson, C. T.; Wang, J.; Roberts, S. B.; Hendrick, J. P.; Anderson, J. J.; Loy, J. K.; Denton, R.; Verdoorn, T. A.; Smith, D. W.; Felsenstein, K. M. *J. Pharmacol. Exp. Ther.* **2005,** *312,* 635.
[44] Hu, B.; Fan, K. Y.; Bridges, K.; Chopra, R.; Lovering, F.; Cole, D.; Zhou, P.; Ellingboe, J.; Jin, G.; Cowling, R.; Bard, J. *Bioorg. Med. Chem. Lett.* **2004,** *14,* 3457.
[45] Ghosh, A. K.; Bilcer, G.; Harwood, C.; Kawahama, R.; Shin, D.; Hussain, K. A.; Hong, L.; Loy, J. A.; Nguyen, C.; Koelsch, G.; Ermolieff, J.; Tang, J. *J. Med. Chem.* **2001,** *44,* 2865.
[46] Brady, S. F.; Singh, S.; Crouthamel, M. C.; Holloway, M. K.; Coburn, C. A.; Garsky, V. M.; Bogusky, M.; Pennington, M. W.; Vacca, J. P.; Hazuda, D.; Lai, M. T. Bioorg. Med. Chem. Lett. **2004,** *14,* 601.
[47] Tung, J. S.; Davis, D. L.; Anderson, J. P.; Walker, D. E.; Mamo, S.; Jewett, N.; Hom, R. K.; Sinha, S.; Thorsett, E. D.; John, V. *J. Med. Chem.* **2002,** *45,* 259.
[48] Hanessian, S.; Yun, H.; Hou, Y.; Yang, G.; Bayrakdarian, M.; Therrien, E.; Moitessier, N.; Roggo, S.; Veenstra, S.; Tintelnot-Blomley, M.; Rondeau, J.-M.; Ostermeier, C.; Strauss, A.; Ramage, P.; Paganetti, P.; Neumann, U.; Betschart, C. *J. Med. Chem.* **2005,** *48,* 5175.

[49] Chen, S. H.; Lamar, J.; Guo, D.; Kohn, T.; Yang, H. C.; McGee, J.; Timm, D.; Erickson, J.; Yip, Y.; May, P.; McCarthy, J. *Bioorg. Med. Chem. Lett.* **2004,** *14,* 245.

[50] Lamar, J.; Hu, J.; Bueno, A. B.; Yang, H. C.; Guo, D.; Copp, J. D.; McGee, J.; Gitter, B.; Timm, D.; May, P.; McCarthy, J.; Chen, S. H. *Bioorg. Med. Chem. Lett.* **2004,** *14,* 239.

[51] Shuto, D.; Kasai, S.; Kimura, T.; Liu, P.; Hidaka, K.; Hamada, T.; Shibakawa, S.; Hayashi, Y.; Hattori, C.; Szabo, B.; Ishiura, S.; Kiso, Y. *Bioorg. Med. Chem. Lett.* **2003,** *13,* 4273.

[52] Kimura, T.; Shuto, D.; Kasai, S.; Liu, P.; Hidaka, K.; Hamada, T.; Hayashi, Y.; Hattori, C.; Asai, M.; Kitazume, S.; Saido, T. C.; Ishiura, S.; Kiso, Y. *Bioorg. Med. Chem. Lett.* **2004,** *14,* 1527.

[53] Kimura, T.; Shuto, D.; Hamada, Y.; Igawa, N.; Kasai, S.; Liu, P.; Hidaka, K.; Hamada, T.; Hayashi, Y.; Kiso, Y. *Bioorg. Med. Chem. Lett.* **2005,** *15,* 211.

[54] Hom, R. K.; Fang, L. Y.; Mamo, S.; Tung, J. S.; Guinn, A. C.; Walker, D. E.; Davis, D. L.; Gailunas, A. F.; Thorsett, E. D.; Sinha, S.; Knops, J. E.; Jewett, N. E.; Anderson, J. P.; John, V. *J. Med. Chem.* **2003,** *46,* 1799.

[55] Hom, R. K.; Gailunas, A. F.; Mamo, S.; Fang, L. Y.; Tung, J. S.; Walker, D. E.; Davis, D.; Thorsett, E. D.; Jewett, N. E.; Moon, J. B.; John, V. *J. Med. Chem.* **2004,** *47,* 158.

[56] Maillaird, M.; Hom, C.; Gailunas, A.; Jagodzinska, B.; Fang, L. Y.; John, V.; Freskos, J. N.; Pulley, S. R.; Beck, J. P.; Tenbrink, R. E. Preparation of substituted amines to treat Alzheimer's disease. WO2002002512, **2002**.

[57] Beck, J. P.; Gailunas, A.; Hom, R.; Jagodzinska, B.; John, V.; Maillaird, M. Preparation of disubstituted amines for treating Alzheimer's disease. WO2002002520, **2002**.

[58] Patel, S.; Vuillard, L.; Cleasby, A.; Murray, C. W.; Yon, J. *J. Mol. Biol.* **2004,** *343,* 407.

[59] Vuillard, L. M. M.; Patel, S. J.; Yon, J. R.; Cleasby, A.; Hamilton, B. J.; Shah, A. Crystal structure of human β-secretase mutants and drug discovery applications. WO2004011641, **2004**.

[60] Uchikawa, O.; Aso, K.; Koike, T.; Tarui, N.; Hirai, K. Preparation of benzamide derivatives as β-secretase inhibitors. WO2004014843, **2004**.

[61] Demont, E. H.; Faller, A.; MacPherson, D. T.; Milner, P. H.; Naylor, A.; Redshaw, S.; Stanway, S. J.; Vesey, D. R.; Walter, D. S. Preparation of hydroxethylamine derivatives for the treatment of Alzheimer's disease. WO2004050619, **2004**.

[62] Pulley, S. R.; Beck, J. P.; Tenbrink, R. E.; Jacobs, J. S. Preparation of macrocycles useful in the treatment of Alzheimer's disease. WO2002100399, **2002**.

[63] Reeder, M. R. Processes for the synthesis of amino acid-related benzyl epoxides used in the production of pharmaceutical agents. WO2002085877, **2002**.

[64] Tenbrink, R.; Maillard, M.; Warpehoski, M. Preparation of substituted hydroxyethylamines as β-secretase inhibitors. WO2003050073, **2003**.

[65] Fang, L. Y.; Hom, R.; John, V.; Maillaird, M. Preparation of substituted amines for treating Alzheimer's disease. WO2002002505, **2002**.

[66] Fobian, Y. M.; Freskos, J. N.; Jagodzinska, B. A preparation of 1,3-diamino-2-hydroxypropane derivatives as β-secretase enzyme inhibitors. WO2004022523, **2004**.

[67] Fang, L. Y.; John, V. Compounds to treat Alzheimer's disease. WO2002002506, **2002**.

[68] John, V.; Maillard, M.; Jagodzinska, B.; Beck, J. P.; Gailunas, A.; Fang, L.; Sealy, J.; Tenbrink, R.; Freskos, J.; Mickelson, J.; Samala, L.; Hom, R. Preparation of N,N'-substituted-1,3-diamino-2-hydroxypropanes for treating Alzheimer's disease. WO2003040096, **2003**.

[69] Yang, W. Preparation of amino carboxamide derivatives as aspartyl protease inhibitors. WO2004147454, **2004**.

[70] Decicco, C. P.; Tebben, A. J.; Thompson, L. A.; Combs, A. P. Novel γ-lactams as β-secretase inhibitors. WO2004013098, **2004**.

[71] Cumming, J. N.; Huang, Y.; Li, G.; Iserloh, U.; Stamford, A.; Strickland, C.; Voigt, J. H.; Wu, Y.; Pan, J.; Guo, T.; Hobbs, D. W.; Le, T. X. H.; Lowrie, J. F. Preparation of cyclic amine BACE-1 inhibitors having a heterocyclic substituent. WO2005014540, **2005**.

[72] John, V.; Tung, J.; Hom, R.; Guinn, A.; Fang, L.; Gailunas, A.; Mamo, S. S. Preparation of statine-derived dipeptides as inhibitors of β-secretase. US6864240, **2005**.

[73] Aquino, J.; John, V.; Tucker, J. A.; Hom, R.; Pulley, S.; Tenbrink, R. Preparation of 2-hydroxy-3-aminoalkylbenzamides as β-secretase inhibitors for the treatment of Alzheimer's disease. WO2004094384, **2004**.

[74] Aquino, J.; John, V.; Tucker, J. A.; Hom, R.; Pulley, S.; Tenbrink, R. Preparation of phenacyl-substituted 2-hydroxy-3-diamino-alkanes as inhibitors of β-secretase. WO2004094413, **2004**.

[75] Tucker, J. A. Preparation of hydroxypropyl amide peptide analogs for the treatment of Alzheimer's disease. WO2005042472, **2005**.

[76] John, V.; Hom, R.; Sealy, J.; Aquino, J.; Probst, G.; Tung, J.; Fang, L. Preparation of N-(3-amino-2-hydroxypropyl)acetamides as aspartyl protease and β-secretase inhibitors for treating conditions associated such as Alzheimer's disease. WO2005070407, **2005**.

[77] John, V.; Maillaird, M.; Fang, L.; Tucker, J.; Brogley, L.; Aquino, J.; Bowers, S.; Probst, G.; Tung, J. Preparation of bicyclic compounds as aspartyl protease and beta secretase inhibitors for treating conditions associated with amyloidosis such as Alzheimer's disease. WO2005087714, **2005**.

[78] John, V.; Maillaird, M.; Tucker, J.; Aquino, J.; Hom, R.; Tung, J.; Dressen, D.; Shah, N.; Neitz, R. J. Preparation of substituted urea and carbamate, phenacyl-2-hydroxy-3-diaminoalkane, and benzamide-2-hydroxy-3-diaminoalkane aspartyl protease and β-secretase inhibitors for treating conditions associated with amyloidosis such as Alzheimer's disease. WO2005087215, **2005**.

[79] John, V.; Maillard, M.; Tucker, J.; Aquino, J.; Jagodzinska, B.; Brogley, L.; Tung, J.; Bowers, S.; Dressen, D.; Probst, G.; Shah, N. Preparation of hydroxyethylamines as aspartyl protease inhibitors for treatment of amyloidosis. WO2005087751, **2005**.

[80] Betschart, C.; Tintelnot-Blomley, M. Macrocyclic compounds having aspartic protease inhibiting activity and pharmaceutical uses thereof. WO2005003106, **2005**.

[81] Auberson, Y.; Betschart, C.; Glatthar, R.; Laumen, K.; Machauer, R.; Tintelnot-Blomley, M.; Troxler, T. J.; Veenstra, S. J. Preparation of macrocyclic lactams for treatment of neurological or vascular disorders related to β-amyloid generation and/or aggregation. WO2005049585, **2005**.

[82] Auberson, Y.; Betschart, C.; Flohr, S.; Glatthar, R.; Simic, O.; Tintelnot-Blomley, M.; Troxler, T. J.; Vangrevelinghe, E.; Veenstra, S. J. A preparation of dibenz[b,f]oxepincarboxamide derivatives, useful for the treatment of neurological and vascular disorders related to β-amyloid generation and aggregation. WO2005014517, **2005**.

[83] Miyamoto, M.; Matsui, J.; Fukumoto, H.; Tarui, N. Preparation of 2-[2-amino- or 2-(N-heterocyclyl)ethyl]-6-(4-biphenylylmethoxy) tetralin derivatives as β-secretase inhibitors. WO2001087293, **2001**.

[84] Ramakrishna, N. V. S.; Kumar, E. K. S. V.; Kulkarni, A. S.; Jain, A. K.; Bhat, R. G.; Parikh, S.; Quadros, A.; Deuskar, N.; Kalakoti, B. S. Indian J. Chem., Sect. B: *Org. Chem. Incl. Med. Chem.* **2001,** *40*B, 539.

[85] Brockhaus, M.; Doebeli, H.; Grueninger, F.; Huguenin, P.; Kitas, E. A.; Nelboeck-Hochstetter, P. Fluorescence and competitive radioligand binding assays for identifying β-secretase inhibitors and for screening agents for treatment of Alzheimer's disease and cerebrovascular amyloidosis. US2003125257, **2003**.

[86] Bhisetti, G. R. S., J. O.; Murcko, M. A.; Lepre, C. A.; Britt, S. D.; Come, J. H.; Deninger, D. D.; Wang, T. Preparation of β-carbolines and other inhibitors of BACE-1 aspartic proteinase useful against Alzheimer's and other BACE-mediated dieseases. WO2002088101, **2002**.

[87] Boss, C.; Bur, D.; Fischli, W.; Jenck, F.; Weller, T. Preparation of piperidines for the treatment of central nervous system disorders. WO2004009549, **2004**.

[88] Boss, C.; Bur, D.; Fischli, W.; Jenck, F.; Weller, T. Preparation of substituted 3- and 4-(aminomethyl)piperidines for use as β-secretase inhibitors in the treatment of Alzheimer's disease. WO2004002483, **2004**.

[89] Annis, D. A.; Athanasopoulos, J.; Curran, P. J.; Felsch, J. S.; Kalghatgi, K.; Lee, W. H.; Nash, H. M.; Orminati, J.-P. A.; Rosner, K. E.; Shipps, G. W.; Thaddupathy, G. R. A.; Tyler, A. N.; Vilenchik, L.; Wagner, C. R.; Wintner, E. A. *Int. J. Mass Spectrom.* **2004,** *238,* 77.

[90] Coburn, C. A.; Stachel, S. J.; Li, Y.-M.; Rush, D. M.; Steele, T. G.; Chen-Dodson, E.; Holloway, M. K.; Xu, M.; Huang, Q.; Lai, M.-T.; DiMuzio, J.; Crouthamel, M.-C.; Shi, X.-P.; Sardana, V.; Chen,

Z.; Munshi, S.; Kuo, L.; Makara, G. M.; Annis, D. A.; Tadikonda, P. K.; Nash, H. M.; Vacca, J. P. *J. Med. Chem.* **2004,** *47,* 6117.

[91] Coburn, C. A.; Stachel, S. J.; Vacca, J. P. Preparation of macrocyclic β-secretase inhibitors for treatment of Alzheimer's disease. WO2004062625, **2004**.

[92] Coburn, C.; Stachel, S. J.; Vacca, J. P. Preparation of macrocyclic β-secretase inhibitors for the treatment of Alzheimer's disease. WO2005018545, **2005**.

[93] Stachel, S. J.; Coburn, C. A.; Steele, T. G.; Jones, K. G.; Loutzenhiser, E. F.; Gregro, A. R.; Rajapakse, H. A.; Lai, M.-T.; Crouthamel, M.-C.; Xu, M.; Tugusheva, K.; Lineberger, J. E.; Pietrak, B. L.; Espeseth, A. S.; Shi, X.-P.; Chen-Dodson, E.; Holloway, M. K.; Munshi, S.; Simon, A. J.; Kuo, L.; Vacca, J. P. *J. Med. Chem.* **2004,** *47,* 6447.

[94] Barrow, J. C.; Coburn, C. A.; Nantermet, P. G.; Selnick, H. G.; Stachel, S. J.; Stanton, M. G.; Stauffer, S. R.; Zhuang, L.; Davis, J. R. Preparation of phenylamides and pyridylamides as β-secretase inhibitors. WO9822494, **2005**.

[95] Coburn, C. A.; Stachel, S. J.; Vacca, J. P. N-alkyl phenylcarboxamide β-secretase inhibitors for the treatment of Alzheimer's disease. WO2005004802, **2005**.

[96] Nantermet, P. G.; Rajapakse, H. A.; Selnick, H. G. Preparation of phenylcarboxylate esters as β-secretase inhibitors for the treatment of Alzheimer's disease. WO2005004803, **2005**.

[97] Nantermet, P. G.; Rajapakse, H. A.; Selnick, H. G. Benzyl ethers and benzylamines as β-secretase inhibitors, their preparation and use for the treatment of Alzheimer's disease. WO2005032471, **2005**.

[98] Nantermet, P. G.; Rajapakse, H. A.; Selnick, H. G.; Stauffer, S. R.; Young, M. B. Preparation of benzyl ethers, benzylamines, pyridylmethyl ethers, and pyridylmethylamines as β-secretase inhibitors for the treatment of Alzheimer's disease. WO2005051914, **2005**.

[99] Demont, E. H.; Redshaw, S.; Walter, D. S. Preparation of hydroxydiaminopropyl tricyclic indolecarboxamides for treatment of β-amyloid related disease. WO2004094430, **2004**.

[100] Willems, H. Preparation of piperazines as β-amyloid converting enzyme (BACE) inhibitors for the treatment of Alzheimer's disease. WO2004020422, **2004**.

[101] Willems, H.; Gordon, R. Protected amino acid derivatives for the treatment of Alzheimer's disease. GB2392443, **2004**.

[102] Willems, H.; Harris, W.; John, D. E. A preparation of triazinoindole derivatives as inhibitors of β-secretase (BACE), useful in the treatment of Alzheimer's disease. WO2004063196, **2004**.

[103] Willems, H.; Harris, W. H. Preparation of N-sulfonyl amino acid derivatives for the treatment of Alzheimer's disease. WO2004020402, **2004**.

[104] Godel, T.; Hilpert, H.; Humm, R.; Rogers-Evans, M.; Rombach, D.; Stahl, C. M.; Weiss, P.; Wostl, W. Preparation of tetronic and tetramic acids as beta-secretase inhibitors. US2005119329, **2005**.

[105] Yehia, N. A. M.; Antuch, W.; Beck, B.; Hess, S.; Schauer-Vukasinovic, V.; Almstetter, M.; Furer, P.; Herdtweck, E.; Domling, A. Bioorg. Med. Chem. Lett. **2004**, *14,* 3121.

[106] Thaisrivongs, S.; Strohbach, J. W. *Biopolymers* **1999,** *51,* 51.

[107] Schmidt, B.; Larbig, G. **2005,** submitted.

[108] Zhu, Z.; McKittrick, B.; Sun, Z.-Y.; Ye, Y. C.; Voigt, J. H.; Strickland, C.; Smith, E. M.; Stamford, A.; Greenlee, W. J.; Wu, Y.; Iserloh, U.; Mazzola, R.; Caldwell, J.; Cumming, J.; Wang, L.; Guo, T.; Le, T. X. H.; Saionz, K. W.; Babu, S. D.; Hunter, R. C. Preparation of heterocyclic aspartyl protease inhibitors for treating various diseases. WO2005058311, **2005**.

[109] Goutte, C.; Tsunozaki, M.; Hale, V. A.; Priess, J. R. *Proc. Natl. Acad. Sci. USA* ***2002*****,** *99,* 775.

[110] Yu, G.; Nishimura, M.; Arawaka, S.; Levitan, D.; Zhang, L.; Tandon, A.; Song, Y. Q.; Rogaeva, E.; Chen, F.; Kawarai, T.; Supala, A.; Levesque, L.; Yu, H.; Yang, D. S.; Holmes, E.; Milman, P.; Liang, Y.; Zhang, D. M.; Xu, D. H.; Sato, C.; Rogaev, E.; Smith, M.; Janus, C.; Zhang, Y.; Aebersold, R.; Farrer, L. S.; Sorbi, S.; Bruni, A.; Fraser, P.; St George-Hyslop, P. *Nature* **2000,** *407,* 48.

[111] Francis, R.; McGrath, G.; Zhang, J.; Ruddy, D. A.; Sym, M.; Apfeld, J.; Nicoll, M.; Maxwell, M.; Hai, B.; Ellis, M. C.; Parks, A. L.; Xu, W.; Li, J.; Gurney, M.; Myers, R. L.; Himes, C. S.; Hiebsch, R.; Ruble, C.; Nye, J. S.; Curtis, D. *Dev*. *Cell* **2002**, *3,* 85.

[112] Lee, S. F.; Shah, S.; Li, H.; Yu, C.; Han, W.; Yu, G. *J. Biol. Chem.* **2002**, *277,* 45013.

[113] Haass, C. *EMBO J.* **2004**, *23,* 483.

[114] Esler, W. P.; Kimberly, W. T.; Ostaszewski, B. L.; Diehl, T. S.; Moore, C. L.; Tsai, J. Y.; Rahmati, T.; Xia, W.; Selkoe, D. J.; Wolfe, M. S. *Nat. Cell Biol.* **2000,** *2,* 428.

[115] Wolfe, M. S.; Xia, W.; Ostaszewski, B. L.; Diehl, T. S.; Kimberly, W. T.; Selkoe, D. *J. Nature* **1999,** *398,* 513.

[116] Li, Y. M.; Xu, M.; Lai, M. T.; Huang, Q.; Castro, J. L.; DiMuzio-Mower, J.; Harrison, T.; Lellis, C.; Nadin, A.; Neduvelil, J. G.; Register, R. B.; Sardana, M. K.; Shearman, M. S.; Smith, A. L.; Shi, X. P.; Yin, K. C.; Shafer, J. A.; Gardell, S. *J. Nature* **2000**, *405,* 689.

[117] Mattson, M. P. *Nature* **2003,** *422,* 385.

[118] Wolfe, M. S.; Xia, W.; Moore, C. L.; Leatherwood, D. D.; Ostaszewski, B.; Rahmati, T.; Donkor, I. O.; Selkoe, D. *J. Biochemistry* **1999,** *38,* 4720.

[119] Laudon, H.; Hansson, E. M.; Melen, K.; Bergman, A.; Farmery, M. R.; Winblad, B.; Lendahl, U.; von Heijne, G.; Naslund, J. *J. Biol. Chem.* **2005**, *280,* 35352.

[120] Beher, D.; Fricker, M.; Nadin, A.; Clarke, E. E.; Wrigley, J. D.; Li, Y. M.; Culvenor, J. G.; Masters, C. L.; Harrison, T.; Shearman, M. S. *Biochemistry* **2003,** *42,* 8133.

[121] Brunkan, A. L.; Martinez, M.; Wang, J.; Walker, E. S.; Beher, D.; Shearman, M. S.; Goate, A. M. *J. Neurochem.* **2005,** *94,* 1315.

[122] Kopan, R.; Ilagan, M. X. Nat. Rev. Mol. Cell. Biol. **2004,** *5,* 499.

[123] Herreman, A.; Serneels, L.; Annaert, W.; Collen, D.; Schoonjans, L.; De Strooper, B. *Nat. Cell Biol.* **2000,** *2,* 461.

[124] Beher, D.; Clarke, E. E.; Wrigley, J. D. J.; Martin, A. C. L.; Nadin, A.; Churcher, I.; Shearman, M. S. *J. Biol. Chem.* **2004,** *279,* 43419.

[125] Nadin, A. J.; Stevenson, G. I. Preparation of peptides as γ-secretase inhibitors. WO2001077144, **2001**.

[126] McLendon, C.; Xin, T.; Ziani-Cherif, C.; Murphy, M. P.; Findlay, K. A.; Lewis, P. A.; Pinnix, I.; Sambamurti, K.; Wang, R.; Fauq, A.; Golde, T. E. *FASEB J.* **2000,** *14,* 2383.

[127] Castro Pineiro, J. L. S., A. L.; Stevenson, G. I. γ-Secretase inhibitors for treatment or prevention of Alzheimer's disease. WO0166564, **2001**.

[128] Esler, W. P.; Kimberly, W. T.; Ostaszewski, B. L.; Ye, W.; Diehl, T. S.; Selkoe, D. J.; Wolfe, M. S. *Proc. Natl. Acad. Sci. USA* **2002,** *99,* 2720.

[129] Dovey, H. F.; John, V.; Anderson, J. P.; Chen, L. Z.; de Saint Andrieu, P.; Fang, L. Y.; Freedman, S. B.; Folmer, B.; Goldbach, E.; Holsztynska, E. J.; Hu, K. L.; Johnson-Wood, K. L.; Kennedy, S. L.; Kholodenko, D.; Knops, J. E.; Latimer, L. H.; Lee, M.; Liao, Z.; Lieberburg, I. M.; Motter, R. N.; Mutter, L. C.; Nietz, J.; Quinn, K. P.; Sacchi, K. L.; Seubert, P. A.; Shopp, G. M.; Thorsett, E. D.; Tung, J. S.; Wu, J.; Yang, S.; Yin, C. T.; Schenk, D. B.; May, P. C.; Altstiel, L. D.; Bender, M. H.; Boggs, L. N.; Britton, T. C.; Clemens, J. C.; Czilli, D. L.; Dieckman-McGinty, D. K.; Droste, J. J.; Fuson, K. S.; Gitter, B. D.; Hyslop, P. A.; Johnstone, E. M.; Li, W. Y.; Little, S. P.; Mabry, T. E.; Miller, F. D.; Audia, J. E. *J. Neurochem.* **2001,** *76,* 173.

[130] Audia, J. E. B., T. C.; Droste, J. J.; Folmer, B. K.; Huffman, G. W.; John, V.; Latimer, L. H.; Mabry, T. E.; Nissen, J. S.; Porter, W. J.; Reel, J.K.; Thorsett, E. D.; Tung, J. S.; Eid, C. N.; Scott, W. L. Preparation of N-(phenylacetyl)di- and tripeptide derivatives for inhibiting β-amyloid peptide release. WO9822494, **1998**.

[131] Lanz, T. A.; Himes, C. S.; Pallante, G.; Adams, L.; Yamazaki, S.; Amore, B.; Merchant, K. M. *J. Pharmacol. Exp. Ther.* **2003,** *305,* 864.

[132] Geling, A.; Steiner, H.; Willem, M.; Bally-Cuif, L.; Haass, C. *EMBO Rep.* **2002,** *3,* 688.

[133] Hadland, B. K.; Manley, N. R.; Su, D.; Longmore, G. D.; Moore, C. L.; Wolfe, M. S.; Schroeter, E. H.; Kopan, R. *Proc. Natl. Acad. Sci. USA* **2001,** *98,* 7487.

[134] Lanz, T. A.; Hosley, J. D.; Adams, W. J.; Merchant, K. M. *J. Pharmacol. Exp. Ther.* **2004,** *309,* 49.

[135] Wong, G. T.; Manfra, D.; Poulet, F. M.; Zhang, Q.; Josien, H.; Bara, T.; Engstrom, L.; Pinzon-Ortiz, M.; Fine, J. S.; Lee, H. J.; Zhang, L.; Higgins, G. A.; Parker, E. M. *J. Biol. Chem.* **2004,** *279,* 12876.

[136] Siemers, E.; Skinner, M.; Dean, R. A.; Gonzales, C.; Satterwhite, J.; Farlow, M.; Ness, D.; May, P. C. *Clin. Neuropharmacol.* **2005**, *28,* 126.

[137] Seiffert, D.; Bradley, J. D.; Rominger, C. M.; Rominger, D. H.; Yang, F.; Meredith, J. E., Jr.; Wang, Q.; Roach, A. H.; Thompson, L. A.; Spitz, S. M.; Higaki, J. N.; Prakash, S. R.; Combs, A. P.; Copeland, R. A.; Arneric, S. P.; Hartig, P. R.; Robertson, D. W.; Cordell, B.; Stern, A. M.; Olson, R. E.; Zaczek, R. *J. Biol. Chem.* **2000,** *275,* 34086.

[138] Zaczek, R.; Olson, R. E.; Seiffert, D. A.; Thompson, L. A. Small molecule ligand inhibitors of β-amyloid peptide production suitable as diagnostic and therapeutic agents. US6737038, **2004**.

[139] Vardy, E. R. L. C.; Catto Andrew, J.; Hooper Nigel, M., Proteolytic mechanisms in amyloid-β metabolism: therapeutic implications for Alzheimer's disease. *Trends Mol. Med.* **2005,** *11,* 464.

[140] Wong, H.-K.; Sakurai, T.; Oyama, F.; Kaneko, K.; Wada, K.; Miyazaki, H.; Kurosawa, M.; De Strooper, B.; Saftig, P.; Nukina, N., β-Subunits of voltage-gated sodium channels are novel substrates of β-Site amyloid precursor protein-cleaving enzyme (BACE1) and γ-secretase. *J. Biol. Chem.* **2005,** *280,* 23009.

[141] Beglopoulos, V.; Sun, X.; Saura, C. A.; Lemere, C. A.; Kim, R. D.; Shen, J. *J. Biol. Chem.* **2004,** *279,* 46907.

[142] Netzer William, J.; Dou, F.; Cai, D.; Veach, D.; Jean, S.; Li, Y.; Bornmann William, G.; Clarkson, B.; Xu, H.; Greengard, P. *Proc. Natl. Acad. Sci. USA* **2003,** *100,* 12444.

[143] Fraering, P. C., γ-Secretase substrate selectivity can be modulated directly *via* interaction with a nucleotide binding site. *J. Biol. Chem.* **2005**, in press.

[144] Petit, A.; Pasini, A.; Alves da Costa, C.; Ayral, E.; Hernandez, J. F.; Dumanchin-Njock, C.; Phiel, C. J.; Marambaud, P.; Wilk, S.; Farzan, M.; Fulcrand, P.; Martinez, J.; Andrau, D.; Checler, F. *J. Neuro. Res.* **2003,** *74,* 370.

[145] Prasad, C. V. C.; Vig, S.; Smith, D. W.; Gao, Q.; Polson, C. T.; Corsa, J. A.; Guss, V. L.; Loo, A.; Barten, D. M.; Zheng, M.; Felsenstein, K. M.; Roberts, S. B. *Bioorg. Med. Chem.* **2004,** *14,* 3535.

[146] Kornilova, A. Y.; Das, C.; Wolfe, M. S. *J. Biol. Chem.* **2003,** *278,* 16470.

[147] Weihofen, A.; Lemberg, M. K.; Friedmann, E.; Rueeger, H.; Schmitz, A.; Paganetti, P.; Rovelli, G.; Martoglio, B. *J. Biol. Chem.* **2003**, *278,* 16528.

[148] Cheng, S.; Comer, D. D.; Mao, L.; Balow, G. P.; Pleynet, D. Aryl compounds and uses in modulating amyloid β. WO20040514, **2004**.

[149] Laras, Y.; Quelever, G.; Garino, C.; Pietrancosta, N.; Sheha, M.; Bihel, F.; Wolfe, M. S.; Kraus, J.-L. *Org. Biomol. Chem.* **2005**, *3,* 612.

[150] Neitzel, M.; Dappen, M. S.; Marugg, J. Preparation of N-(oxoazepanyl) benzenesulfonamides and related derivatives as γ-secretase inhibitors for treating Alzheimer's disease. WO2005042489, **2005**.

[151] Galley, G.; Goodnow, R. A.; Peters, J.-U. Preparation of 1,4-benzoxazepin-3-ones as inhibitors of γ-secretase for the treatment of Alzheimer's disease. US20040503, **2004**.

[152] Flohr, A.; Galley, G.; Jakob-Roetne, R.; Kitas, E. A.; Peters, J.-U.; Wostl, W. Preparation of dibenzoazepinylmalonamides, dibenzooxepinylmalonamides, benzodiazepinylmalonamides, and related compounds as γ-secretase inhibitors for treatment of Alzheimer's disease. US2005054633, **2005**.

[153] Churcher, I.; Harrison, T.; Kerrad, S.; Oakley, P. J.; Shaw, D. E.; Teall, M. R.; Williams, S. Preparation of aryl cyclohexyl sulfones as γ-secretase inhibitors useful against Alzheimer's disease. WO2004031137, **2004**.

[154] Audia, J. E.; Nissen, J. S.; Mabry, T. E.; McDaniel, S.; Porter, W. J.; Henry, S. S.; Britton, T. C.; Reel, J. K.; Droste, J. J.; Mitchell, D.; Hay, L. A.; Shi, Q.; Bender, M. H.; Boggs, L. N.; Cramer, J. W.; Czilli, D.; Dieckman, D. K.; Garner, C. O.; Gitter, B.; Hyslop, P. A.; Johnstone, E. M.; Li, W. Y.; Little, S. P.; McMillian, C.; Miller, F. D.; Yin, T.; May, P.; Thorsett, E. D.; Lattimer, L. H.; Tung, J. S.; Folmer, B. K.; Fang, L. Y.; Neitz, J.; Wu, J.; Dovey, H. F.; Freedman, S. B.; Schenk, D. B. Abstracts of Papers, 228th ACS National Meeting, Philadelphia, PA, United States, August 22-26, **2004**, MEDI.

[155] Annaert, W.; De Strooper, B.; Langedijk, J. P. M. Peptides derived from amyloid precursor protein inhibiting specific cleaving activities of presenilins and therapeutic use for Alzheimer's disease. WO2004026331, **2004**.

[156] Beher, D.; Bettati, M.; Checksfield, G. D.; Churcher, I.; Doughty, V. A.; Oakley, P. J.; Quddus, A.; Teall, M. R.; Wrigley, J. D. Preparation of tetrahydrocarbazole-1-alkanoic acids for the treatment of Alzheimer's disease and related conditions. WO2005013985, **2005**.

[157] Weggen, S.; Eriksen, J. L.; Das, P.; Sagi, S. A.; Wang, R.; Pietrizik, C. U.; Findlay, K. A.; Smith, T. E.; Murphy, M. P.; Bulter, T.; Kang, D. E.; Marquez-Sterling, N.; Golde, T. E.; Koo, E. H. *Nature* **2001,** *414,* 212.

DOI: 10.1002/cbic.200((Please insert last 6 DOI digits))

Pharmacophore model of BACE-1 inhibitors.

Ensemble-docking approach on BACE-1: Pharmacophore Perception and Directives for Drug Development

Vittorio Limongelli,[a] Luciana Marinelli,*[a] Sandro Cosconati,[a] Hannes A. Braun,[b] Boris Schmidt[b], and Ettore Novellino[a]

β-Secretase (BACE-1), a key enzyme in the etiopathogenesis and progression of Alzheimer Disease, is at the focus of medicinal chemistry efforts both in pharmaceutical industry and in academia. Despite the availability of diverse peptidomimetic BACE-1 inhibitors, non-peptidic compounds suitable for oral delivery and transport across the blood brain barrier are in great demand. Here, a number of active and structurally diverse inhibitors was selected and subjected to an ensemble-docking into BACE-1 X-ray structures. The calculated bioactive conformations of these inhibitors allow us to build an exhaustive pharmacophore model, which captures both the common geometric and electronic features essential for enzyme inhibition. The model is intended to aid the rational design of new BACE-1 inhibitors and can be used in pharmacophore- and/or structure-based virtual screening techniques. Furthermore, a comparison of BACE/cathepsin D X-ray structures was made with the aim to provide guidelines for the design of BACE-selective inhibitors.

Introduction

Alzheimer disease (AD) is a cerebral neurodegenerative pathology that is characterized by the progressive formation of insoluble amyloid plaques and fibrillary tangles.[1] Although AD is the most common cause of dementia in western industrialized countries, up to now there is no approved causal treatment. The available symptomatic treatments or disease modifiers provide only limited benefits to the affected people. Approved drugs, such as Vitamin E and AChE inhibitors, slow down, but do not stop disease progression.[2] Thus, a growing need exists for new effective therapies with a specific mode of action, which allow to control onset and progression of the disease. Over the last decade great attention has been paid to the cascade of physiological events that contribute or accompany AD.[3],[4],[5] It is generally accepted that the β-amyloid precursor protein (APP) is cleaved by two proteases to generate the 40/42 amino acid long amyloid-β peptides (Aβ) Increased Aβ formation results in extracellular amyloid plaques deposition and is accompanied by the intracellular formation of neurofibrillary tangles in the brain.[5],[6] The neurotoxicity associated with Aβ oligomerisation is assumed to cause neuronal death, brain inflammation, and finally AD.[7] The APP is processed via the major α- or the minor β-secretase pathway, the latter produces fragments, that are further processed by γ-secretase.[8] Differently from the nonpathogenic products of α-secretase, the β-secretase pathway produces pathogenic Aβ peptides. After the demonstration that β-secretase (BACE-1), a member of the pepsin family of aspartyl proteases, is the rate-limiting enzyme in the production of Aβ,[9] and that its genetic depletion in mice abolishes β-amyloid formation without major side effects,[10] BACE-1 has emerged as leading target for therapeutic treatment of Alzheimer disease.[11] Recently BACE-1 was shown to control myelination of peripheral nerves in the late foetal development, the relevance of this finding to chronic treatment of adults will have to be considered.[12]

Up to now, several X-ray structures of BACE-1 (hereinafter "BACE") have been reported, either in the apo form (PDB codes: 1SGZ and 1W50), either in complex with large-size peptidomimetic ligands (1FKN, 1M4H, 1XN2, 1XN3, 1XS7, 2F3E, 1YM2, 1YM4, 2B8L, 2B8V and 2FDP), or with rather small inhibitors (1W51, 1TQF, 2G94). An important advance in the elucidation of inhibitor-BACE recognition process has been provided by the 1W51 structure, where the enzyme has been cocrystallized with the inhibitor 1.[13] Figure 1 highlights the main interactions between **1** and the BACE-1 enzyme.

Insert Figure 1

A detailed comparison of the available X-ray structures

[a] *Dr. V. Limongelli, Prof. Dr. L. Marinelli, Dr. S. Cosconati, Prof. Dr. E. Novellino*
Dipartimento di Chimica Farmaceutica e Tossicologica
Università di Napoli "Federico II"
Via D. Montesano 49, 80131 Napoli, Italy
E-mail: lmarinel@unina.it
[b] *Dr. H. A. Braun, Prof. Dr. B. Schmidt*
Clemens Schöpf-Institute of Chemistry and Biochemistry
Darmstadt University of Technology
Petersenstr. 22, D-64287 Darmstadt, Germany

suggests that BACE can adopt at least two major conformations mainly differing in the FLAP region, which can adopt an open and a closed conformation in the ligand free and ligand bound enzyme, respectively. Thanks to the availability of all these structures, great strides in the development of new BACE inhibitors have been made by both academic and industrial research groups.

Many noncleavable transition state isosters were designed as new inhibitors on the basis of initial kinetics and substrate specificity data.[14] Most of these peptide ananlogues mimic the scissile amide bond of the endogenous substrates.[15],[16] The hydroxyethylenes derivates, such as OM99-2 and OM00-3, represented the first class of highly potent BACE inhibitors.[14]. The employment of the statine moiety led to the peptidomimetic compound **2** (IC_{50} = 20 nM), which features non peptidic portions at both C- and N-termini.[18] In the effort to reduce the peptidic character of the first inhibitors, numerous hydroxyethylamine-containing compounds were investigated as new BACE inhibitors. Among them, inhibitors **3** and **4** are of particular interest for their low nanomolar activity (IC_{50} = 1 and 1.4 nM, respectively) and for the originality of their structures, being the secondary amine of HEA arranged in a six-membered cycle.[19] With the aim of achieving selectivity for BACE over other aspartic proteases, a sulphonylamide group has been introduced in an HEA derivative leading to compound **6**.[20] Recently, high BACE-1 selective compounds, (e.g. compound 5, IC_{50} = 4 nM) featuring a $\Psi(CH_2NH)$ reduced amide bond, were reported by Coburn et al.[21]

Despite this considerable progress, it is worth noting that the majority of the reported peptidomimetics with low nanomolar activity in BACE-1 enzymatic assays are poorly active in cell-based assays because of the limited penetration across cell membranes. Thus, non-peptidic inhibitors with lower molecular weight, suitable for oral delivery and transport through cell membranes and the blood-brain barrier are still in great demand. In spite of all efforts made by the pharmaceutical companies and academic groups, non-peptidic leads for BACE inhibition are still few.[22] Thus, BACE turns out to be a structurally challenging target having on one hand multiple sites for effective binding and, on the other hand an high homology with other aspartyl proteases such as cathepsin D, pepsin, renin. Currently, medicinal chemists can choose among a number of novel approaches for drug discovery such as high-throughput in vitro screening, combinatorial chemistry, focused library or pharmacophore-based and/or target structure-based virtual screening (VS), being the latter two approaches increasingly used having the advantage to avoid long and expensive experimental efforts. However, the pharmacophore-based VS is exclusively possible when a trustworthy pharmacophore model exists, while the structure-based VS needs the design of a proper protocol as it is well known that several features, as the charge state of potential-interactive residues, the protein conformations (apo and ligand bound), the docking methods and the scoring functions can all deeply affect the success rate. In this regard, the work of Polgàr et al.[23] is particularly helpful, as the influence of protonation state of catalytic Asp residues of BACE (D32 and D228) as well as the enzyme conformations were investigated in a comparative VS. From this study, it emerges that the monoprotonated form ($D228^-$, D32) of the BACE catalytic site gave better enrichment factor compared to the default protonation state (D32 and D228 deprotonated), and ligands can find proper poses easier in a ligand-bound structure (FLAP closed), than in the unbound form (FLAP open). Interestingly, the introduction of pharmacophore constraints in the docking calculations improved enrichment factors for both structures (bound and unbound), reducing ligands false positive poses and increasing the inactive drop-out rate.

In structure-based VS, a 3-D pharmacophore model can be used either to constrict the number of possible ligands poses either to pre-screen compounds databases, both helping to pursue a more accurate and saving time simulations. The pharmacophore constraints used in the study of Polgàr et al. were retrieved from a patent document, where a congeneric series of BACE-1 inhibitors were presented.[24]

Here, with the aim to extend our understanding of inhibitors binding at the BACE-1 catalytic site and to provide an exhaustive structure-based pharmacophore model, a number of active and structurally diverse inhibitors (**1-6**) was selected and subjected to an ensemble molecular docking process into BACE X-ray structures. The superimposition of the calculated bioactive conformations of these inhibitors let us capture both the common geometric and electronic features essential for ligand recognition and enzyme inhibition. Furthermore, in order to achieve BACE-1 selective inhibition a comparison of the X-ray structures of BACE-1 and the cathepsin D was made to better understand the structural and chemical differences in their respective catalytic sites.

The elucidation of the different binding modes of the diverse ligands on one hand, and the developed pharmacophore model on the other, are intended to furnish a support for pharmacophore- and structure-based VS techniques and a source for the optimization of the screened compounds as well as of the already-known leads.

Insert Chart 1

Results and Discussion

X-ray Structures Selection for the Ensemble Docking Studies.

Even today, a major hurdle for successful molecular docking is protein flexibility. At the present time, many effective methods are available for docking a flexible ligand into a rigid protein, while docking calculations including target flexibility still remain problematic, both in terms of computational time and efficiency. In this respect, BACE shows the type of flexibility that can pose challenging problems in docking simulations as the enzyme is known to undergo a massive rearrangement of the FLAP region (residues 68-74) during association with ligands and a certain mobility is expected for the "10S loop" (residues 9-14). To the best of our knowledge, no docking program, that attempts to include wide flexibility of the protein, has been extensively validated so far. Fortunately, in the case of BACE, numerous crystallographic structures exist enabling us to use an ensemble of enzyme conformations for our docking calculations. Docking a ligand into a battery of binding pockets is a strategy to deal with protein flexibility, although it is still far from perfection.

A comparative structural analysis of all available BACE structures revealed that the FLAP region is always in the closed conformation whenever an inhibitor, either peptidomimetic or non-peptidomimetic, is bound. Because ligands **1-6** are substrate analogues that interact with the FLAP-closed form of BACE, we

limited our studies to all BACE structures with a FLAP closed conformation (PDB codes: 1FKN, 1M4H, 1TQF, 1XN2, 1XN3, 1XS7, 1YM2, 1YM4, 2B8L, 2B8V, 2FDP, 2G94, 2F3E, 2F3F). With the aim of reducing the BACE structure redundancy, only the most divergent structures were considered for our docking calculations.

To assess the differences among the BACE structures, they were superimposed on the alpha carbon atoms (Cα) using 1W51 structure as reference. Interestingly, the FLAP closed conformations are all surprisingly similar regardless of the inhibitor type bound, while some differences were found in the side chain conformations of few residues with the most notable one residing in Q73 (Figure 2). Additionally, some expected flexibility is also found in various residues lining the binding site cleft such as R128, T231, D307 and D235.

From the comparative analysis of BACE X-ray structures, it clearly emerges that the "10S loop", a short loop located between two strands at the base of the S3 subpocket, shows mainly three low-energy conformations, an open (1FKN, 1XN3, 1XN2, 1XS7, 1YM2, 1M4H, 2F3F, 2G94) a closed (1W51, 1FDP, 2B8L, 2B8V, 1YM4, 2F3E) and an outlier conformation (1TQF) (Figure 2).

In view of the capability of "10S loop" in affecting the shape of the S3 subpocket (S3sp) and thus the ligand binding,[25] the inclusion of such structural variability in a docking study becomes of fundamental importance. Thus, 1FKN,[26] 1W51,[13] and 1TQF,[27] were chosen for our docking experiments as they cover the experimentally observed motions of the "10S loop" as well as of some residues in the catalytic site such as Q73, R128, R307, R235, and T231. Two additional structures were considered (1XN3 and 2G94)[28],[29] so as to include additional conformers of Q73 and R235 residues. Thus, each ligand was docked in a total of five BACE structures (1FKN, 1W51,1TQF, 2G94, 1XN3).

Insert Figure 2

Assessment of the Docking Program.

Although Autodock program is the most widely used docking program[30] and has been extensively validated, it is well-known that each docking algorithm performs better for certain protein systems than for others, thus the reliability of a docking program towards the target of interest has always to be assessed. Furthermore, testing a program by docking a ligand into its native protein is intrinsically biased because the protein has already changed its shape to better accommodate the ligand and this unavoidably affects positively docking results. Here, with the aim of accurately evaluating the program performances on the studied system, a cross-docking experiment of **1** in its native enzyme (1W51) and in four non-native enzyme conformations (1FKN,1TQF, 2G94 and 1XN3) was conducted. It is generally accepted that a successful docking result reproduces the crystallographic conformation of a ligand in the complex structure within ~2 Å of RMSD on all ligand atoms and that the first-ranked docked conformation (herein referred as ranking conformation) should be always the preferable one. On the other hand, from our experience in the case of Autodock program, the lowest energy docked conformation of the most populated cluster (herein referred as cluster conformation) has to be taken into account as well. Indeed, in the case of BACE, in two complexes, 1W51 and 2G94, the conformation calculated by AutoDock with the lowest free energy of binding belongs to the most populated cluster, thus, no ambiguity exists for the selection of the "best" binding pose. Autodock program well reproduced the experimental binding mode of **1** (Figure 2) both in native (1W51) and non native (2G94) enzyme structure, with an RMSD values of 0.4 and 0.6 Å, respectively. For the other three enzyme structures, good results were obtained considering the cluster conformations (0.59 Å for both 1FKN and 1TQF, and 1.20 Å for 1XN3) while the accuracy in reproducing the X-ray conformation lowered when the ranking conformation is considered only (2.9 Å for 1FKN, 3.4 Å for 1TQF and 2.8 Å for 1XN3). Our test experiments confirmed that Autodock program can be successfully applied to BACE-1 in order to predict the binding modes of small peptidomimetic ligands such as **1-6**, although whenever the ranking conformation does not correspond to the cluster one, both solutions have to be taken in consideration. The final choice between the ranking and the cluster conformations will be governed by their coherency with experimental data, when available (e.g. SARs).

Docking Results.

Docking of 2. Due to the undetermined absolute stereochemistry of the carbon atom attached to the biphenyl ring of compound **2**[18] both stereoisomers were subjected to docking calculations.

Docking of **2** with the (*R*) absolute stereochemistry revealed that in four out of five calculations (1TQF, 1W51, 1XN3 and 2G94) comparable results were found for all the predicted ranking conformations. Using as receptor 1FKN, docking of **2** did not succeed in predicting a plausible binding mode, therefore it was omitted from the comparison. As depicted in Figure 3, the (S) statine isoster places the hydroxyl group in between the catalytic dyad allowing the simultaneous interaction with D32 and D228 as previously observed in others X-ray complexes (e.g. 1FKN).

Insert Figure 3

The difluorobenzyl moiety of **2** (P1) occupies the aromatic pocket S1, analogue to the corresponding benzyl group of **1**. Noteworthy, due to the withdrawing property of the fluorine atoms present on the aromatic system of **2**, the charge transfer interactions of the P1 branch in **2** with the Y71, W108 and P115 aromatic rings are expected to be stronger with respect to those observed for compound **1**. Analogue to **1**, the calculated binding mode preserves the H-bond with G34 backbone CO, while two additional H-bonds with T72 and T231 side chains are present (Figure 3).

Unfortunately, a direct comparison between the potency of **2** (IC_{50} = 20 nM) and 1 (IC_{50} = 200 nM) is not meaningful, this is due to the different biological assays. Differently from **1**, compound **2** features an isopropyl group (P1') which establishes hydrophobic contacts with I226 and V332 side chains (S1' pocket) while the biphenyl moiety deepens into a narrow passage (S3sp) mainly formed by two glycines (G13 and G230). An interesting feature of **2**, which certainly contributes to its great potency (IC_{50} = 20 nM), is the aminocyclohexanedicarboxylate moiety (P2'), which was inserted to mimic the C-termini of the first known peptidic inhibitors.[14],[17] Indeed, docking results confirm that this P2' moiety entirely fills the S2' hydrophobic pocket with both the carboxylate groups engaging a charged-reinforced H-bond with the guanidine group of R128.

Docking of **2** with biphenyl unit attached in the (*S*) configuration gave for three out of five docking calculations (1FKN, 1XN3 and 2G94) a slightly different binding conformation in comparison to that found for the (*R*) isomer. Indeed, the main interactions with the enzyme are well conserved for this isomer while some differences come out for the N-terminal moiety (P3 branch). Here, the biphenyl group points into the S3sp, similarly to the (*R*) isomer, while the hydroxyl function due to its (*S*) stereochemistry is now incapable to interact with T231. Although it is not known which is the most active diastereoisomer, it has been reported that one isomer is 100 fold more active than the other.[18] Our docking results do not clearly discriminate between the two analyzed isomers. Nevertheless, the low convergence of docking results for the (*S*)-isomer allow us to hypothesize a weaker binding to BACE if compared to the (*R*)-isomer.

However, the proposed binding modes are in alignment with the available SARs data.[18] Indeed, analogues of **2**, featuring non acidic aminocyclohexanedicarboxylate derivatives, do not interact with R128, this results in loss of activity.[18]

Furthermore, the replacement of the aminocyclohexanedicarboxylic moiety by 4-aminomethylbenzoic acid, presenting only one acidic function, caused a 10-fold loss of activity thus demonstrating the contribution of both acidic groups for the enzyme binding. Interestingly, the aminocyclohexanedicarboxylic methylester derivative displays only a 10 fold decrease in the inhibitory activity. These data are in accordance with our results, which place the aminocyclohexanedicarboxylic near to R128, where the carbonyl of the methyl ester forms a H-bond with the guanidine side chain.

Docking of 3 and 4. The binding pose of **3** does not substantially change when different enzyme structures are used and basically resembles the binding position found for **1** and **2**. As depicted in Figure 4a, the hydroxyl group of the HEA core H-bonds with D32, while the protonated secondary amine, which differs from **1** by the locked conformation of the 6-membered ring. It engages a salt bridge with D228 and H-bonds with G34. Interestingly, all HEA derivatives feature an unusual stereochemistry at the secondary alcohol (R absolute configuration). A secondary amine in the HEA derivatives causes the interaction with D228, which would be lost by the inversion of the stereochemistry at the secondary alcohol. The benzyl ring (P2') is stacked in between the Y198 and Y71 residues (S2' pocket), while the ligand amide group H-bonds with G230 and Q73 backbones. Analogue to **2**, the difluorobenzyl branch (P1) fills the S1 pocket shaped by Y71, F108 and W115 residues (Figure 4a).

Insert Figure 4

While the above-described interactions are conserved in all five BACE structures, an ambiguity was encountered for the relative position of the imidazolidinone moiety. Ligand docking into 1W51 and 1XN3 structures placed the imidazolidinone so as to allow the carbonyl group to H-bond with T232 backbone, the benzyl group (P2) to establish a cation-π interaction with the guanidine group of R235 and the N-alkyl substituent to thread into the narrow S3 subpocket (S3sp) (Figure 4a). However, ligand docking into 1FKN and 1TQF structures, placed the imidazolidinone ring so that the phenyl ring pointed to the S3sp, while the alkyl chain pointed out of the enzyme. In this case, ensemble docking leads to two comparable but not equal conformations. A subsequent analysis of BACE structures suggests that the different conformations of the R235 side chain are mainly responsible for the divergent results. More precisely, in 1W51 and 1XN3 structures, the R235 side chain is optimally oriented to engage a cation-π interaction with the phenyl ring of **3** (Figure 4a), while in 1FKN and 1TQF structures, the R235 guanidine group partially occludes the catalytic site. as to prevent the placement of the phenyl group. Indeed, both ligand conformations are feasible, Nevertheless, the orientation of the N-alkyl substituent into the S3sp and the benzyl moiety towards the external part of the enzyme maximizes the interaction with the protein by allowing the formation of a H-bond with T232 and a cation-π interaction with R235. Further support for this hypothesis is provided by recent X-ray studies outlining the importance of the interactions with T232 and R235.[31]

Similarly to **3**, the HEA isoster in **4** well interacts with both the catalytic aspartates as well as with G34 (Figure 4b). The benzyl and difluorobenzyl moieties of the ligand optimally fill S2' and the S1 pockets, respectively, while the isophthalamide group lies in the S2 open region with one of the two amide functions H-bonding with G230 and Q73. Interestingly, the methoxymethyl substituent of the pyrrolidine protrudes above the S3sp, where polar interactions with R307 and T232 side chains occur. The high potencies of **3** and **4** (IC_{50} = 1 nM, IC_{50} = 1.4 nM, respectively) suggest that T232, R235 and R307 are further points of ligand attachment strengthening the inhibitor binding.

Docking of 5 and 6. Ensemble docking experiments on **5** and **6** showed for both of them convergence of results. In fact, all docking calculations apart from one (1W51) detected a single solution which is at the same time the ranking and cluster conformation.

The protonated nitrogen of **5** was found to interact with D228 while the isobutylamide branch (P2') engages H-bonds with T72 and G34 placing the alkyl chain into the hydrophobic S2' pocket (Figure 5a). The n-propyl branch (P1') lies in S1' pocket shaped by hydrophobic aminoacids such as I226, V332 and Y198. The benzyl group (P1) is placed into the aromatic cage S1 with the adjacent amide group forming two H-bonds with G230 and Q73. Comparing the binding modes of the docked ligands, we noticed that H-bonds with G230, T72 or Q73 backbones are frequently present and this seems to be important for high BACE inhibitory activity.[32] Interestingly, in all five BACE structures used for the ensemble docking, the *N*-methyl methylsulfonamide group (P2) was found in a polar region among N233, S325 and R235, mostly interacting with the latter residue. The proposed location of the sulfonamide function is in line with the recently reported X-ray structures of BACE complexed with sulfonamide-containing ligands.[20],[27],[29],[32]

The difluorobenzyl branch deepens inside the narrow channel in the S3sp engaging a T-shape interaction with Tyr14 (Figure 5a). It is interesting to note that this channel constitutes the access to an additional small pocket lined by hydrophobic residues (L152, L154, V31 and Y14) and up to date no inhibitor has entirely filled this newly identified pocket.

The hydrophobic interactions of the n-propyl branch (P1') in the S1' pocket are supported by SAR data which show a slight decrease of activity for the ethyl and/or methyl (P1') substituent.[21] Furthermore, additional SARs suggest that an H-bond donor on P2' substituent can be important for BACE activity

and this is in agreement with our finding of an H-bond interaction between the isobutylamide branch and the G34 backbone.

Due to the structural similarity, compound **6** docked in a mode similar to **5**. Nevertheless, being **6** an HEA derivate, it contacts both D32 and D228, as described for all the others HEA derivates. While the benzyl group (P1) deepens into the S1 pocket, the sulfonamide group engages an electrostatic interaction with R235 (Figure 5b).

Insert Figure 5

The two cyclopropyl branches of **6** fit in the hydrophobic S1' pocket and S3sp, respectively. Despite the structural similarity, compounds **5** and **6** show different activities (IC_{50} = 4 and 35 nM, respectively). According to our docking results, this difference in potency has to be ascribed to the additional interactions established by **5**, which occupies S3sp, S1' and S2' pocket, while **6** just partially occupies the S3sp and S1'pocket and does not fill the S2' pocket at all.

Pharmacophore fingerprints and guidelines for drug design.

The superimposition of the calculated bioactive conformations of inhibitors **1-6** (Figure 6a) allowed us to capture both the common geometric and electronic features essential for ligand recognition and enzyme inhibition. From the analysis of the interactions established between the ligands and the enzyme, it is apparent that both polar and hydrophobic interactions are equally important in the inhibitor-enzyme recognition process.

Despite the structural diversity, compounds **1-6** are linked by five highly conserved pharmacophoric points (blue spheres in Figure 6b and 6c): three H-bond donors (D1, D2 and D3), one acceptor (A4) and one hydrophobic centre (H5). All compounds, with the exception of **5**, feature an interaction point with D32 (D1) and with the other catalytic aspartate (D228) through the D2 point. This observation confirms the importance of the interaction with the two catalytic aspartates of the binding site for an effective enzyme inhibition. Moreover, all compounds, apart from **2**, present the D2 point. This highlights the convenient insertion of a protonable amine in this position to achieve simultaneous interaction with D228 and G34 residues. As shown in Figure 6c, the D3 point donates an H-bond to G230 backbone CO while the H-bond acceptor A4 interacts with either T72 or Q73 backbone NHs. It is noteworthy how these two latter points (D3 and A4) represent an ancestral inheritance of the endogenous ligands of BACE where these points are normally filled by an amide moiety of the peptidic backbone.

Despite the relevance of such polar features, the hydrophobic point H5, constantly present in **1-6**, underlines the essential role of a hydrophobic group in this position, interacting with the S1 pocket residues Y71, W108 and F115. (Figure 6c).

The frequent occurrence of D1, D2, D3, A4 and H5 pharmacophoric points in the analysed compound set (Table 1) suggests that these are the indispensable features for ligand recognition. Unfortunately these interactions do not offer the key to selective BACE inhibition. This is due to the conservation of the majority of their corresponding interacting residues in others proteases such as cathepsin D as discussed hereafter.

From our docking results, four additional pharmacophore points, represented as cyan spheres in Figure 6b and 6c, emerge. They are mostly hydrophobic (H6, H7 and H9), with the exception of one, that can be either hydrophobic or a polar (H/A8).

Insert Figure 6

The H6 point represents a hydrophobic feature able to reach the S2' pocket (Figure 5c). The structural variability of this feature (Figure 6a) demonstrates that, although an aromatic substituent in H6 is not mandatory (see compounds **2** and **5**), an hydrophobic group is required due to the nonpolar character of the S2' pocket. It is worth noting that in all analysed compounds, only **2** features the H6 point optimally functionalized having two carboxyl groups that establish a double salt bridge with R128. Such an interaction is particularly interesting being R128 an unique feature of BACE enzyme. In order to achieve a better pharmacokinetic profile preserving a good inhibitory potency, the acidic functions present in the H6 point could be methylated not preventing the ability to H-bond with R128.

The additional point H7 finds place in the hydrophobic S1' pocket (I226, V332 and Y198) where, due to its limited dimension, only an alkyl or cycloalkyl chain with at maximum three carbon atoms, seems to be tolerated. This position was recently employed to achieve selective BACE inhibition and should be investigated further.[33]

Another pharmacophoric point, which may be exploited to achieve BACE-selectivity, is represented by the H/A8 point, which is located in the S2 open region and can be either hydrophobic or polar. An H-bond acceptor in this position, such as a sulfonamide (compounds **5** and **6**), or an hydrophobic phenyl ring (compound **3**) can interact with the surrounding residues such as N233, R235 and S325. These three residues are peculiar to BACE in comparison to others proteases, thus this interaction is expected to have an important role in BACE selectivity. Our observation is in accordance with the recently reported X-ray analysis of co-crystallized complexes of selective BACE inhibitors featuring a sulfonamide group as H/A8 point.[27],[29]

After the superposition of all compounds in their predicted binding poses, it clearly emerges a different sized branch as H9 point indicating that aliphatic, as well as aromatic branches are well tolerated in the S3sp. The extension of this pocket mainly depends on the conformation of 10S loop, but it has to be pointed out that among all analysed compounds, only inhibitor **5** goes across the S3sp, reaching with its aromatic system the inner hydrophobic pocket made by L152, L154, VI31 and Y14 residues. In the design of new BACE inhibitors, this cavity should be explored further, as demonstrated for the renin inhibitor aliskiren.[34] Comparing the BACE and renin cavities, we noticed that they have chemical and structural differences, which offer further chances to improve inhibitor selectivity.

Insert Table 1

Insert Table 2

The compounds **1-6** are characterized by five to eight identified pharmacophoric points (Table 1); appropriate chemical modifications can result in more potent analogues. For instance, the BACE binding affinity of compound **5** may be improved by the addition of an hydroxyl group on the carbon of the $\Psi(CH_2NH)$

reduced amide bond so as to present the D1 point and complete the nine-point pharmacophore.

Regarding compound **1**, the substitution of the *n*-propyl chain with a benzyl moiety may optimize the interactions with the BACE S3sp and the addition of an H-bond acceptor in position 2 on the isophthalamide group such as a sulfonate or carbonyl group may provide the basis for BACE selectivity.

So far, only one pharmacophore model derived from a congeneric series of BACE inhibitors has been disclosed via a patent application by Vertex.[24] The authors proposed that the flap is shifted and stabilised in an open conformation in the presence of their inhibitors.

Comparing the Vertex pharmacophore model with ours, we found that the two models are rather similar regarding the pharmacophoric points interacting with residues unaffected by flap movement. In particular, the Vertex model shares a pattern of three H-bond donors, and two hydrophobic points corresponding to D1, D2 and D3 and H5 and H6 in our model. Despite the general coherency of the chemical features of these points in both pharmacophoric models, the reported distances between them diverge to a large extent. For instance, in our model, the distance between D1 and D2 and D1 and D3 is maximum 2.9 and 3.8 Å respectively, (see Figure 6b) while in the Vertex model both range from 4 to 5 Å. Moreover, the D1-H6 distance is calculated as a range of 4.2-7.8 Å in our pharmacophore model and this value is very low in comparison to the minimum distance of 8 Å reported for the corresponding points in the Vertex model (HB-1 and HPB-3, respectively). This discrepancy may be due to the fact that Vertex model places the HPB-3 point in a different pocket of the S2' region.

The discrepancies found between the two pharmacophoric models can be assigned to the different compounds used for model generation. The Vertex pharmacophore derived from a congeneric series based on a piperazine scaffold which are thought to stabilize the flap in on open conformation. Consequently, in their pharmacophoric model, an additional hydrophobic point referred as HPB-2 is involved in the interactions with the flap pocket (W76, F108, F109, W115 and I102). Here, we have used BACE with the flap in a closed conformation, thus this pocket is no longer present. Consequently the HPB-2 point has to be considered a typical feature of the open flap pharmacophore model.

With respect to the Vertex model, our model offers an accurate description of three new pharmacophoric points: A4, H7 and H9, which are particularly important for selective BACE inhibition.

The structural diversity of the compounds used in our study contributes to the value of our pharmacophore model, which is also substantiated by the X-ray structure of the binding conformation of compound **1**, perfectly filling seven pharmacophoric points.

The design of new BACE inhibitors has to consider the other human aspartic proteases which could be potentially inhibited by BACE ligands, such as renin, napsin-A, and B, cathepsin-E, pepsinogen-A, and C and cathepsin-D. Indeed, the catalytic domain of BACE is similar to that of other aspartyl proteases and the interactions of these enzymes with their inhibitors do not diverge too much from those we observed in the case of BACE. For instance, most of the human aspartyl proteases accept a phenylalanine analogue in P1. The selectivity versus BACE over other human aspartic proteases is required to avoid adverse side effects and is thus mandatory for clinical development of BACE inhibitors. For instance, inhibition of cathepsin D, which is largely expressed in all cells controlling their protein catabolism,[35] would mean a likely consuming of that BACE inhibitor as well as the occurrence of probable toxicity.

Therefore we performed a structure-based sequence alignment of BACE and cathepsin D in order to investigate the differences in their binding sites. The superposition of BACE and cathepsin D three-dimensional structures reveals that the two enzymes display very similar residues in their binding sites and consequently possess a similar shape, which is visualised by their Connolly surfaces in Figure 7. Besides the catalytic dyad, several residues important for the ligands recognition such as G34 or G230 (G35 and G233 in cathepsin D) are conserved. As shown in Figure 7, the shape of the hydrophobic S1 and S2' pockets is equivalent in BACE and cathepsin D. However, a careful comparison of the two binding sites reveals several important points of diversification (Figure 7).

Insert Figure 7

Probably the most striking difference is located near to the catalytic dyad and thus easily accessible to the inhibitors; it concerns the S2 pocket, which presents the polar triplet N233-R235-S325 in BACE and the hydrophobic triplet L236-V238-M307 in cathepsin D. In line with this observation, a series of highly selective inhibitors containing a sulfonyl group in the P2 branch interacts with the residues of the BACE S2 region.[27],[28] Besides the different character of the S2 region in BACE and cathepsin D, the space available for ligand binding in cathepsin D is limited by the M307 and M309 side chains; these are replaced by less space spacious residues in BACE (S325 and S327). This finding suggests the incorporation of bulky P2 branches, functionalized with polar groups capable to interact with the BACE triplet (N233-R235-S325).

The superposition of BACE and cathepsin D reveals significant differences in the length and sequence of the loop defining the S1'/S3' pocket. Indeed, this loop is shorter in BACE (S327, S328, T329 and G330) than in cathepsin D, which presents a long loop of ten residues containing a rigid section called proline loop (P312, P313, P314, S315, G316 and P317).

This relevant difference indicates an alternative way to achieve BACE/cathepsin D selectivity. In fact, a properly oriented bulky moiety on the P1' substituent will occupy the BACE S1'pocket and will not be tolerated by cathepsin D. Moreover, the exchange of BACE-K224 to E227 in cathepsin D, suggests the insertion of a hydrogen bond acceptor or a positively charged group on the bulky moiety. To our knowledge, only few peptidic inhibitors targeted an interaction with K224.[14],[17]

Another dissimilarity between BACE and cathepsin D resides in the S2' pocket, where R128 is replaced by V144 in cathepsin D. Therefore, inhibitors including one or more acidic functions on the P2' branch are expected to favour interaction with BACE. The cathepsin D flap region, where G79 replaces the BACE-T72, offers another opportunity for enhanced selectivity. The last divergence of BACE/cathepsin D resides in the region above the

S3 pocket. Here, as shown in Figure 7, two basic amino acids (R307 and K321) are replaced by two hydrophobic residues (L292 and L303) in cathepsin D. Thus, compounds presenting an interaction with R307 and/or K321 (e.g. 4) may contribute to selective BACE inhibition.

Mapping our pharmacophore model into the BACE/cathepsin D superposed structures, two main issues can be inferred. Firstly, it is apparent how conserved pharmacophoric points (blue spheres in Figure 7) are essential for ligand recognition in both enzymes. These pharmacophoric points are placed in a region where all residues are conserved, therefore these points cannot confer selectivity.

On the contrary, some additional points (cyan spheres in Figure 7) are located in regions, which are dissimilar in BACE and cathepsin D. In particular, the H/A8 has to be considered critical for the improvement of ligand potency and selectivity by allowing the interaction with the basic triplet (N233, R235 and S325) present in BACE and not in the homologous cathepsin D. Similarly, the H6 and H7 points both offer the opportunity to obtain compounds featuring an acidic groups or a H-bond acceptor on the P1' and P2' branches so as to allow an interaction with R128 and K224 residues, which are only expressed in BACE.

In conclusion, despite the high sequence homology between BACE and cathepsin D, we have identified a distinctive fingerprint of the BACE catalytic site that is worth targeting in the effort to achieve potent and selective inhibitors.

Insert Table 3

Conclusion

In the present paper an ensemble-docking approach was undertaken on six highly potent BACE inhibitors identifying for all of them plausible binding modes. A common pharmacophore model linking the multiple structural classes of inhibitors was derived. This allowed us to capture both the geometric and electronic features essential for ligand recognition and enzyme inhibition. In particular, we identified a nine points pharmacophore model outlining the relative distances among them. Interestingly, five of these points are present in all inspected ligands; they can be referred to as essential features for ligand recognition. Whereas the others four points have been defined as accessory points of interaction. An accurate structural comparison of BACE and cathepsin D was made to support the rational design of BACE-selective inhibitor. Despite the high degree of similarity, many structural differences were identified and highlighted; these can be used to achieve or enhance a selective BACE inhibition.

Both, the elucidation of the binding modes of the diverse ligands, and the development of an exhaustive structure-based pharmacophore model are expected to provide a support for pharmacophore- and structure-based VS techniques and a source for the optimization of screen derived hits as well as of established leads.

Computational Methods

Molecular modeling calculations and graphics manipulations were performed on a Silicon Graphics Octane2 workstation equipped with two 2600 MHz R14000 processors using the SYBYL7.2 software package.[36] Automated docking calculations were performed using version 3.0.5 of the AutoDock program.[37]

Ligand setup: The protonation state of ligands **1-6** was calculated using MarvinSketch tools (available at http://www.chemaxon.com/marvin/doc/dev/example-sketch1.1.html) at the pH value of the corresponding biological essay. The absolute stereochemistry of each ligand was considered as reported in literature. Due to the undetermined stereochemistry on the *N*-terminal hydroxyl group of compound **2**, both possible isomers were taken into account for the docking calculations. For **2**, **3** and **4** the Cambridge Structural Database (CSD)[38] was searched for the conformational preference of the cyclohexyl and the piperazinone moieties. Energy minimizations of the obtained structures were achieved with the TRIPOS force field using the SYBYL/MAXIMIN2 minimizer by applying the BFGS (Broyden, Fletcher, Goldfarb and Shannon) algorithm[39] with a convergence criterion of 0.001 kcal/mol. Partial atomic charges were assigned by using the Gasteiger-Marsili formalism.[40] All the relevant torsion angles were treated as rotatable during the docking process, allowing thus a search of the conformational space.

Protein setup: All the X-ray structures of BACE (PDB entry codes = 1FKN, 1W51, 1TQF, 1XN3 and 2G94)[13],[26],[27],[28],[29] were set up for docking as follows: polar hydrogens were added using the BIOPOLYMERS module of the SYBYL program (the side chain of Asp32 was taken as protonated[23],[41] while all other Asp, Glu, Lys and Arg side chains were considered ionized and all His were considered neutral by default), Kollman united-atom partial charges were assigned and all waters were removed. In order to optimize the side chains and the hydrogen positions, the protein structures were minimized using both steepest descent and conjugate gradient, keeping the backbone atoms constrained, employing the DISCOVER program with the CVFF force field.[42] ADDSOL utility of the AutoDock program was used to add salvation parameters to the protein structures and the grid maps representing the proteins in the docking process were calculated using AutoGrid. The grids, one for each atom type in the ligand, plus one for electrostatic interactions, were chosen to be large enough to include not only the catalytic site, but also a significant part of the protein around it. As a consequence, for all docking calculations, the dimensions of grids map was 60 x 60 x 60 Å with a grid-point spacing of 0.375 Å. The centre of the grid was set to be coincident with one of the two oxygens of Asp228.

Docking simulation: Docking simulations of compounds **1-6** were carried out using the Lamarckian Genetic Algorithm and applying a protocol with an initial population of 50 randomly placed individuals, a maximum number of 1.0×10^6 energy evaluations, a mutation rate of 0.02, a crossover rate of 0.80, and an elitism value of 1. Proportional selection was used, in which the average of the worst energy was calculated over a window of the previous 10 generations. The pseudo-Solis and Wets algorithm with a maximum of 300 interactions was applied for the local search. 100 independent docking runs were carried out for each ligand, clustering together the resulting conformations which differ by less than 2.0 Å in positional root-mean-square deviation (rmsd). The result with the lowest free energy of binding was taken as the representative of each cluster.

Energy refinement of the BACE-1/ligand complexes. Energy optimizations of the obtained complexes were carried out using 3000 steps of steepest descent followed by 2000 steps of conjugated gradient algorithm employing the CVFF force field as implemented in the DISCOVER program.[42] Only the ligand and the side chains of all residues within a radius of 8 Å around the ligand were allowed to relax. Connolly surfaces of BACE and Cathepsin D were calculated using PyMOL software.[43]

Keywords: BACE-1 inhibitors; ensemble-docking; pharmacophore model; molecular modeling; medicinal chemistry.

[1] G. G. Glenner, C. W. Wong, *Biochem. Biophys. Res. Commun.* **1984**, *120*, 885-890.

[2] R. C. Petersen, R. G. Thomas, M. Grundman, D. Bennett, R. Doody, S. Ferris, D. Galasko, S. Jin, J. Kaye, A. Levey, E. Pfeiffer, M. Sano, C. H. van Dyck, L. Thal, *J. New England J. Med.* **2005**, *352*, 2379-2388.

[3] a) D. K. Lahiri, M. R. Farlow, K. Sambamurti, N. H. Greig, E. Giacobini, L. S. A. Schneider, *Curr. Drug Targets* **2003**, *4*, 97-112; b) M. Citron, *Neurobiol. Aging* **2002**, *23*, 1017-1022.

[4] R. Vassar, *Adv. Drug Delivery Rev.* **2002**, *54*, 1589-1602.

[5] S. Roggo, S. *Curr. Top. Med. Chem.* **2002**, *2*, 359-370.

[6] a) R. Vassar, B. D. Bennett, S. Babu-Khan, S. Kahn, E. A. Mendiaz, P. Denis, D. B. Teplow, S. Ross, P. Amarante, R. Loeloff, Y. Luo, S. Fisher, J. Fuller, S. Edenson, J. Lile, M. A. Jarosinski, A. L. Biere, E. Curran, T. Burgess, J. C. Louis, F. Collins, J. Treanor, G. Rogers, M. Citron, *Science* **1999**, *286*, 735-741; b) X. Lin, G. Koelsch, S. Wu, D. Downs, A. Dashti, J. Tang, *Proc. Natl. Acad. Sci. U.S.A.* **2000**, *97*, 1456-1460; c) S. Sinha, I. Lieberburg, *Proc. Natl. Acad. Sci. U.S.A.* **1999**, *96*, 11049-11053.

[7] a) D. J. Selkoe, *Nature* **1999**, *399* (67388 Suppl), A23-A31; b) D. J. Selkoe, *Physiol. Rev.* **2001**, *81*, 741-766.

[8] a) H. Josien, *Curr. Opin. Drug Discov. Devel.* **2002**, *5*, 513-25; b) V. John, J. P. Beck, M. J. Bienkowski, S. Sinha, R. L. Heinrikson, *J. Med. Chem.* **2003**, *46*, 4625-30.

[9] D. H. Small, C. A. McLean, *J. Neurochem.* **1999**, *73*, 443-449.

[10] Y. Luo, B. Bolon, S. Kahn, B. D. Bennett, S. Babu-Khan, P. Denis, W. Fan, H. Kha, J. Zhang, Y. Gong, L. Martin, J. Louis, Q. Yan, W. G. Richards, M. Citron, R. Vassar, *Nat. Neurosci.* **2001**, *4*, 231-232.

[11] L. A. Thompson, J. J. Brown, F. C. Zusi, *Curr. Pharm. Des.* **2005**, *11*, 3383-3404.

[12] M. Willem, A. N. Garratt, B. Novak, M. Citron, S. Kaufmann, A. Rittger, B. DeStrooper, P. Saftig, C. Birchmeier, C. Haass, *Science* **2006**, 314, 664-666.

[13] a) M. Maillard, C. Hom, A. Gailunas, B. Jagodzinska, L. Y. Fang, J. Varghese, J. N. Freskos, S. R. Pulley, J. P. Beck, R. E. Tenbrink, Patent WO 02/02512, **200**;. b) L. Vuillard, S. Patel, J. Yon, A. Cleasby, B. Hamilton, A. Shah, Patent WO 04/011641, **2004**; c) S. Patel, L. Vuillard, A. Cleasby, C. W. Murray, J. Yon, *J .Mol. Biol.* **2004**, *343*, 407-416.

[14] R. Turner, G. Koelsch, L. Hong, P. Castenheira, A. K. Ghosh, J. Tang, *Biochemistry* **2001**, *40*, 10001-10006.

[15] a) B. Schmidt, H. A. Braun, R. Narlawar, *Curr. Med. Chem.* **2005**, *12*, 1677-1695; b) B. Schmidt, S. Baumann, H. A. Braun, G. Larbig, *Curr. Top. in Med. Chem.* **2006**, *6*, 377-392.

[16] V. John, J. P. Beck, M. J. Bienkowski, S. Sinha, R. L. Heinrikson, *J. Med. Chem.* **2003**, *46*, 4625-4630.

[17] a) A. K. Ghosh, L. Hong, J. Tang, *Curr. Med. Chem.* **2002**, *9*, 1135-1144; b) A. K. Ghosh, D. Shin, D. Downs, G. Koelsch, X. Lin, J. Ermolieff, J. Tang, *J. Am. Chem. Soc.* **2000**, *122*, 3522-3523.

[18] R. K. Hom, L. Y. Fang, S. Mamo, J. S. Tung, A. C. Guinn, D. E. Walker, D. L. Davis, A. F. Gailunas, E. D. Thorsett, S. Sinha, J. E. Knops, N. E. Jewett, J. P. Anderson, V. John, *J. Med. Chem.* **2003**, *46*, 1799-1802.

[19] J. N. Cumming, Y. Huang, G. Li, U. Iserloh, A. Stamford, C. Strickland, J. H. Voigt, Y. Wu, J. Pan, T. Guo, D. W. Hobbs, T. X. H. Le, J. F. Lowrie, Patent WO 05/014540, **2005**.

[20] S. J. Stachel, C. A. Coburn, T. G. Steele, M. Crouthamel, B. L. Pietrak, M. Lai, M. K. Holloway, S. K. Munshi, S. L. Grahama, J. P. Vacca, *Bioorg. Med. Chem. Lett.* **2006**, *16*, 641-644.

[21] C. A. Coburn, S. J. Stachel, K. G. Jones, T. G. Steele, D. M. Rush, J. DiMuzio, B. L. Pietrak, M. Lai, Q. Huang, J. Lineberger, L. Jin, S. Munshi, M. K. Holloway, A. Espeseth, A. Simon, D. Hazuda, S. L. Grahama, J. P. Vacca *Bioorg. Med. Chem. Lett.* **2006**, *16*, 3635-3638.

[23] T. Polgár, G. M. Keserű, *J. Med. Chem.* **2005**, *48*, 3749-3755.

[22] V. John, *Curr. Top. Med. Chem.* **2006**, 6, 569-578.

[24] G. R. Bhisetti, J. O. Saunders, M. A. Murcko, C. A. Lepre, S. D. Britt, J. H. Come, D. D. Deninger, T. Wang, Patent WO 02/088101, **2002**.

[25] G. B. McGaughey, D. Colussi, S. L. Graham, M. T. Lai, S. K. Munshi, P. G. Nantermet, B. Pietrak, H. A. Rajapakse, H. G. Selnick, S. R. Stauffer, M. K. Holloway, *Bioorg. Med. Chem. Lett.* **2006** Nov 6; [Epub ahead of print].

[26] L. Hong, G. Koelsch, X. Lin, S. Wu, S. Terzyan, A. K. Ghosh, X. C. Zhang, J. Tang, *Science* **2000**, *290*, 150-153.

[27] C. A. Coburn, S. J. Stachel, Y. M. Li, D. M. Rush, T. G. Steele, E. Chen-Dodson, M. K. Holloway, M. Xu, Q. Huang, M. T. Lai, J. DiMuzio, M. C. Crouthamel, X. P. Shi, V. Sardana, Z. Chen, S. Munshi, L. Kuo, G. M. Makara, D. A. Annis, P. K. Tadikonda, H. M. Nash, J. P. Vacca, T. Wang, *J. Med. Chem.* **2004**, *47*, 6117-6119.

[28] R. T. Turner III, L. Hong, G. Koelsch, A. K. Ghosh, J. Tang, *Biochemistry* **2005**, *44*, 105-112.

[29] A. K. Ghosh, N. Kumaragurubaran, L. Hong, H. Lei, K. A. Hussain, C. Liu, T. Devasamudram, V. Weerasena, R. Turner, G. Koelsch, G. Bilcer, J. Tang, *J. Am. Chem. Soc.* **2006**, *128*, 5310-5311.

[30] S. F. Sousa, P. A. Fernandes, M. J. Ramos, *Proteins* **2006**, *65*,15-26.

[31] a) J. N. Freskos, Y. M. Fobian, T. E. Benson, M. J. Bienkowski, D. L. Brown, T. L. Emmons, R. Heintz, A. Laborde, J. J. McDonald, B. V. Mischke, J. M. Molyneaux, J. B. Moon, P. B. Mullins, P. D. Bryan, D. J. Paddock, A. G. Tomasselli, G. Winterrowd, *Bioorg. Med. Chem. Lett.* **2006** Oct 4; [Epub ahead of print]; b) J. N. Freskos, Y. M. Fobian, T. E. Benson, J. B. Moon, M. J. Bienkowski, D. L. Brown, T. L. Emmons, R. Heintz, A. Laborde, J. J. McDonald, B. V. Mischke, J. M. Molyneaux, P. B. Mullins, P. D. Bryan, D. J. Paddock, A. G. Tomasselli, G. Winterrowd, *Bioorg Med Chem Lett.* **2006** Oct 4; [Epub ahead of print].

[32] H. A. Rajapakse, P. G. Nantermet, H. G. Selnick, S. Munshi, G. B. McGaughey, S. R. Lindsley, M. B. Young, M. T. Lai, A. S. Espeseth, X. P. Shi, D. Colussi, B. Pietrak, M. C. Crouthamel, K. Tugusheva, Q. Huang, M. Xu, A. J. Simon, L. Kuo, D. J. Hazuda, S. Graham, J. P. Vacca, *J. Med. Chem.*; **2006**, Nov 10; [Ahead of print].

[33] S. F. Brady, S. Singh, M. C. Crouthamel, M. K. Holloway, C. A. Coburn, V. M. Garsky, M. Bogusky, M. W. Pennington, J. P. Vacca, D. Hazuda, M. T. Lai, *Bioorg Med Chem Lett.* **2004**, *14*, 601-604.

[34] J. Rahuel, V. Rasetti, J. Maibaum, H. Rueger, R. Goschke, N. C. Cohen, S. Stutz, F. Cumin, W. Fuhrer, J. M. Wood, M. G. Grutter, *Chem. Biol.* **2000**, *7*, 493-504.

[35] S. Diment, M. S. Leech, P. D. Stahl, *J. Biol. Chem.* **1988**, *263*, 6901-6907.

[36] *SYBYL Molecular Modelling System*, version 7.2; Tripos Inc.: St. Louis, MO, 2003.

[37] G. M. Morris, D. S. Goodsell, R. S. Halliday, R. Huey, W. E. Hart, R. K. Belew, A. J. Olson, *J. Comput. Chem.* **1998**, *19*, 1639-1662.

[38] F. H. Allen, S. Bellard, M. D. Brice, B. A. Cartwright, A. Doubleday, H. Higgs, T. Hummelink, B. G. Hummelink-Peters, O. Kennard, W. D. S. Motherwell, *Acta Crystallogr.* **1979**, *B35*, 2331-2339.

[39] J. Head, M. C. Zerner, *Chem. Phys. Lett.* **1985**, *122*, 264-274.

[40] J. Gasteiger, M. Marsili, *Tetrahedron* **1980**, *36*, 3219-3228.

[41] a) N. Moitessier, E. Therrien, S. A. Hanessian, *J. Med. Chem.* **2006**, *49*, 5885-5894; b) H. Park, S. Lee, *J. Am. Chem. Soc.* **2003**, *125*, 16416-16422.

[42] a) DISCOVER, Version 95.0; BIOSYM Technologies, 10065 Barnes Canyon Rd, San Diego, CA 92121; b) A. F. Hagler, S. Lifson, P. Dauber, *J. Am. Chem. Soc.* **1979**, *101*, 5122-5130.

[43] DeLano Scientific LLC, The PyMOL Molecular Graphics System, 2002, http:// www.pymol.org.

Received: ((will be filled in by the editorial staff))
Published online: ((will be filled in by the editorial staff))

Chart 1. Chemical structures of docked compounds.

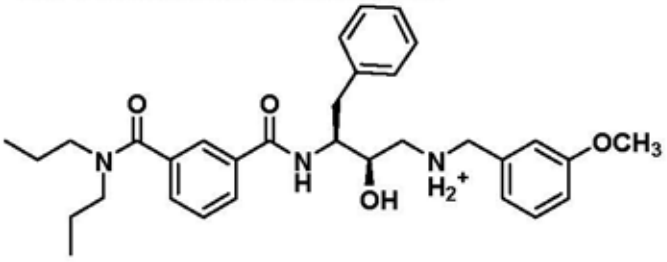

1

(IC_{50} = 200 nM)

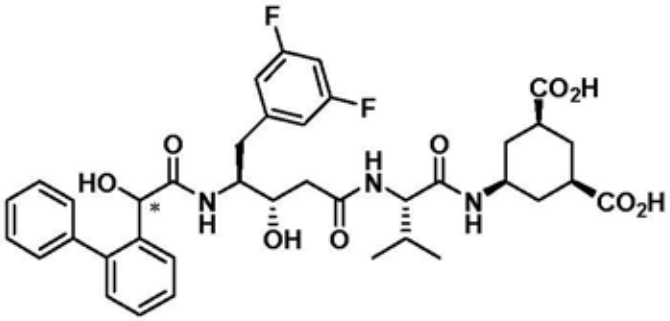

2

(IC_{50} = 20 nM)

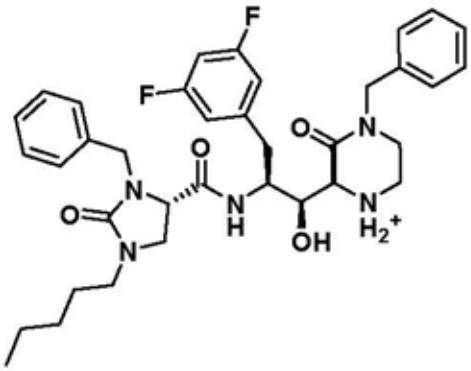

3

(IC_{50} = 1 nM)

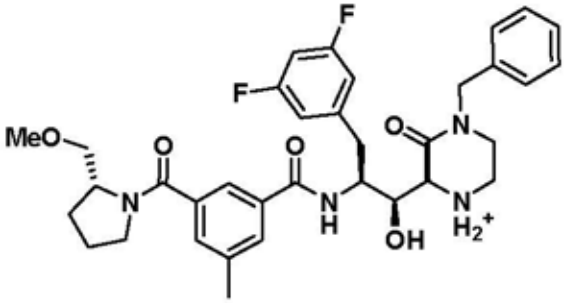

4

(IC_{50} = 1.4 nM)

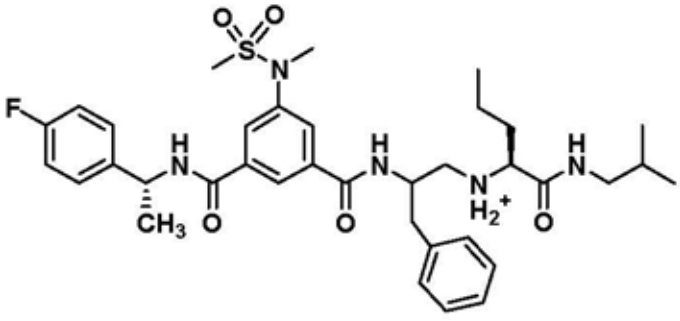

5

(IC_{50} = 4 nM)

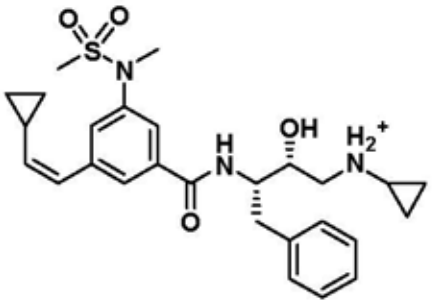

6

(IC_{50} = 35 nM)

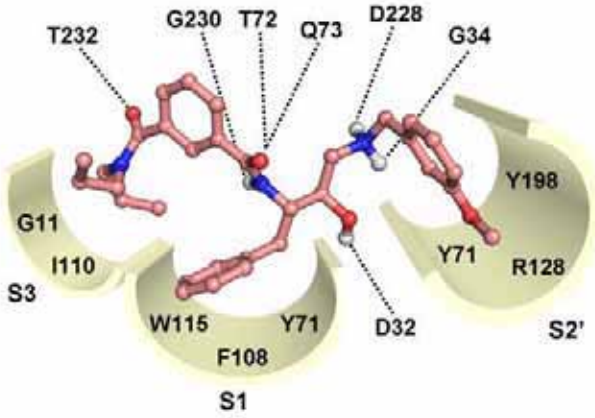

Figure 1

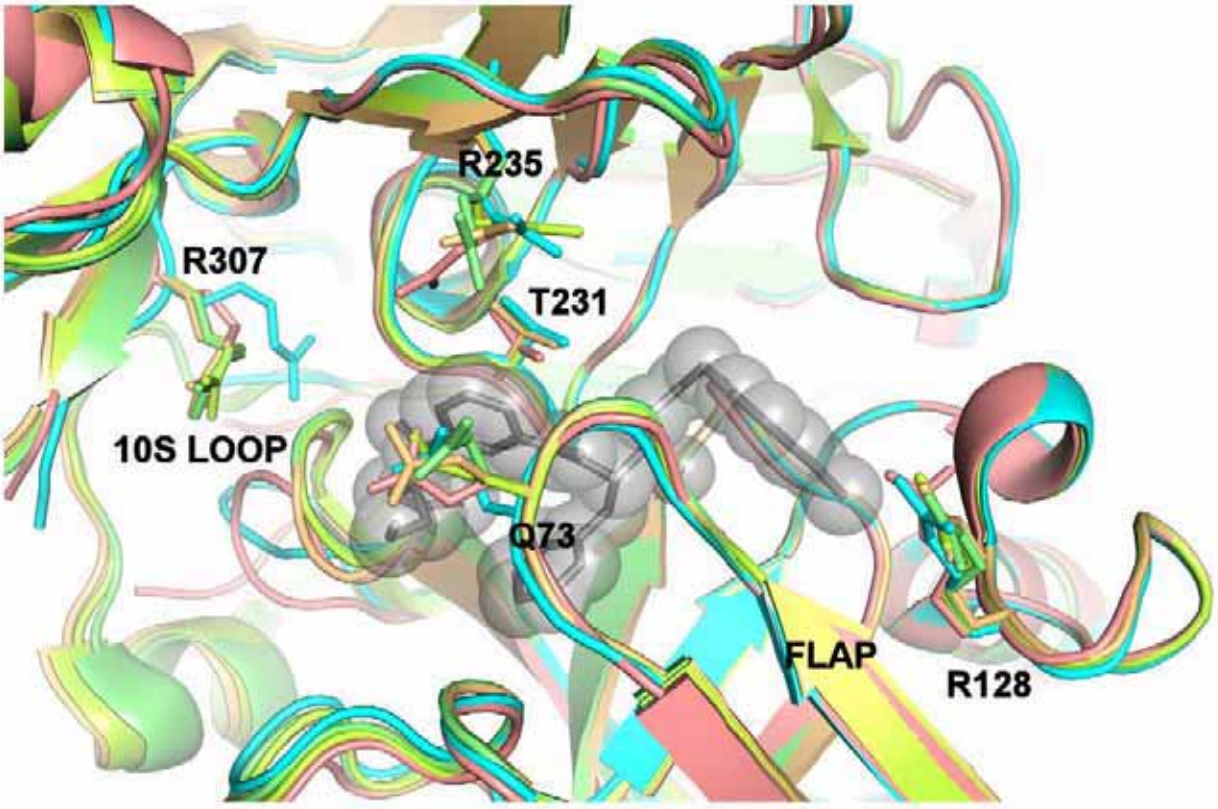

Figure 2

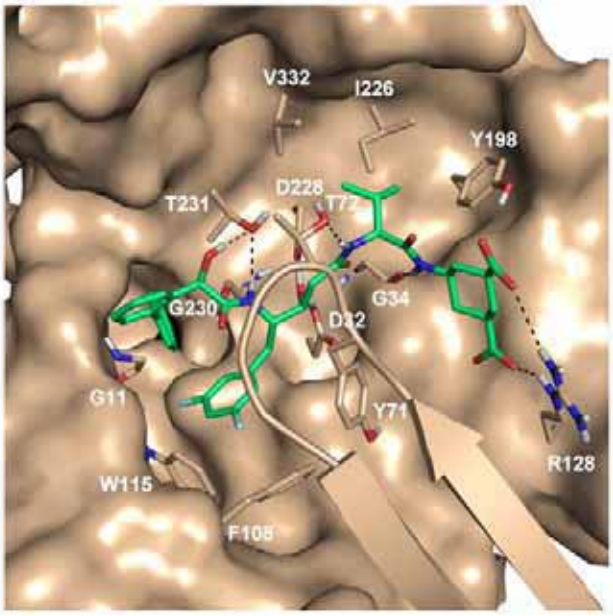

Figure 3

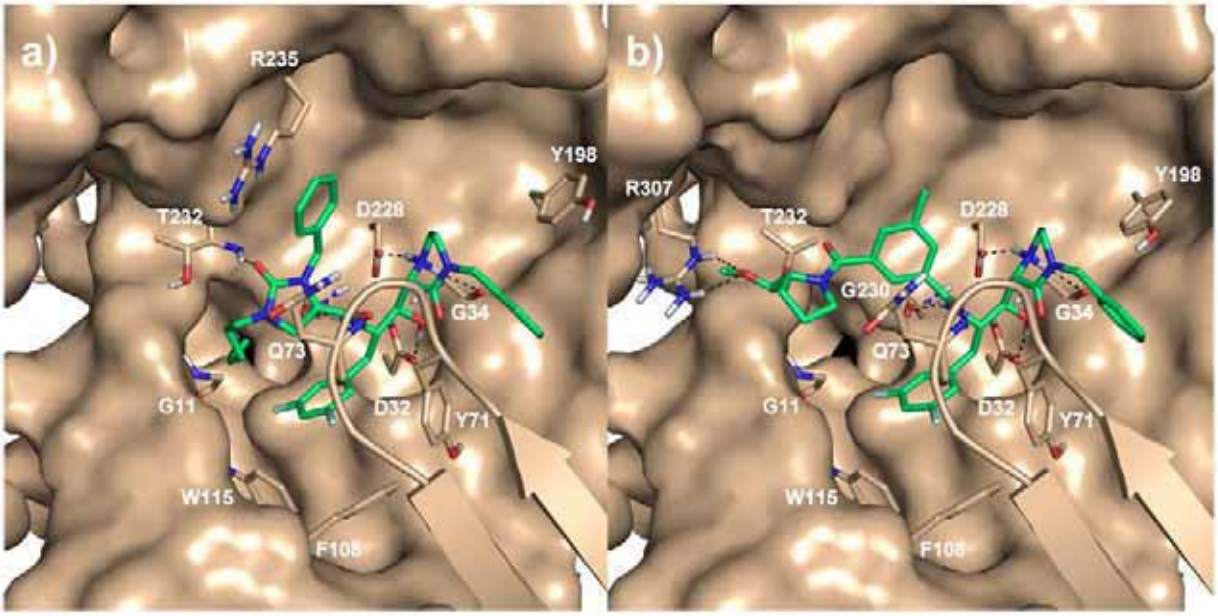

Figure 4

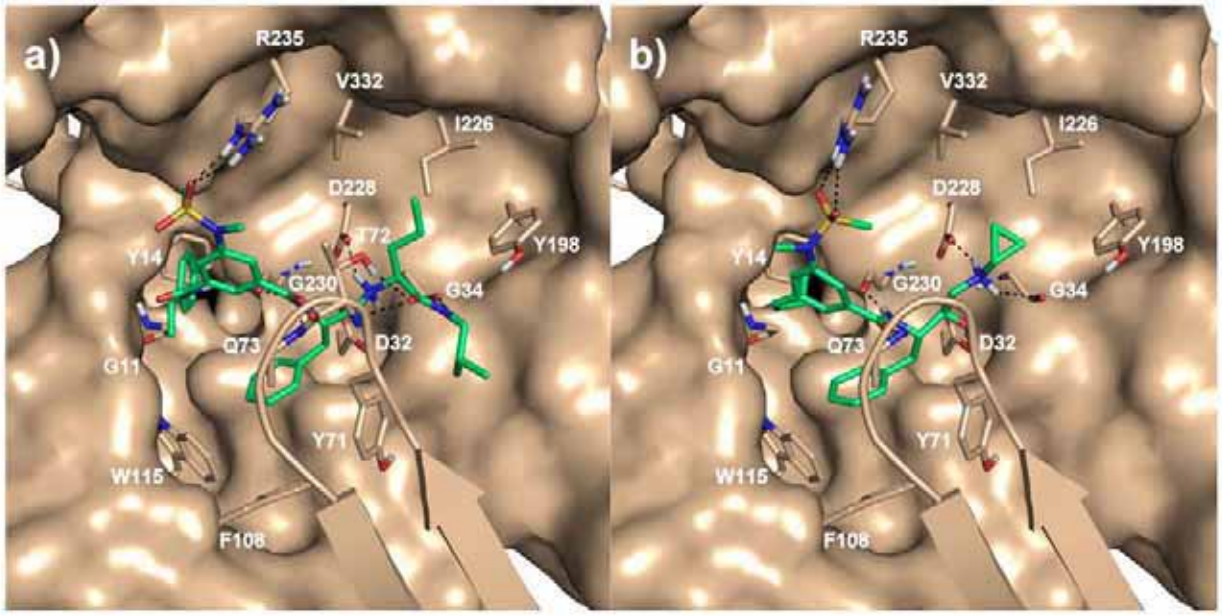
a)
R235
V332
I226
D228
T72
Y198
Y14
G230
G34
Q73
D32
G11
Y71
W115
F108
b)
R235
V332
I226
D228
Y198
Y14
G230
G34
Q73
D32
G11
Y71
W115
F108

Figure 5

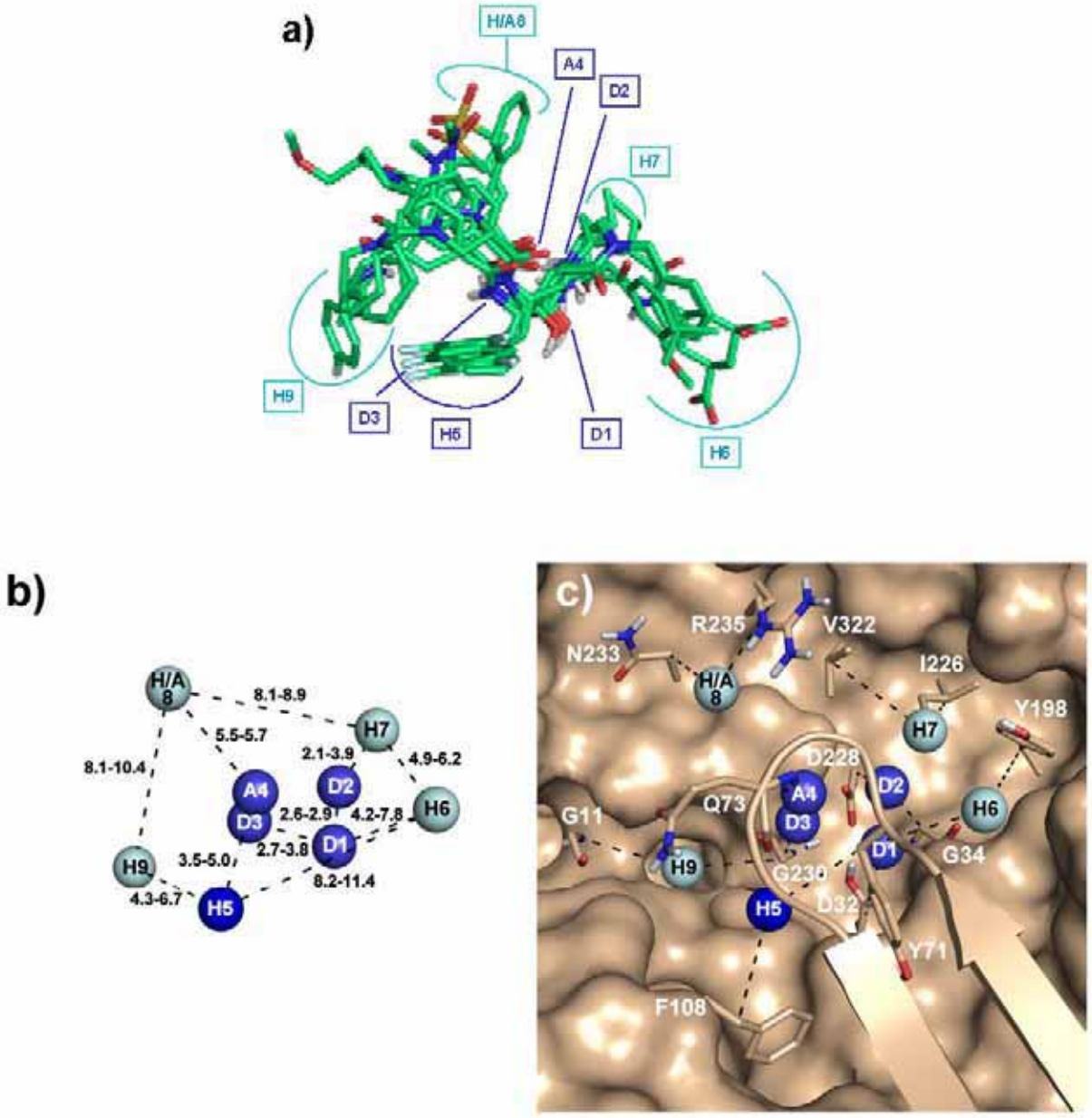
a)
H/A8
A4
D2
H7
H9
D3
H5
D1
H6
b)
H/A 8
8.1-8.9
H7
5.5-5.7
2.1-3.9
4.9-6.2
8.1-10.4
A4
D2
D3
2.6-2.9
4.2-7.8
H6
H9
3.5-5.0
2.7-3.8
D1
8.2-11.4
4.3-6.7
H5
c)
R235
V322
N233
H/A 8
I226
Y198
H7
D228
D2
A4
Q73
G11
D3
H6
H9
D1
G34
G230
H5
D32
Y71
F108

Figure 6

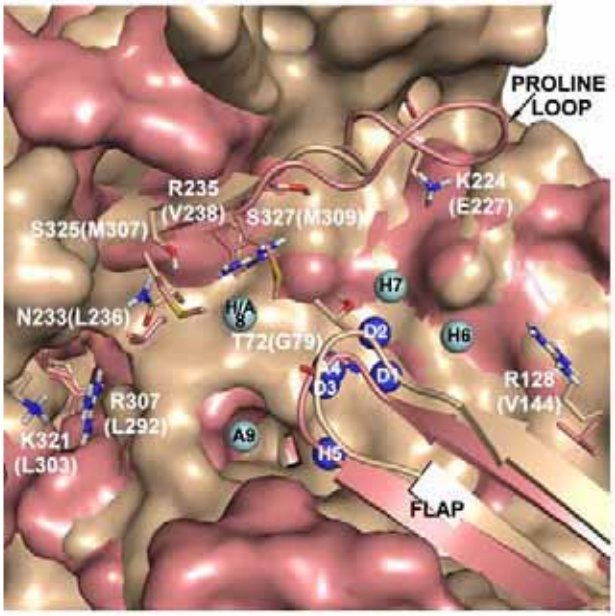

Figure 7

Captions:

Figure 1. Schematic representation of the main interactions of **1** with the BACE catalytic site.

Figure 2. Cartoon representation of the BACE X-ray structures used for the ensemble-docking study (1W51, 1FKN, 1TQF, 1XN3, 2G94 are in pink, green, cyan, yellow and orange, respectively) with **1** shown as grey sticks and transparent grey spheres; hydrogen atoms are omitted for clarity reason. The most flexible residues, emerged from the BACE X-ray structures superposition, are represented in stick mode and coloured according to the BACE structures colour code.

Figure 3. Binding mode of compound **2** (green) into BACE catalytic site represented as Connolly surface. The ligand and the interacting residues are shown in stick representation and coloured by atom type, while the FLAP region is represented as cartoon. Hydrogen bonds are represented with dashed black lines. All nonpolar hydrogens were removed for clarity.

Figure 4. Binding modes of compound **3** (a) and **4** (b) into BACE catalytic site.

Figure 5. Binding modes of compound **5** (a) and **6** (b) into BACE catalytic site.

Figure 6. a) Overlay of bioactive conformations of compounds **1-6** on the experimentally determined bound conformation of **1**. The pharmacophoric points are colour coded as conservative (blue) or additional (cyan). The non polar hydrogens are omitted for clarity. The letter "A" corresponds to an H-bond acceptor group, "D" to an H-bond donor, while "H" to an hydrophobic group. "A/H" means that an H-bond acceptor or an hydrophobic group is tolerated. b) Tridimensional representation of the distances between the identified pharmacophoric points. The distances are reported in Å and represent the minimum and the maximum value found in the proposed bioactive conformations of **1-6**. The distances were calculated considering the nitrogen and oxygen atoms of the H-bond acceptor and donor groups, the sulphur atom of the sulphonamide function, the centroids of the aromatic rings, the centre of mass of the alkyl and cycloalkyl groups. c) Mapping of the pharmacophoric points into the BACE catalytic site represented as Connolly surface. Interactions between the pharmacophoric points and some BACE residues are highlight by black dashed lines.

Figure 7. Superposition of BACE (pink) and cathepsin D (brown) structures represented as Connolly surfaces. The pharmacophoric points were mapped into the BACE enzyme. Mutated residues in the binding pocket are shown in stick representation and labelled with the one-letter amino acid code. The letters and the number in parentheses refer to the cathepsin D enzyme.

Tables:

Table 1. Pharmacophoric points present in ligands **1-6**.

Compounds	Points
1	D1-D2-D3-A4-H5-H6-H9
2	D1-H5-H6-H7-H9
3	D1-D2-D3-A4-H5-H6-H/A8-H9
4	D1-D2-D3-A4-H5-H6
5	D2-D3-A4-H5-H6-H7-H/A8-H9
6	D1-D2-D3-A4-H5-H7-H/A8-H9

Table2. Distances (Å) between the pharmacophoric points and the BACE interacting residues. The distances were calculated considering the pharmacophoric points and each Cβ of the corresponding residues, Cα were taken into account for glycine residues.

Pharmacophoric Points	Interacting Residues	Distances
D1	D32	4.9
D2	G34	3.7
	D228	4.5
D3	G230	4.4
A4	Q73	4.5
H5	Y71	5.4
	P108	8.9
H6	Y71	5.4
	Y198	8.1
H7	I226	6.0
	V332	6.4
H/A8	R235	5.6
	N233	5.3
H9	G11	5.1
	G230	4.5

Table 3. Main dissimilarities in BACE and Cathepsin-D catalytic sites.

Binding Site Location	BACE residues	Cathepsin D residues
S2 Open Region	N233	L236
	R235	V238
	S325	M307
	S327	M309
S1' pocket	K224	E227
Loop between S1' and S2'	S328, T329 and G330	D310, I311, P312, P313, P314, S315, G316, P317 and L318
S2' pocket	R128	V144
Flap Region	T72	G79
Others	R307	L292
	K321	L303

Röntgenstrukturanalyse von (*S*,*S*)-97

Table 1. Crystal data and structure refinement for 1037.

Identification code	1037 (649 F2B)
Empirical formula	C15 H22 I N O3
Formula weight	391.24
Temperature	299(2) K
Wavelength	0.71073 A
Crystal system, space group	Monoclinic, C 2
Unit cell dimensions	a = 20.303(5) A alpha = 90 deg. b = 5.182(2) A beta = 99.04(2) deg. c = 16.780(3) A gamma = 90 deg.
Volume	1743.5(9) A^3
Z, Calculated density	4, 1.490 Mg/m^3
Absorption coefficient	1.843 mm^-1
F(000)	784
Crystal size	0.40 x 0.12 x 0.05 mm
Theta range for data collection	4.20 to 25.67 deg.
Limiting indices	-24<=h<=24, -4<=k<=6, -20<=l<=20
Reflections collected / unique	4902 / 2338 [R(int) = 0.0538]
Completeness to theta = 25.67	95.4 %
Absorption correction	Empirical
Max. and min. transmission	0.992 and 0.567
Refinement method	Full-matrix least-squares on F^2
Data / restraints / parameters	2338 / 2 / 195
Goodness-of-fit on F^2	1.201
Final R indices [I>2sigma(I)]	R1 = 0.0820, wR2 = 0.1384
R indices (all data)	R1 = 0.1433, wR2 = 0.1559
Absolute structure parameter	0.06(8)
Largest diff. peak and hole	0.613 and -0.465 e.A^-3

Table 2. Atomic coordinates (x 10^4) and equivalent isotropic displacement parameters (A^2 x 10^3) for 1037.
U(eq) is defined as one third of the trace of the orthogonalized Uij tensor.

	x	y	z	U(eq)
I(1)	4044(1)	9938(5)	-888(1)	108(1)
O(1)	4876(4)	7488(15)	2796(6)	65(3)
O(2)	2748(3)	9730(20)	134(4)	55(2)
O(3)	4151(4)	4500(20)	2151(5)	55(2)
N(1)	4014(4)	8824(17)	1961(5)	44(3)
C(1)	3871(6)	8200(30)	196(8)	69(4)
C(2)	3390(4)	9720(30)	619(6)	39(3)
C(3)	3351(5)	8680(20)	1451(7)	38(3)
C(4)	2835(4)	10130(40)	1863(6)	53(3)
C(5)	2820(5)	9300(30)	2718(8)	56(4)
C(6)	3203(6)	10570(30)	3356(9)	71(5)
C(7)	3201(8)	9670(60)	4140(8)	92(5)
C(8)	2843(8)	7610(40)	4310(12)	92(5)
C(9)	2473(8)	6320(30)	3670(12)	83(5)
C(10)	2471(6)	7130(30)	2899(10)	70(4)
C(11)	4331(6)	6660(30)	2292(8)	41(3)
C(12)	5332(7)	5530(30)	3228(10)	71(5)
C(13A)	5770(20)	7150(70)	3917(18)	101(17)
C(13B)	5963(16)	7320(60)	3460(20)	64(12)
C(14)	4970(8)	4030(30)	3800(9)	96(7)
C(15)	5612(7)	3910(30)	2649(12)	95(6)

Table 3. Bond lengths [A] and angles [deg] for 1037.

I(1)-C(1)	2.107(13)
O(1)-C(11)	1.352(14)
O(1)-C(12)	1.482(16)
O(2)-C(2)	1.423(9)
O(2)-H(2O)	0.8200
O(3)-C(11)	1.191(15)
N(1)-C(11)	1.366(15)
N(1)-C(3)	1.480(12)
N(1)-H(1N)	0.8600
C(1)-C(2)	1.517(17)
C(1)-H(1A)	0.9700
C(1)-H(1B)	0.9700
C(2)-C(3)	1.508(15)
C(2)-H(2)	0.9800
C(3)-C(4)	1.538(16)
C(3)-H(3)	0.9800
C(4)-C(5)	1.503(16)
C(4)-H(4A)	0.9700
C(4)-H(4B)	0.9700
C(5)-C(6)	1.387(18)
C(5)-C(10)	1.387(19)
C(6)-C(7)	1.40(2)
C(6)-H(6)	0.9300
C(7)-C(8)	1.35(3)
C(7)-H(7)	0.9300
C(8)-C(9)	1.38(2)
C(8)-H(8)	0.9300
C(9)-C(10)	1.360(19)
C(9)-H(9)	0.9300
C(10)-H(10)	0.9300
C(12)-C(15)	1.47(2)
C(12)-C(14)	1.51(2)
C(12)-C(13B)	1.58(2)
C(12)-C(13A)	1.58(2)
C(13A)-H(13A)	0.9600
C(13A)-H(13B)	0.9600
C(13A)-H(13C)	0.9600
C(13B)-H(13D)	0.9600
C(13B)-H(13E)	0.9600
C(13B)-H(13F)	0.9600
C(14)-H(14A)	0.9600
C(14)-H(14B)	0.9600
C(14)-H(14C)	0.9600
C(15)-H(15A)	0.9600
C(15)-H(15B)	0.9600
C(15)-H(15C)	0.9600

C(11)-O(1)-C(12)	118.5(10)
C(2)-O(2)-H(2O)	109.5
C(11)-N(1)-C(3)	121.5(9)
C(11)-N(1)-H(1N)	119.3
C(3)-N(1)-H(1N)	119.3
C(2)-C(1)-I(1)	112.8(9)
C(2)-C(1)-H(1A)	109.0
I(1)-C(1)-H(1A)	109.0
C(2)-C(1)-H(1B)	109.0
I(1)-C(1)-H(1B)	109.0
H(1A)-C(1)-H(1B)	107.8
O(2)-C(2)-C(3)	110.8(8)

O(2)-C(2)-C(1)	109.5(10)
C(3)-C(2)-C(1)	112.3(10)
O(2)-C(2)-H(2)	108.0
C(3)-C(2)-H(2)	108.0
C(1)-C(2)-H(2)	108.0
N(1)-C(3)-C(2)	110.1(8)
N(1)-C(3)-C(4)	109.7(9)
C(2)-C(3)-C(4)	112.4(9)
N(1)-C(3)-H(3)	108.2
C(2)-C(3)-H(3)	108.2
C(4)-C(3)-H(3)	108.2
C(5)-C(4)-C(3)	113.9(11)
C(5)-C(4)-H(4A)	108.8
C(3)-C(4)-H(4A)	108.8
C(5)-C(4)-H(4B)	108.8
C(3)-C(4)-H(4B)	108.8
H(4A)-C(4)-H(4B)	107.7
C(6)-C(5)-C(10)	117.5(14)
C(6)-C(5)-C(4)	120.4(13)
C(10)-C(5)-C(4)	122.0(13)
C(5)-C(6)-C(7)	118.8(17)
C(5)-C(6)-H(6)	120.6
C(7)-C(6)-H(6)	120.6
C(8)-C(7)-C(6)	123.2(18)
C(8)-C(7)-H(7)	118.4
C(6)-C(7)-H(7)	118.4
C(7)-C(8)-C(9)	117.6(18)
C(7)-C(8)-H(8)	121.2
C(9)-C(8)-H(8)	121.2
C(10)-C(9)-C(8)	120.8(16)
C(10)-C(9)-H(9)	119.6
C(8)-C(9)-H(9)	119.6
C(9)-C(10)-C(5)	122.1(15)
C(9)-C(10)-H(10)	119.0
C(5)-C(10)-H(10)	119.0
O(3)-C(11)-O(1)	128.1(12)
O(3)-C(11)-N(1)	125.6(10)
O(1)-C(11)-N(1)	106.3(11)
C(15)-C(12)-O(1)	110.2(12)
C(15)-C(12)-C(14)	113.6(12)
O(1)-C(12)-C(14)	109.5(12)
C(15)-C(12)-C(13B)	97(2)
O(1)-C(12)-C(13B)	98.2(16)
C(14)-C(12)-C(13B)	126.8(18)
C(15)-C(12)-C(13A)	124(2)
O(1)-C(12)-C(13A)	103.4(19)
C(14)-C(12)-C(13A)	94.7(18)
C(13B)-C(12)-C(13A)	33.6(18)
C(12)-C(13A)-H(13A)	109.5
C(12)-C(13A)-H(13B)	109.5
C(12)-C(13A)-H(13C)	109.5
C(12)-C(13B)-H(13D)	109.5
C(12)-C(13B)-H(13E)	109.5
H(13D)-C(13B)-H(13E)	109.5
C(12)-C(13B)-H(13F)	109.5
H(13D)-C(13B)-H(13F)	109.5
H(13E)-C(13B)-H(13F)	109.5
C(12)-C(14)-H(14A)	109.5
C(12)-C(14)-H(14B)	109.5
H(14A)-C(14)-H(14B)	109.5
C(12)-C(14)-H(14C)	109.5
H(14A)-C(14)-H(14C)	109.5
H(14B)-C(14)-H(14C)	109.5

C(12)-C(15)-H(15A)	109.5
C(12)-C(15)-H(15B)	109.5
H(15A)-C(15)-H(15B)	109.5
C(12)-C(15)-H(15C)	109.5
H(15A)-C(15)-H(15C)	109.5
H(15B)-C(15)-H(15C)	109.5

Symmetry transformations used to generate equivalent atoms:

Table 4. Anisotropic displacement parameters (A^2 x 10^3) for 1037. The anisotropic displacement factor exponent takes the form: -2 pi^2 [h^2 a*^2 U11 + ... + 2 h k a* b* U12]

	U11	U22	U33	U23	U13	U12
I(1)	86(1)	169(1)	70(1)	29(1)	14(1)	8(1)
O(1)	55(6)	34(5)	90(7)	4(5)	-35(5)	1(5)
O(2)	32(4)	51(6)	74(5)	4(7)	-15(3)	-8(6)
O(3)	47(5)	24(6)	86(6)	0(5)	-17(4)	-2(5)
N(1)	26(5)	39(8)	63(6)	3(5)	-1(4)	-5(4)
C(1)	47(8)	78(11)	74(10)	19(8)	-14(7)	3(7)
C(2)	18(5)	38(7)	57(6)	-3(8)	-9(4)	7(7)
C(3)	8(5)	32(7)	71(8)	0(6)	-5(5)	-1(5)
C(4)	27(5)	59(8)	72(7)	16(11)	0(5)	7(9)
C(5)	8(5)	68(13)	91(9)	-4(8)	9(5)	8(7)
C(6)	65(8)	64(13)	84(10)	-8(9)	15(7)	-7(9)
C(7)	87(10)	120(16)	64(9)	-7(15)	2(7)	-10(17)
C(8)	49(10)	115(17)	114(15)	8(13)	20(10)	5(10)
C(9)	69(11)	68(12)	115(15)	22(10)	23(10)	-12(8)
C(10)	35(8)	85(13)	88(12)	12(9)	3(7)	-6(8)
C(11)	22(6)	46(11)	53(8)	2(7)	-8(6)	4(7)
C(12)	60(9)	49(11)	89(11)	1(10)	-32(8)	15(9)
C(13A)	120(30)	90(30)	70(20)	40(20)	-50(20)	-30(20)
C(13B)	60(20)	50(20)	60(20)	20(20)	-50(20)	-5(18)
C(14)	107(13)	94(19)	77(10)	5(10)	-19(9)	45(11)
C(15)	42(8)	78(15)	165(17)	40(12)	14(9)	19(8)

Table 5. Hydrogen coordinates (x 10^4) and isotropic displacement parameters (A^2 x 10^3) for 1037.

	x	y	z	U(eq)
H(2O)	2611	8247	69	66
H(1N)	4205	10301	2051	52
H(1A)	3694	6477	79	82
H(1B)	4293	8028	555	82
H(2)	3549	11505	676	47
H(3)	3218	6867	1398	46
H(4A)	2933	11966	1861	64
H(4B)	2396	9877	1550	64
H(6)	3456	12007	3263	85
H(7)	3459	10531	4565	110
H(8)	2846	7073	4840	110
H(9)	2223	4888	3768	100
H(10)	2226	6201	2479	84

H(13A)	6122	6084	4188	122
H(13B)	5494	7730	4297	122
H(13C)	5957	8613	3683	122
H(13D)	5869	8603	3843	77
H(13E)	6069	8149	2989	77
H(13F)	6335	6289	3704	77
H(14A)	4706	5187	4065	115
H(14B)	5289	3176	4196	115
H(14C)	4685	2766	3502	115
H(15A)	5994	3002	2923	114
H(15B)	5743	4971	2233	114
H(15C)	5282	2687	2414	114

Table 6. Torsion angles [deg] for 1037.

I(1)-C(1)-C(2)-O(2)	65.2(13)
I(1)-C(1)-C(2)-C(3)	-171.3(8)
C(11)-N(1)-C(3)-C(2)	-119.9(12)
C(11)-N(1)-C(3)-C(4)	116.0(12)
O(2)-C(2)-C(3)-N(1)	-176.8(11)
C(1)-C(2)-C(3)-N(1)	60.4(13)
O(2)-C(2)-C(3)-C(4)	-54.2(15)
C(1)-C(2)-C(3)-C(4)	-177.0(10)
N(1)-C(3)-C(4)-C(5)	-52.7(15)
C(2)-C(3)-C(4)-C(5)	-175.5(11)
C(3)-C(4)-C(5)-C(6)	92.7(16)
C(3)-C(4)-C(5)-C(10)	-82.3(14)
C(10)-C(5)-C(6)-C(7)	-2(2)
C(4)-C(5)-C(6)-C(7)	-177.1(14)
C(5)-C(6)-C(7)-C(8)	0(3)
C(6)-C(7)-C(8)-C(9)	1(3)
C(7)-C(8)-C(9)-C(10)	0(3)
C(8)-C(9)-C(10)-C(5)	-2(2)
C(6)-C(5)-C(10)-C(9)	3(2)
C(4)-C(5)-C(10)-C(9)	177.9(13)
C(12)-O(1)-C(11)-O(3)	2(2)
C(12)-O(1)-C(11)-N(1)	-178.2(12)
C(3)-N(1)-C(11)-O(3)	8(2)
C(3)-N(1)-C(11)-O(1)	-172.5(9)
C(11)-O(1)-C(12)-C(15)	61.2(17)
C(11)-O(1)-C(12)-C(14)	-64.5(16)
C(11)-O(1)-C(12)-C(13B)	162(2)
C(11)-O(1)-C(12)-C(13A)	-165(2)

Symmetry transformations used to generate equivalent atoms:

Table 7. Hydrogen bonds for 1037 [A and deg.].

D-H...A	d(D-H)	d(H...A)	d(D...A)	<(DHA)
N(1)-H(1N)...O(3)#1	0.86	2.18	2.965(14)	150.8
O(2)-H(2O)...O(2)#2	0.82	1.97	2.791(4)	177.3

Symmetry transformations used to generate equivalent atoms:
#1 x,y+1,z #2 -x+1/2,y-1/2,-z

Lebenslauf

Persönliche Daten

Name:	Hannes Braun
Geburtsdatum/-ort:	03. März 1979 in Pforzheim
Staatsangehörigkeit:	deutsch
Familienstand:	ledig

Ausbildung

06/1997	Reifeprüfung in Bad Ischl / Österreich
09/1997-06/1998	Grundwehrdienst in Lahnstein
10/1998 - 09/2000	Grundstudium Chemie, Albert-Ludwigs-Universität Freiburg
10/2000 - 05/2003	Hauptstudium Chemie, TU Darmstadt
06/2003 - 12/2003	Diplomarbeit bei Prof. Dr. B. Schmidt, TU Darmstadt „Selektive Inhibition des Proteasoms“
seit 02/2004	Doktorand bei Prof. Dr. B. Schmidt, Technische Universität Darmstadt
07/2004 - 09/2004	Trinity College Dublin / Irland bei Dr. D. G. Lloyd, Computergestütztes Design von BACE-Inhibitoren

Veröffentlichungen

Siehe Anhang, S. 146.

Hannes Braun
Gundolfstr. 24

64287 Darmstadt

25.04.2007

Eidesstattliche Erklärung

Ich erkläre hiermit an Eides Statt, dass ich meine Dissertation selbständig und nur mit den angegebenen Hilfsmitteln angefertigt habe.

Hannes Braun
Gundolfstr. 24

64287 Darmstadt

25.04.2007

Erklärung

Ich erkläre hiermit, noch keinen Promotionsversuch unternommen zu haben.